Publication No. 02-002-023

EVALUATION OF PHOSPHATIC CLAY DISPOSAL AND RECLAMATION METHODS

Volume 5: Shear Strength Characteristics of Phosphatic Clays

Prepared by Ardaman & Associates, Inc.

under a grant sponsored by the

Florida Institute of Phosphate Research

Bartow, Florida

July, 1983

FLORIDA INSTITUTE OF PHOSPHATE RESEARCH

EVALUATION OF PHOSPHATIC CLAY DISPOSAL AND RECLAMATION METHODS

Volume 5: Shear Strength Characteristics of Phosphatic Clays

Research Project FIPR 80-02-002
Final Report, July 1983

Prepared by

Ardaman & Associates, Inc.
8008 South Orange Avenue
Orlando, Florida 32809

Principal Investigators

Anwar E. Z. Wissa
Nadim F. Fuleihan
Thomas S. Ingra

Prepared for

Florida Institute of Phosphate Research
1855 West Main Street

Bartow, Florida 33830

FIPR Program Managers

David P. Borris
Henry L. Barwood

DISCLAIMER

EVALUATION OF PHOSPHATIC CLAY DISPOSAL AND RECLAMATION METHODS

Research Project FIPR 80-02-002

PREFACE

As part of a Florida Institute of Phosphate Research project titled "Evaluation of Phosphatic Clay Disposal and Reclamation Methods", Ardaman & Associates, Inc. performed a comprehensive study to evaluate the engineering properties of a wide range of phosphatic clays and sand-clay mixes, and developed a methodology for forecasting the performance of phosphatic clay settling areas during disposal and reclamation. The findings of this study are presented in a series of six complementary volumes.

Laboratory evaluations of the engineering properties of phosphatic clays and sand-clay mixes were performed on phosphatic clays from twelve different mine sites. Volumes 1, 2 and 3 titled "Index Properties of Phosphatic Clays", "Mineralogy of Phosphatic Clays", and "Sedimentation Behavior of Phosphatic Clays", respectively, present extensive data on the twelve clay sources selected in the study. The findings were used to screen the samples and select six clays covering the full range of anticipated behavioral characteristics. The selected clays were subjected to a comprehensive testing program for determining engineering parameters pertaining to consolidation and strength. Extensive sophisticated testing of three of the six phosphatic clays and corresponding sand-clay mixes was subsequently undertaken. The results are presented in Volumes 4 and 5 titled "Consolidation Behavior of Phosphatic Clays" and "Shear Strength Characteristics of Phosphatic Clays", respectively.

Concurrent with the laboratory evaluation of phosphatic clay engineering properties, a theoretical model to evaluate disposal systems was developed. The finite difference program SLURRY can also be used in reclamation planning. In an attempt to verify and refine the prediction modeling technique, a preliminary field investigation program at six phosphatic clay settling areas ranging from retired to active sites was undertaken. Volume 6 discusses the theoretical model and presents a comparison of predictions based on laboratory data and actual field measurements.

A more extensive second phase field testing program is proposed to further refine and improve predictive capability based on actual field conditions. Conventional phosphatic clay disposal and the sand-clay mix disposal methods can then be critically evaluated for phosphatic clays with differing characteristics to quantify advantages/disadvantages of disposal/reclamation methods and outline their relative merits. The results should allow mine planners to select an optimum disposal method based on the clay characteristics at a particular mine.

EVALUATION OF PHOSPHATIC CLAY DISPOSAL AND RECLAMATION METHODS

Volume 5: Shear Strength Characteristics of Phosphatic Clays

Research Project FIPR 80-02-002
Final Report, July 1983

ABSTRACT

The undrained stress-strain-strength characteristics of six normally consolidated phosphatic clays were investigated via isotropically consolidated undrained triaxial compression tests (CIUC). The remolded phosphatic clay undrained shear strength at low effective stresses was determined from viscosity and laboratory vane measurements. The effects of strength anisotropy and stress history were evaluated for three phosphatic clays via K_O- consolidated undrained triaxial compression ($\overline{CK_oUC}$), triaxial extension ($\overline{CK_oUE}$) and direct simple shear (CK_oUDSS) tests. The undrained behavior of normally consolidated sand-clay mixes at sand-clay ratios of 1:1 and 3:1 was investigated for three phosphatic clays using $\overline{CIUC}$ and CK_oUDSS tests. Clays selected for the evaluation of anisotropic and stress history effects and for the sand-clay mix study generally bracketed the range of plasticity and settling, consolidation and strength behavior reported for phosphatic clays. A total of 44 $\overline{CIUC}$, 3 $\overline{CK_OUC}$, 4 $\overline{CK_OUE}$ and 25 CK_oUDSS tests were performed as part of this investigation.

The remolded undrained shear strength of phosphatic clays at low effective stresses is of interest in determining the impact of an accidental spill from the disposal system and/or for evaluating the shear strength of re-worked or displaced clay. Phosphatic clays are highly plastic and not anticipated to be very sensitive to loss of shear strength upon disturbance. Nevertheless, viscosity and laboratory vane measurements indicate that at a liquidity index in excess of 1.0 (solids contents less than 25 to 40%), the phosphatic clays are moderately sensitive with sensitivities ranging from about 1.5 to 3.5 depending on the plasticity of the clay. Phosphatic clays appear to be less sensitive at lower liquidity indices (higher solids contents).

Results of $\overline{CIUC}$ and CK_oUDSS tests confirmed the applicability of the normalized soil parameter concept to phosphatic clays. Moreover, the shear strength of phosphatic clays was determined to be strain rate sensitive although to a lesser extent than anticipated based on the high plasticity of these clays. This finding is, consistent

with the relatively low rates of secondary compression measured on phosphatic clays (Volume 4). It also implies that phosphatic clays are not as susceptible to undrained creep deformations as originally anticipated.

Highly plastic phosphatic clays were not expected to exhibit significant anisotropic behavior. Nevertheless, their stress-strain-strength characteristics were determined to be moderately affected by the direction of loading. For example, the undrained shear strength, s_u, normalized with respect to the one-dimensional vertical effective consolidation stress, $\bar{\sigma}_{vc}$, was determined to be affected by stress system and inherent anisotropy. $s_u/\bar{\sigma}_{vc}$ ratios of 0.28 or more characterized normally consolidated phosphatic clays sheared in compression, whereas an $s_u/\bar{\sigma}_{vc}$ ratio of about 0.225 was characteristic of a direct simple shear stress system. When the effects of strain compatibility for the different stress systems along a failure surface were taken into consideration, the normalized undrained shear strength ratio, $s_u/\bar{\sigma}_{vc}$, of normally consolidated phosphatic clays was determined to equal 0.22 to 0.24, which is in good agreement with data on other natural sedimentary type deposits of lower plasticity. CK_oUDSS test results were in excellent agreement with the selected design parameters. $s_u/\bar{\sigma}_{vc}$ values were not significantly different for all phosphatic clays investigated and no consistent trends with phosphatic clay plasticity could be detected. Hence, the normalized properties determined in this investigation are probably applicable to a wide range of phosphatic clays.

The undrained Young's secant modulus, E_u, of phosphatic clays was determined to be highly stress-level dependent as expected. However, all phosphatic clays seem to exhibit approximately the same magnitude of normalized modulus, E_u/s_u, irrespective of plasticity. At a stress level of 50% (factor of safety = 2.0), phosphatic clays are characterized by an E_u/s_u ratio of 250 to 370. Although the data are consistent, the undrained modulus is higher than one would expect for such plastic materials implying smaller undrained deformations upon loading than would occur with high plasticity natural sedimentary clay deposits consolidated to the same effective stress.

The effective angle of internal friction, $\bar{\phi}$ determined from undrained shear tests generally ranged from 28^o to 35° and averaged about 30° at maximum obliquity. These friction angles are much higher than expected for highly plastic clays. A lower drained friction angle of 25° is recommended for evaluating long-term stability problems.

The effect of stress history and overconsolidation due to desiccation and/or pre-loading produced significant changes in the stress-strain-strength behavior of phosphatic clays. The normalized undrained shear strength ratio, $s_u/\bar{\sigma}_{vc}$, was determined to increase with increased overconsolidation ratio (OCR) in accordance with the relationship $s_u/\bar{\sigma}_{vc}$ = 0.225 $(OCR)^{0.8}$ based on CK_oUDSS data. Moreover, the normalized undrained modulus, E_u/s_u, decreased with increasing overconsolidation ratio particularly at overconsolidation ratios in excess of 2.

The addition of tailings sand to phosphatic clays caused subtle changes to the undrained stress-strain-strength characteristics of the sand-clay mix, namely: (i) a reduction in the strain at failure and more prominent strain softening effects; (ii) an increase in the normalized undrained modulus E_u/s_u; and (iii) a slight to moderate increase in the angle of internal friction, $\bar{\phi}$, by about 2 to 3 degrees. The $s_u/\bar{\sigma}_v$ ratio of normally consolidated phosphatic clays from CK_0UDSS tests increased slightly from an average of 0.225 to 0.228 by increasing the sand-clay ratio (SCR) from 0:1 to 1:1. The normalized undrained shear strength ratio $s_u/\bar{\sigma}_{vc}$ decreased moderately to about 0.196 at a sand-clay ratio of 3:1. Trends were consistent for all three phosphatic clays investigated. Most of the above trends reflect the change in plasticity of the sand-clay mix and the transition from a highly plastic clay (SCR = 0:1) to a much leaner clay (SCR = 3: 1).

Although the $s_u/\bar{\sigma}_{vc}$ ratios of phosphatic clays and sand-clay mixes are not significantly different, the undrained shear strength, s_u, of a sand-clay mix *in situ* is expected to be higher, at least during disposal, because of the higher effective stresses caused by the weight of the sand. Nevertheless, if sand is used as a cap placed atop the phosphatic clay (disposed of without sand), the undrained shear strength of the phosphatic clay *in situ* would ultimately exceed that of the sand-clay mix.

ACKNOWLEDGEMENTS

The support and sponsorship provided by the Florida Institute of Phosphate Research to conduct this investigation is gratefully acknowledged. The cooperation and assistance provided by the various mining companies named in this report and their representatives during collection of clay samples is greatly appreciated, namely:

- Agrico Chemical Company
- AMAX Phosphate, Inc.
- Beker Phosphates
- Brewster Phosphates
- CF Mining Corporation
- Estech, Inc.
- Hopewell Land Corporation
- International Minerals and Chemicals Corporation
- Mobil Chemical Company
- Occidental Chemical Company
- United States Steel Corporation Agrichemicals Division
- W. R. Grace & Company

The permission to publish information provided by: Mr. John Cameron of New Wales Chemicals, International Minerals and Chemicals Corporation; Mr. Steve Olson of Agrico Chemical Company; and Mr. Troy Deal of Aztec Development Company from in-house reports prepared by Ardaman & Associates, Inc. is appreciated.

The authors would like to acknowledge the assistance of Dr. Charles C. Ladd, Professor of Civil Engineering at the Constructed Facilities Division of the Department of Civil Engineering, Massachusetts Institute of Technology, Cambridge, Massachusetts. Dr. Ladd and his associates performed the specialized K_o-consolidated undrained strength testing presented in this volume. Dr. Ladd's comments on the test data are also gratefully acknowledged.

TABLE OF CONTENTS

TABLE OF CONTENTS (cont'd)

TABLE OF CONTENTS (cont'd)

LIST OF TABLES

LIST OF FIGURES

LIST OF FIGURES (cont'd)

LIST OF FIGURES (cont'd)

LIST OF FIGURES (cont'd)

LIST OF FIGURES (cont'd)

LIST OF FIGURES (cont'd)

LIST OF FIGURES (cont'd)

SYMBOLS

NOTE: Prefix Δ indicates a change or an increment.
Suffix "f" indicates a final or failure condition.
Subscript "o" indicates an initial condition.
A bar over a stress indicates an effective stress.
A bar over a property indicates value in terms of effective stress.
A bar over a test indicates that pore pressures were measured.

INDEX AND CLASSIFICATION PROPERTIES

e	Void Ratio
LI	Liquidity Index
LL	Liquid Limit
NC	Normally Consolidated
OC	Overconsolidated
OCR	Overconsolidated Ratio $=\bar{\sigma}_{vm}/\bar{\sigma}_{vc}$
PI	Plasticity Index
PL	Plastic Limit
S	Solids Content
SCR	Sand-Clay Ratio
w_n,w	Water Content
γ_d	Dry Density
γ_t	Total Unit Weight
γ_w	Unit Weight of Water

STRESS, STRAIN, MODULUS AND STRENGTH PARAMETERS

A	Skempton's Shear Pore Pressure Parameter $A = (\Delta u - \Delta\sigma_3)/(\Delta\sigma_1 - \Delta\sigma_3)$
B	Skempton's Hydrostatic Pore Pressure Parameter $B = \Delta u/\Delta\sigma_3$
$\bar{c}$	Intercept of Mohr-Coulomb Failure Envelope or Effective Cohesion Intercept
E_u	Undrained Young's Secant Modulus
E_{u50}	E_u at Stress Level of 50%
K_o	Coefficient of Earth Pressure at Rest
K_s	Anisotropic Strength Ratio $= s_u(H)/s_u(V)$

SYMBOLS (cont'd)

$\bar{p}$	Average Effective Principal Stress = 0.5 $(\bar{\sigma}_1 + \bar{\sigma}_3)$
q	Half Principal Stress Difference = 0.5 $(\sigma_1 - \sigma_3)$ = Maximum Shear Stress
q_f	q at Failure = maximum q
Δq_f	Increment of Shear Stress to Cause Failure
s_u	Undrained Shear Strength
$s_u(H)$	Undrained Shear Strength with Major Principal Stress in Horizontal Direction
$s_u(V)$	Undrained Shear Strength with Major Principal Stress in Vertical Direction
$s_u(\theta)$	Undrained Shear Strength with Major Principal Stress at Angle θ to the Horizontal
$s_u(45)$	Undrained Shear Strength with Major Principal Stress at 45^{o} to the Horizontal
$s_u(LV)$	Remolded Undrained Shear Strength Measured with Laboratory Vane
$s_u(DSS)$	Undrained Shear Strength in Direct-Simple Shear = $s_u(45)$
$s_u(TC)$	Undrained Shear Strength in Compression = $s_u(V)$
$s_u(TE)$	Undrained Shear Strength in Extension = $s_u(H)$
u	Pore Water Pressure or Excess Pore Pressure Generated During Undrained Shear
V	Volume
V_o	Initial Volume
γ	Shear Strain
$\dot{\gamma}$	Shear Strain Rate
ε	Linear or Axial Strain
$\dot{\varepsilon}$	Linear or Axial Strain Rate
ε_v	Vertical Strain
$\sigma, \bar{\sigma}$	Normal Total Stress, Normal Effective Stress
$\sigma_1, \sigma_2, \sigma_3$	Principal Stresses (major, intermediate and minor, respectively)
$\bar{\sigma}_c$	Effective Consolidation Pressure (isotropic)
σ_h	Horizontal Normal Stress
$\bar{\sigma}_{hc}$	Effective Horizontal Consolidation Stress (normal)
$\sigma_v, \bar{\sigma}_v$	Vertical Normal Stress, Vertical Normal Effective Stress
$\bar{\sigma}_{vc}$	Effective Vertical Consolidation Stress
$\bar{\sigma}_{vf}$	Final Vertical Effective Stress
$\bar{\sigma}_{vo}$	Initial Vertical Effective Stress
$\bar{\sigma}_{vm}$	Maximum Past Pressure

SYMBOLS (cont'd)

τ	Shear Stress
τ_f	Shear Stress at Failure
τ_{ff}	Shear Stress at Failure on Failure Plane
τ_h	τ on Horizontal Plane (direct-simple shear test)
$(\tau_h)max$	Maximum Shear Stress τ on Horizontal Plane
τ_y	Yield Stress (viscosity test)
$\bar{\phi}$	Slope of Mohr-Coulomb Failure Envelope or Effective Angle of Internal Friction
$\bar{\phi}_d$	$\bar{\phi}$ from Drained Tests
ϕ_m	Mobilized $\bar{\phi}$
$\bar{\phi}_u$	$\bar{\phi}$ from Undrained Tests

STRESS-SYSTEM AND LABORATORY TESTING TERMINOLOGY

CU	Consolidated-Undrained Shear Test
$\overline{CIU}$	Isotropically Consolidated-Undrained Shear Test
$\overline{CIU}C$	$\overline{CIU}$ Triaxial Compression Test
$\overline{CIU}E$	$\overline{CIU}$ Triaxial Extension Test
$\overline{CK_oU}$	K_o Consolidated-Undrained Shear Test
$\overline{CK_oU}C$	$\overline{CK_oU}$ Triaxial Compression Test
$\overline{CK_oU}DSS$	$\overline{CK_oU}$ Direct-Simple Shear Test
$\overline{CK_oU}E$	$\overline{CK_oU}$ Triaxial Extension Test
DSS	Direct-Simple Shear
LV	Laboratory Vane
PSA	Plane Strain Active
PSP	Plane Strain Passive
TC	Triaxial Compression
TE	Triaxial Extension

MISCELLANEOUS

m	Exponent Coefficient in Undrained Shear Strength Versus Overconsolidation Ratio Equation
NSP	Normalized Soil Parameters
r	Correlation Coefficient
SHANSEP	Stress History and Normalized Soil Engineering Properties
λ	Semi-Log Linear Regression Coefficient (intercept) in s_u(LV) Versus Solids Content Equation
ψ	Semi-Log Linear Regression Coefficient (slope) in s_u(LV) Versus Solids Content Equation

Section 1

RESEARCH BACKGROUND AND OBJECTIVES

1.1 Introduction

Little published data are available on the shear strength characteristics of phosphatic clays. The only comprehensive data are limited to results from a series of direct-simple shear tests performed at the Massachusetts Institute of Technology on one phosphatic clay (Roma, 1976). Since reclamation emphasis is often on land use and rapid land reclamation, the shear strength characteristics of phosphatic clays and sand-clay mixes as a function of consolidation stress and stress history are needed.

Although phosphatic clays are flocculated and highly plastic and would, therefore, not be expected to be very sensitive nor to exhibit significant anisotropic behavior, the limited data available indicate that these clays may be susceptible to loss of strength upon disturbance or remolding (Bromwell and Radan, 1979), and that their stress-strain-strength characteristics may be affected by the direction of loading (anisotropic behavior).

Based on general observations reported by Ladd et al. (1977), the highly plastic phosphatic clays are expected to have a very low undrained shear modulus and exhibit highly time dependent stress-strain-strength behavior. Consequently, loads placed on reclaimed phosphatic clay deposits may undergo significant initial settlements (undrained shear deformations) and subsequent large undrained creep deformations.

One objective of this study, therefore, was to determine the range of stress-strain-strength behavior of phosphatic clays and sand-clay mixes, and establish correlations between index properties and strength parameters. The strength properties and behavior of interest include:

- The undrained shear strength, s_u, drained friction angle, $\bar{\Phi}_d$, and undrained Young's secant modulus, E_u. The strength parameters s_u and $\bar{\Phi}_d$ are necessary to determine the short-term and long-term bearing capacity and/or stability of constructed facilities placed on reclaimed phosphatic clays, respectively. The undrained modulus, E_u, is necessary to estimate the initial undrained settlement of loads placed on the surface of reclaimed phosphatic clay deposits.

- The effects of anisotropy. The effects of inherent and stress induced anisotropy on strength and undrained deformations can lead to changes in behavior during undrained shear depending on the direction of the major principal stress imposed by the applied loading along a failure surf ace. The resulting strengths may be less than determined from conventional tests, which can have important implications if low factors of safety are used. Special K_o-consolidated undrained triaxial compression and extension tests with pore pressure measurements

($\overline{CK_0UC}$ and $\overline{CK_0UE}$) and K_o-consolidated undrained direct-simple shear tests (CK_0UDSS) are generally performed to investigate the effect of varying stress systems on the shear strength behavior of clays.

- The effects of stress history. The effects of stress history on shear strength due to desiccation and/or pre-loading produce significant changes in strength behavior relative to the behavior of normally consolidated clays. Since reclaimed settling areas will likely always contain an upper overconsolidated "crust", the effect of stress history on strength is of interest.

- The effects of strain rate. The strength of highly plastic clays is generally very sensitive to time and creep effects (or strain rate effects). Hence, the highly plastic phosphatic clays are expected to be highly strain rate sensitive.

- The effect of sand-clay ratio. The effect of sand-clay ratio on stress-strain-strength behavior is important for evaluating the relative advantages or disadvantages of sand-clay mix disposal methods.

- The applicability of the Stress History and Normalized Soil Engineering Properties (SHANSEP) approach. Based on previous research on soft clays (see Ladd and Foott, 1974 and Ladd et al., 1977), it is expected that phosphatic clays and sand-clay mixes would exhibit "normalized behavior". Accordingly, the normally consolidated undrained shear strength and undrained Young's secant modulus should be related to the vertical effective consolidation stress, $\bar{\sigma}_{vc}$ (i.e., unique $s_u/\bar{\sigma}_{vc}$, $E_u/\bar{\sigma}_{vc}$ and E_u/s_u ratios). For overconsolidated clays the $s_u/\bar{\sigma}_{vc}$ and E_u/s_u ratios should also be uniquely related to the overconsolidation ratio.

Once strength parameters ($s_u/\bar{\sigma}_{vc}$, $\bar{\phi}$, E_u/s_u) are well defined for a wide range of phosphatic clays and sand-clay mixes, correlations can be established with index properties. Further, after establishing the basic normalized parameters, the task of predicting the strength in reclaimed phosphatic clay disposal facilities can be greatly simplified and the surcharge loads and degree of consolidation required to attain a desired strength can be determined. The normalized parameters can therefore be used to comprehensively evaluate phosphatic clay disposal and reclamation methods.

1.2 Previous Research

1.2.1 Undrained Shear Strength

A series of K_0-consolidated undrained direct simple shear tests (CK_0UDSS) were performed by Roma (1976) on a sample of phosphatic clay from the IMC-Noralyn mine. The clay had a plasticity index of 139% and a liquid limit of 190%, which are characteristic of an average plasticity phosphatic clay.* A total of four tests were performed, three on normally consolidated samples and one at an overconsolidation ratio, OCR, of 4.0.** The normally consolidated (NC) normalized undrained shear strength ratio from the CK_oUDSS tests, $s_u(DSS)/\bar{\sigma}_{vc}$, varied from 0.220 to 0.227 for the three tests with an average of 0.224. At an overconsolidation ratio of 4.0, $s_u(DSS)/\bar{\sigma}_{vc}$ equalled 0.656. Hence, over the overconsolidation ratio range of 1.0 to 4.0, $s_u(DSS)/\bar{\sigma}_{vc}$ increased according to the relationship $s_u(DSS)/\bar{\sigma}_{vc} = 0.224\,(OCR)^{0.78}$.

Figure 1-1 compares the normalized $s_u/\bar{\sigma}_{vc}$ versus OCR relationship from CK_oUDSS tests for the IMC-Noralyn phosphatic clay and six naturally occurring clays. As shown, the behavior of the highly plastic phosphatic clay is not significantly different from clays with substantially lower plasticity (i.e., plasticity indices of 20 to 75% in comparison to 139%).

The normalized undrained shear strength ratio, $s_u/\bar{\sigma}_c$, from isotropically consolidated triaxial compression undrained shear tests with pore pressure measurements ($\overline{CIU}C$) has been investigated for several phosphatic clays from five mine sites by Ardaman & Associates, Inc. in conjunction with site specific projects at the Occidental-Suwannee River, USSAC-Fort Meade, IMC-Kingsford and Brewster-Lonesome mines, and at an old mine pit near CF Chemicals-Bartow. The Occidental, USSAC, and "CF" phosphatic clays were obtained from undisturbed samples. The IMC and Brewster clays were re-sedimented in the laboratory. The $s_u/\bar{\sigma}_c$ ratios determined for the phosphatic clays with widely varying plasticity are tabulated below:

Phosphatic Clay	PI (%)	Measured $s_u/\bar{\sigma}_c$	Inferred $s_u/\bar{\sigma}_{vc}$
Occidental-Suwannee River	221	0.32-0.39	0.30-0.33
USSAC-Fort Meade	213	0.40	0.35
IMC-Kingsford	177	0.36	0.29
USSAC-Fort Meade	175	0.36	0.33
Brewster-Lonesome	171	0.30-0.37	0.27-0.31
USSAC-Fort Meade	155	0.36	0.30
IMC-Kingsford	152	0.32-0.37	0.29-0.32
Occidental-Suwannee River	140	0.39	0.35
Old Pit near CF Chemicals-Bartow	119	0.28	0.25
Old Pit near CF Chemicals-Bartow	94	0.29-0.32	0.28
Average		0.35	0.30
Range		0.28-0.40	0.25-0.35

*Refer to Volume 1, Section 2.5, for the plasticity characteristics of phosphatic clays. (All phosphatic clays are highly plastic CH clays.)

**Overconsolidation ratio, OCR, is defined as the ratio $\bar{\sigma}_{vm}/\bar{\sigma}_{vc}$, where $\bar{\sigma}_{vm}$ is the maximum past vertical effective consolidation stress and $\bar{\sigma}_{vc}$ is the vertical effective consolidation stress.

The undrained effective stress paths and relevant test data for 13 $\overline{\text{CIUC}}$ tests from the five sites are presented in Figure 1-2. As shown and tabulated above, the $s_u/\bar{\sigma}_c$ ratio varied widely from 0.28 to 0.40 with an average value of about 0.35. Further, there is no relationship between plasticity and $s_u/\bar{\sigma}_c$ for the phosphatic clays. The $s_u/\bar{\sigma}_c$ values are somewhat higher than typically expected for highly plastic clays, but agree with $s_u/\bar{\sigma}_c$ values measured on clays of much lower plasticity.

The undrained shear strength ratio normalized with respect to the one-dimensional vertical effective consolidation stress, $\bar{\sigma}_{vc}$, rather than the isotropic stress, $\bar{\sigma}_c$ may be backfigured from CIUC tests by assuming that the phosphatic clays exhibit strength principles in accordance with the "simple clay model" (Ladd, 1964). In accordance with this principle and arbitrarily assuming a coefficient of earth pressure at rest, K_o, of 0.60, $s_u/\bar{\sigma}_{vc}$ may be determined from the effective stress paths presented in Figure 1-2. The resulting inferred values of $s_u/\bar{\sigma}_{vc}$ are tabulated above adjacent to the $s_u/\bar{\sigma}_c$ values. As shown, the scatter in $s_u/\bar{\sigma}_{vc}$ is generally less than observed for $s_u/\bar{\sigma}_c$. The phosphatic clays exhibited an $s_u/\bar{\sigma}_{vc}$ ratio in triaxial compression on the order of 0.30 essentially independent of plasticity, which implies that phosphatic clays will likely exhibit essentially the same undrained shear strength at the same effective stress. On the other hand, $s_u(\overline{\text{CIUC}})/\bar{\sigma}_{vc}$ was found to be 34% higher than $s_u(\text{CK}_o\text{UDSS})/\bar{\sigma}_{vc}$ as determined by Roma (1976), and hence, phosphatic clays may be more susceptible to anisotropic effects than inferred from their high plasticity.

1.2.2 Undrained Modulus

Values of normalized undrained Young's secant modulus, E_u/s_u, versus the applied shear stress level, τ_h/s_u, from CK_oUDSS tests on normally consolidated naturally occurring clays are shown in Figure 1-3 (Ladd et al., 1977). Although the trends are similar regarding the variation in modulus with stress level during undrained shear, E_u/s_u generally decreases substantially with increasing plasticity and organic content of the soil. Values of E_u/s_u reported by Roma (1976) for the IMC-Noralyn phosphatic clay are also shown on Figure 1-3. The reported values are considerably higher than expected for a clay with such a high plasticity and agree with E_u/s_u values for clays with lower plasticity indices of 40 to 75%.

The normalized undrained Young's secant modulus versus stress level from $\overline{\text{CIUC}}$ tests for the five normally consolidated phosphatic clays listed in Figure 1-2 are summarized in Figure 1-4. At a high stress level of 80%, the value of E_u/s_u, generally varies from 50 to 120 for the five normally consolidated phosphatic clays regardless of the plasticity of the clay. E_u/s_u increases with decreasing stress level to values of 300 to 1000 at a stress level of 20%. These values are in general agreement with E_u/s_u ratios from CK_oUDSS tests reported by Roma (1976) and also indicate that E_u/s_u values for phosphatic clays are higher than expected for clays of such high plasticity.

1.2.3 Angle of Internal Friction

As shown in Figure 1-2, the angle of internal friction or effective friction angle, $\bar{\phi}$, measured in $\overline{\text{CIUC}}$ tests generally ranges from 26° to 33° with a representative value at maximum obliquity of 30 . This friction angle is substantially higher than expected for the highly plastic phosphatic clays. The angle of internal friction applicable for drained conditions, $\bar{\phi}_d$, is generally lower than $\bar{\phi}_u$ determined from undrained tests at maximum obliquity.

1.3 Purpose of Investigation

Available strength data for phosphatic clays, although limited, clearly indicate that the behavior of phosphatic clays is often not consistent with the behavior expected from established correlations with plasticity on naturally occurring clays. Additionally, there are no comprehensive data reported on the strength behavior of sand-clay mixes. Accordingly, as part of research project FIPR 80-02-002 "Evaluation of Phosphatic Clay Disposal and Reclamation Methods" performed for the Florida Institute of Phosphate Research, twelve phosphatic clays, sampled from various mine sites, were investigated via laboratory vane, viscometer determinations, and $\overline{\text{CIUC}}$ and $\overline{\text{CK}_0\text{U}}$ strength tests to determine the range of stress-strain-strength behavior of Florida phosphatic clays. Strength tests were also performed on sand-clay mixes from three selected phosphatic clays with widely varying plasticity. The mine sites were selected to provide a range of geographic locations and mining concerns. The locations of the mine sites are illustrated in Figure 1-5 and the specific settling areas sampled and sampling dates are summarized in Table 1-1.

One purpose of performing the strength tests for the present investigation was to establish the range in stress-strain-strength behavior of phosphatic clays and sand-clay mixes and to determine the applicability of the Stress History and Normalized Soil Engineering Properties (SHANSEP) design methodology for phosphatic clays and sand-clay mixes. Once the strength characteristics of the phosphatic clays are fully established, the study would achieve the following additional purposes:

- Allow the determination of the shear strength of phosphatic clays and sand-clay mixes at low effective stresses to enable evaluation of the impact of an accidental spill from the disposal system.

- The use of normalized shear strength properties provide an estimate of the strength of a clay or sand-clay mix from a given mine as a function of consolidation stress and stress history. These data allow determination of the surcharge load, degree of consolidation and/or degree of desiccation required to achieve a given strength to support the required loads. They are also valuable for determining the earliest time that a surcharge, such as tailings sand, can be applied without generating extensive "mud-waving".

- The normalized shear strength properties of sand-clay mixes will allow determination of whether this disposal method results in poor, marginal or good foundation conditions relative to phosphatic clay without sand. This is important to evaluate the relative merits of the sand-clay mix disposal method versus conventional disposal techniques.

- The normalized undrained modulus of phosphatic clays and sand-clay mixes will permit assessment of undrained deformations caused by application of loads on reclaimed disposal areas.

1.4 Scope of Investigation

The scope of the investigation included determining the strength behavior of six of the twelve phosphatic clays sampled as part of this project. The six clays were selected to represent a range in properties of phosphatic clays based on index tests (Volume 1), mineralogy (Volume 2), and settling tests (Volume 3). The strength characteristics of sand-clay mixes were investigated for three of the six clays. The specific tests performed are summarized in Figure 1-6.

The strength characteristics of normally consolidated phosphatic clays determined from laboratory vane, viscometer, $\overline{CIUC}$ and $\overline{CK_oU}$ tests are first reported in Section 2. Test procedures and methodologies are also detailed in Section 2. The effects of stress history on phosphatic clay strength behavior are presented in Section 3. Section 4 discusses the strength characteristics of sand-clay mixes. Recommended properties for use in design and prediction are presented in each section.

Table 1-1

MINE SITES AND SETTLING AREAS SELECTED FOR PHOSPHATIC CLAY LABORATORY INVESTIGATIONS

Mine	Settling Area	Sampling Date
Agrico-Saddle Creek	Settling Area-2	1-28-81
AMAX-Big Four	Settling Area BF-1	6-05-81
Beker-Wingate Creek	Pilot Plant Samples	6-05-81
Brewster-Haynsworth	Settling Area-L	1-27-81
CF Mining-Hardee	Settling Area N-1	1-28-81
Estech-Watson	Settling Area 13	4-10-81
Hopewell-Hillsborough	Pilot Plant Samples	3-04-81
IMC-Noralyn	Settling Area N-14	2-23-81
Mobil-Nichols	Settling Area N-3	1-28-81
Occidental-Suwannee River	Settling Area-8	2-02-81
USSAC-Rockland	Settling Area-6	1-28-81
WR Grace-Four Corners	Pilot Plant Samples	9-11-81

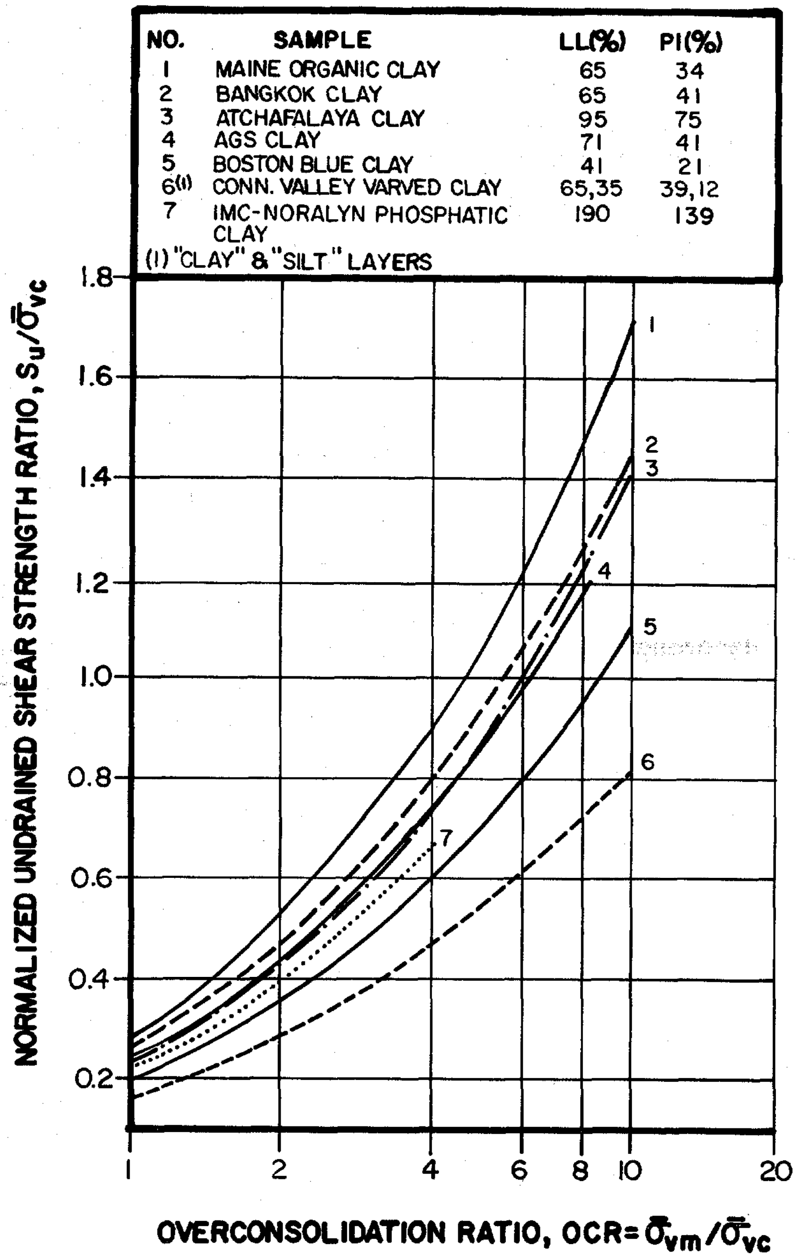

SOURCE: ADAPTED FROM ROMA, J.R. (1976). "GEOTECHNICAL PROPERTIES OF PHOSPHATIC CLAYS," M.S. THESIS, DEPARTMENT OF CIVIL ENGINEERING, M.I.T. CAMBRIDGE, MASSACHUSETTS.

OVERCONSOLIDATION RATIO VS. NORMALIZED UNDRAINED SHEAR STRENGTH RATIO FROM CK_oUDSS TESTS ON SEVERAL CLAYS

FIGURE 1-1

SYMBOL	PHOSPHATIC CLAY	LL (%)	PI (%)	INITIAL ω_n (%)	INITIAL γ_t (pcf)	PRE-SHEAR ω_n (%)	PRE-SHEAR γ_t (pcf)	$S_u/\bar{\sigma}_c$	At $(\bar{\sigma}_1 - \bar{\sigma}_3)_{max}$ ξ (%)	At $(\bar{\sigma}_1 - \bar{\sigma}_3)_{max}$ $\bar{\phi}$	At $(\bar{\sigma}_1 - \bar{\sigma}_3)_{max}$ A FACTOR	At $(\bar{\sigma}_1 / \bar{\sigma}_3)_{max}$ ξ (%)	At $(\bar{\sigma}_1 / \bar{\sigma}_3)_{max}$ $\bar{\phi}$	At $(\bar{\sigma}_1 / \bar{\sigma}_3)_{max}$ A FACTOR
●	BREWSTER-LONESOME	216	171	195.1 123.7	78.0 86.7	96.1 110.3	92.0 89.1	0.30 0.37	8.1 6.8	25.6° 30.5°	0.97 0.88	8.1 10.0	25.6° 32.0°	0.97 0.97
⊙	OLD PIT NEAR CF CHEMICALS-BARTOW	119 119 143	94 94 119	80.9 39.7 83.8	96.8 91.0 82.3	61.5 22.8 74.6	103.0 129.9 98.2	0.29 0.32 0.28	6.9 7.5 5.8	27.0° 25.8° 22.5°	1.11 - 1.00	9.5 10.1 8.6	27.8° 26.8° 23.7°	1.18 - 1.10
⊡	IMC-KINGSFORD	202 202 209	152 152 177	178.0 180.4 240.6	79.0 86.0 75.2	120.3 104.0 145.5	88.0 91.3 84.5	0.32 0.37 0.36	9.8 9.2 7.6	30.8° 31.4° 32.1°	1.04 0.89 0.96	12.2 10.5 9.6	31.5° 31.6° 32.4°	1.11 0.94 1.04
▲	USSAC-FORT MEADE	263 224 179	213 175 155	125.8 172.0 128.9	85.0 83.1 -	111.0 118.4 103.2	89.4 87.0 -	0.40 0.36 0.36	6.8 8.7 7.8	34.9° 32.7° 31.5°	0.88 0.99 -	6.8 10.4 14.6	34.9° 33.2° 32.3°	0.88 1.01 -
△	OCCIDENTAL-SUWANNEE RIVER	171 264 264	140 221 221	130.6 158.8 69.8	- - -	86.6 103.2 38.6	- - -	0.39 0.32 0.39	10.2 10.0 7.9	37.70 34.3° 33.6°	- - -	12.4 12.3 9.5	38.4° 35.2° 34.2°	- - -

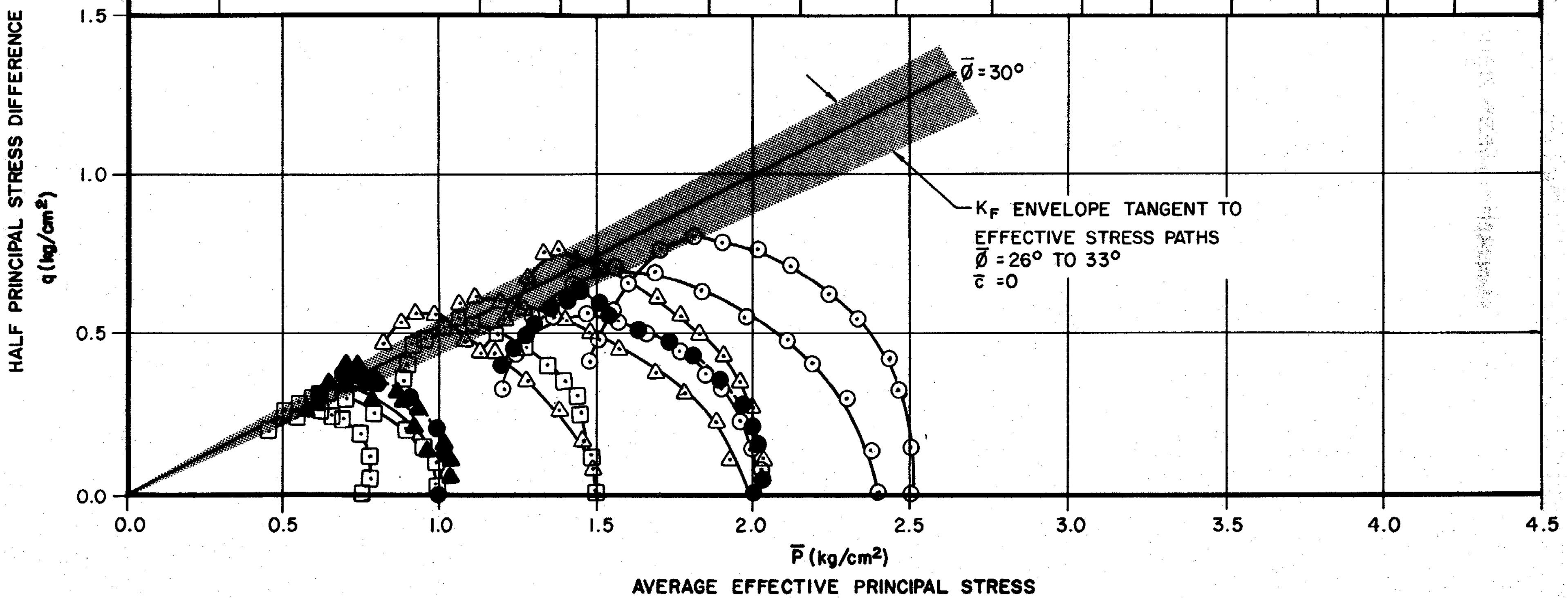

FIGURE 1-2

UNDRAINED EFFECTIVE STRESS PATHS FROM $\overline{\text{CIUC}}$ TESTS ON NORMALLY CONSOLIDATED PHOSPHATIC CLAYS FROM FIVE SITES

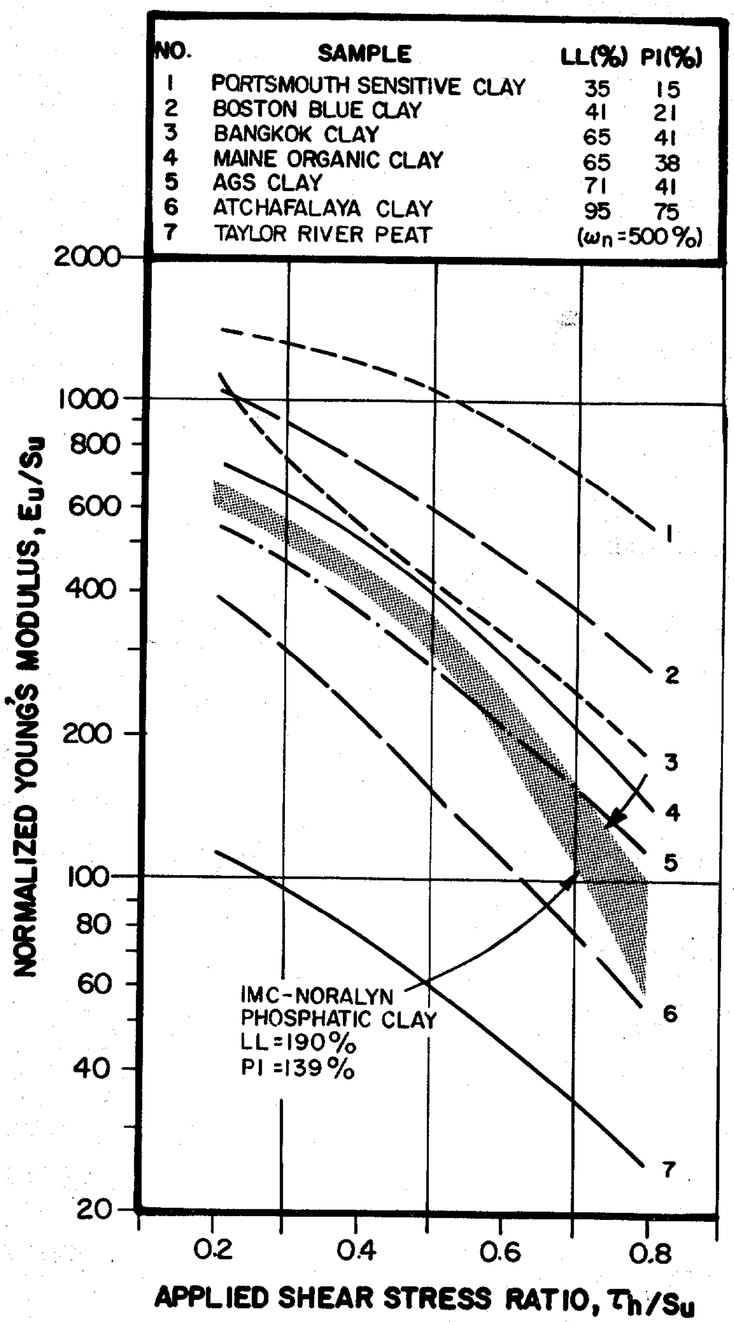

SOURCE: ADAPTED FROM ROMA, J.R. (1976). "GEOTECHNICAL PROPERTIES OF PHOSPHATIC CLAYS," M.S. THESIS, DEPARTMENT OF CIVIL ENGINEERING, M.I.T. CAMBRIDGE, MASSACHUSETTS.

NORMALIZED UNDRAINED YOUNG'S SECANT MODULUS VS. STRESS RATIO FROM CK_oUDSS TESTS ON SEVERAL NORMALLY CONSOLIDATED CLAYS

FIGURE 1-3

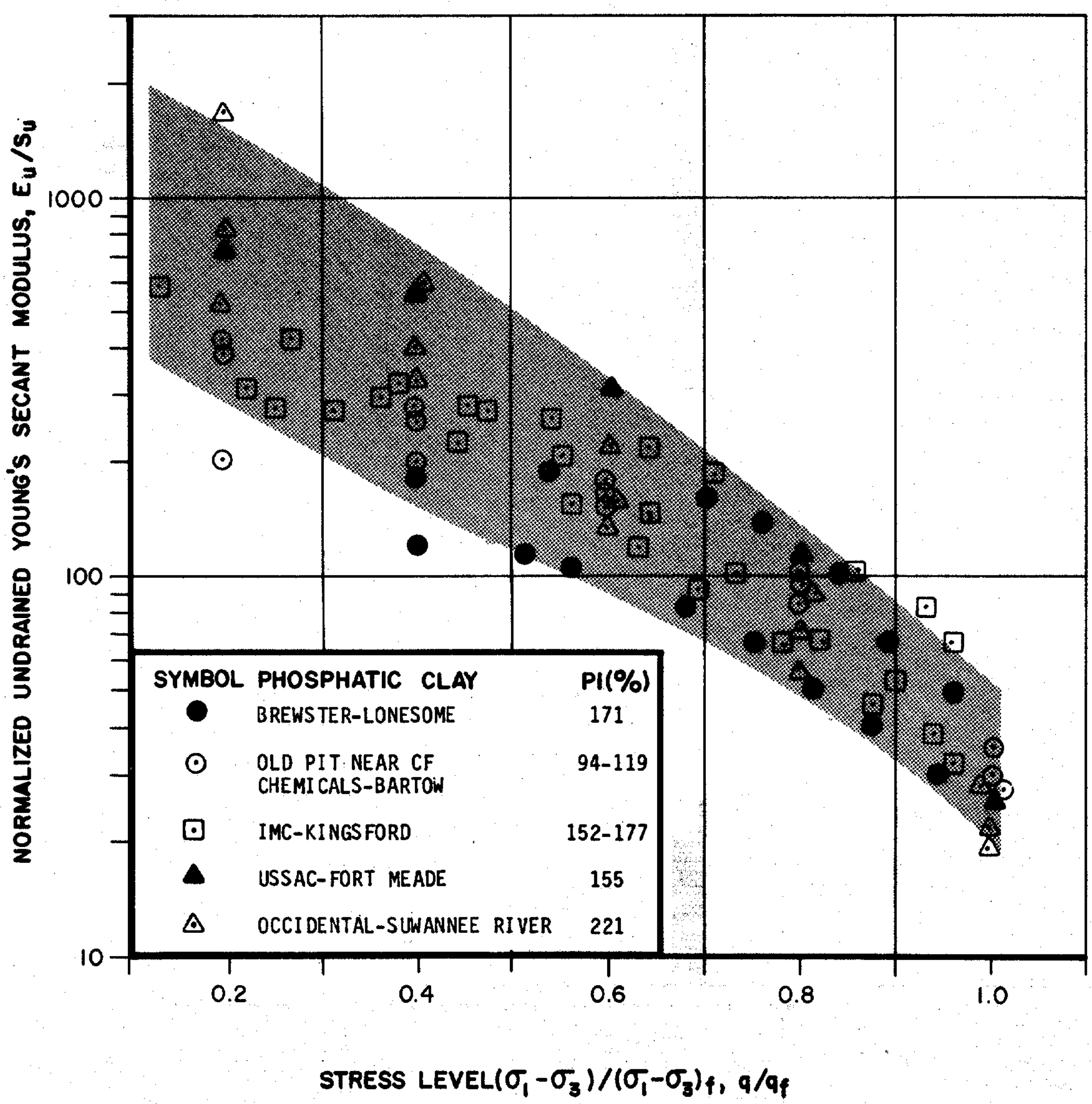

NORMALIZED UNDRAINED YOUNG'S SECANT MODULUS VERSUS STRESS LEVEL FROM $\overline{\text{CIU}}$C TESTS ON NORMALLY CONSOLIDATED PHOSPHATIC CLAYS FROM FIVE SITES

FIGURE 1-4

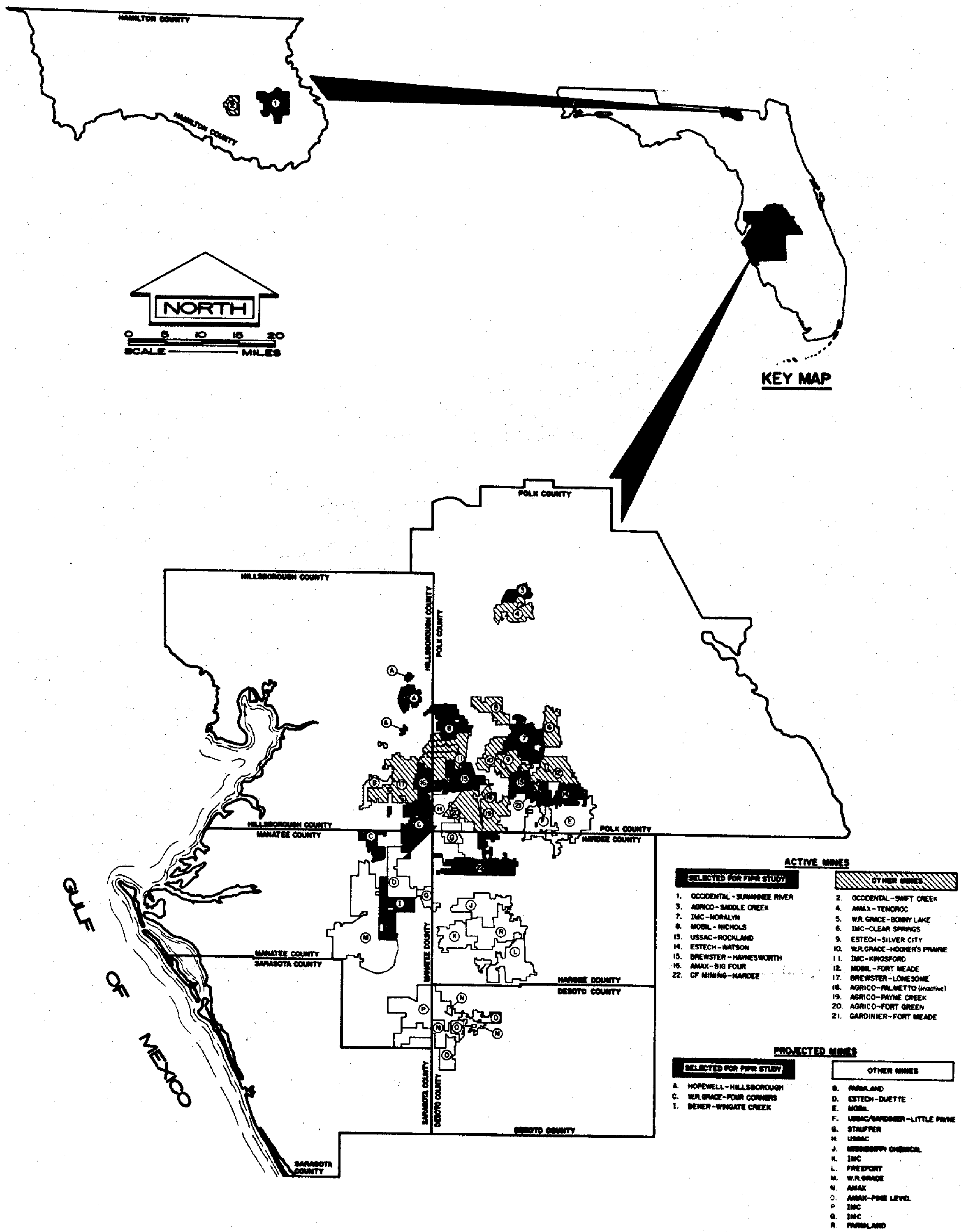

MINE SITES SELECTED FOR INVESTIGATION

FIGURE 1-5

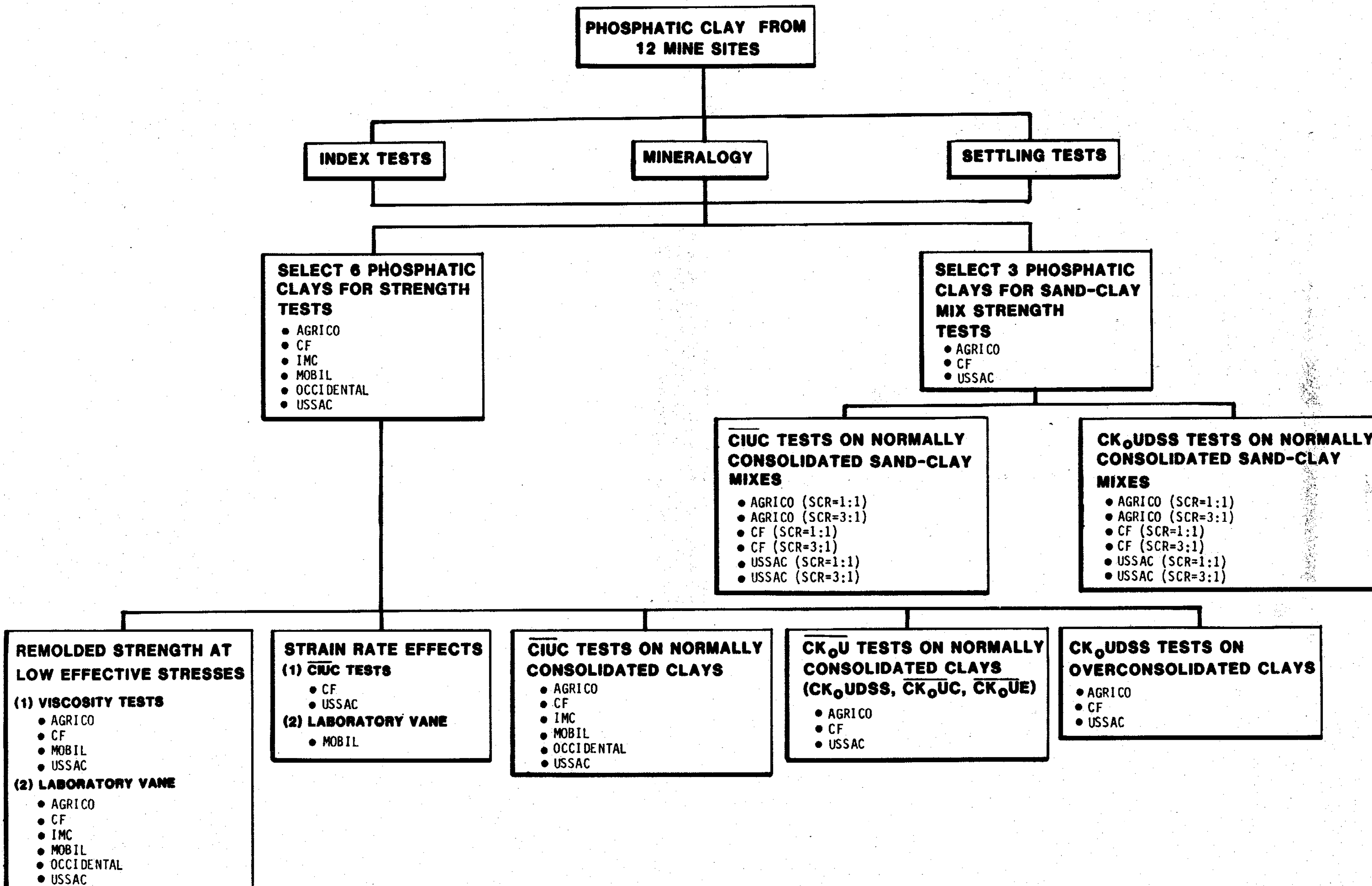

FIGURE 1-6

EXPERIMENTAL SCHEME FOR EVALUATION OF STRENGTH BEHAVIOR

Section 2

STRESS-STRAIN-STRENGTH PROPERTIES OF NORMALLY CONSOLIDATED PHOSPHATIC CLAYS

2.1 Remolded Undrained Shear Strength at Low Effective Stresses

As clay slurry is discharged into a settling area, the phosphatic clay gradually transitions from a viscous fluid to a soil with particle to particle contact characterized by a shear strength which is a function of the effective consolidation stress.

The remolded shear strength of phosphatic clays is a measure of the shear strength of the clay upon disturbance or after extensive straining. Sensitive clays generally exhibit a substantial reduction in shear strength with remolding due to alterations to the particle arrangement and structure of the clay matrix. (Sensitivity is defined as the ratio of undisturbed to remolded strength.) Because of their high plasticity, however, phosphatic clays are not anticipated to be very sensitive.

The remolded undrained shear strength of phosphatic clays at low effective stresses is of interest in determining the extent of phosphatic clay flow and flood-plain coverage that may result from accidental spills or an embankment failure. It is also relevant in assessing the stability of an embankment or other constructed facility erected on phosphatic clay wherein the clay is disturbed via displacement and/or re-worked to promote displacement prior to or during construction.

2.1.1 Undrained Strength from Viscosity Tests

Viscosity determinations were made on five phosphatic clays at varying solids contents using a Brookfield viscosimeter. The test method and results were detailed in Volume 1 “Index Properties of Phosphatic Clays”, Section 4. The yield stress, τ_y, determined for the Bingham plastic model can be considered equivalent to the remolded undrained shear strength, s_u, at very low effective stresses. The results for five phosphatic clays are reproduced in Figure 2-1 (Figure 4-12 of Volume 1).

As shown in Figure 2-1, a correlation between moisture content and undrained shear strength at very high moisture contents was found. In developing this correlation, the shear strength at the liquid limit was assumed equal to 25 g/cm^2 as recommended by Casagrande (1932). The remolded undrained shear strength was found to: (i) increase with decreasing moisture content, (increasing solids content); and (ii) increase with increasing liquid limit at a given moisture content, in accordance with the equation:

$$\tau_y = 10^{\{10.34-5.21 \log(w) + 0.014(LL)\}} \qquad (1)$$

where τ_y is the yield stress or remolded undrained shear strength in g/cm^2; w is the water content expressed as a percentage; and LL is the liquid limit expressed as a percentage. The correlation coefficient, r, of 0.933 indicates that 87% of the variability in shear strength is accounted for by changes in the moisture content and liquid limit.

The liquidity index, LI, relates the moisture content of a clay to its Atterberg limits by the expression:

$$LI = (w - PL)/PI \tag{2}$$

where PL is the plastic limit and PI the plasticity index. Liquidity indices of 1.0 and 0.0 imply that the moisture content is at the liquid and plastic limits, respectively. A correlation between liquidity index and remolded shear strength was developed and is reproduced in Figure 2-2 (Figure 4-13 of Volume 1). The correlation is in the form:

$$\tau_y = 10^{\{-3.382 + (4.792/LI)\}} \tag{3}$$

where τ_y is expressed in units of g/cm^2. This unique correlation for phosphatic clays physically indicates that the remolded shear strength increases with decreasing liquidity index, i.e., with decreasing water content and/or increasing plasticity. The correlation coefficient of 0.974 implies that the variability in liquidity index explains 95% of the variability in remolded undrained shear strength. The relationship is applicable for liquidity indices in excess of 3.

2.1.2 Undrained Strength from Laboratory Vane Tests

A series of laboratory vane (LV) shear tests were performed on six phosphatic clays remolded to varying solids contents. Three different four-bladed vanes having a height to diameter ratio of about 1.33 were used in this investigation, with diameters ranging from 0.5 inches to 1.5 inches. As illustrated in Figure 2-3, the shear strength, s_u(LV), of the highly plastic phosphatic Clays can be sensitive to strain rate, $\dot{\gamma}$, effects. The effect of strain rate, however, is insignificant at rates of rotation less than about 15°/minute. Accordingly, all determinations reported below are based on tests performed at a rate of rotation of 8°/minute (about 0.1°/second).

Results of laboratory vane tests are summarized in Figure 2-4. As shown, the remolded undrained shear strength, s_u(LV), increases with increased solids content (or reduced water content). Moreover, at the same solids content, the higher plasticity clay (e.g., Agrico-Saddle Creek) exhibits a higher remolded vane undrained shear strength than lower plasticity clays (e.g., CF Mining-Hardee). Results of semi-log linear regressions performed on the data in Figure 2-4 for each phosphatic clay are presented in Figure 2-5. The regression analyses indicate the validity of a relationship of the form:

$$s_u(LV) = 10^{(\lambda + \psi S)} \tag{4}$$

where: $\lambda = -3.165 + 0.0085\ (PI)$
$\psi = 0.097$

and where: $s_u(LV)$ is the remolded laboratory vane undrained shear strength expressed in units of lb/ft^2; S is the solids content expressed as a percentage; and PI is the plasticity index expressed as a percentage.

When the water content of the clay is normalized with respect to the liquidity index, LI, the following unique correlation between s (LV) and LI (illustrated in Figure 2-6) is found applicable for phosphatic clays with varying characteristics:

$$s_u(LV) = 29.31\ (LI)^{-3.634} \tag{5}$$

where $s_u(LV)$ is expressed in units of lb/ft^2. The correlation coefficient of 0.98 for the log-log linear regression indicates that the variability in liquidity index explains 96% of the variability in remolded undrained shear strength.

The remolded undrained shear strength of the highly plastic phosphatic clays is compared to that of relatively lower plasticity naturally occurring clays with plasticity indices of 14 to 65% in Figure 2-7. As shown, the relationship between liquidity index and remolded undrained shear strength for the phosphatic clays is consistent with that for other clays at liquidity indices in excess of 0.9. At lower liquidity indices, the phosphatic clays seem to exhibit a higher remolded shear strength inferring that the highly plastic phosphatic clays are not as sensitive as other naturally occurring clays at increased solids contents.

The vertical effective consolidation stress, $\bar{\sigma}_{vc}$, corresponding to the solids content at which laboratory vane tests were performed was determined from compressibility relationships presented in Volume 4, "Consolidation Behavior of Phosphatic Clays". Figure 2-8 presents a plot of the remolded undrained shear strength, $s_u(LV)$, versus the effective consolidation stress. As shown, at the same vertical effective consolidation stress, the lower plasticity CF Mining-Hardee clay apparently exhibits a higher remolded shear strength than higher plasticity clays, whereas, as previously shown- in Figure 2-4, a reverse trend prevails when the remolded shear strength is compared at the same solids content. The remolded normalized undrained shear strength ratios, $s_u(LV)/\bar{\sigma}_{vc}$, for each phosphatic clay are compared in Figure 2-9. The data indicate that:

- At liquidity indices in excess of about 1.0, the phosphatic clays are apparently sensitive with remolded $s_u(LV)/\bar{\sigma}_{vc}$ ratios ranging from about 0.16 for the CF Mining-Hardee clay to 6.06 for the Agrico-Saddle Creek clay. The phosphatic clays appear to be less sensitive at lower liquidity indices as evidenced by an increase in $s_u(LV)/\bar{\sigma}_{vc}$ ratios.
- Assuming that the normally consolidated undisturbed $s_u/\bar{\sigma}_{vc}$ ratio does not vary significantly between phosphatic clays (as will be demonstrated in subsequent sections), the lower plasticity CF Mining-Hardee clay is apparently less sensitive than the higher plasticity Agrico-Saddle Creek clay! This is evident by comparing the remolded $s_u(LV)/\bar{\sigma}_{vc}$ ratio for both clays. Other phosphatic clays exhibit a remolded $s_u(LV)/\bar{\sigma}_{vc}$ ratio between the two extremes.

The remolded undrained shear strengths from viscosity tests and laboratory vane tests are compared and plotted versus liquidity index in Figure 2-10. A least squares log-log linear regression on the combined data reveals a correlation of the form:

$$s_u(\text{remolded}) = 32.91\ (LI)^{-4.332} \qquad (6)$$

where s_u is expressed in units of lb/ft^2. The correlation exhibits a correlation coefficient of 0.979 and is applicable to liquidity indices ranging from about 0.6 to more than 10.

2.2 Undrained Properties of Normally Consolidated Phosphatic Clays from $\overline{CIU}C$ Tests

2.2.1 Test Methods and Test Procedures

Twenty-six isotropically consolidated triaxial compression undrained shear tests with pore pressure measurement ($\overline{CIU}C$ tests) were performed on six selected phosphatic clay samples obtained from different mine sites. The shear tests were strain controlled and the rate of strain was slow enough to allow for pore pressure equilization during undrained shear.

Test specimens were trimmed from larger block samples pre-consolidated under one-dimensional Ko-conditions from a slurry to effective vertical consolidation stresses of 0.3 to 0.5 kg/cm^2. K_o-consolidation was performed in the laboratory on a sedimented slurry using one load increment applied in large consolidometers to produce samples that permit handling and trimming. The consolidometer used produced block samples 25.7 cm in diameter with heights generally ranging from 10 to 15 cm. Triaxial test specimens were trimmed from these larger samples to standard triaxial dimensions of 8.0 cm in height and approximately 3.6 cm in diameter.

$\overline{CIU}C$ tests were conducted according to the procedures described in Bishop and Henkel (1962). After trimming test specimens, the samples were placed on the triaxial cell pedestal, vertical filter strips were installed and the specimen enclosed in prophylactic membranes applied to the exterior surfaces. After filling the triaxial cell with de-aired water, a backpressure of several kg/em was applied to saturate the sample. The test specimen was then isotropically consolidated in increments to an effective consolidation pressure, $\bar{\sigma}_c$, generally ranging from 1.0 to 2.0 kg/cm^2. The drainage valve was then closed and the pore pressure response measured. A B-factor of 100% indicated that the samples were saturated. During shear, pore pressures were measured with a rigid, flush-diagram pressure transducer. The signals from the transducers, load cell, and DCDT strain gauge were monitored with a digital voltmeter and recorded electronically on magnetic tape with a data acquisition system for subsequent processing.

Three to six CIUC tests were performed at varying consolidation pressure, $\bar{\sigma}_c$, on each of six phosphatic clays. The isotropic pre-shear effective consolidation pressure generally ranged from 1.0 to 2.0 kg/cm^2. Hence, the samples were consolidated prior to shear to effective stresses 2 to 4 times the maximum vertical effective stress used during sample preparation. All test samples were, therefore, normally consolidated. Various isotropic consolidation stresses, $\bar{\sigma}_c$, were used to confirm that the phosphatic clays exhibit normalized behavior and to determine the applicability of the Normalized Soil Parameter (NSP) concept to phosphatic clays (see Ladd and Foott, 1974). A clay exhibiting normalized behavior will yield values of normalized undrained shear strength, $s_u/\bar{\sigma}_c$, and normalized modulus, $E_u/\bar{\sigma}_c$ or E_u/s_u, that are constant for samples consolidated to differing effective stresses in excess of the maximum past pressure.

2.2.2 Stress-Strain Behavior

The undrained stress-strain-strength behavior of phosphatic clays from $\overline{\text{CIU}}\text{C}$ tests is presented in appropriate figures in Appendix A for the Agrico-Saddle Creek, CF Mining-Hardee, IMC-Noralyn, Mobil-Nichols, Occidental-Suwannee River and USSAC-Rockland phosphatic clay samples. Representative effective stress paths and stress-strain behavior from typical tests are summarized in this section along with relevant findings.

Stress path and normalized stress strain data from 10 tests (that are best representative of the 26 tests performed) are plotted in Figures 2-11 and 2-12, respectively. These results are for specimens sheared at an axial (vertical compression) strain rate, $\dot{\varepsilon}_v$, of 1%/hour. As shown in Figure 2-11, the stress paths for all phosphatic clays are similar exhibiting a pore pressure A-factor at "failure", i.e., at maximum principal stress difference $(\sigma_1-\sigma_3)\text{max}$, of about 1.0 with the more plastic Agrico-Saddle Creek clay exhibiting an A-factor on the order of 1.2. The stress paths are typical of those characteristic of normally consolidated soft clays.

The effective stress paths in Figure 2-11 and the stress-strain and pore pressure behavior depicted in Figure 2-12 support the applicability of the normalized soil parameter (NSP) concept to phosphatic clays. The maximum stress difference generally occurred at failure strains ranging from about 7% to 12%. Strain softening effects are not significant at large strains as depicted in Figure 2-12. Moreover, the undrained behavior of the highly plastic phosphatic clays is similar within the wide range of clay plasticity investigated.

2.2.3 Strain Rate Effect

In addition to $\overline{\text{CIU}}\text{C}$ tests performed at a strain rate $\dot{\varepsilon}_v$ of 1%/hour, tests were performed on the USSAC-Rockland and CF Mining-Hardee clays at strain rates of 0.36%/hour and 5.1%/hour to investigate the effect of strain rate on the undrained shear strength. (Test results are detailed in Appendix A: samples labeled S1 through S9 were sheared at 1%/hour; samples labeled S were sheared at 0.36%/hour; and samples labeled F were sheared at 5.1%/hour.) The effect of strain rate on the undrained shear strength ratio, $s_u/\bar{\sigma}_c$, is illustrated in Figure 2-13 based on test results performed on phosphatic clay and other highly plastic clays. As shown, increasing the strain rate beyond 1%/hour can cause a significant increase in undrained strength. Accordingly, all triaxial tests used in our evaluation were performed at strain rates of 1%/hour or less.

2.2.4 Undrained Shear Strength

The normalized undrained shear strength ratio, $s_u/\bar{\sigma}_c$, of phosphatic clays averaged about 0.33* with little variability with plasticity, except for the very highly plastic Agrico-Saddle Creek clay which exhibited a lower $s_u/\bar{\sigma}_c$ ratio (on the order of 0.28) as illustrated in Figure 2-14, primarily due to a higher A-factor at failure.** (The undrained shear strength, s_u, is defined herein as half the maximum principal stress difference, q, at failure; i.e., $s_u = q_f = 0.5(\sigma_1-\sigma_3)_{max}$; $\bar{\sigma}_c$ is the isotropic pre-shear effective consolidation stress.)

The undrained shear strength ratio normalized with respect to the one-dimensional vertical effective consolidation stress, $\bar{\sigma}_{vc}$, rather than the isotropic stress, $\bar{\sigma}_c$, may be backfigured from $\overline{\text{CIU}}$C tests by assuming that phosphatic clays exhibit basic strength principles in accordance with Ladd's "simple clay model" (Ladd, 1964). In accordance with this hypothesis and by arbitrarily assuming a coefficient of earth pressure at rest $K_o = 0.6^{\dagger}$, $s_u/\bar{\sigma}_{vc}$ may be directly determined from the effective stress paths presented in Appendix A. The resulting average values of $s_u/\bar{\sigma}_{vc}$ and the range measured for each phosphatic clay are presented in the lower graph of Figure 2-14. As shown, the scatter in the resulting $s_u/\bar{\sigma}_{vc}$ values is less than that observed for $s_u/\bar{\sigma}_c$. Phosphatic clays generally exhibit an $s_u/\bar{\sigma}_{vc}$ ratio in triaxial compression of 0.28 ± 0.02 irrespective of plasticity. (For comparison, $s_u/\bar{\sigma}_{vc}$ values from $\overline{\text{CK}_o\text{U}}$C tests - see Section 2.3 - are also plotted in Figure 2-14.) In summary, the following normalized undrained shear strength ratios are believed representative of phosphatic clays based on $\overline{\text{CIU}}$C test data:

Phosphatic Clay	PI (%)	$s_u/\bar{\sigma}_c$	$s_u/\bar{\sigma}_{vc}$
Agrico-Saddle Creek	222	0.28	0.26
IMC-Noralyn	181	0.33	0.28
Mobil-Nichols	164	0.34	0.29
USSAC-Rockland	160	0.30	0.28
Occidental-Suwannee River	142	0.33	0.30
CF Mining-Hardee	113	0.33	0.29

These values are generally consistent with those determined on 10 other phosphatic clays of varying plasticity with plasticity indices ranging from 94% to 221% (see Section 1.2.1). Since $s_u/\bar{\sigma}_{vc}$ is similar for all phosphatic clays tested, a gross average value $s_u/\bar{\sigma}_{vc} = 0.28$ may be used for other phosphatic clays in the

---

*Values of $s_u/\bar{\sigma}_c$ as high as 0.4 have been reported by other investigators. Such high values are not believed characteristic of the highly plastic phosphatic clays.

**Other high plasticity phosphatic clays (PI = 175 to 221%) do not reflect lower $s_u/\bar{\sigma}_c$ values as observed for the Agrico-Saddle Creek clay (see data in Section 1.2.1).

†See Section 2.3.3

absence of laboratory test data. This value is characteristic of the shear strength in compression, s (V), when the clay is sheared with the major principal stress in the vertical direction. The normalized. undrained shear strength ratio of 0.28 is slightly higher than expected for the highly plastic phosphatic clays.

2.2.5 Undrained Modulus

The undrained modulus governs the magnitude of undrained deformations resulting from loading a phosphatic clay deposit. Values of Young's secant undrained modulus, E_u, are highly dependent on stress level.

Values of E_u/s_u (normalized secant modulus with respect to the undrained shear strength) from CIUC tests are presented in Figure 2-15 as a function of stress level q/q_f (where q is the maximum shear stress for a particular loading, or half the principal stress difference; and q_f is the value of q at maximum stress difference $(\sigma_1-\sigma_3)_{max}$, i.e., at failure). As shown in Figure 2-15, the undrained modulus decreases substantially with increased stress level. Moreover, the higher plasticity phosphatic clays seem to exhibit a higher E_u/s_u than lower plasticity clays which was not expected! At a stress level of 50%, all phosphatic clays exhibit an undrained modulus higher than one would expect for such plastic materials. For the high plasticity Agrico-Saddle Creek clay, E_u/s_u decreases from about 2000 at a stress level of 20% to about 150 at a stress level of 80%. The relatively "low" plasticity CF Mining-Hardee clay E_u/s_u ratio decreases from about 400 to 80 as the stress level increases from 20 to 80% of the undrained shear strength. Corresponding E_u/s_u values for the USSAC-Rockland clay (PI = 160%) of 600 and 90, respectively, are probably representative of a wide range of phosphatic clays. The trends, magnitudes and variability in E /s are also consistent with data obtained on other phosphatic clays (see Figure 1-4). Note that the undrained modulus can also be highly dependent on the type of shear test or stress system.

2.2.6 Angle of Internal Friction

The effective angle of internal friction, $\bar{\phi}$, is required for evaluating the drained class of stability problems which are performed to assess long-term stability when consolidation due to loading (or unloading) of a clay deposit has been completed. This class of stability problems can be important but, in conjunction with construction on a soft phosphatic clay deposit where the undrained case governs, the angle of internal friction is generally not as important as the undrained shear strength.

The effective angle of internal friction, $\bar{\phi}$, was determined from $\overline{\text{CIU}}\text{C}$ tests on six phosphatic clays at maximum obliquity, maximum stress difference, and tangency to the effective stress paths (see Appendix A). Figure 2-11 illustrated the typical range in Mohr-Coulomb failure envelopes for normally consolidated phosphatic clays which are characterized by zero effective cohesion ($\bar{c}$ = 0) and an angle of internal friction from undrained tests, $\bar{\phi}_u$, generally ranging from 28° to 35° and averaging about 30°. Figure 2-16 presents the average values and ranges in $\bar{\phi}_u$ from $\overline{\text{CIU}}\text{C}$ tests on the six phosphatic clays. (For comparison, $\bar{\phi}_u$ values from $\overline{\text{CK}_o\text{U}}\text{C}$ tests - see Section 2.3 - are also plotted on Figure 2-16).

Although there is some variability in the test data, there is no consistent trend with plasticity. A gross average $\bar{\phi}_u$ value at maximum obliquity on the order of 30° is representative of the angle of friction from $\overline{\text{CIU}}\text{C}$ tests on a wide range of phosphatic clays.* A somewhat lower value of 28° is arbitrarily selected as applicable at maximum stress difference.

Ladd (1971) concluded that, for normally consolidated clays, the angle of internal friction under drained conditions, $\bar{\phi}_d$, is generally up to 3 degrees lower than $\bar{\phi}_u$ at maximum obliquity. Hence, in the absence of drained tests and on the basis of $\overline{\text{CIU}}\text{C}$ tests, $\bar{\phi}_d$ of phosphatic clays is anticipated to be on the order of 27°. This friction angle is much higher than expected for the highly plastic phosphatic clays based on correlations with plasticity presented in NAVFAC DM-7 (1971) wherein $\bar{\phi}_d$ is on the order of 20°. Moreover, some K_o-consolidated tests indicate that $\bar{\phi}_u$ at maximum oblquity can be as low as 26°. Hence, $\bar{\phi}_d$ probably lies between 25° and 27°. Accordingly, a drained effective friction angle, $\bar{\phi}_d$, of 25° is recommended for the drained class of stability problems.

2.3 Properties of Normally Consolidated Phosphatic Clays from K_o-Consolidated Undrained Strength Tests with Differing Stress System

2.3.1 Overview of Anisotropic Behavior

Ladd et al, (1977) present a comprehensive review of anisotropy and effect of stress system on the undrained behavior of clay deposits. Sedimentary clay deposits have a preferred particle orientation: during one-dimensional deposition and subsequent consolidation, clay particles tend to be oriented horizontally. This inherent anisotropy can lead to changes in behavior during undrained shear depending on the direction of the major principal stress, σ_1, imposed by the applied loading relative to the preferred particle orientation.

Moreover, because the coefficient of earth pressure at rest, $K_o = \bar{\sigma}_{hc}/\bar{\sigma}_v$ (where $\bar{\sigma}_{hc}$ is the effective horizontal consolidation stress under one-dimensional loading), is always less than unity for normally consolidated *in situ* clay deposits, the clay will also exhibit stress system induced anisotropy. This is caused by the differing increments of shear stress required to produce failure as the direction of the major principal stress at failure, σ_{1f}, is varied. Theoretically, the stress system induced anisotropy is also applicable to an isotropic material, even one that has no inherent anisotropy. The combined effect of both inherent and stress induced anisotropy components on the undrained behavior and shear strength of clays can be determined by performing special laboratory tests.

Several stress systems exist along a typical failure surface as illustrated in Figure 2-17. Where the major principal stress at failure, σ_{1f}, acts in the vertical direction, a plane strain active (PSA) or triaxial compression (TC) stress system

*Including data on other phosphatic clays investigated by Ardaman & Associates, Inc. (see Section 1.2.3).

prevails; where σ_1 acts in the horizontal direction, a plane strain passive (PSP) or triaxial extension (TE) condition characterizes the stress system; when σ_{1f} acts at 45° to the vertical, direct simple shear (DSS) conditions prevail. For σ_{1f} acting at 0°, 90° and 45° to the vertical direction, the corresponding undrained shear strength is denoted by $s_u(V)$, $s_u(H)$ and $s_u(45°)$, respectively. Alternatively, the following notations can be used: $s_u(TC)$, $s_u(TE)$ and $s_u(DSS)$, respectively.

Lean sensitive clays are generally characterized by a high degree of anisotropy: their $s_u(H)/s_u(V)$ ratio can be as low as 0.5. Although all clays exhibit anisotropic behavior, highly plastic relatively insensitive clays such as phosphatic clays are anticipated to exhibit a much lower degree of anisotropy than lower plasticity clays.

2.3.2 Test Methods and Test Procedures

Three phosphatic clays representative of the range in plasticity determined on samples obtained from twelve differing mine sites were subjected to special undrained shear tests to determine their anisotropic behavior. The clays selected for this investigation were from the Agrico-Saddle Creek mine (PI = 222%), the USSAC-Rockland mine (PI = 160%), and the CF Mining-Hardee mine (PI = 113%).

Test specimens were trimmed from larger block samples pre-consolidated from a slurry to effective vertical consolidation stresses of 0.3 to 0.5 kg/cm^2 as described in Section 2.2.1. Test specimens were trimmed from these large samples to standard dimensions: 8.0 cm in height and about 3.6 cm in diameter for triaxial specimens; and 2.0 cm in height with a diameter of about 8.0 cm for direct simple shear test specimens.

All test samples were subjected to Ko-consolidation (prior to undrained shear) to vertical effective stresses in excess of that used during sample preparation. Hence, all samples were normally consolidated. K_o-consolidation was used to simulate the in situ state of stress. A total of three K_o-consolidated triaxial compression undrained shear tests with pore pressure measurement ($\overline{CK_oUC}$ tests), four K_o-consolidated triaxial extension undrained shear tests with pore pressure measurement ($\overline{CK_oUE}$ tests), and six K_o-consolidated direct simple shear undrained shear tests (CK_oUDSS) were performed. The shear tests were strain controlled and the rate of strain was slow enough to allow for pore pressure equilization during undrained shear.

The $\overline{CK_oUC}$ tests were conducted in much the same manner as $\overline{CIUC}$ tests (Section 2.2.1) except that K_o-consolidation was used prior to shear and consolidation proceeded in small increments to minimize undrained shear deformations. The ratio of the vertical stress (from hanger dead weights) to cell pressure was adjusted from one consolidation increment to the other in order to maintain one-dimensional consolidation. This was monitored by comparing the cumulative volume change of the test specimen to the total vertical strain in order to maintain them equal. The pre-shear effective vertical consolidation stress ranged from 0.65 to 0.8 kg/cm^2. Hence, the samples were consolidated prior to shear to effective stresses approximately 1.5 times the maximum vertical effective stress used during sample preparation. Samples were then sheared in the same manner as $\overline{CIUC}$ tests at a controlled axial strain rate (vertical compression), $\dot{\epsilon}_v$, of 0.5%/hour.

The $\overline{CK_oUE}$ specimens were consolidated in the same manner as described for $\overline{CK_oUC}$ tests. (The vertical load during consolidation was applied by means of air pressure rather than dead load hanger.) Spiral filter strips in lieu of vertical filter strips were used on $\overline{CK_oUE}$ test specimens. During undrained shear, the cell pressure was kept constant and the vertical stress was reduced at an axial strain (vertical extension) controlled rate, $\dot{\epsilon}_v$, of 0.5%/hour.

The CK_oUDSS tests were performed in a modified Geonor Direct Simple Shear Device using the procedures outlined by Bjerrum and Landva (1966). The cylindrical test specimen was prepared by means of a special cutting frame and shoe which allows trimming and aligning the sample for placement within a wire reinforced rubber membrane which prevents lateral deformation during consolidation. The volume of the sample is maintained constant during shear by automatic adjustment of the normal load to keep a constant sample height and, hence, model undrained shear. Two CK_oUDSS tests were performed on each of 3 phosphatic clays at pre-shear effective vertical consolidation stresses of 1.0 (or 0.8) kg/cm^2 and 2.0 kg/cm^2 to confirm the applicability of the NSP concept to phosphatic clays. Based on extensive experience with CK_oUDSS tests, a controlled shear strain rate, $\dot{\gamma}$, of 3 to 6%/hour was used to achieve pore pressure equilization.

The undrained shear strength, s_u, from triaxial tests is defined herein as half the maximum principal stress difference, q, at failure, i.e., $s_u = q_f = 0.5(\sigma_1 - \sigma_3)_{max}$. For CK_oUDSS tests, undrained failure is defined as the peak horizontal shear stress, τ_h, i.e., $s_u = (\tau_h)_{max}$. The stress τ_h is the applied shear stress on the horizontal plane which causes shear by inducing lateral movement of the top cap.

2.3.3 Coefficient of Earth Pressure at Rest

No direct measurement of the coefficient of earth pressure at rest, K_o, of phosphatic clays was made. K_o is the ratio of horizontal to vertical effective consolidation stress under one-dimensional loading and as such defines the *in situ* state of stress normally encountered.

Although a direct measurement of K_o was not made, values of K_o can be estimated from the consolidation phase of $\overline{CK_oUC}$ and $\overline{CK_oUE}$ tests. Consolidation increments when the clay is normally consolidated can be used to determine K_o values for normally consolidated phosphatic clays. Plots of cumulative vertical strain versus volumetric strains during K_o-consolidation in triaxial tests are presented in Figure 2-18. Although the final vertical strain, ϵ_v, was not always equal to the volumetric strain, $\Delta V/V_o$, as one would expect during K_o-consolidation, the data during virgin compression (last few consolidation increments) were generally parallel to the K_o-theoretical line ($\epsilon_v = \Delta V/V_o$). Hence, the final consolidation stresses were close to a K_o-condition.

Values of K_o for normally consolidated phosphatic clays determined from the consolidation phase of $\overline{CK_oUE}$ and $\overline{CK_oUC}$ tests are tabulated below:

Phosphatic Clay	K_o Individual Data	K_o Average
Agrico-Saddle Creek (PI = 222%)	0.50; 0.60	0.55
USSAC-Rockland (PI = 160%)	0.51; 0.53	0.52
CF Mining-Hardee (PI = 113%)	0.49; 0.67; 0.70	0.62

Some of the data show considerable scatter and the K_o-data, particularly for the Agrico-Saddle Creek and, USSAC-Rockland phosphatic clays, are lower than expected for such plastic material. Figure 2-19 compares measured data to empirical correlations with. plasticity index, PI, and angle of internal friction, $\bar{\phi}$, presented by Alpan (1967), Brooker and Ireland (1965) and Ladd et al. (1977). As shown, the measured K_o-data for two of the clays (Agrico and CF) are substantially lower than expected based on plasticity. The unanticipated low values may be partly due to the fact that the friction angle, $\bar{\phi}$, of phosphatic clays is much higher than expected for such highly plastic material (see Section 2.2.6 and Figure 2-16). In the absence of reliable direct K_o-measurement and in light of the data and correlations in Figure 2-19, it is tentatively recommended that a K_o-value on the order of 0.62 be used to characterize the *in situ* one-dimensional state of stress of normally consolidated phosphatic clays.

2.3.4 Results of $\overline{CK_oU}C$ and $\overline{CK_oU}E$ Tests

Stress path data from $\overline{CK_oU}C$ and $\overline{CK_oU}E$ tests on normally consolidated Agrico-Saddle Creek, USSAC-Rockland and CF Mining-Hardee phosphatic clays are presented in Figures 2-20, 2-21 and 2-22, respectively. Normalized stress-strain and pore pressure data for all three clays are presented in Figure 2-23 and 2-24 for $\overline{CK_oU}C$ and $\overline{CK_oU}E$ tests, respectively. Figure 2-25 summarizes the normalized undrained Young's secant modulus, E_u/s_u, versus shear stress level, $\Delta q/\Delta q_f$, from $\overline{CK_oU}C$ and $\overline{CK_oU}E$ tests (where Δq is the increment of half principal stress difference from K_o-conditions, and Δq_f is Δq at failure, i.e., at maximum stress difference).

2.3.4.1 $\overline{CK_oU}C$ Tests

The $\overline{CK_oU}C$ effective stress paths (Figures 2-20 through 2-22) are reasonably consistent with expected behavior for normally consolidated highly plastic materials. The mobilized angle of internal friction, $\bar{\phi}_m$, at maximum stress difference equalled 26.0°, 26.3° and 22.0° for the Agrico, USSAC and CF clays, respectively. The pore pressure A-factor at maximum stress difference averaged about 0.85 which is slightly lower than expected. The normalized undrained shear strength ratio, $s_u(\overline{CK_oU}C)/\bar{\sigma}_{vc}$, equalled 0.315, 0.327 and 0.271 for the Agrico, USSAC and CF clays, the first two values being slightly higher than anticipated.

The effective angle of internal friction at maximum obliquity equalled 39.8°, 33.4° and 26.0° for the Agrico, USSAC and CF clays. These values, particularly for the Agrico and USSAC clays, are much higher than expected for such highly plastic material.

The stress-strain behavior in Figure 2-23 indicates that failure occurred at very small strains of about 0.3 to 0.4% for the Agrico and USSAC clays, and at approximately 2.5% strain for the CF Mining clay. The Agrico and CF clays exhibited moderate strain softening behavior. The USSAC clay depicted substantial strain softening effects.

In summary, K_o-consolidated phosphatic clays sheared in triaxial compression exhibit a normalized undrained shear strength slightly higher than expected probably because of a somewhat high angle of internal friction and a somewhat low A-factor at failure. The very low strains at failure observed for the USSAC and Agrico clays and the moderate to substantial strain softening effects are normally more characteristic of lean sensitive clays than highly plastic materials.

The effect of K_o-consolidation versus isotropic consolidation of phosphatic clays can be assessed by comparing $\overline{CIUC}$ test data (Section 2.2) to $\overline{CK_oUC}$ test data. The data show that K_o-consolidation:

- Substantially decreases the strain at failure from 7% or 12% to less than 3%; and causes more significant strain softening behavior.

- Has little effect on the normalized undrained shear strength ratio considering the limited number of $\overline{CK_oUC}$ tests and the scatter depicted in Figure 2-14. Average values of $s_u/\bar{\sigma}_{vc}$ are tabulated below for comparison:

Phosphatic Clay	PI (%)	$s_u(\overline{CIUC})/\bar{\sigma}_c$	$s_u(\overline{CIUC})/\bar{\sigma}_{vc}$	$s_u(\overline{CK_oUC})/\bar{\sigma}_{vc}$
Agrico-Saddle Creek	222	0.28	0.26	0.31
USSAC-Rockland	160	0.30	0.28	0.33
CF Mining-Hardee	113	0.33	0.29	0.27
Gross Average		0.30	0.28	0.30

Based on the above and other data presented in Figure 2-14, an $s_u(V)/\bar{\sigma}_{vc}$ ratio in compression on the order of 0.28 is recommended for normally consolidated phosphatic clay irrespective of plasticity.

- Causes a decrease in $\bar{\phi}$ at maximum stress difference but not necessarily at maximum obliquity as was illustrated in Figure 2-16. (A friction angle, $\bar{\phi}$ =25°, is recommended for the drained class of stability problems as detailed in Section 2.2.6).

- Apparently causes a decrease in the A-factor at failure particularly for the highly plastic USSAC and Agrico clays.

- Causes an increase in the normalized undrained modulus as evidenced by comparison of E_u/s_u data in Figures 2-15 and 2-25. This stiffening effect may be caused by the smaller increment in shear stress required to produce failure in $\overline{CK_oUC}$ tests, but is difficult to ascertain because of the scatter in the data and limited number of $\overline{CK_oUC}$ tests performed. The undrained modulus from $\overline{CK_oUC}$ tests is much higher than expected for such highly plastic material. $\overline{CIUC}$ data (Figure 2-15) are also higher than anticipated, but seem more reasonable in spite of the scatter between various phosphatic clays.

2.3.4.2 $\overline{CK_oUE}$ Tests

The shape of the $\overline{CK_oUE}$ effective stress paths (Figures 2-20 through 2-22) and normalized stress-strain curves (Figure 2-24) are reasonable, but the samples continue to strain harden to extremely large strains resulting in values of $s_u/\bar{\sigma}_{vc}$ and $\bar{}$ that are too high. The A-factors at failure (0.82 to 0.95) are reasonable and the normalized pore pressure behavior, $\Delta u/\bar{\sigma}_{vc}$, is reasonable (considering that the tests were performed by reducing the vertical stress and, hence, comparison of the pore pressure behavior in compression - Figure 2-23 - and extension - Figure 2-24 - has to take into account changes in the minor principal stress $\Delta\sigma_3$, i.e., one should compare $(\Delta u - \Delta\sigma_3)/\bar{\sigma}_{vc}$ rather than $\Delta u/\bar{\sigma}_{vc}$).

The strain hardening behavior, even at extremely large strains in excess of 25%, resulted in values of $s_u/\bar{\sigma}_{vc}$ and $\bar{\phi}$ that are considered too high to be representative of phosphatic clay behavior. Moreover, three out of four $\overline{CK_oUE}$ tests gave small negative values for the effective minor principal stress at failure, $\bar{\sigma}_{3f}$ (with values of $\bar{\sigma}_{3f}/\bar{\sigma}_{vc}$ of -0.01, -0.10 and -0.20), which is physically not possible since tension cannot exist between the test specimen and its end caps. Three of the "measured" $s_u(\overline{CK_oUE})/\bar{\sigma}_{vc}$ ratios of 0.36, 0.42 and 0.44 are unusually high particularly in light of the fact that $s_u(H)$ is expected to be less than $s_u(V)$, i.e., $s_u(\overline{CK_oUE})$ should be lower than $s_u(\overline{CK_oUC})$. The resulting angles of internal friction at maximum stress difference of more than 40^o are clearly not realistic (although the large strains at failure are not unreasonable because of the 90 degree rotation in principal planes).

The reason for this unusual behavior is not clear particularly because the cells had good quality low-friction pistons, spiral filter strips were used, and no obvious signs of sample necking were observed. Nevertheless, necking of the sample if prevalent and unaccounted for would give an undrained strength and angle of friction that are too high.

Because of the unrealistic high values of $s_u/\bar{\sigma}_{vc}$ and $\bar{\phi}$ "measured" in $\overline{CK_oUE}$ tests and the possibility of undetected sample necking particularly at large strains, it is considered prudent to arbitrarily terminate the effective stress paths and stress strain curves at a vertical extension strain of about 7 to 8%; the corresponding angle of internal friction "mobilized" at these strains is on the order of 30^o (for the USSAC and Agrico clays, and is slightly higher for the CF clay). The resulting undrained shear strength ratio in triaxial extension, $s_u(H)/\bar{\sigma}_{vc}$, is then found equal to about 0.245 for all three phosphatic clays.

As shown in Figure 2-25, the normalized modulus, E_u/s_u, from triaxial extension tests is lower than that from $\overline{CK_oUC}$ tests (and even lower than that from $\overline{CIUC}$ tests - Figure 2-15). This behavioral trend was expected because of the substantially larger increment in shear stress required to produce failure in $\overline{CK_oUE}$ tests corresponding to a passive (extension) stress system.

2.3.5 Results of CK_oUDSS Tests

Results of CK_oUDSS tests on normally consolidated phosphatic clays are summarized in Figures 2-26 through 2-29. Samples of each phosphatic clay consolidated to differing $\bar{\sigma}_{vc}$ of 0.8 kg/cm^2 (or 1.0 kg/cm^2) and 2.0 kg/cm^2 (or 2.2 kg/cm^2) yielded fairly consistent (constant) normalized behavior as illustrated in Figures 2-26 and 2-28, confirming the applicability of the normalized soil parameter (NSP) concept to phosphatic clays. Moreover, the undrained behavior and normalized properties of the Agrico, USSAC and CF clays are very similar (as depicted in Figures 2-27 and 2-28) even though these clays cover a wide range of clay plasticity (PI = 113% to 222%). Hence, the normalized properties determined in this investigation are probably applicable to most, if not all, Florida phosphatic clays since there were no detectable or consistent trends with plasticity.

The normalized stress paths in Figure 2-26 show a continuous decrease in vertical effective stress during undrained shear, which is typical of CK_oUDSS tests performed on normally consolidated clays. The stress-strain behavior in Figure 2-28 is also consistent with that observed on other naturally occurring clay deposits. The undrained shear strength is mobilized at very large shear strains, γ, with a shear strain at failure, γ_f, of about $19.4 \pm 3.2\%$. There is little strain softening observed after failure as illustrated in Figure 2-28.

The normalized $s_u(DSS)/\bar{\sigma}_{vc}$ ratio ranged from: 0.222 to 0.226 for the Agrico clay; 0.212 to 0.227 for the USSAC clay; and 0.228 to 0.231 for the CF clay. Average values of 0.224, 0.220 and 0.229 are characteristic of the Agrico, USSAC and CF clays, respectively. Roma (1976) reports a value of 0.224 for an IMC-Noralyn clay with a plasticity index of 139%. A gross average $s_u(DSS)/\bar{\sigma}_{vc}$ value of 0.225 is believed characteristic of a large number of phosphatic clays since very little variability was observed in CK_oUDSS tests for the clays investigated.

Although CK_oUDSS test results yield accurate estimates of the undrained shear strength, only limited significance should be given to the values of the effective friction angle, $\bar{\phi} = \arctan(\tau_h/\bar{\sigma}_v)$ in Figure 2-27, because of unknown stress conditions within the sample (Ladd and Edgers, 1971; Ladd et al., 1972). Nevertheless, $\bar{\phi}$ equalled 21.4° and 27.2° at failure and at maximum "obliquity", respectively. These values are lower than those determined from $\overline{CIU}C$ and $\overline{CK_oU}C$ tests (Figure 2-16), but are not considered as reliable.

Values of the normalized undrained Young's secant modulus, E_u/s_u, are presented in Figure 2-29 as a function of stress level, τ_h/s_u. As shown, the undrained modulus decreases substantially with increased stress level. Moreover, all phosphatic clays seem to exhibit approximately the same magnitude of modulus* particularly at stress levels in excess of about 40%. At a stress level of 50%, phosphatic clays are characterized by an E_u/s_u ratio of about 250 to 370.

*This is also true for the IMC-Noralyn phosphatic clay (PI = 139%) investigated by Roma (1976); see Figure 1-3.

Although the data are consistent, the E_u/s_u ratio is higher than expected for such plastic materials.

The CK_oUDSS E_u/s_u versus stress level data are much more consistent and the trends more realistic than those from $\overline{CIUC}$ tests (Figure 2-15). Moreover the data lies between that from $\overline{CK_oUC}$ and $\overline{CK_oUE}$ tests (Figure 2-25). Hence the E_u/s_u data from CK_oUDSS tests would probably give the most realistic estimate of undrained deformations. The data in Figure 2-29 indicate that E_u/s_u decreases from 600 or more at a stress level of 20%, to 50 or 100 at a stress level of 80%. These values which are higher than one would have predicted based on the plasticity of phosphatic clays imply smaller undrained deformations than would occur with high plasticity natural sedimentary clay deposits (consolidated to the same effective stress).

2.4 Recommended Properties of Normally Consolidated Phosphatic Clay for Use in Design and Predictions

2.4.1 Effect of Anisotropy and Strain Compatibility on Undrained Shear Strength Ratio

A summary of the undrained shear strength ratios, $s_u/\bar{\sigma}_{vc}$, from various types of strength tests and for various stress systems is presented in Figure 2-30 for normally consolidated phosphatic clays. As indicated by the anistropic strength ratio, $s_u(H)/s_u(V)$, of 0.87, the phosphatic clays are shown to be slightly more anisotropic than anticipated considering the extremely high plasticity of these clays (PI = 113% to 222%). Moreover, all three phosphatic clays investigated yielded approximately the same $s_u/\bar{\sigma}_{vc}$ ratio for a given stress system irrespective of plasticity. Hence, the reported normalized undrained shear strength ratios are characteristic for a large number of phosphatic clays.

The recommended undrained shear strength ratios for the differing stress systems, i.e., $s_u(V) = s_u(TC)$; $s_u(H) = s_u(TE)$; and $s_u(45^o) = s_u(DSS)$, are shown on Figure 2-30. A comparison of the normalized undrained strength ratio, $s_u/\bar{\sigma}_{vc}$, from various types of strength tests has to take into account the mobilized strain at failure. Noting that the shear strain, γ, is related to the axial strain, ϵ_v, by the relationship $\gamma = 1.5\ \epsilon_v$ in triaxial tests, one can compare $s_u/\bar{\sigma}_{vc}$ and γ_f (γ at failure) from the various tests:

Type of Test	Stress System	$s_u/\bar{\sigma}_{vc}$	γ_f, %
$\overline{CIUC}$	TC; $s_u = s_u(V)$	$0.280^{\pm}$	10.5-18.0
$\overline{CK_oUC}$	TC; $s_u = s_u(V)$	0.280	0.5-3.8
CK_oUDSS	DSS; $s_u = s_u(45^o)$	0.225	19.4 ± 3.2
$\overline{CK_oUE}$	TE; $s_u = s_u(H)$	0.245	12.0-30.0

In addition to the wide variation in the strain at failure, the degree of strain softening behavior is different for the various stress systems, with the most prominent strain softening effect observed in $\overline{CK_oUC}$ tests. Variables that appear to influence the shear strain at failure include: (i) the degree of rotation in principal planes, the larger strains at failure being characteristic of the larger degree of principal plane rotation which necessitates a larger increment in shear stress to cause failure; and (ii) the degree of anisotropic consolidation with K_o-consolidation yielding lower strains at failure in triaxial compression than isotropic consolidation.

Figures 2-31, 2-32 and 2-33 compare measured $\overline{CK_oU}C$, CK_oUDSS and $\overline{CK_oU}E$ stress-strain data for the Agrico-Saddle Creek, USSAC-Rockland and CF Mining-Hardee clays, respectively. Ladd et al. (1972) and Ladd (1975) present a simplified methodology that accounts for strain compatibility in determining the appropriate average $s_u/\bar{\sigma}_{vc}$ to account for the varying modes of failure illustrated in Figure 2-17. The large difference in the shear strain at failure with the varying stress systems makes it very unlikely that the peak strength can be mobilized simultaneously all along a potential failure surface. By averaging the values of $q/\bar{\sigma}_{vc}$ from triaxial compression and extension tests and $\tau_h/\bar{\sigma}_{vc}$ from DSS tests at the same shear strain, one could estimate the maximum mobilized resistance based on the average of the three stress systems. This should provide a more realistic $s_u/\bar{\sigma}_{vc}$ to be used in conjunction with undrained stability analyses, and accounts, at least empirically, for the effects of strain compatibility along the failure surface.

In the preceding presentation, the undrained shear strength from triaxial tests was taken equal to the maximum half principal stress difference (i.e., $s_u = q_f$) which is appropriate for undrained $\phi = 0$ stability analyses where the failure planes in the active and passive wedges are taken at 45^o to the horizontal plane. These values are also applicable for bearing capacity type analyses. On the other hand, if he shear strength is to be applied to an actual circular arc failure surface or to active and passive wedges at $45^o \pm \bar{\phi}/2$ from the horizontal plane (where $\bar{\phi}$ is arbitrarily selected as the effective angle of internal friction from undrained tests at maximum stress difference, i.e., $\bar{\phi}_u = 28^o$ for phosphatic clays, as outlined in Section 2.2.6), then the undrained shear strength should be taken equal to the shear stress at failure on the failure plane, τ_{ff}, resulting in $s_u = \tau_{ff} = q_f \cos\bar{\phi}_u = q_f \cos 28^o = 0.883\ q_f$. The mobilized undrained shear stress at a given shear strain would then equal q and $q\cos 28^o$, respectively, for consistency with the two definitions of undrained strength outlined above.

The simplified strain compatibility concept was applied to the $\overline{CK_oU}C$, CK_oUDSS and $\overline{CK_oU}E$ stress-strain data of each phosphatic clay illustrated in Figures 2-31 through 2-33. The resulting mobilized undrained shear strength ratios versus shear strain are presented as a shaded band in Figures 2-34 through 2-36 bounded by upper and lower curves corresponding to a mobilized shear stress at failure, q_f, equal to $1/3\{\tau_h + q(TC) + q(TE)\}$ and $1/3\{\tau_h + q(TC)\cos 28^o + q(TE)\cos 28^o\}$, respectively.* The maximum mobilized shear stress occurs at a shear strain of about 12% for all 3 phosphatic clays. The dashed lines in Figures 2-34 through 2-36 represent the corresponding mobilized strength if the $\overline{CK_oU}E$ data at large strains are not discarded. These results indicate a continued small increase in τ_f

*Where $\overline{CK_oU}E$ data is suspect at large strains (Figures 2-31 through 2-33), q(TE) was taken equal to q(TC) at the corresponding shear strain.

at large strains, but the data is suspect as previously noted. Moreover, it is appropriate to consider that failure has occurred when shear strains on the order of 12% have been experienced.

The undrained shear strengths of the three phosphatic clays are almost identical based on the simplified strain compatibility concept. The mobilized shear strengths are compared in Figure 2-37 as well as with CK_oUDSS data. Pertinent design values are tabulated below:

Phosphatic Clay	PI (%)	Mobilized $s_u/\bar{\sigma}_{vc}$ ($s_u = q_f$)	Mobilized $s_u/\bar{\sigma}_{vc}$ ($s_u = q_f \cos 28^o$)	$s_u(CK_oUDSS)/\bar{\sigma}_{vc}$
Agrico-Saddle Creek	222	0.249	0.228	0.224
USSAC-Rockland	160	0.235	0.215	0.220
CF Mining-Hardee	113	0.239	0.220	0.229
Recommended Design Value for Phosphatic Clays		0.240	0.220	0.225

Moreover, the mobilized shear stress in TC, TE and DSS at the design shear strain of about 12% are almost equal as illustrated below, inferring a relatively low degree of anisotropy (as expected) when strain compatibility is taken into account:

		Mobilized $s_u/\bar{\sigma}_{vc}$					
		$s_u = q_f$			$s_u = q_f \cos 28^o$		
Phosphatic Clay	PI (%)	TC	DSS	TE	TC	DSS	TE
Agrico-Saddle Creek	222	0.287	0.212	0.245	0.253	0.212	0.216
USSAC-Rockland	160	0.243	0.207	0.243	0.215	0.207	0.215
CF Mining-Hardee	113	0.247	0.220	0.247	0.218	0.220	0.218
Average		0.259	0.213	0.245	0.229	0.213	0.216

Based on the preceding evaluations, a design $s_u/\bar{\sigma}_{vc}$ value equal to 0.24 is recommended for use in bearing capacity undrained $\phi = 0$ type analyses on normally consolidated phosphatic clays. A design $s_u/\bar{\sigma}_{vc}$ value of 0.22 is judged more appropriate for use in circular arc type stability analyses.

For a wedge type failure surface, the appropriate normalized mobilized shear strengths for use in the active, central and passive wedges correspond to $s_u/\bar{\sigma}_{vc}$ values of 0.259, 0.213 and 0.245, respectively, when the active and passive wedges are taken at 45^o to the horizontal plane. If actual failure surfaces at $45^o \pm \bar{\phi}/2$ from the horizontal plane ($\bar{\phi} = 28^o$) are used for the active and passive wedges, respectively, corresponding $s_u/\bar{\sigma}_{vc}$ values of 0.229, 0.213 and 0.216 should be used in the active, central and passive wedges. However, because anisotropy is so small at the failure strain, one could also use the average $s_u/\bar{\sigma}_{vc}$ ratios of 0.24 or 0.22 in all portions of the sliding block failure surface (depending on the assumptions assumed for the active and passive failure planes).

The normalized design undrained shear strength ratios of 0.22 to 0.24 selected as representative for a wide range of normally consolidated phosphatic clays are in excellent agreement with field test section results for other natural sedimentary type deposits and test data on laboratory sedimented clay samples from these deposits. As noted by Mesri (1975), the *in situ* $s_u/\bar{\sigma}_{vc}$ ratio appropriate for use in stability analyses appears to fall within a fairly narrow range for most soft homogeneous sedimentary clays. Phosphatic clays appear to conform to this finding.

Figure 2-37 compares the design $s_u/\bar{\sigma}_{vc}$ values with data from CK_oUDSS tests at $(\tau_h)_{max}$. As shown, $s_u(CK_oUDSS)/\bar{\sigma}_{vc}$ equals about 0.225, lies between the $s_u/\bar{\sigma}_{vc}$ design values of 0.22 and 0.24, and is, therefore, in excellent agreement with the recommended values. One might, therefore, simply use the CK_oUDSS, $s_u/\bar{\sigma}_{vc}$ = 0.225 in stability and bearing capacity undrained type analyses on normally consolidated phosphatic clays. The CK_oUDSS test, therefore, appears to provide reasonable design strengths.

2.4.2 Undrained Deformations

As detailed in Section 2.3.5, the normalized undrained Young's secant modulus data, E_u/s_u, versus stress level from CK_oUDSS tests (presented in Figure 2-29) are recommended for use in predicting undrained deformations of normally consolidated phosphatic clays. As shown in Figure 2-29, E_u/s_u exhibits a large decrease with increasing stress level and values are generally in good agreement for all phosphatic clays investigated.

The data in Figure 2-29 indicate that E_u/s_u decreases from about 500 (range of 400 to 900) at a factor of safety of 3, to about 300 (range of 250 to 370) at a factor of safety of 2, to about 150 (range of 120 to 200) at a factor of safety of 1.5. These values are higher than one would have predicted based on the high plasticity of phosphatic clays; they imply smaller undrained deformations than would occur with other high plasticity natural sedimentary clay deposits (consolidated to the same effective stress). The relatively high undrained modulus is nevertheless consistent with a somewhat lower coefficient of secondary compression than anticipated (see Volume 4, "Consolidation Behavior of Phosphatic Clays") and a lower sensitivity to strain rate effects than expected for such plastic material (see Figure 2-13).

2.4.3 Effective Stress Failure Envelope

For drained effective stress type stability analyses that may be performed to assess long-term performance of normally consolidated phosphatic clays, an effective angle of internal friction, $\bar{\phi}_d$, equal to 25^o is recommended as was outlined in Section 2.2.6. (Normally consolidated phosphatic clays are characterized by zero effective cohesion.)

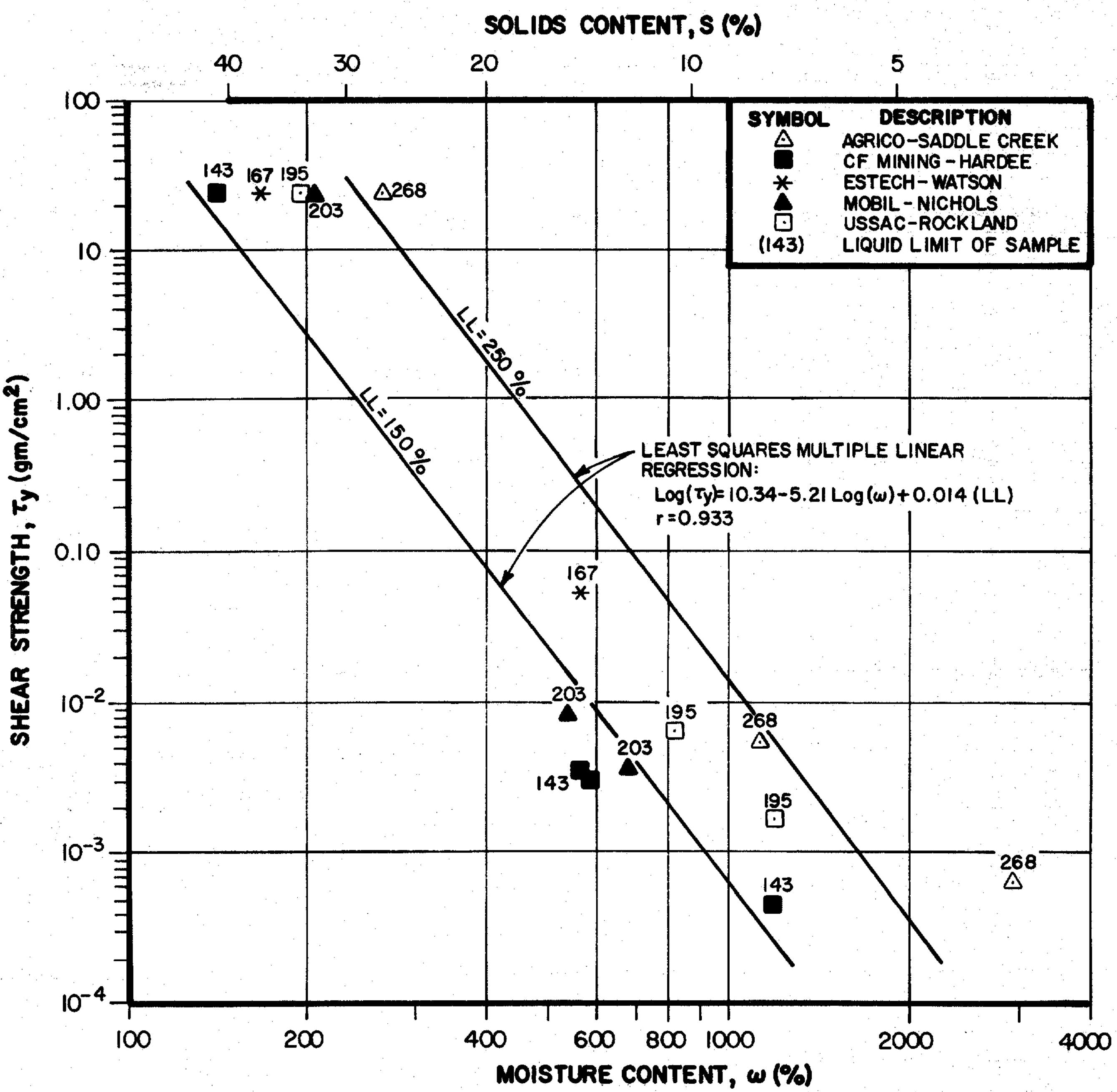

MOISTURE CONTENT VS. SHEAR STRENGTH FOR PHOSPHATIC CLAYS FROM VISCOSITY TESTS

FIGURE 2-1

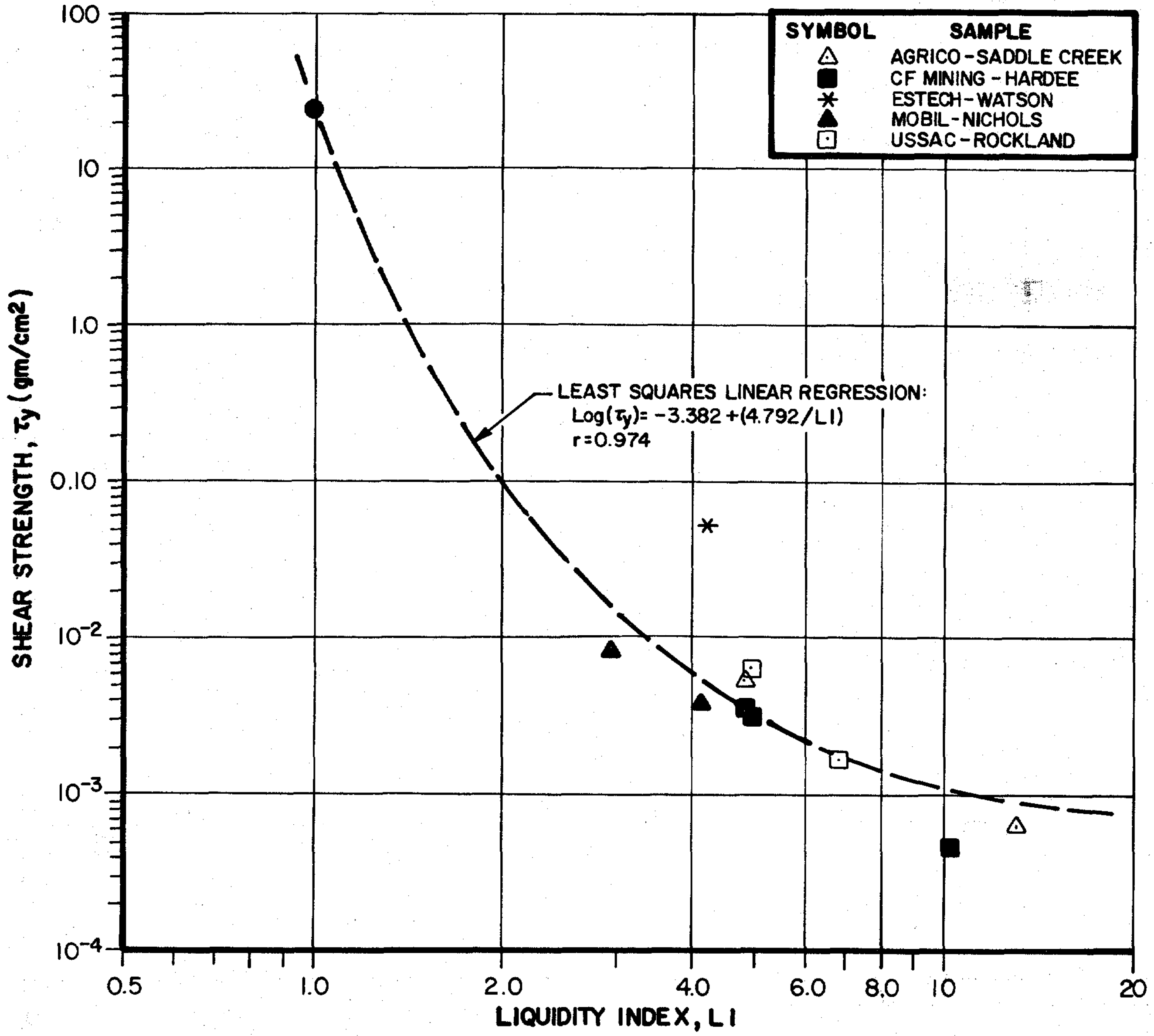

LIQUIDITY INDEX VS. SHEAR STRENGTH FOR PHOSPHATIC CLAYS FROM VISCOSITY TESTS

FIGURE 2-2

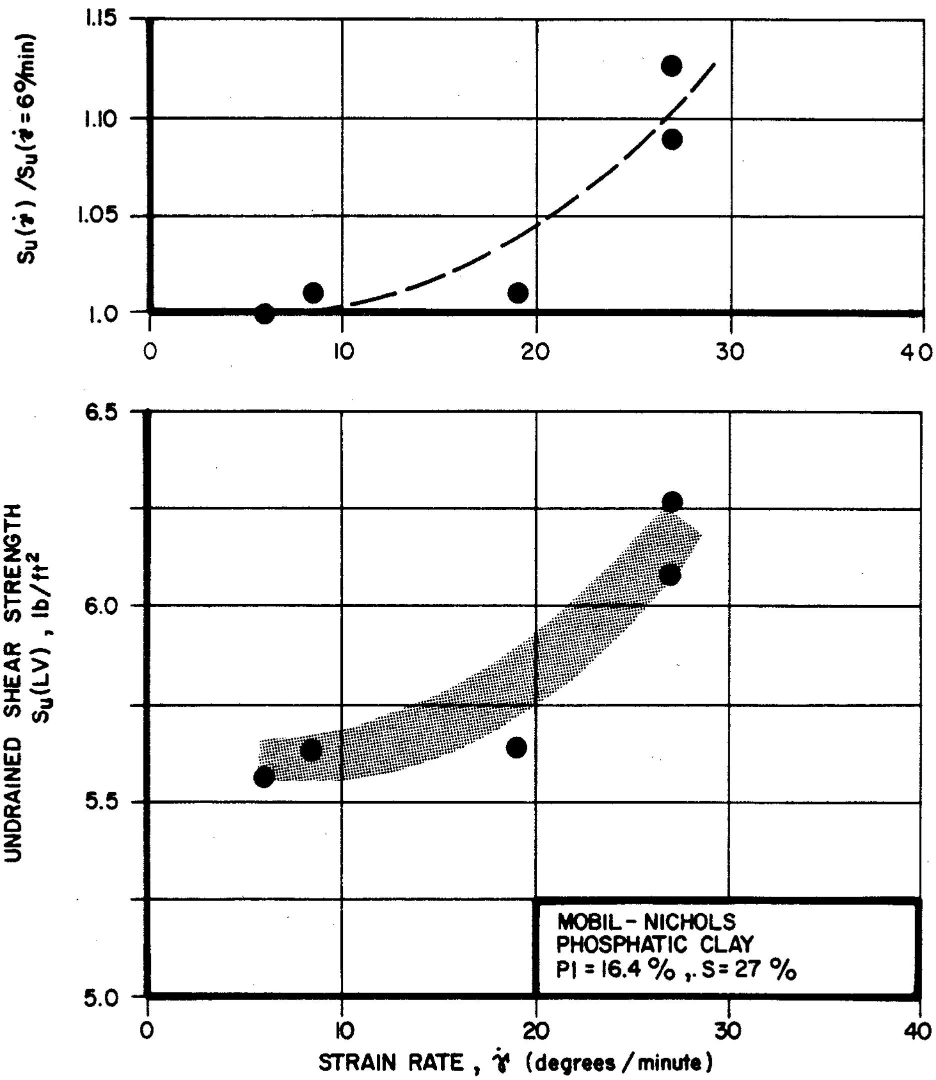

EFFECT OF STRAIN RATE ON LAB VANE REMOLDED UNDRAINED SHEAR STRENGTH

FIGURE 2-3

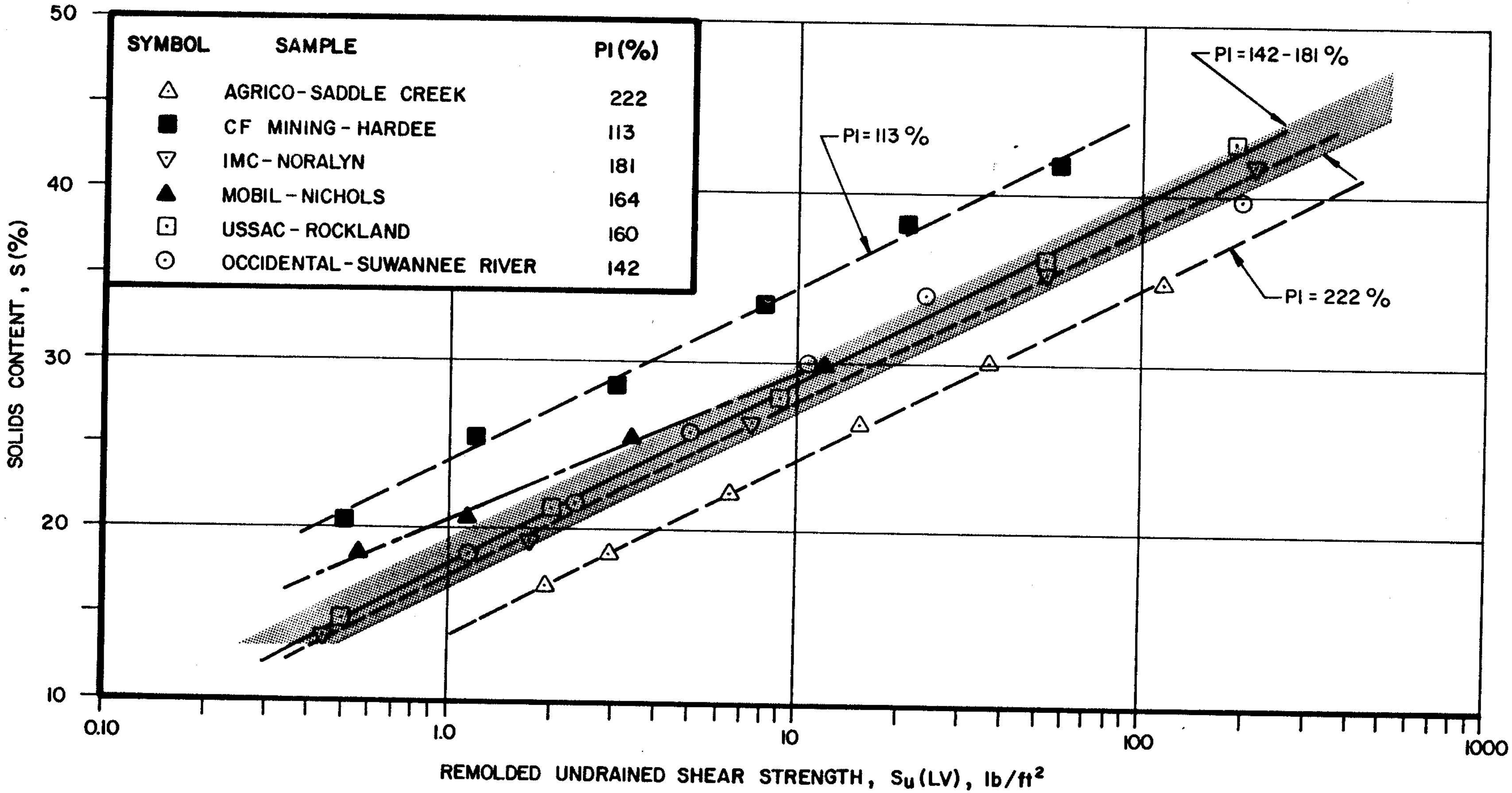

FIGURE 2-4

SOLIDS CONTENT VERSUS LAB VANE REMOLDED UNDRAINED SHEAR STRENGTH

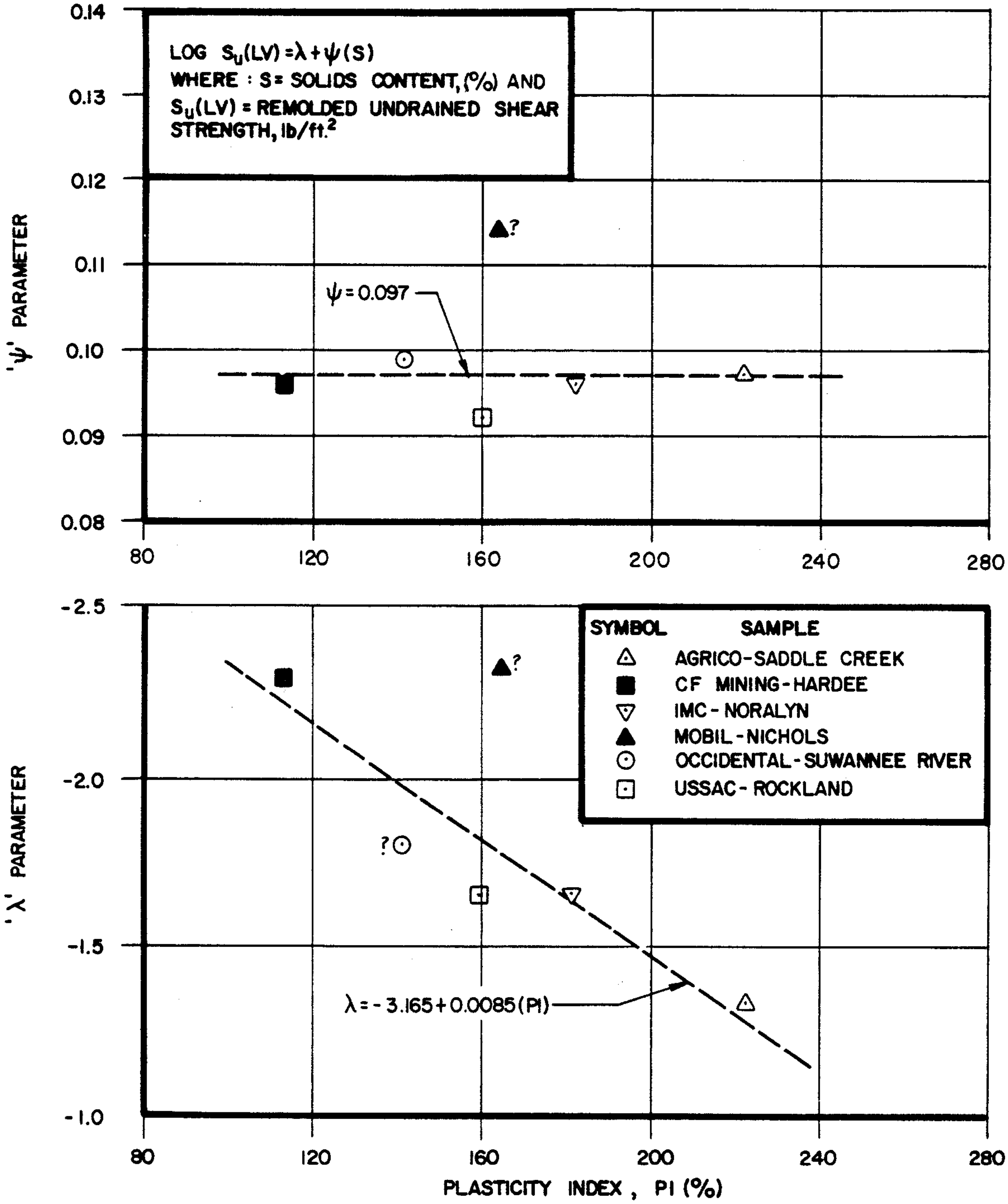

RESULTS OF REGRESSION ANALYSES ON LABORATORY VANE REMOLDED UNDRAINED SHEAR STRENGTH

FIGURE 2-5

FIGURE 2-6

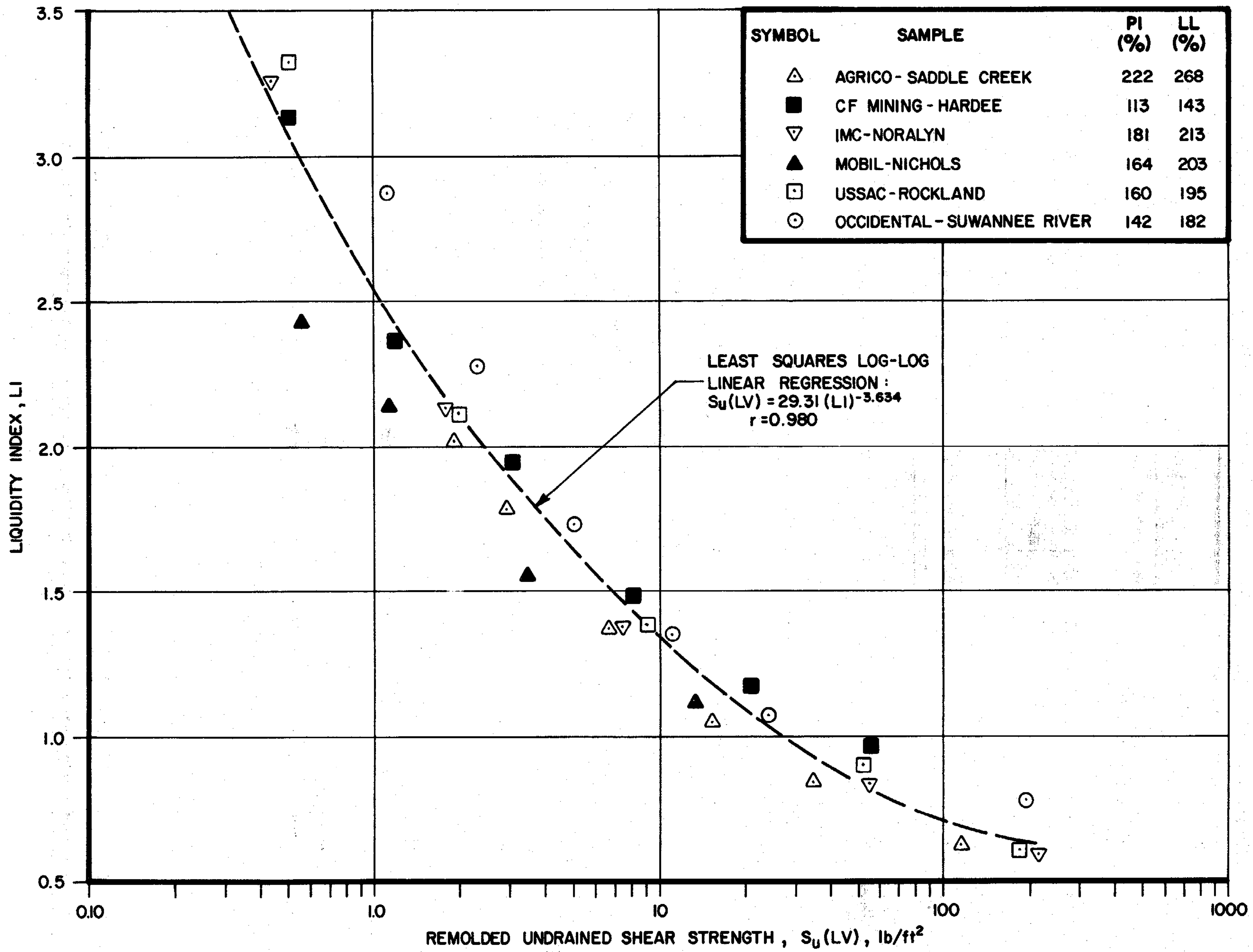

LIQUIDITY INDEX VERSUS LAB VANE REMOLDED UNDRAINED SHEAR STRENGTH

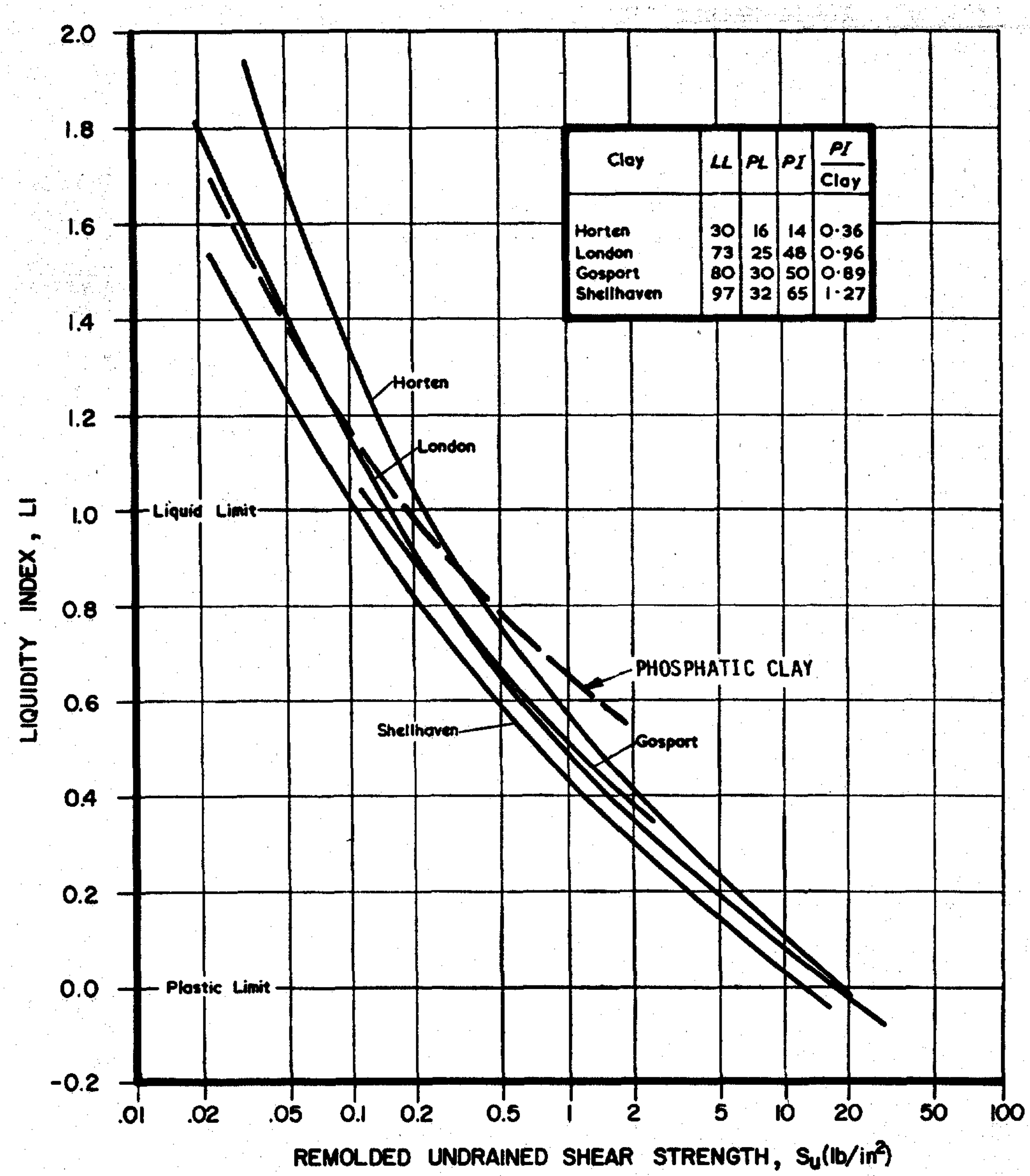

SOURCE: ADAPTED FROM SKEMPTON, A.W. AND NORTHEY, R.D. (1952). "THE SENSITIVITY OF CLAYS". GEOTECHNIQUE. VOLUME III

REMOLDED UNDRAINED SHEAR STRENGTH VERSUS LIQUIDITY INDEX

FIGURE 2-7

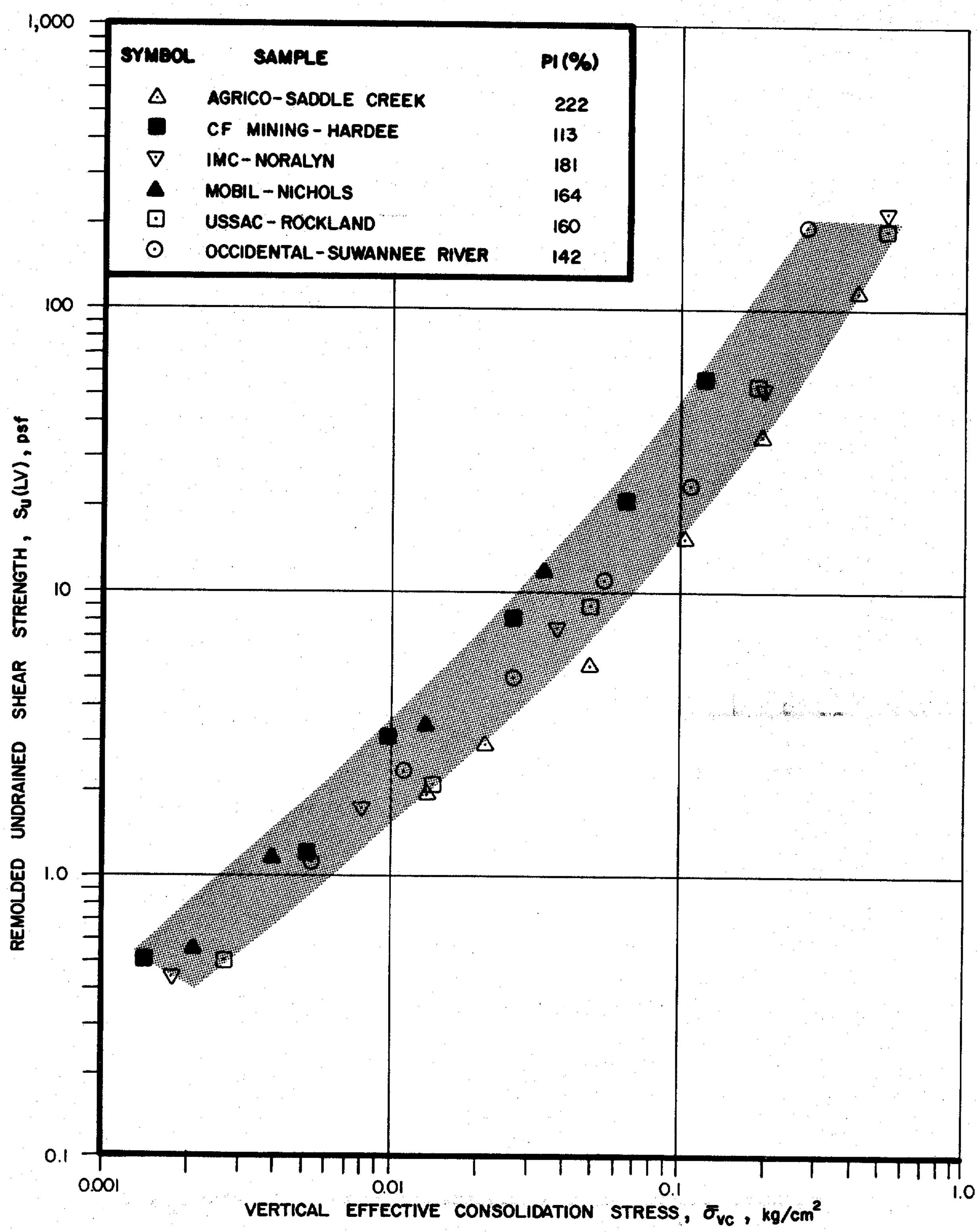

LAB VANE REMOLDED UNDRAINED SHEAR STRENGTH VERSUS CONSOLIDATION STRESS

FIGURE 2-8

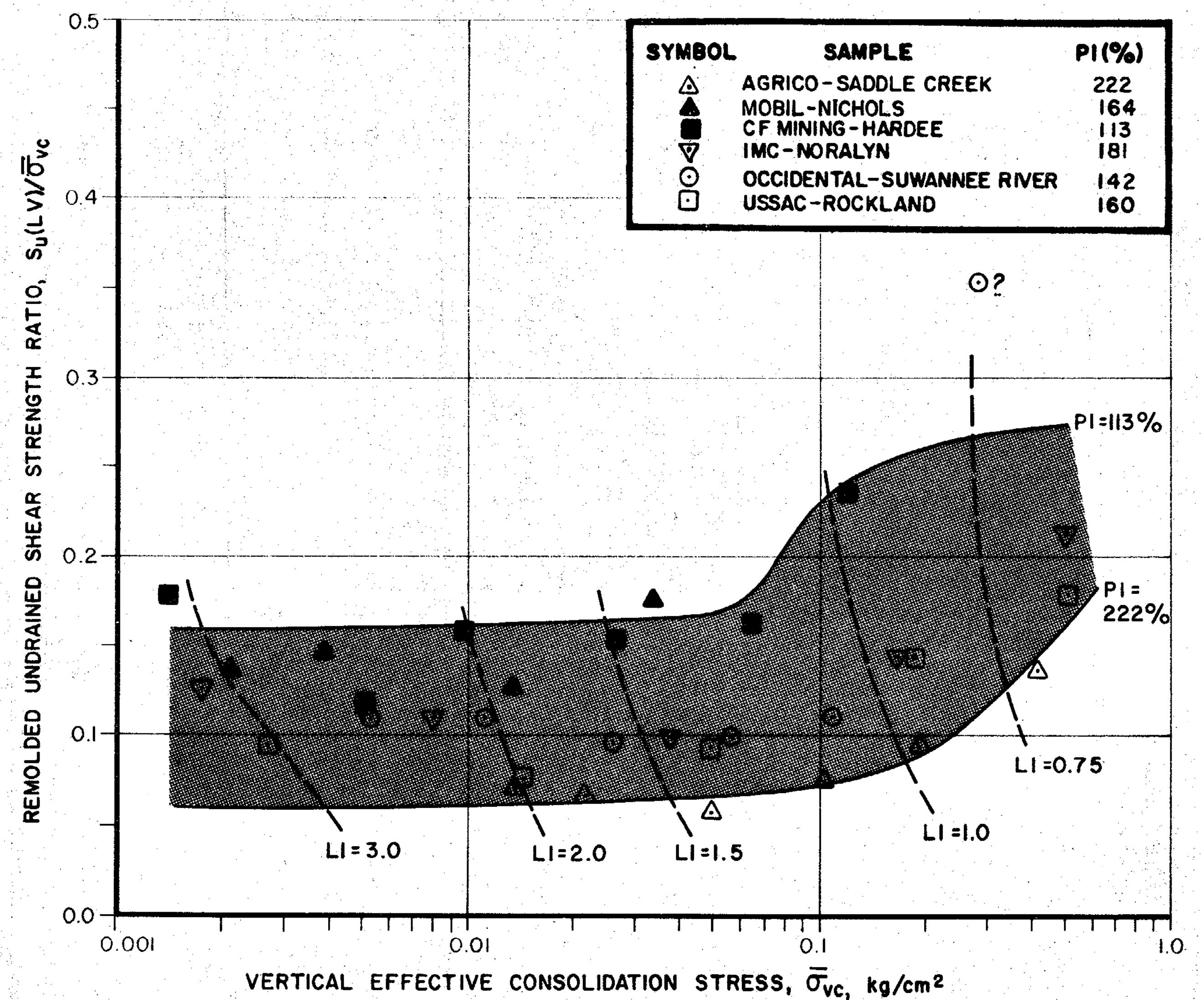

FIGURE 2-9

REMOLDED NORMALIZED UNDRAINED SHEAR STRENGTH RATIO OF PHOSPHATIC CLAYS

FIGURE 2-10

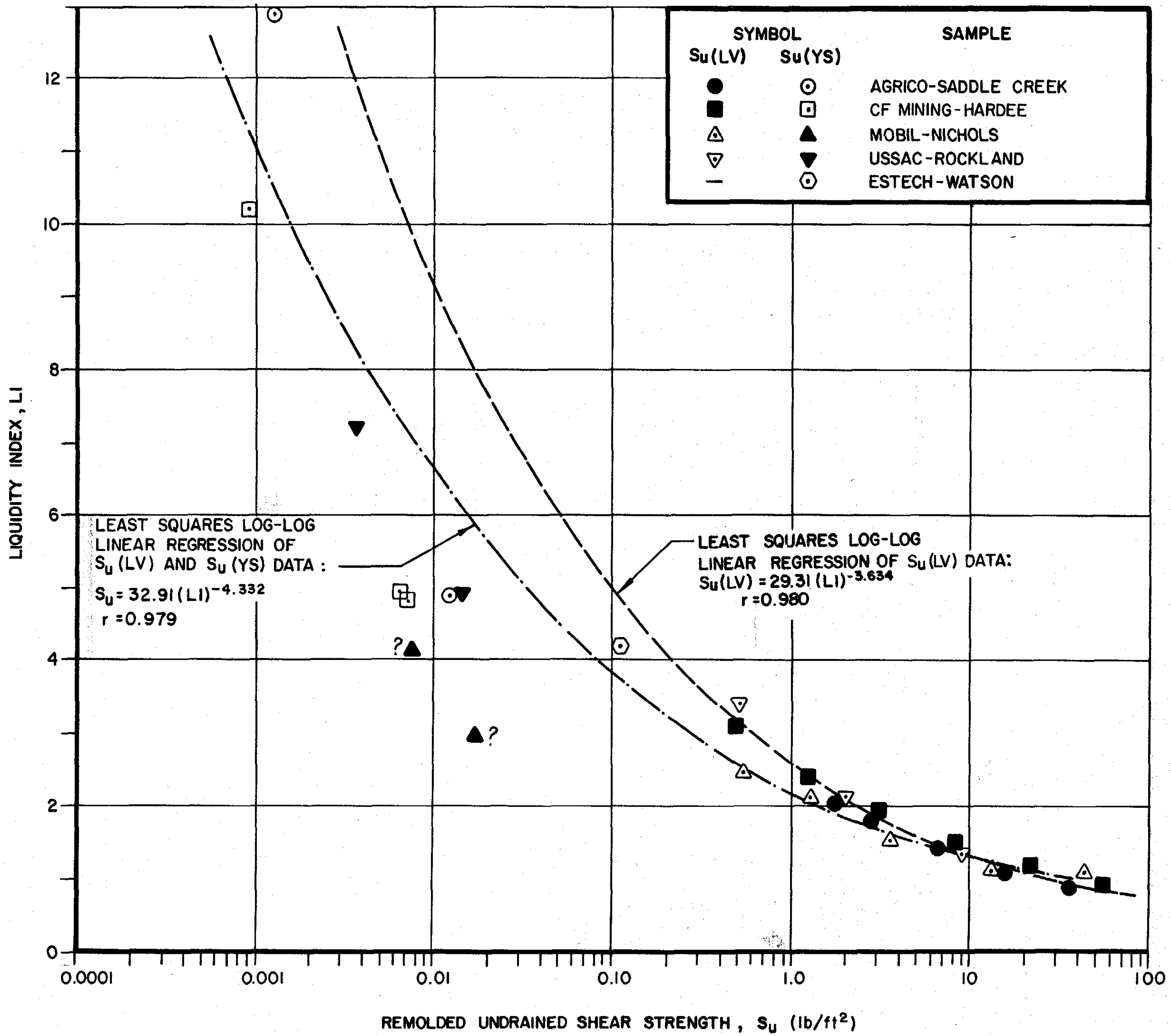

LIQUIDITY INDEX VERSUS REMOLDED LAB VANE AND YIELD STRESS UNDRAINED SHEAR STRENGTH

SYMBOL	SAMPLE	LL (%)	PI (%)	SPECIMEN	INITIAL ω_n (%)	INITIAL γ_t (pcf)	PRE-SHEAR ω_n (%)	PRE-SHEAR γ_t (pcf)	$S_u/\bar{\sigma}_c$	At $(\bar{\sigma}_1-\bar{\sigma}_3)_{max}$ ξ (%)	$\bar{\phi}$ (°)	A FACTOR	At $(\bar{\sigma}_1/\bar{\sigma}_3)_{max}$ ξ (%)	$\bar{\phi}$ (°)	A FACTOR
△	AGRICO-SADDLE CREEK	268	222	S8	190.1	77.7	109.4	90.0	0.27	6.9	28.2	1.28	10.9	29.8	1.42
				S9	205.1	76.9	130.6	86.5	0.29	6.7	29.5	1.14	10.6	31.1	1.26
■	CF MINING-HARDEE	143	113	S1	111.5	90.1	86.6	95.4	0.32	5.7	28.6	1.03	9.6	28.8	1.17
				S3	113.4	91.3	116.4	88.9	0.34	7.4	29.3	0.92	9.5	29.9	0.97
▽	IMC-NORALYN	213	181	S2	168.8	81.2	104.0	91.4	0.35	12.4	30.8	0.96	14.3	31.4	0.98
				S4	140.3	84.3	114.3	89.4	0.32	7.5	29.5	1.05	11.3	31.1	1.17
▲	MOBIL-NICHOLS	203	164	S3	122.5	86.8	89.2	95.4	0.34	12.0	32.4	1.02	14.4	33.2	1.05
⊙	OXY-SUWANNEE RIVER	182	142	S4	146.4	76.1	91.7	93.7	0.32	8.7	33.0	1.14	13.0	35.6	1.25
⊡	USSAC-ROCKLAND	195	160	S1	143.4	85.2	110.0	90.1	0.33	8.4	32.4	1.05	12.8	34.8	1.16
				S4	139.6	85.5	91.3	94.1	0.28	8.9	26.8	1.23	9.4	26.8	1.26

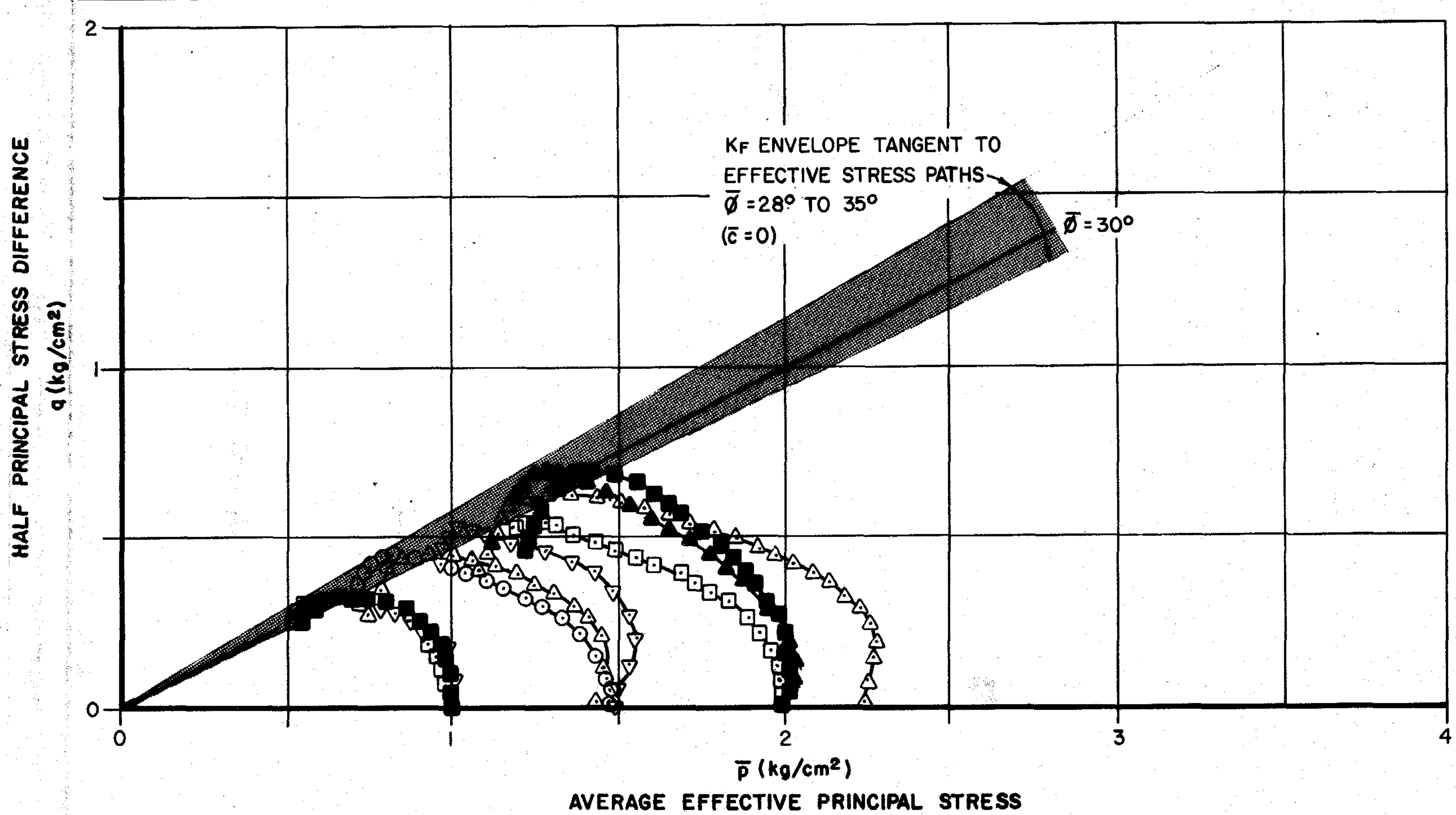

FIGURE 2-11

UNDRAINED EFFECTIVE STRESS PATHS FROM REPRESENTATIVE CIUC TESTS ON NORMALLY CONSOLIDATED PHOSPHATIC CLAY

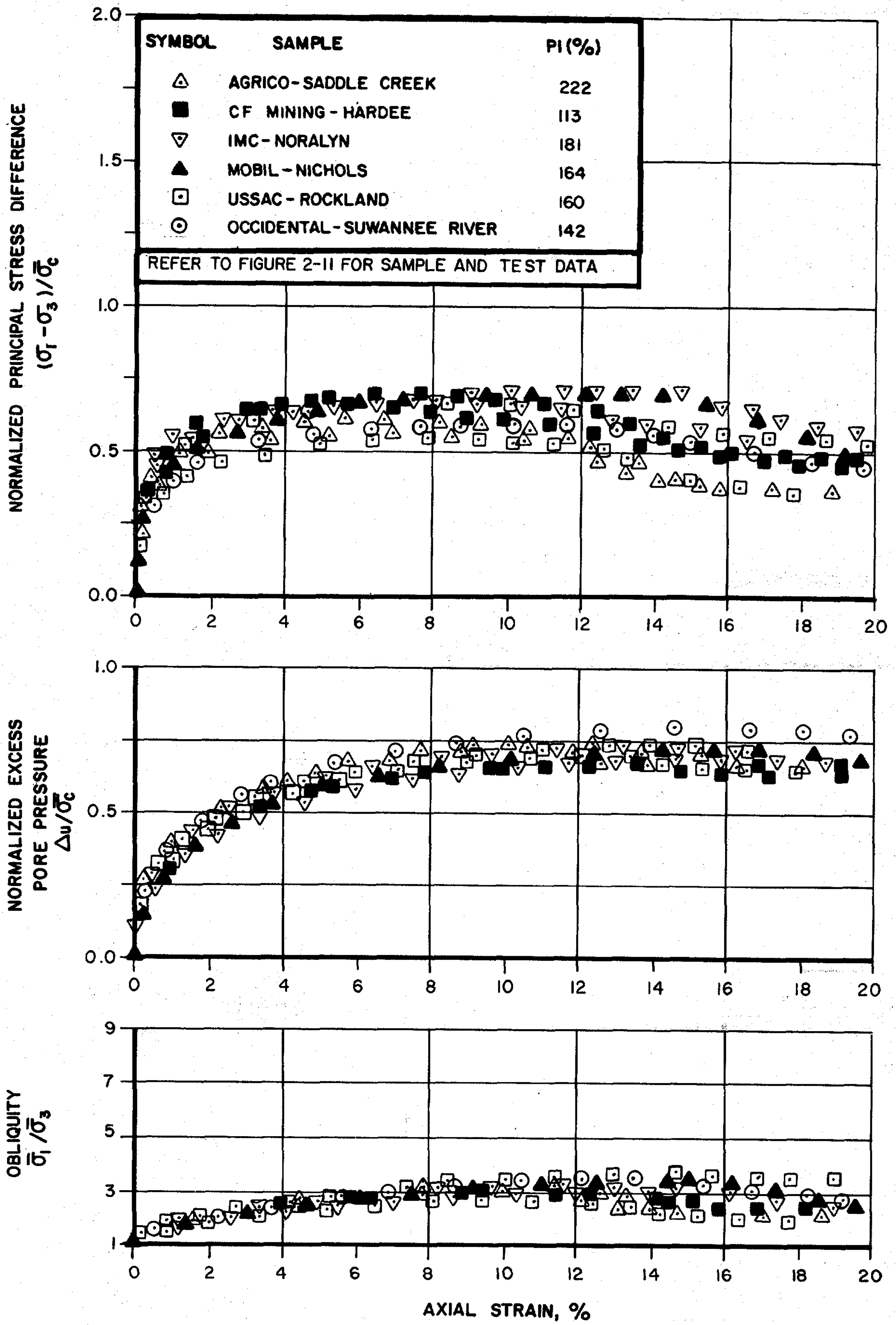

UNDRAINED STRESS-STRAIN BEHAVIOR FROM REPRESENTATIVE CIUC TESTS ON NORMALLY CONSOLIDATED PHOSPHATIC CLAY

FIGURE 2-12

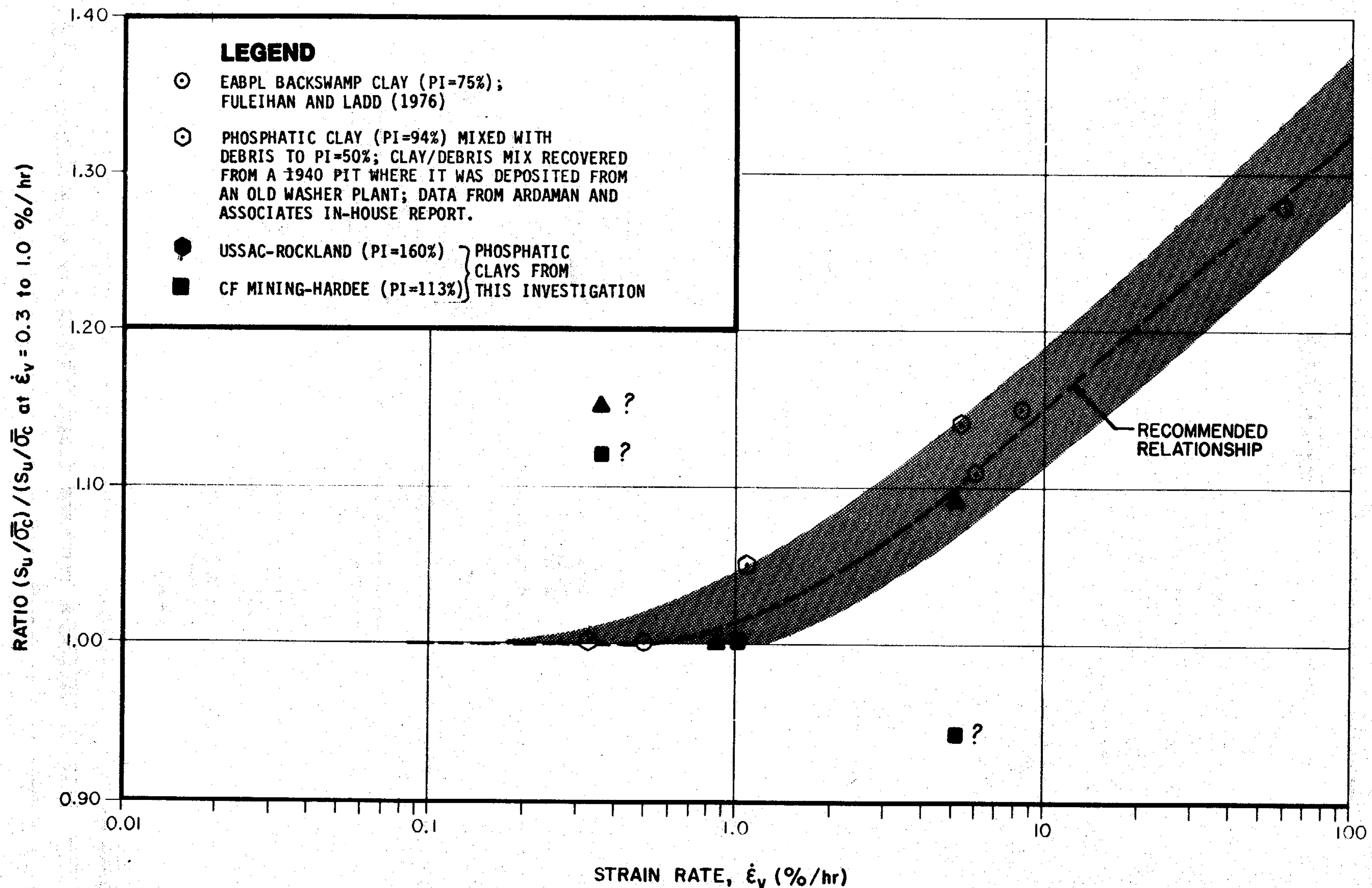

FIGURE 2-13

EFFECT OF STRAIN RATE ON NORMALIZED UNDRAINED SHEAR STRENGTH RATIO FROM $\overline{\text{CIUC}}$ TESTS ON NORMALLY CONSOLIDATED CLAY

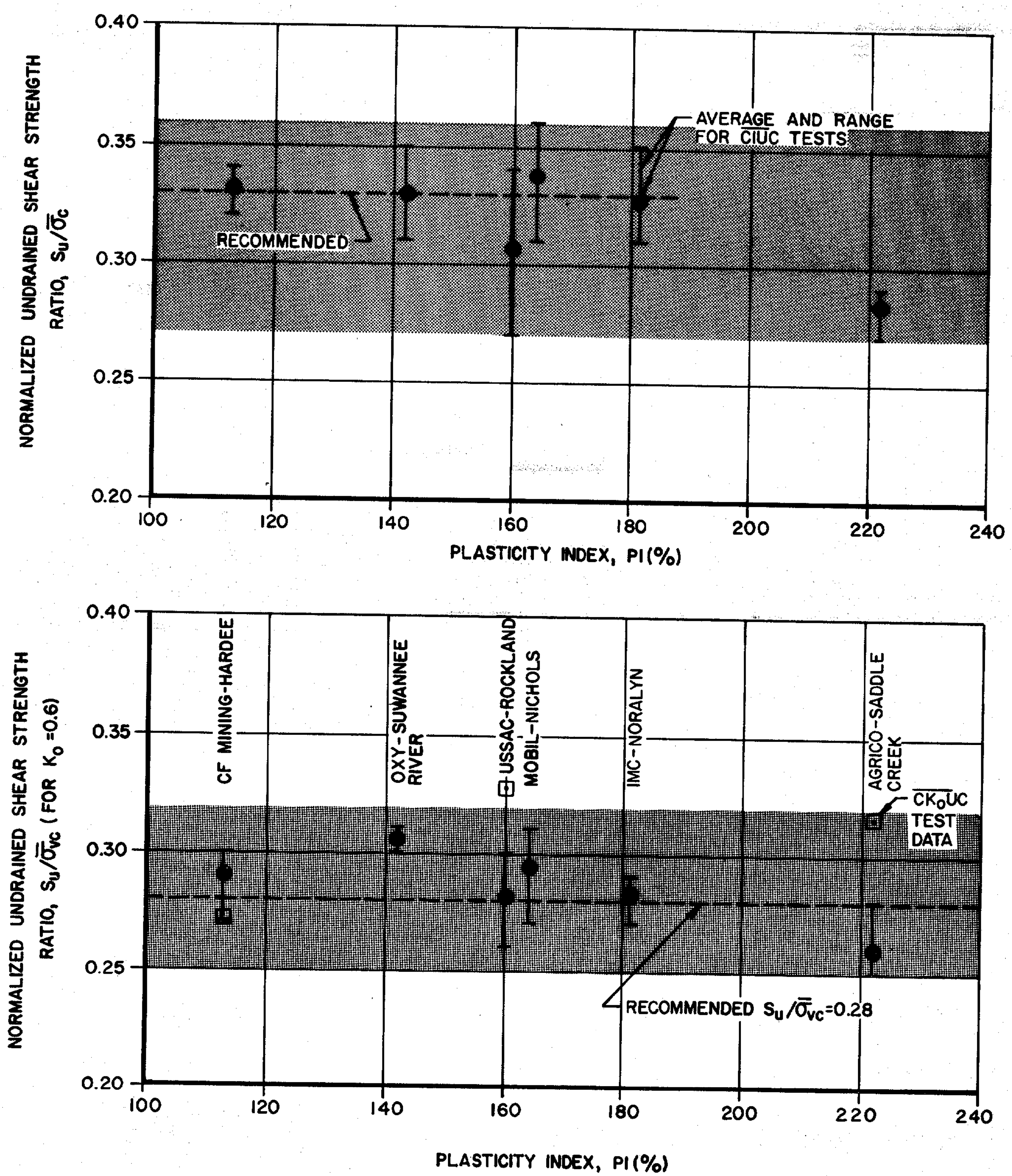

NORMALIZED UNDRAINED SHEAR STRENGTH RATIO VERSUS PLASTICITY INDEX FROM $\overline{CIUC}$ TESTS ON NORMALLLY CONSOLIDATED PHOSPHATIC CLAYS

FIGURE 2-14

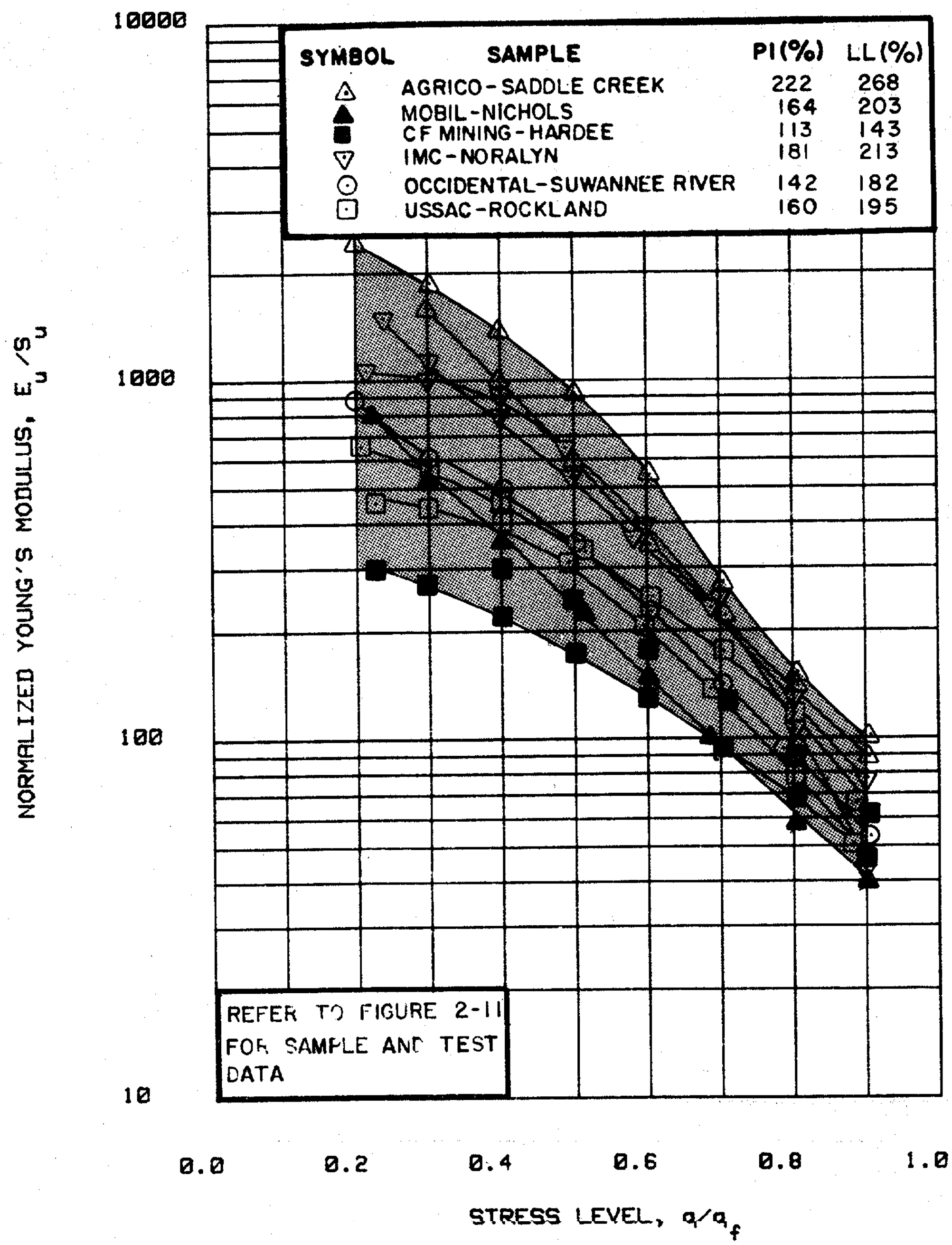

NORMALIZED UNDRAINED YOUNG'S SECANT MODULUS VERSUS STRESS LEVEL FROM REPRESENTATIVE $\overline{\text{CIUC}}$ TESTS ON NORMALLY CONSOLIDATED PHOSPHATIC CLAYS

FIGURE 2-15

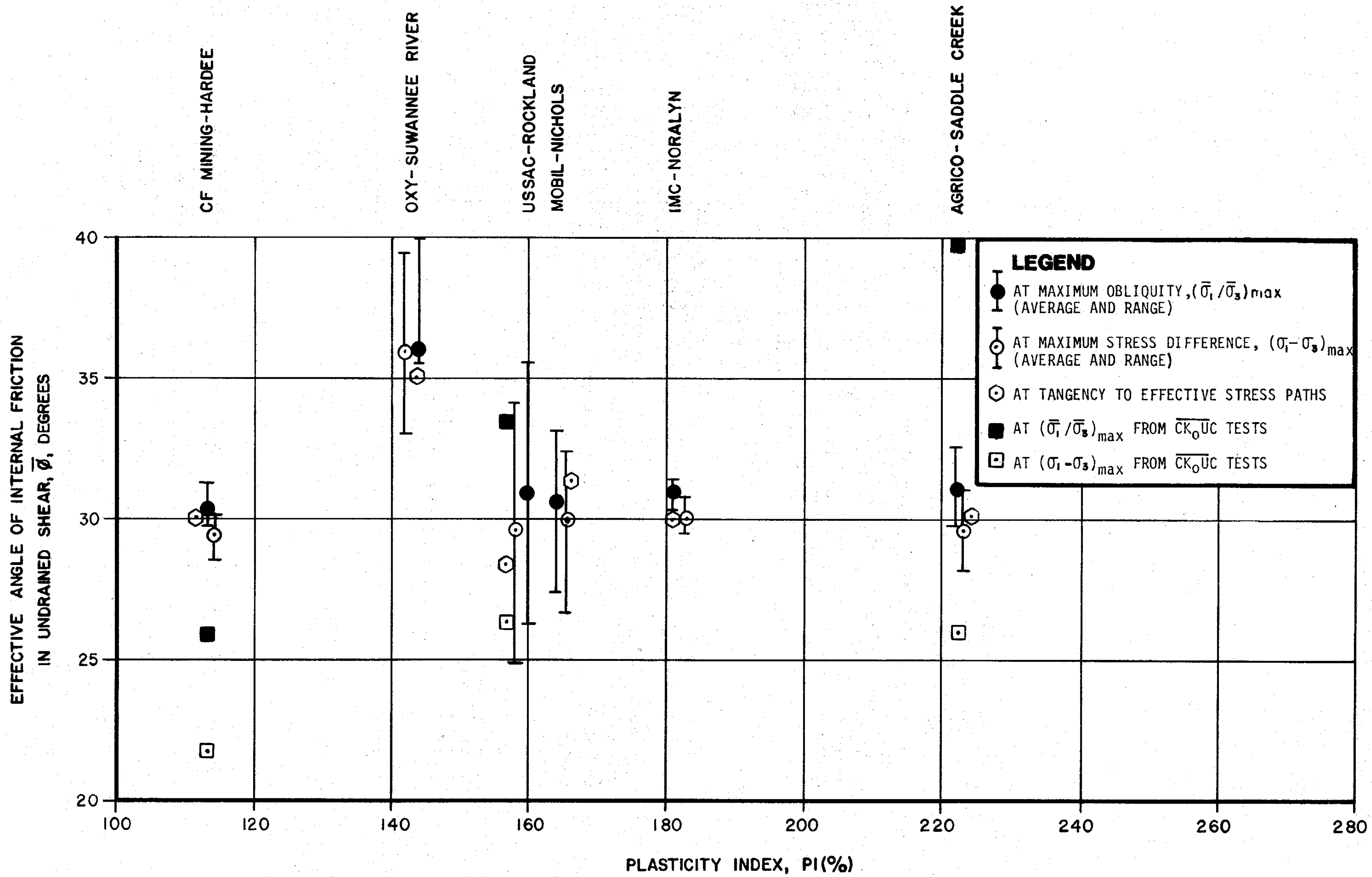

FIGURE 2-16

EFFECTIVE ANGLE OF INTERNAL FRICTION VERSUS PLASTICITY INDEX FROM $\overline{CIUC}$ AND $\overline{CK_oUC}$ TESTS ON NORMALLY CONSOLIDATED PHOSPHATIC CLAYS

FIGURE 2-17

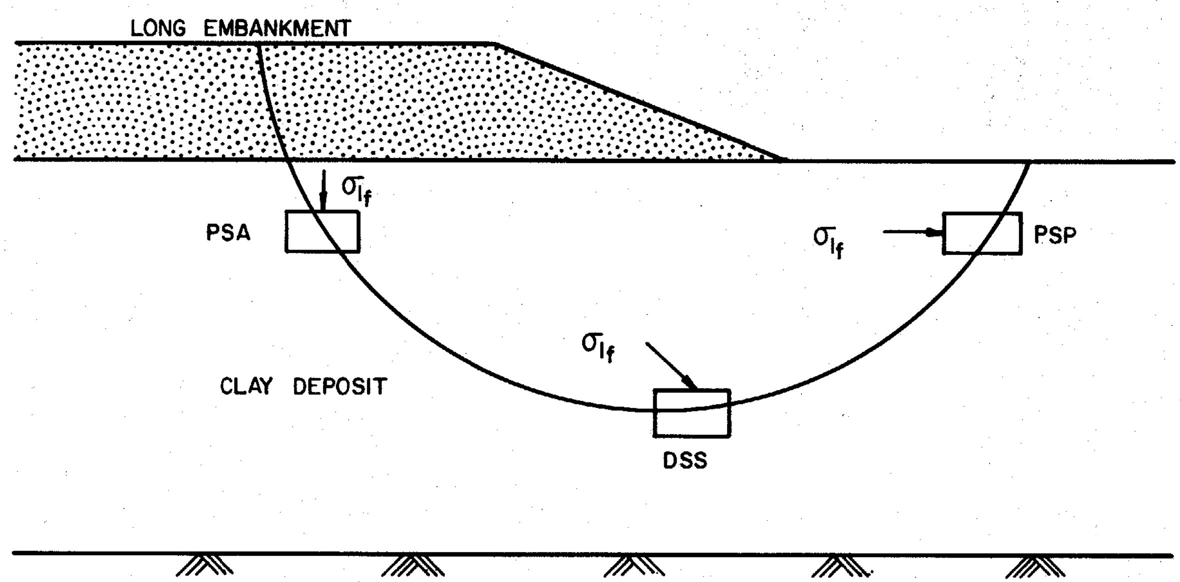

STRESS SYSTEMS ALONG A TYPICAL FAILURE SURFACE

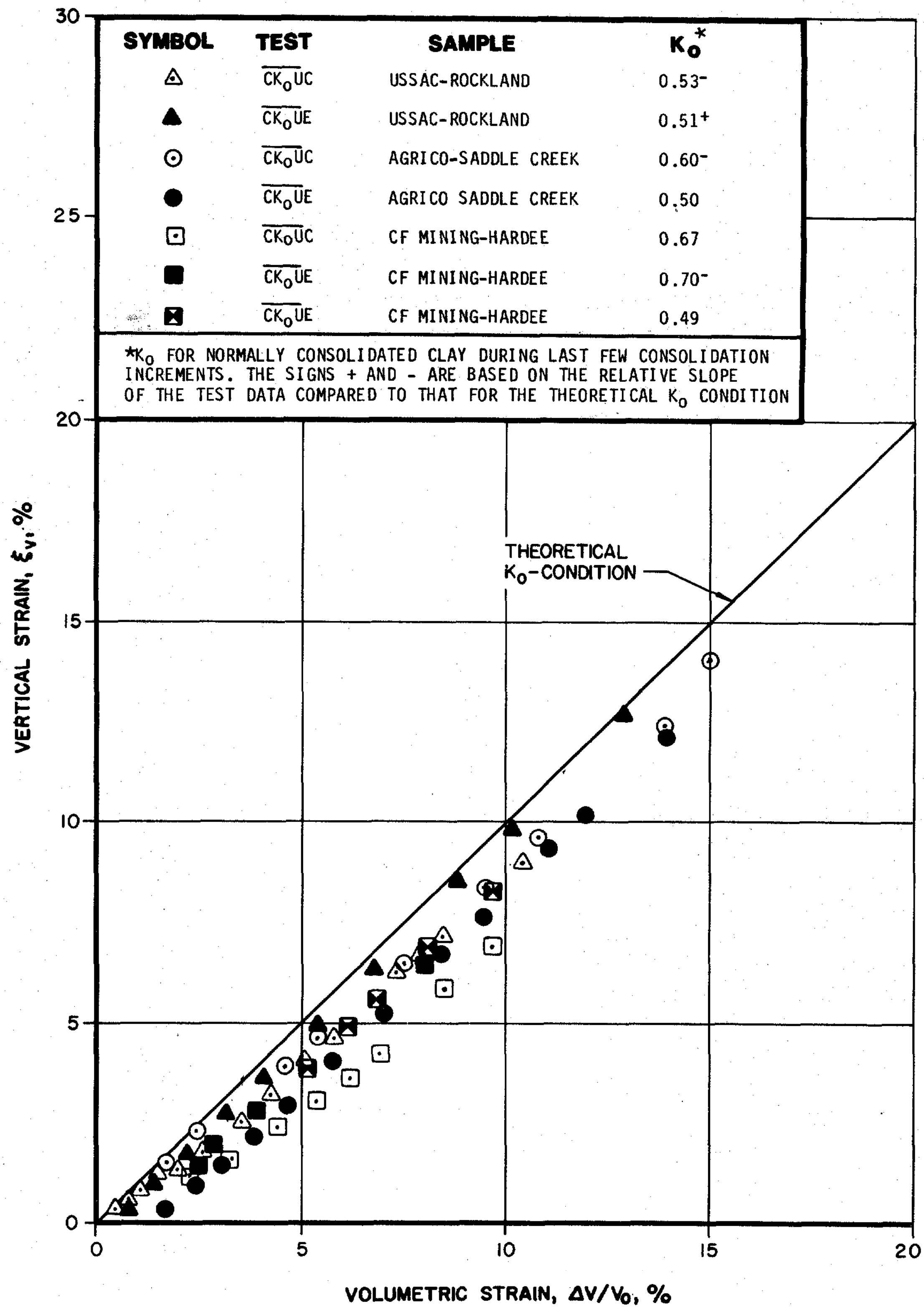

VERTICAL VERSUS VOLUMETRIC CONSOLIDATION STRAIN FROM $\overline{CK_oU}$ TRIAXIAL TESTS ON PHOSPHATIC CLAY

FIGURE 2-18

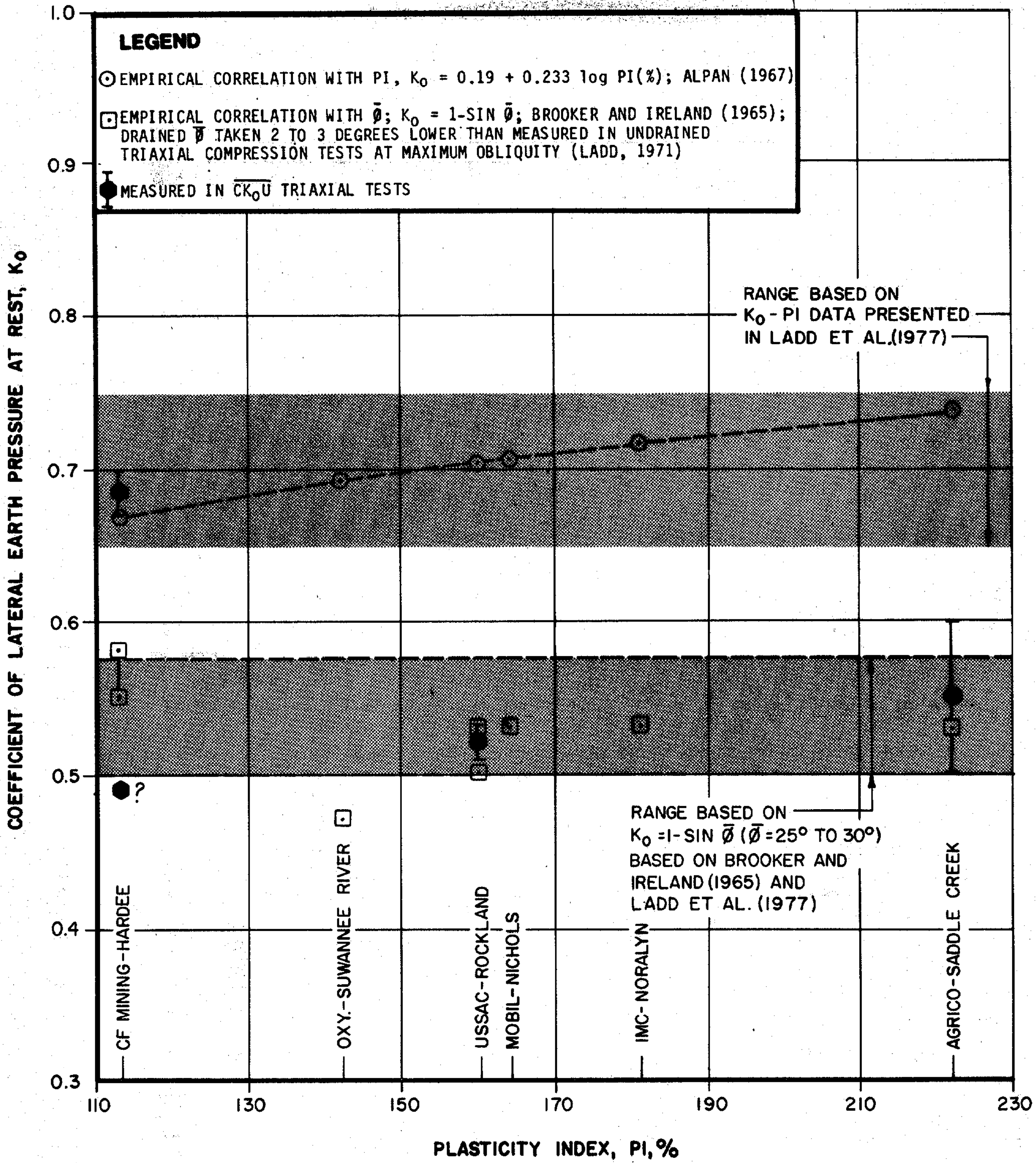

K_o VERSUS PLASTICITY INDEX OF NORMALLY CONSOLIDATED PHOSPHATIC CLAYS

FIGURE 2-20

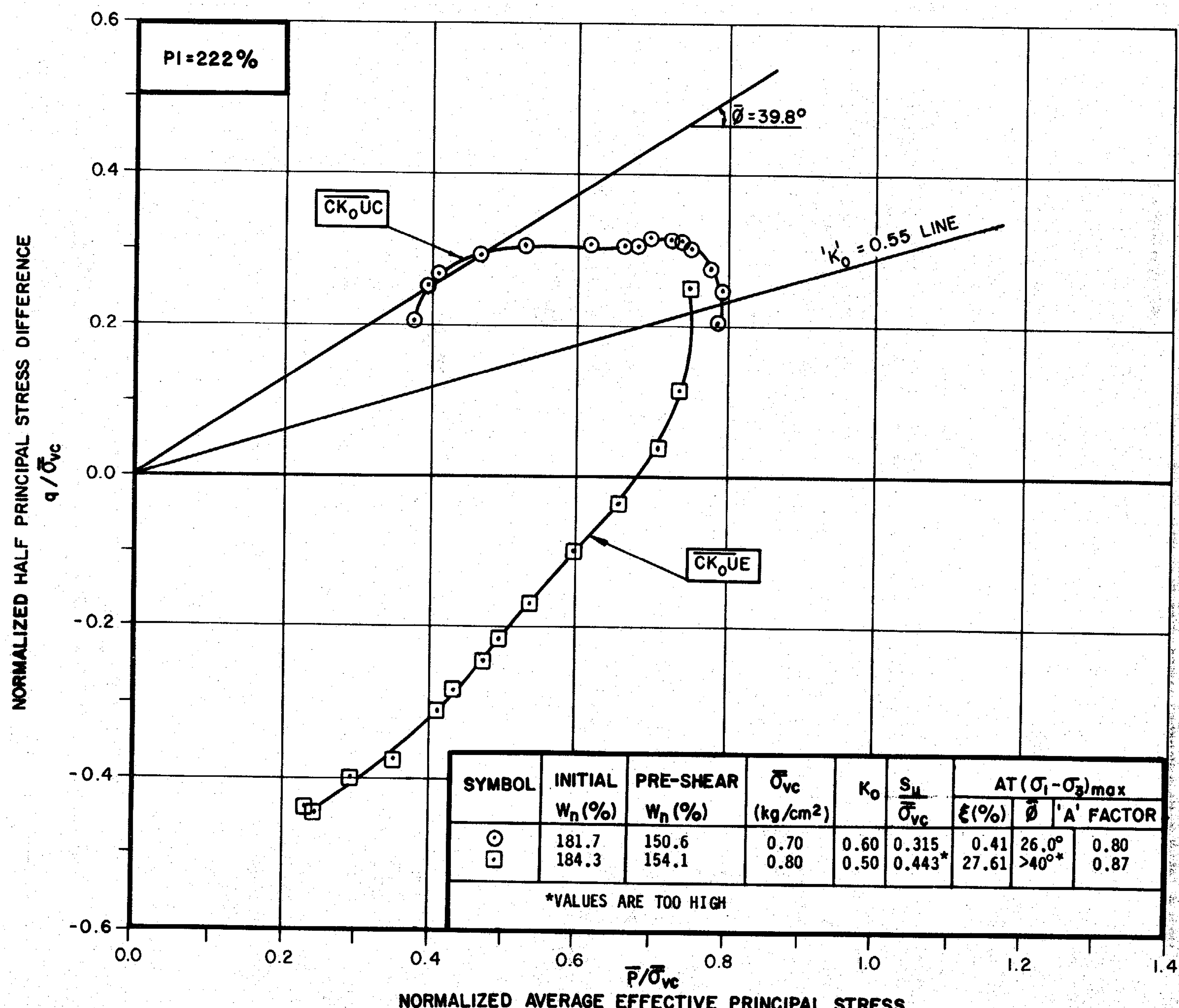

SYMBOL	INITIAL W_n (%)	PRE-SHEAR W_n (%)	$\bar{\sigma}_{vc}$ (kg/cm²)	K_o	$S_u/\bar{\sigma}_{vc}$	AT $(\sigma_1-\sigma_3)max$ ϵ (%)	$\bar{\phi}$	'A' FACTOR
⊙	181.7	150.6	0.70	0.60	0.315	0.41	26.0°	0.80
⊡	184.3	154.1	0.80	0.50	0.443*	27.61	>40°*	0.87

*VALUES ARE TOO HIGH

NORMALIZED UNDRAINED EFFECTIVE STRESS PATHS FROM $\overline{CK_oUC}$ AND $\overline{CK_oUE}$ TESTS ON AGRICO-SADDLE CREEK NORMALLY CONSOLIDATED PHOSPHATIC CLAY

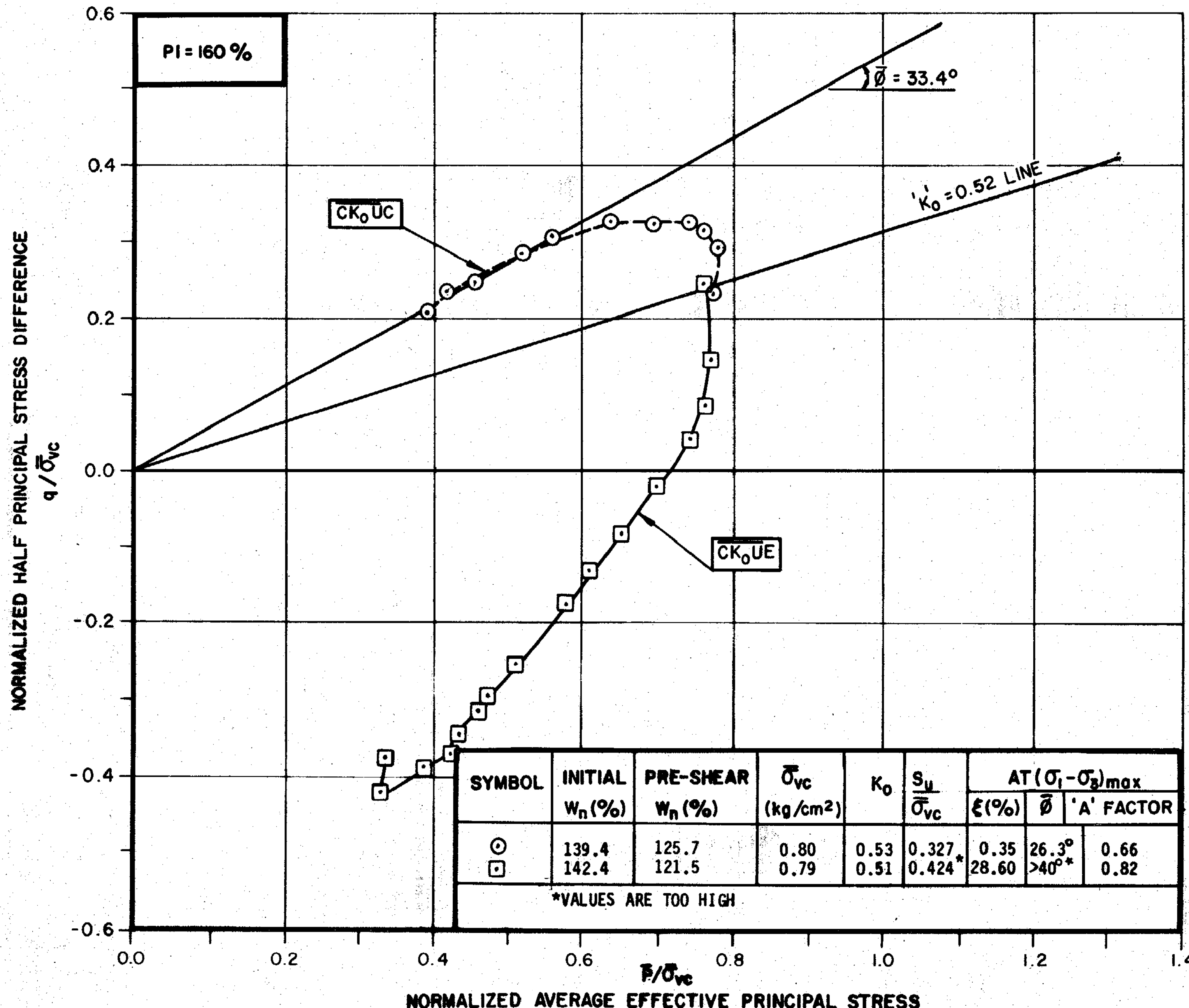

SYMBOL	INITIAL W_n (%)	PRE-SHEAR W_n (%)	$\bar{\sigma}_{vc}$ (kg/cm²)	K_o	$S_u/\bar{\sigma}_{vc}$	AT $(\sigma_1-\sigma_3)_{max}$ ϵ (%)	$\bar{\phi}$	'A' FACTOR
⊙	139.4	125.7	0.80	0.53	0.327	0.35	26.3°	0.66
⊡	142.4	121.5	0.79	0.51	0.424*	28.60	>40°*	0.82

*VALUES ARE TOO HIGH

NORMALIZED UNDRAINED EFFECTIVE STRESS PATHS FROM $\overline{CK_oUC}$ AND $\overline{CK_oUE}$ TESTS ON USSAC-ROCKLAND NORMALLY CONSOLIDATED PHOSPHATIC CLAY

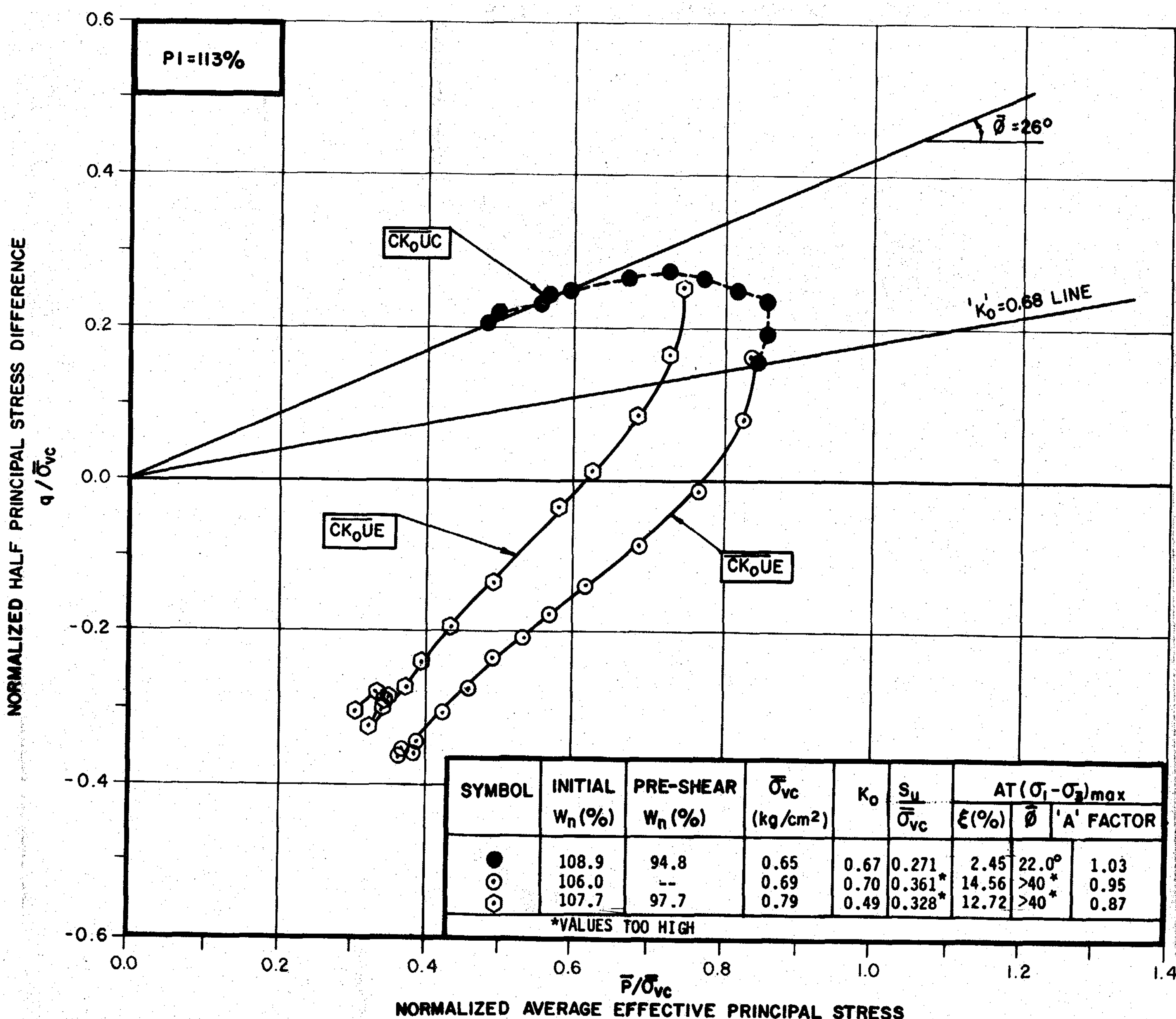

SYMBOL	INITIAL W_n (%)	PRE-SHEAR W_n (%)	$\bar{\sigma}_{vc}$ (kg/cm²)	K_o	$S_u/\bar{\sigma}_{vc}$	AT $(\sigma_1-\sigma_3)_{max}$ ϵ (%)	$\bar{\phi}$	'A' FACTOR
●	108.9	94.8	0.65	0.67	0.271	2.45	22.0°	1.03
⊙	106.0	--	0.69	0.70	0.361*	14.56	>40*	0.95
⬡	107.7	97.7	0.79	0.49	0.328*	12.72	>40*	0.87

*VALUES TOO HIGH

FIGURE 2-22

NORMALIZED UNDRAINED EFFECTIVE STRESS PATHS FROM $\overline{CK_oUC}$ AND $\overline{CK_oUE}$ TESTS ON CF MINING-HARDEE NORMALLY CONSOLIDATED PHOSPHATIC CLAY

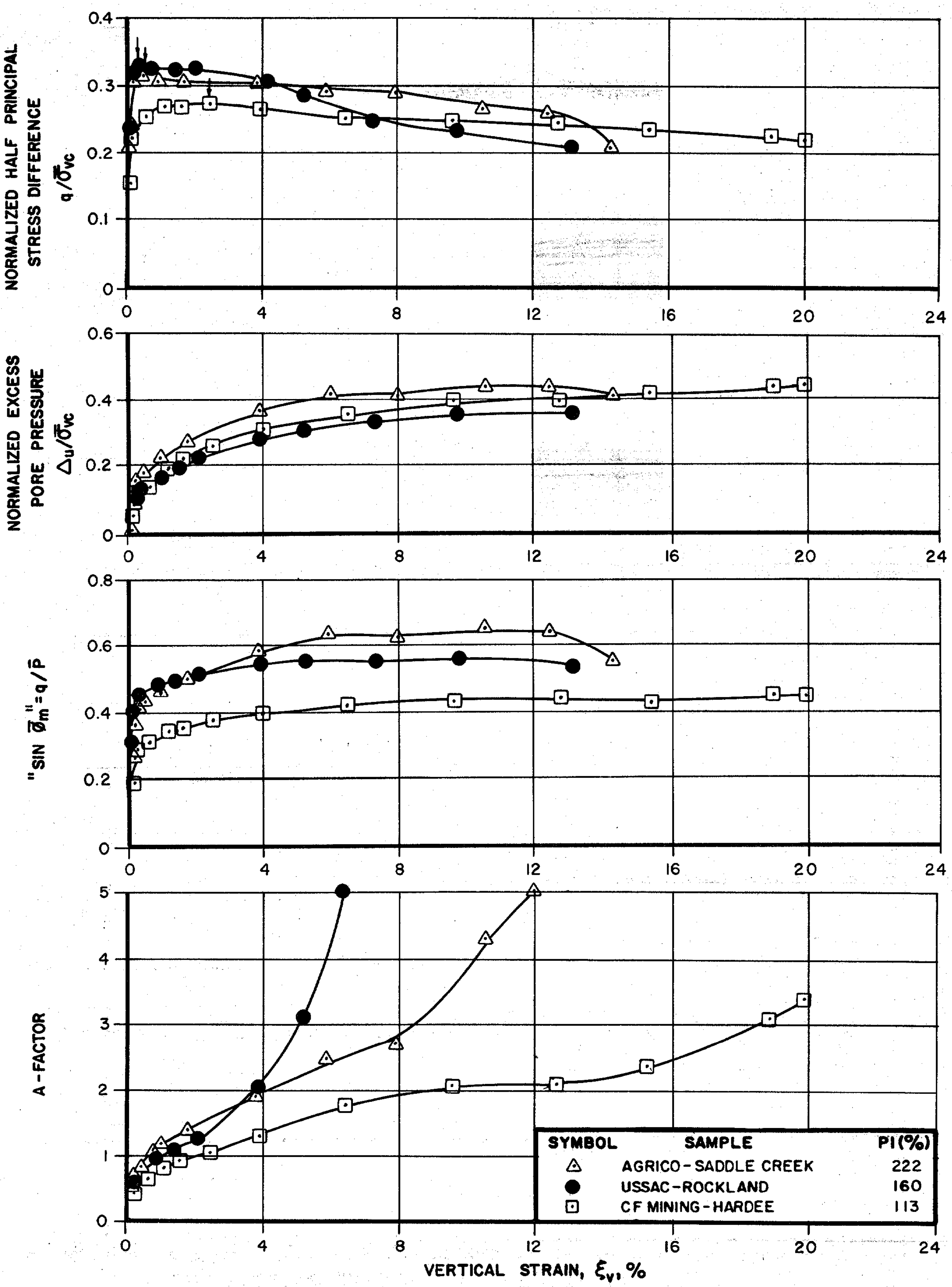

UNDRAINED STRESS-STRAIN BEHAVIOR FROM $\overline{CK_oUC}$ TESTS ON NORMALLY CONSOLIDATED PHOSPHATIC CLAYS

FIGURE 2-23

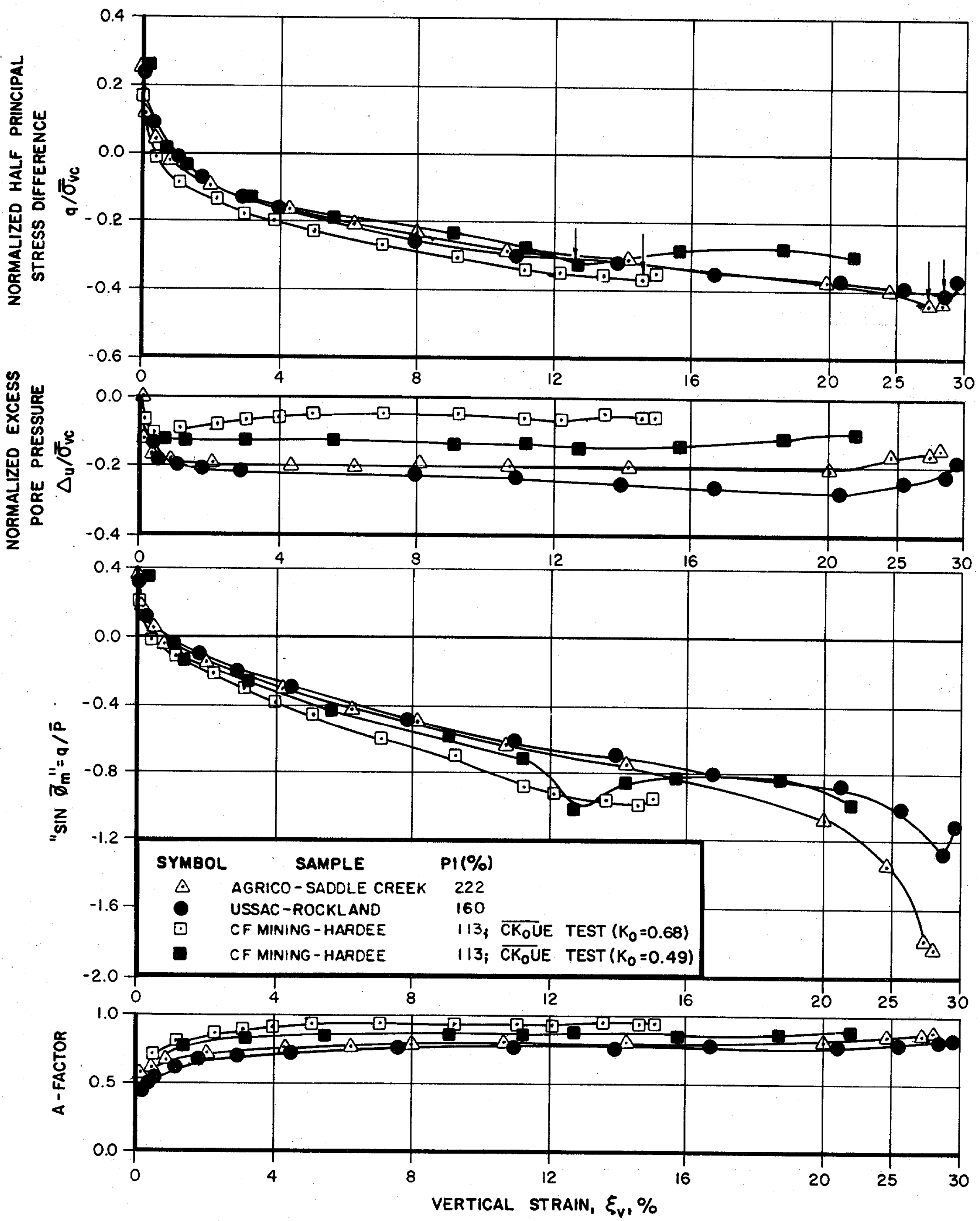

UNDRAINED STRESS-STRAIN BEHAVIOR FROM $\overline{CK_oU}E$ TESTS ON NORMALLY CONSOLIDATED PHOSPHATIC CLAYS

FIGURE 2-24

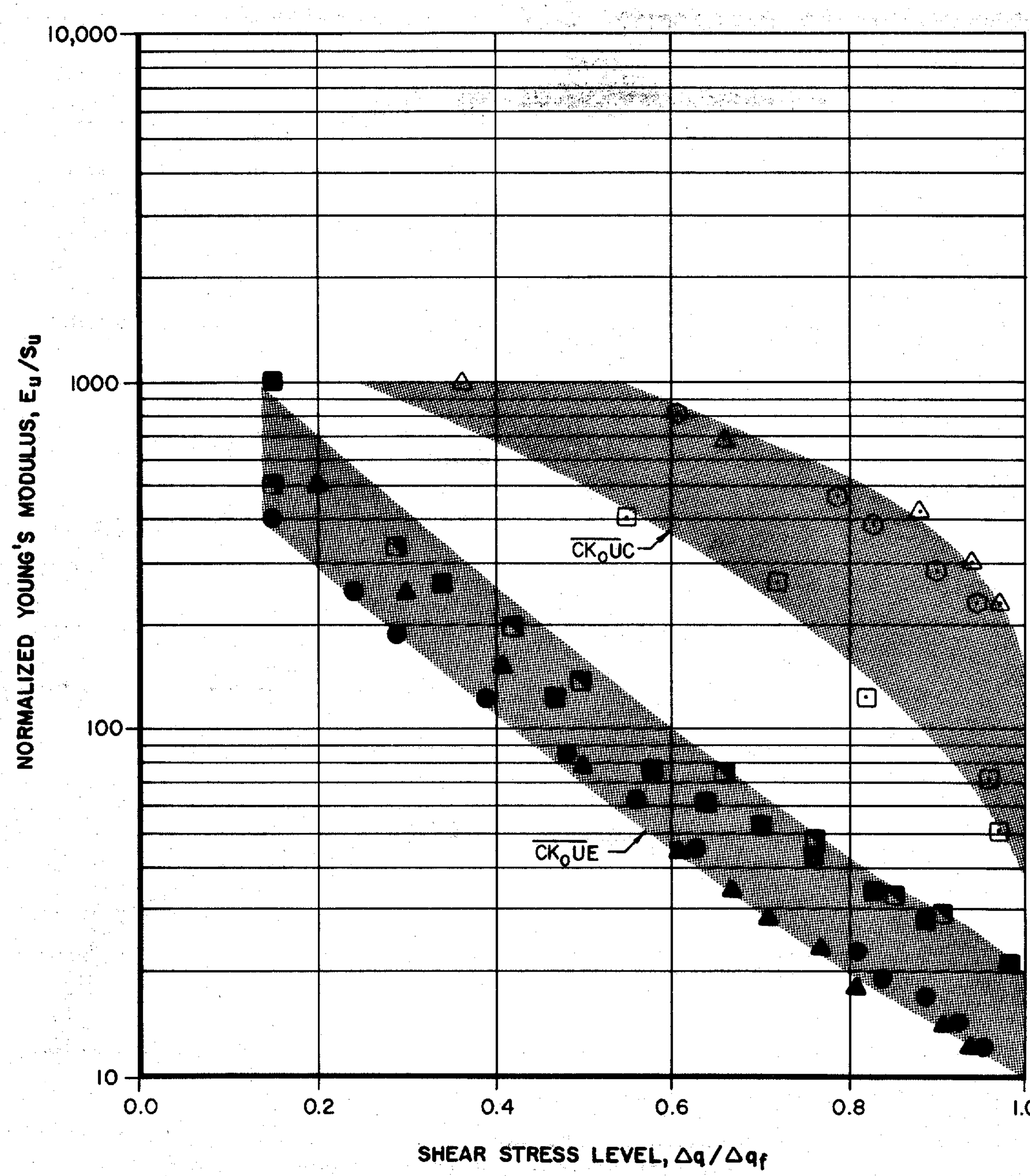

SYMBOL	TEST	SAMPLE	LL(%)	PI(%)
△ ▲	$\overline{CK_oUC}$ $\overline{CK_oUE}$	AGRICO-SADDLE CREEK	268	222
⊙ ●	$\overline{CK_oUC}$ $\overline{CK_oUE}$	USSAC-ROCKLAND	195	160
⊡ ■ ◪	$\overline{CK_oUC}$ $\overline{CK_oUE}$ $\overline{CK_oUE}$	CF MINING-HARDEE	143	113

NORMALIZED UNDRAINED YOUNG'S SECANT MODULUS VERSUS STRESS LEVEL FROM $\overline{CK_oUC}$ AND $\overline{CK_oUE}$ TESTS ON NORMALLY CONSOLIDATED PHOSPHATIC CLAY

FIGURE 2-25

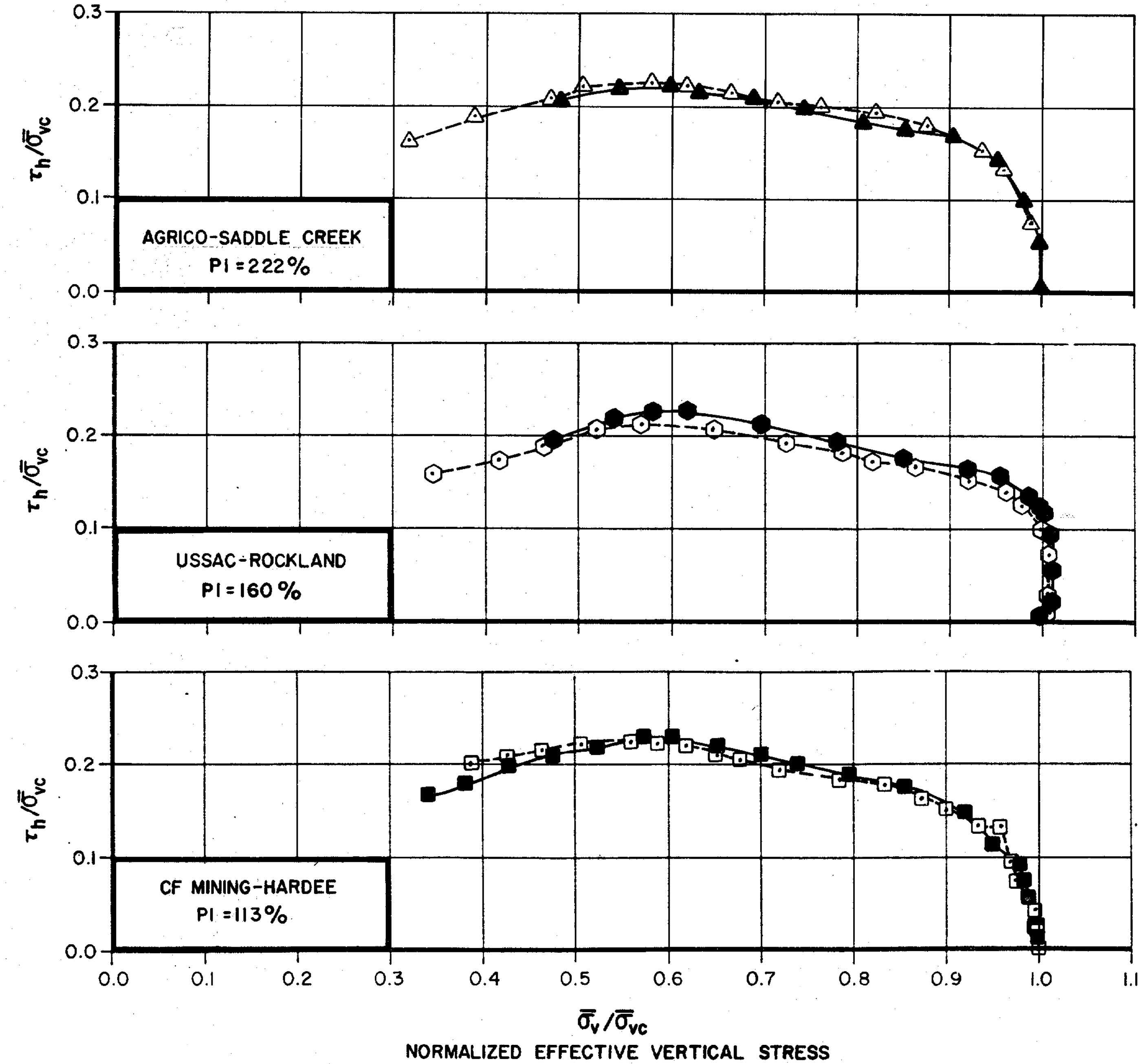

SAMPLE	SYMBOL	SPECIMEN	INITIAL w_n(%)	PRE SHEAR w_n(%)	$\bar{\sigma}_{vc}$ (kg/cm²)	AT τ_h max			
						γ(%)	$\tau_h/\bar{\sigma}_{vc}$	$\bar{\sigma}_v/\bar{\sigma}_{vc}$	E_{u50}/S_u
AGRICO-SADDLE CREEK	▲	B1	192.3	164.1	0.80	19.6	0.222	0.609	360
	△	B2	187.8	133.9	2.00	18.0	0.226	0.579	340
USSAC-ROCKLAND	⬢	C1	136.5	111.6	1.04	23.7	0.227	0.580	308
	⬡	C2	139.8	88.6	2.24	22.0	0.212	0.567	250
CF MINING-HARDEE	⊡	A1	105.4	110.8	0.80	14.6	0.228	0.571	370
	■	A2	107.8	73.4	2.01	18.4	0.231	0.585	240

UNDRAINED EFFECTIVE STRESS PATHS FROM CK_oUDSS TESTS ON NORMALLY CONSOLIDATED PHOSPHATIC CLAY

FIGURE 2-26

FIGURE 2-27

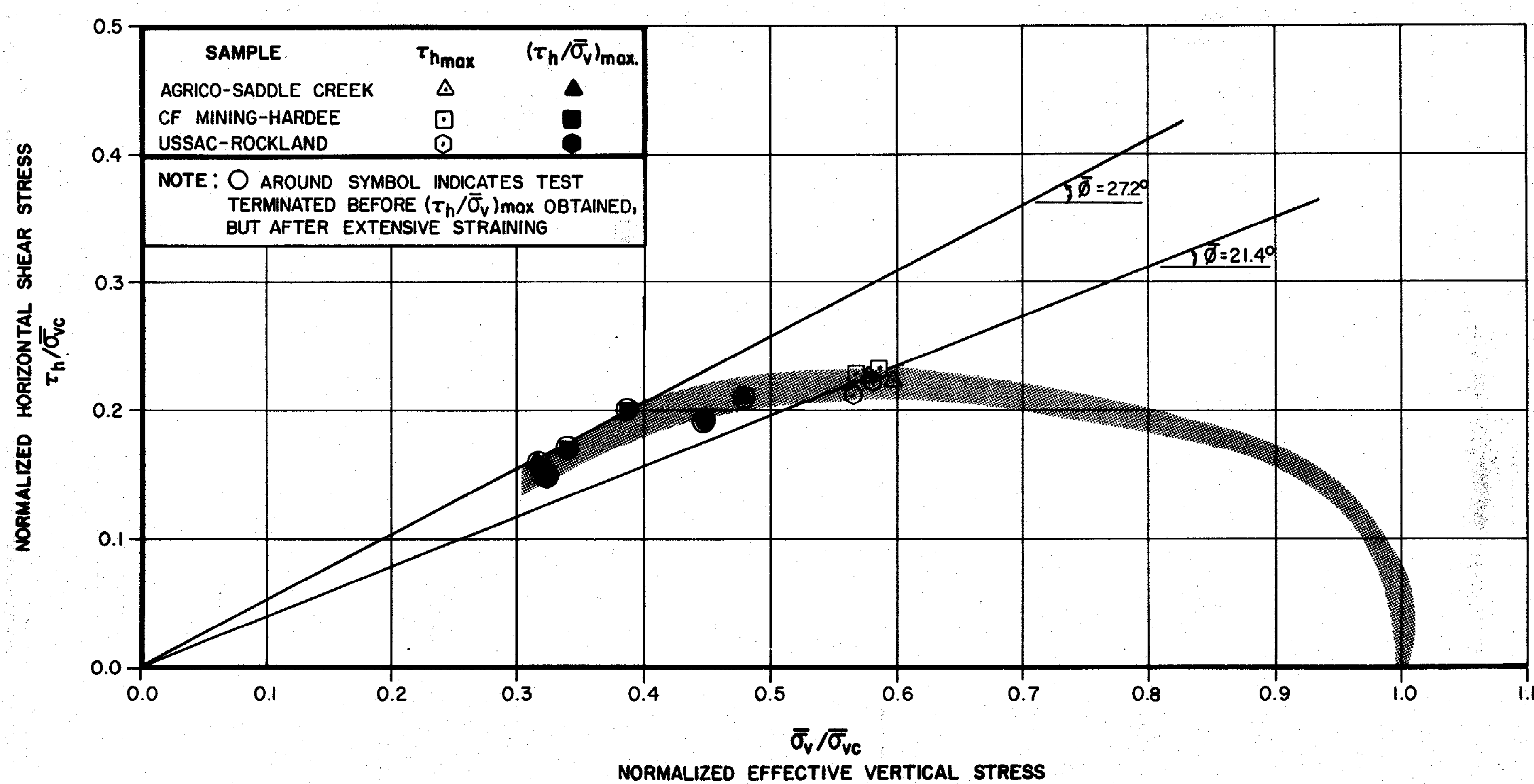

EFFECTIVE FRICTION ANGLE FROM CK_0UDSS TESTS ON NORMALLY CONSOLIDATED PHOSPHATIC CLAYS

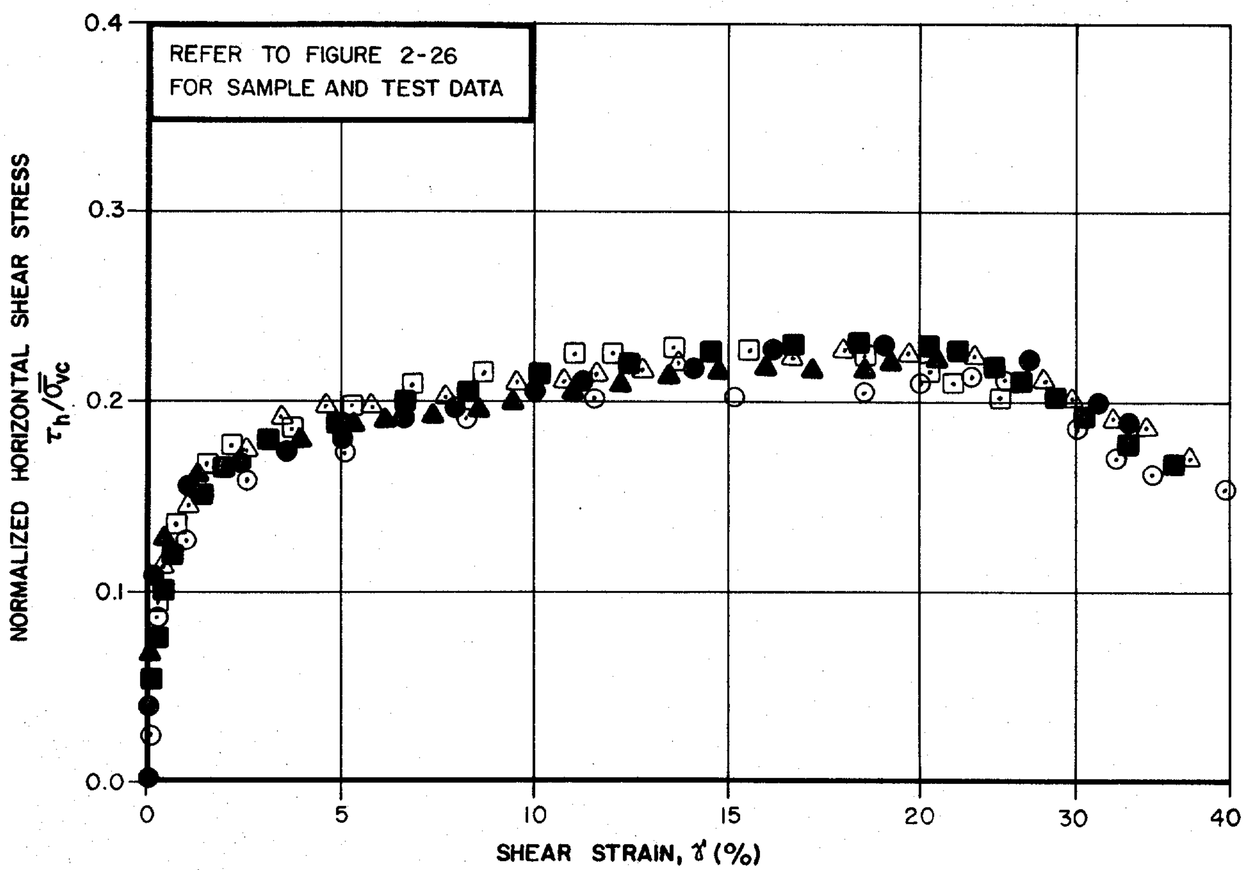

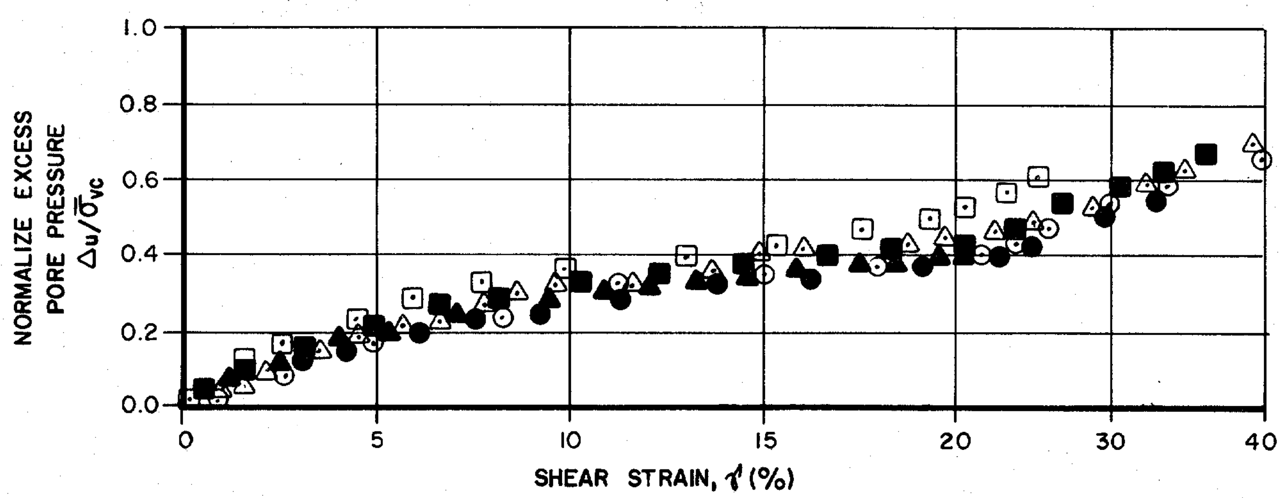

SAMPLE	PI(%)	SYMBOL	SPECIMEN	$\bar{\sigma}_{vc}$ (kg/cm²)
AGRICO-SADDLE CREEK	222	▲ △	B1 B2	0.80 2.00
USSAC-ROCKLAND	160	● ⊙	C1 C2	1.04 2.24
CF MINING-HARDEE	113	⊡ ■	A1 A2	0.80 2.01

UNDRAINED STRESS-STRAIN BEHAVIOR FROM CK_oUDSS TESTS ON NORMALLY CONSOLIDATED PHOSPHATIC CLAYS

FIGURE 2-28

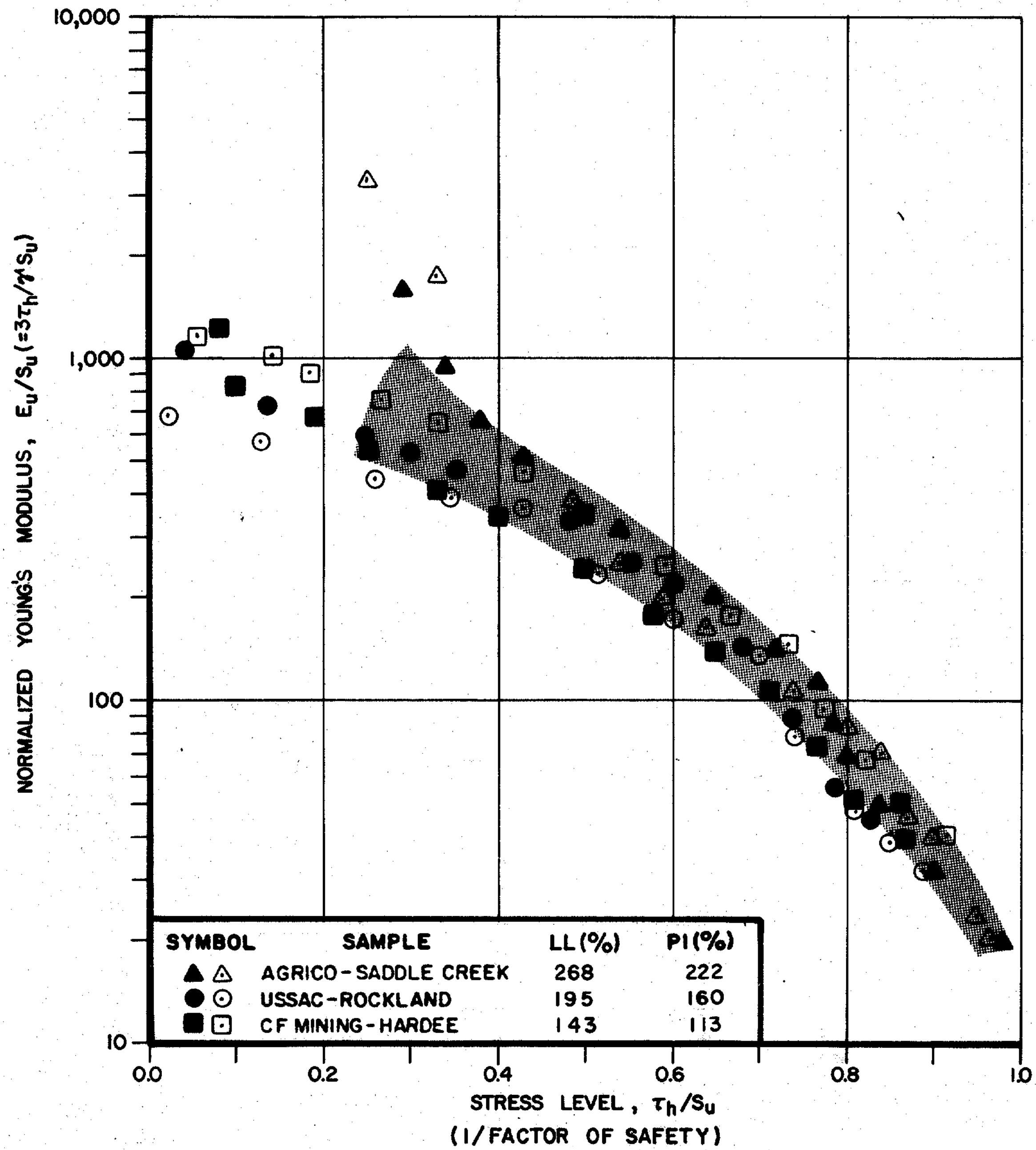

NORMALIZED UNDRAINED YOUNG'S SECANT MODULUS VERSUS STRESS LEVEL FROM CK_oUDSS TESTS ON NORMALLY CONSOLIDATED PHOSPHATIC CLAY

FIGURE 2-29

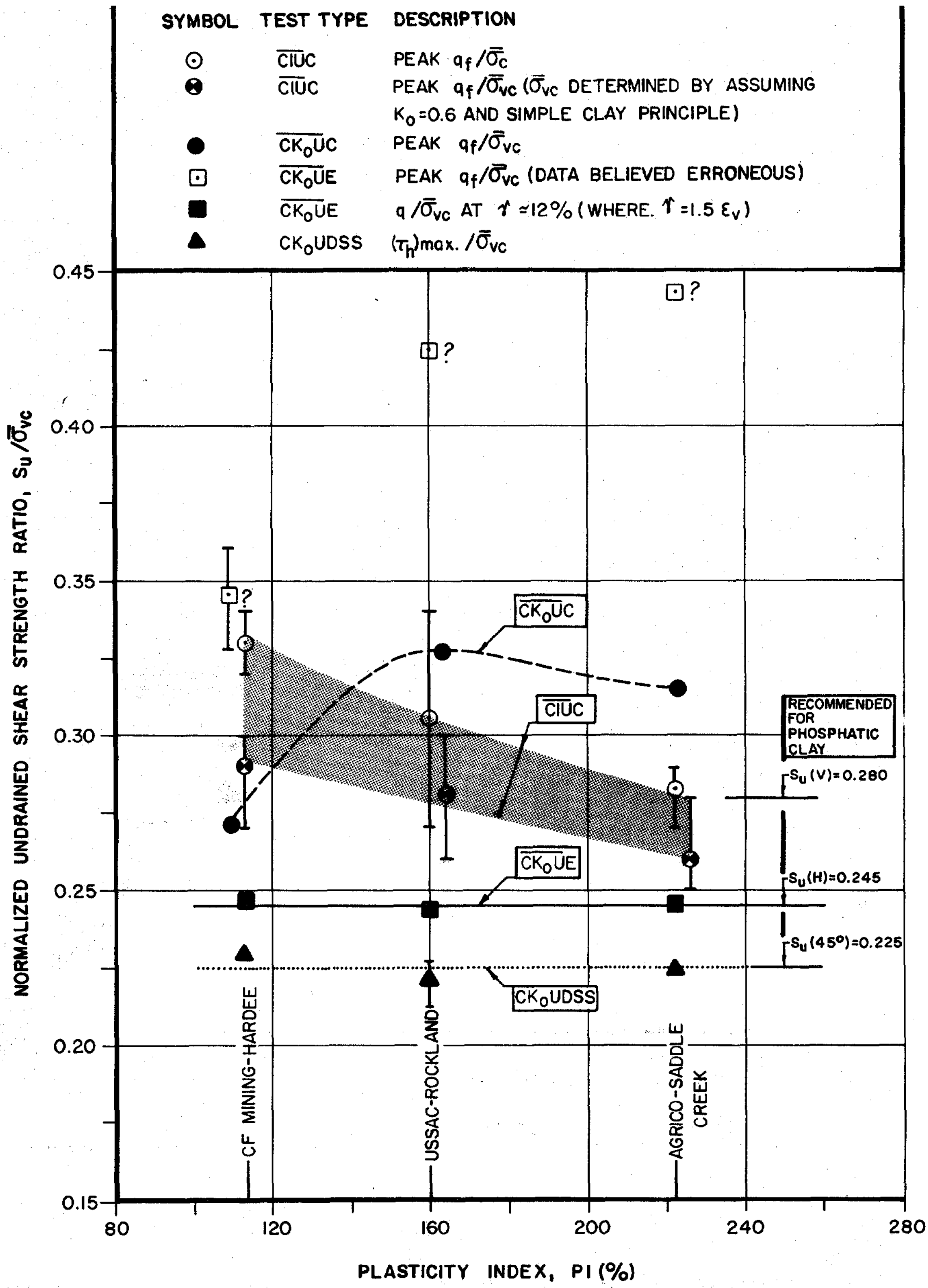

SUMMARY OF NORMALIZED STRESS SYSTEM UNDRAINED SHEAR STRENGTH RATIO VERSUS PLASTICITY INDEX FOR NORMALLY CONSOLIDATED PHOSPHATIC CLAYS

FIGURE 2-30

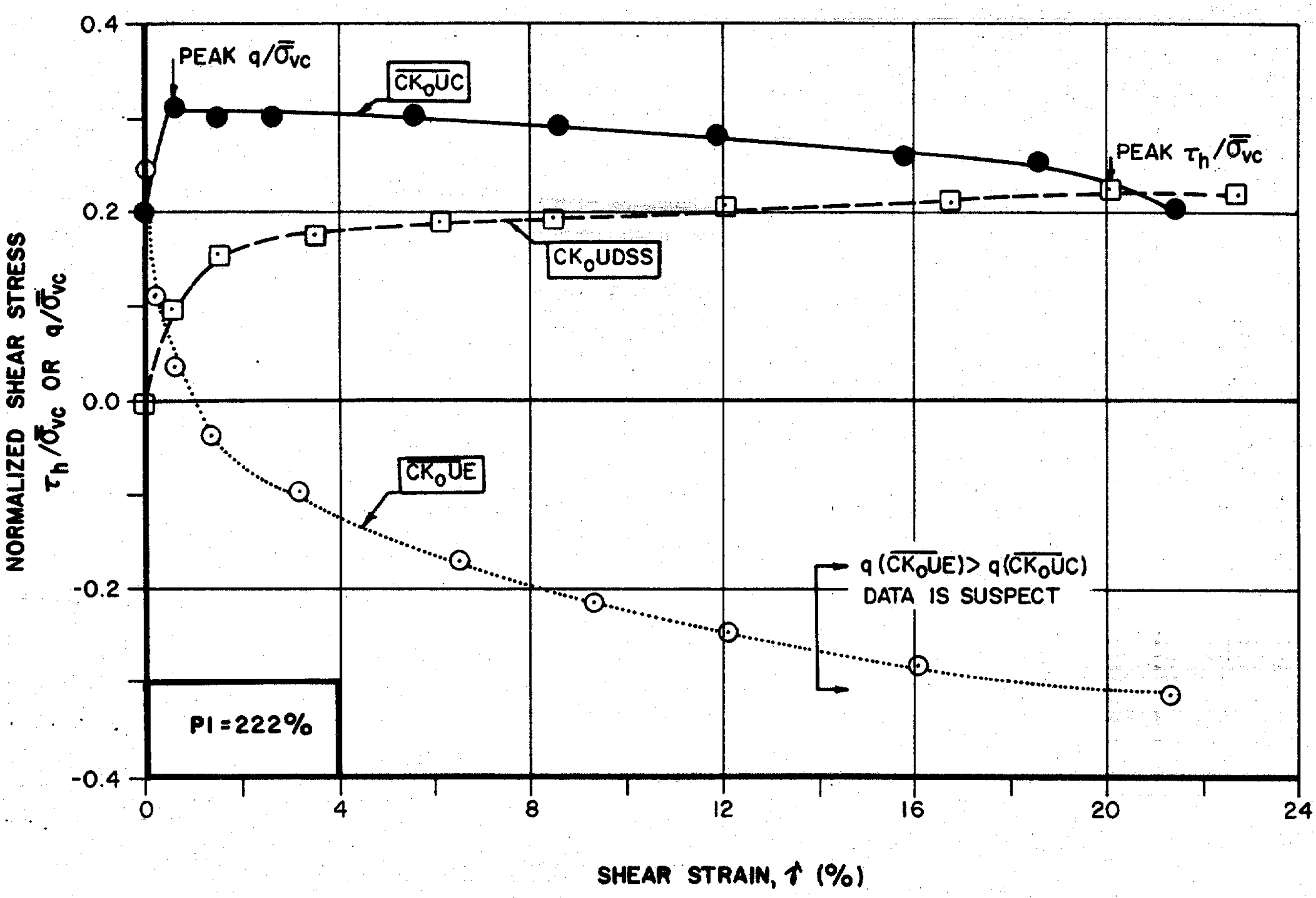

NORMALIZED SHEAR STRESS VERSUS SHEAR STRAIN AS A FUNCTION OF STRESS SYSTEM FROM $\overline{CK_oU}$ TESTS ON AGRICO-SADDLE CREEK NORMALLY CONSOLIDATED PHOSPHATIC CLAY

FIGURE 2-31

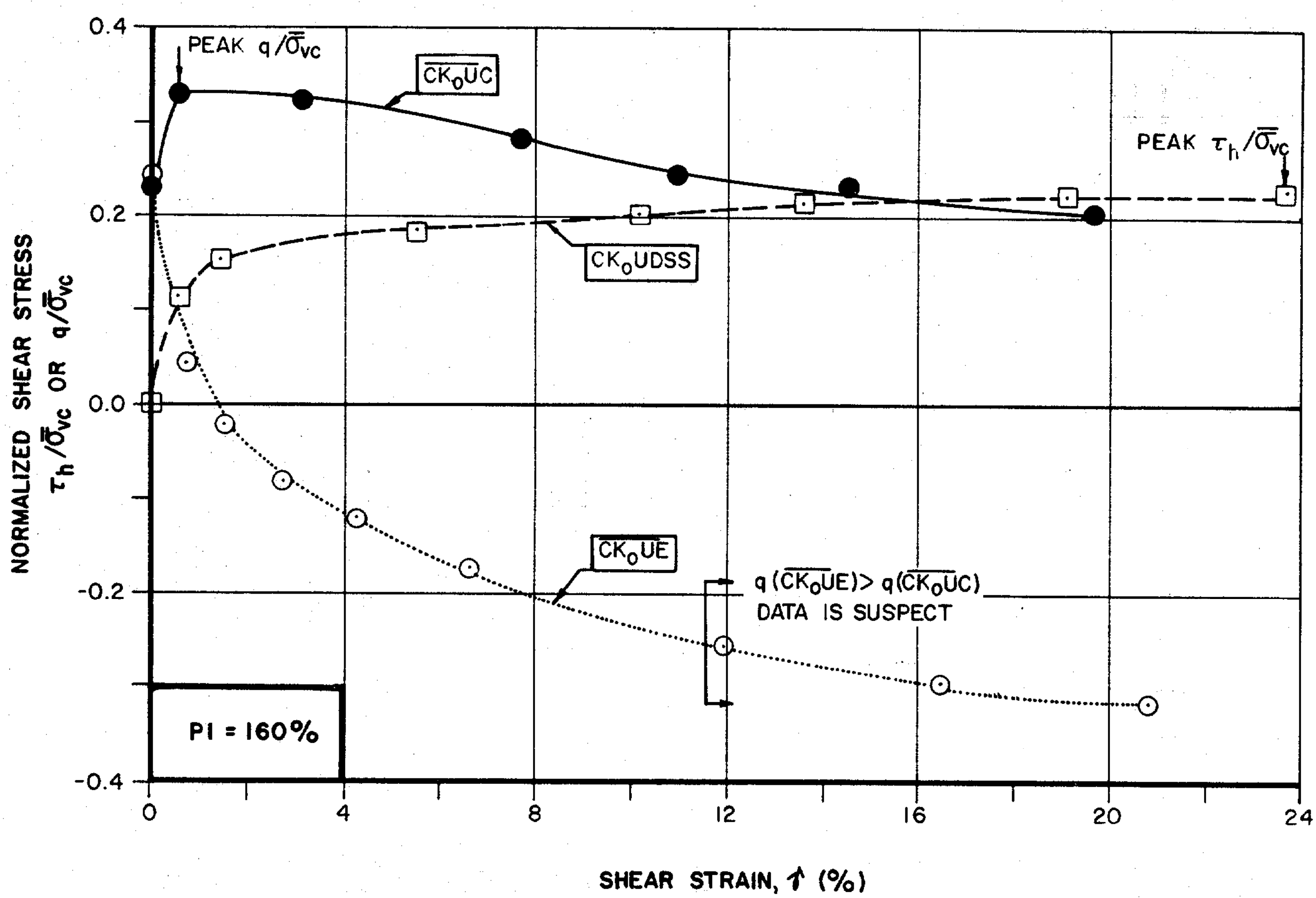

NORMALIZED SHEAR STRESS VERSUS SHEAR STRAIN AS A FUNCTION OF STRESS SYSTEM FROM $\overline{CK_oU}$ TESTS ON USSAC-ROCKLAND NORMALLY CONSOLIDATED PHOSPHATIC CLAY

FIGURE 2-32

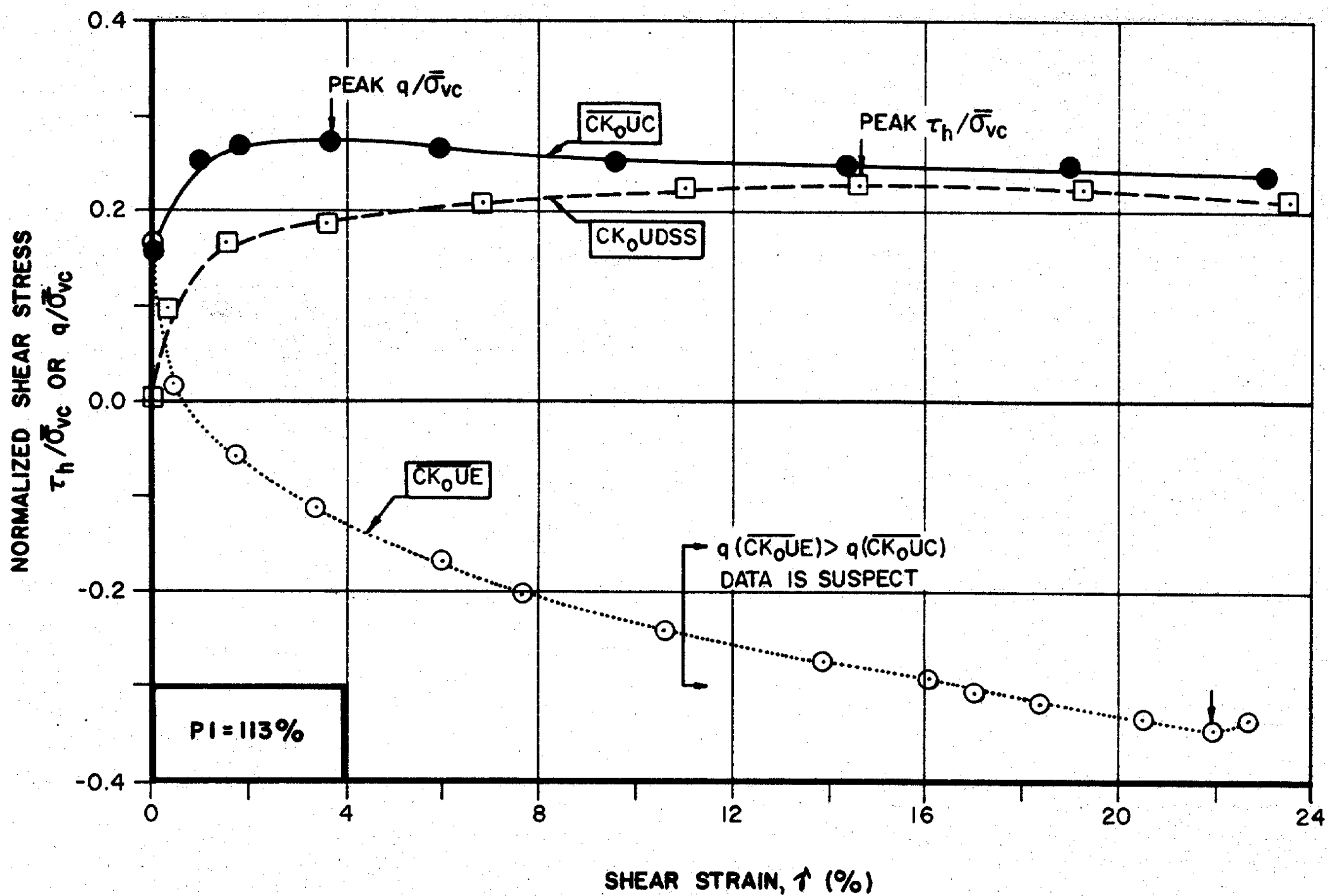

NORMALIZED SHEAR STRESS VERSUS SHEAR STRAIN AS A FUNCTION OF STRESS SYSTEM FROM $\overline{CK_oU}$ TESTS ON CF MINING-HARDEE NORMALLY CONSOLIDATDED PHOSPHATIC CLAY

FIGURE 2-33

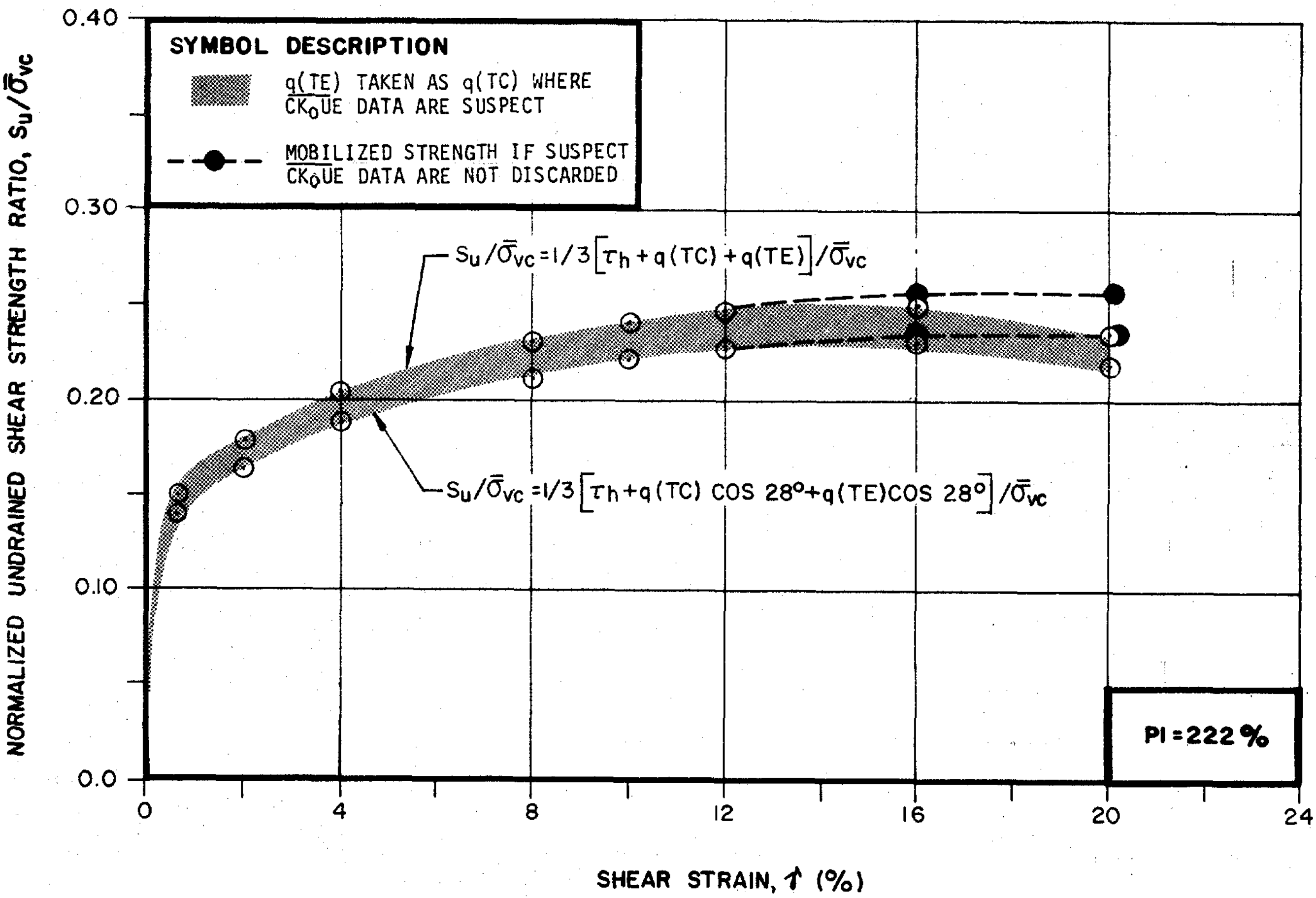

EFFECT OF STRAIN COMPATIBILITY ON NORMALIZED UNDRAINED SHEAR STRENGTH RATIO FROM $\overline{CK_0U}$ TESTS ON NORMALLY CONSOLIDATED AGRICO-SADDLE CREEK PHOSPHATIC CLAY

FIGURE 2-34

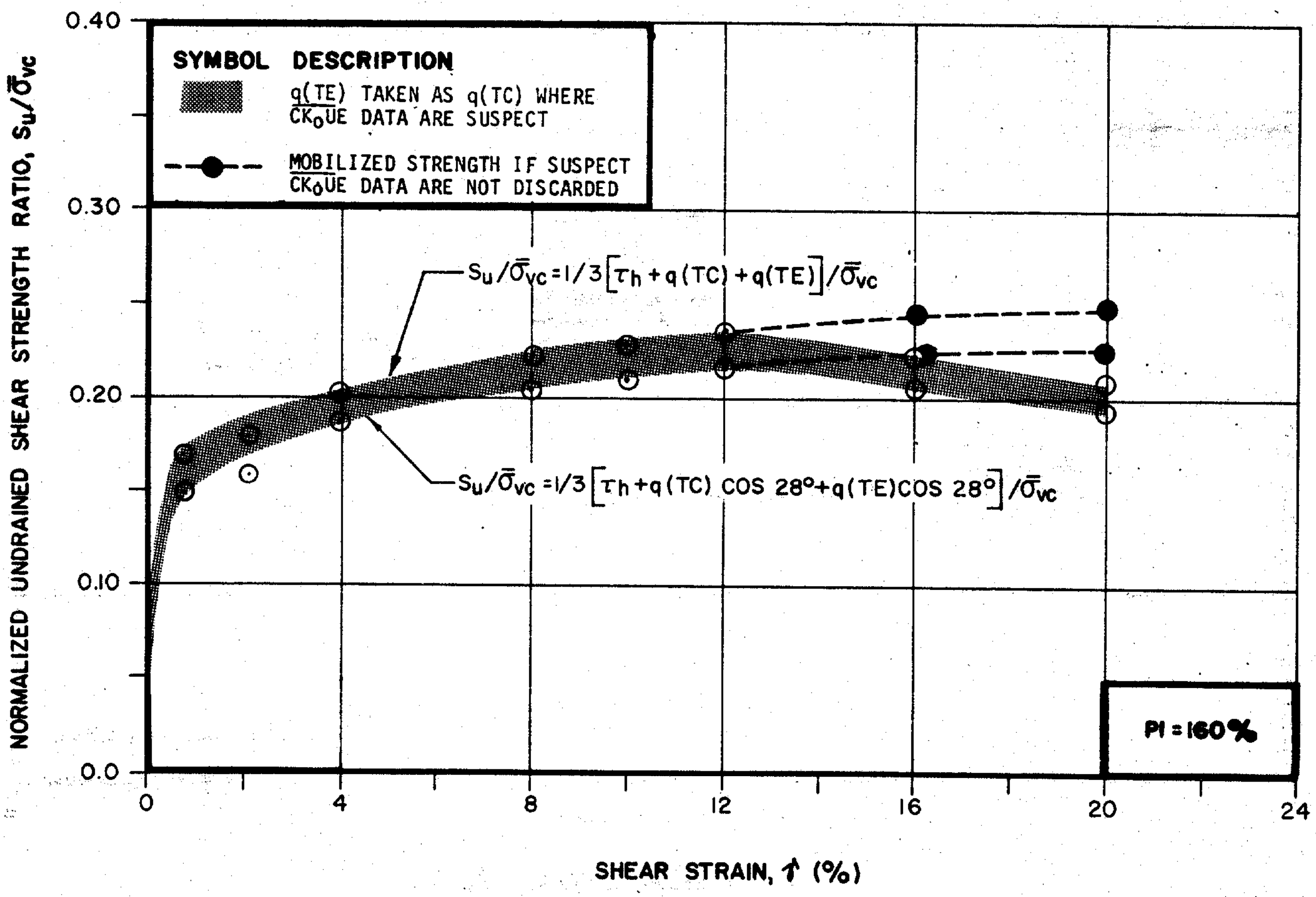

EFFECT OF STRAIN COMPATIBILITY ON NORMALIZED UNDRAINED SHEAR STRENGTH RATIO FROM $\overline{CK_oU}$ TESTS ON NORMALLY CONSOLIDATED USSAC-ROCKLAND PHOSPHATIC CLAY

FIGURE 2-35

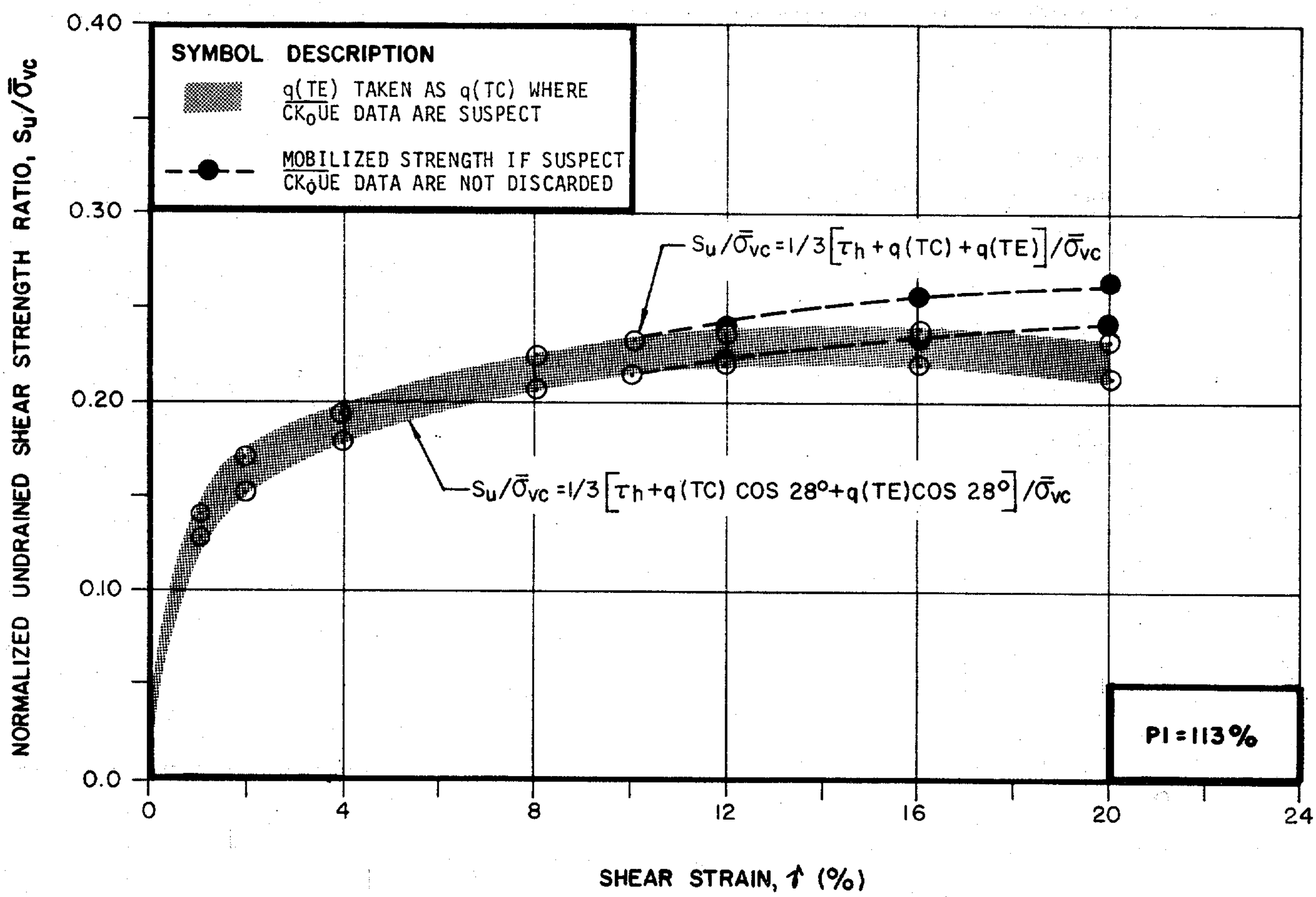

EFFECT OF STRAIN COMPATIBILITY ON NORMALIZED UNDRAINED SHEAR STRENGTH RATIO FROM $\overline{CK_oU}$ TESTS ON NORMALLY CONSOLIDATED CF MINING-HARDEE PHOSPHATIC CLAY

FIGURE 2-36

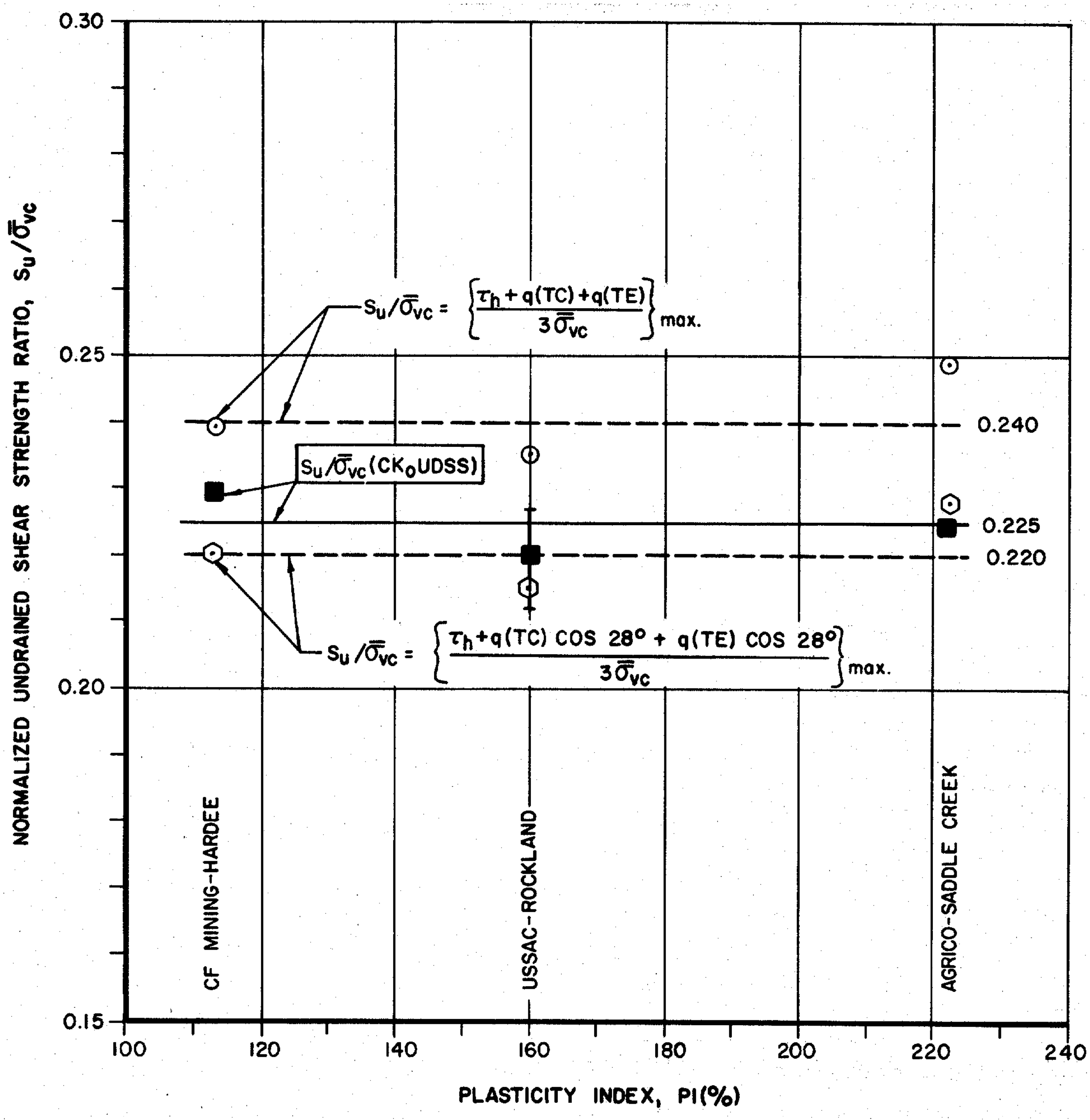

RECOMMENDED DESIGN UNDRAINED SHEAR STRENGTH RATIO FOR NORMALLY CONSOLIDATED PHOSPHATIC CLAYS

FIGURE 2-37

Section 3

STRESS-STRAIN-STRENGTH PROPERTIES OF OVERCONSOLIDATED PHOSPHATIC CLAYS

3.1 Test Methods and Test Procedures

Three phosphatic clays representative of the range in plasticity determined on samples obtained from twelve differing mine sites were subjected to CK_oUDSS tests to determine the effect of stress history on the undrained behavior and undrained shear strength. The clays selected for this investigation were from the Agrico-Saddle Creek mine (PI = 222%), the USSAC-Rockland mine (PI = 160%), and the CF Mining-Hardee mine (PI = 113%). CK_oUDSS tests were performed because, as demonstrated in Section 2.4, the CK_oUDSS test results provide a reasonably reliable estimate for the *in situ* undrained shear strength and undrained modulus.

Test specimens were prepared as described in Section 2.3.2 in conjunction with CK_oUDSS tests performed on normally consolidated phosphatic clay samples, i.e., phosphatic clays having an overconsolidation ratio, OCR, of unity. (OCR = $\bar{\sigma}_{vm}/\bar{\sigma}_{vc}$ where $\bar{\sigma}_{vm}$ is the maximum past pressure or maximum effective vertical consolidation stress to which the clay was subjected). The *in situ* clay may exhibit an overconsolidation ratio in excess of unity if allowed to desiccate and form a surface crust and/or if previously pre-loaded to higher effective stresses than existing *in situ*.

Since phosphatic clays were shown to exhibit normalized behavior (Section 2), the normalized soil parameter variation with overconsolidation ratio was determined by first reconsolidating the test samples under K_o-conditions to the virgin compression line, i.e., to $\bar{\sigma}_{vc}$ = 2.0 kg/cm^2, and then reducing the vertical effective stress to either 1.0 kg/cm^2 or 0.5 kg/cm^2 yielding overconsolidation ratios of 2 and 4, respectively, prior to undrained shear. The consolidation and rebound in the CK_oUDSS test apparatus were used to eliminate the effects of sample disturbance and adequately define stress conditions prior to shear.

CK_oUDSS test data on normally consolidated phosphatic clays (OCR = 1.0) were presented in Section 2. In addition to CK_oUDSS tests performed on normally consolidated phosphatic clays, tests were performed on each of 3 phosphatic clays at overconsolidation ratios of 2 and 4. A total of 12 CK_oUDSS tests, therefore, were performed on phosphatic clays at overconsolidation ratios of 1, 2 and 4. Test procedures were in accordance with the methodology outlined in Section 2.3.2.

3.2 Coefficient of Earth Pressure at Rest

Section 2.3.3 recommended that a K_o-value on the order of 0.62 be used to characterize the *in situ* one dimensional state of stress of normally consolidated (NC) phosphatic clays; i.e., K_o(NC) = 0.62.

No measurements of the coefficient of earth pressure at rest, K_o, of overconsolidated (OC) phosphatic clays was made. However, based on data presented by Ladd et al. (1977) correlating the ratio $K_o(OC)/K_o(NC)$ to plasticity, the following relationship is judged applicable in the absence of specific test data on phosphatic clays:

$$K_o(OC) = K_o(NC) \cdot OCR^{0.35} = 0.62(OCR)^{0.35} \quad (1)$$

The resulting $K_o(OC)$ values are applicable to K_o during unloading of a phosphatic clay deposit. Corresponding K_o values at overconsolidation ratios of 2 and 4 are predicted to equal 0.79 and 1.00, respectively.

3.3 **Stress-Strain Behavior**

Normalized effective stress paths at varying overconsolidation ratios (OCR = 1, 2 and 4) for the Agrico, USSAC and CF clays are presented in Figures 3-1, 3-2 and 3-3, respectively. The normalized stress-strain behavior is depicted in Figures 3-4, 3-5 and 3-6, respectively.

The normalized stress-strain and pore pressure data in Figures 3-4, 3-5 and 3-6 are consistent and show:

- large shear strains at failure ranging from 16% to 22%.
- a marked increase in $s_u/\bar{\sigma}_{vc}$ with increasing overconsolidation ratio.
- development of negative pore pressures during undrained shear (in lieu of positive pore pressures) with increased overconsolidation ratio.
- an increase in pore pressures after failure for overconsolidated samples and a correspondingly more marked strain softening behavior.

These behavioral trends are also characteristic of CK_oUDSS test results on a wide variety of clays.

3.4 **Undrained Shear Strength Ratio**

The increase in the undrained shear strength ratio, $s_u/\bar{\sigma}_{vc}$, with overconsolidation ratio from CK_oUDSS tests performed on the three phosphatic clays is illustrated in Figures 3-7, 3-8 and 3-9. A marked similarity in trends is observed in spite of significant differences in plasticity. Ladd et al. (1977) recommend a relationship of the form:

$$s_u/\bar{\sigma}_{vc} = (s_u(NC)/\bar{\sigma}_{vc})OCR^m \quad (2)$$

This relationship is shown to apply to phosphatic clays with m-values ranging from 0.78 to 0.84, and averaging about 0.80. Figure 3-10 summarizes $s_u/\bar{\sigma}_{vc}$ data versus overconsolidation ratio for all three phosphatic clays. The data depict a slight increase in the $s_u/\bar{\sigma}_{vc}$ ratio with reduced clay plasticity at high overconsolidation ratios (i.e., OCR = 4), but the data is somewhat limited and, therefore, not conclusive. Good agreement is obtained for all three phosphatic clays tentatively justifying use of the following average relationship in conjunction with phosphatic clays:

$$s_u/\bar{\sigma}_{vc} = 0.225\ (\mathrm{OCR})^{0.80} \qquad (3)$$

The normalized $s_u/\bar{\sigma}_{vc}$ ratio based on the above equation is predicted to equal 0.225, 0.392 and 0.682 at overconsolidation ratios of 1, 2 and 4, respectively.

3.5 Undrained Modulus

Variations in the normalized undrained Young's secant modulus, E_u/s_u, with stress level and overconsolidation ratio are illustrated in Figures 3-11, 3-12 and 3-13 for the Agrico-Saddle Creek, USSAC-Rockland, and CF Mining-Hardee clays, respectively. In spite of some scatter in the data, the trends observed are similar for all three clays. Figure 3-14 presents an overview of the data from tests performed on all three clays. As shown, E_u/s_u decreases with increased overconsolidation ratio particularly at OCR values in excess of 2. These trends are in agreement with behavioral trends characteristic of most cohesive soils.

Figure 3-15 illustrates the degree of scatter in E_u/s_u versus overconsolidation ratio at stress levels of 33% and 67%, corresponding to factors of safety of 3 and 1.5. As shown, the scatter between tests on a given phosphatic clay at the same overconsolidation ratio can be as large as the scatter from one phosphatic clay to the other. Hence, a single relationship between E_u/s_u and overconsolidation ratio is recommended for all three phosphatic clays with the band showing potential deviations in E_u/s_u at a given overconsolidation ratio. Figure 3-16 presents the variation in E_u/s_u versus overconsolidation ratio at factors of safety of 3, 2 and 1.5. The trends are consistent with the observed behavior of many sedimentary clay deposits (Ladd et al., 1977). Nevertheless, the E_u/s_u values are higher than one would have predicted based on the high plasticity of phosphatic clays.

3.6 Effective Stress Failure Envelope

For drained effective stress type stability analyses that may be performed to assess long-term performance of normally consolidated phosphatic clays, an effective angle of internal friction, $\bar{\phi}_d$, equal to 25° was recommended with zero effective cohesion (Section 2.4.3). Ladd et al. (1972) suggest on the basis of limited data for other clays, a value of effective cohesion, $\bar{c}$, for overconsolidated clays of 0.02 to 0.05 times the maximum past pressure (and a slightly reduced angle of internal friction).

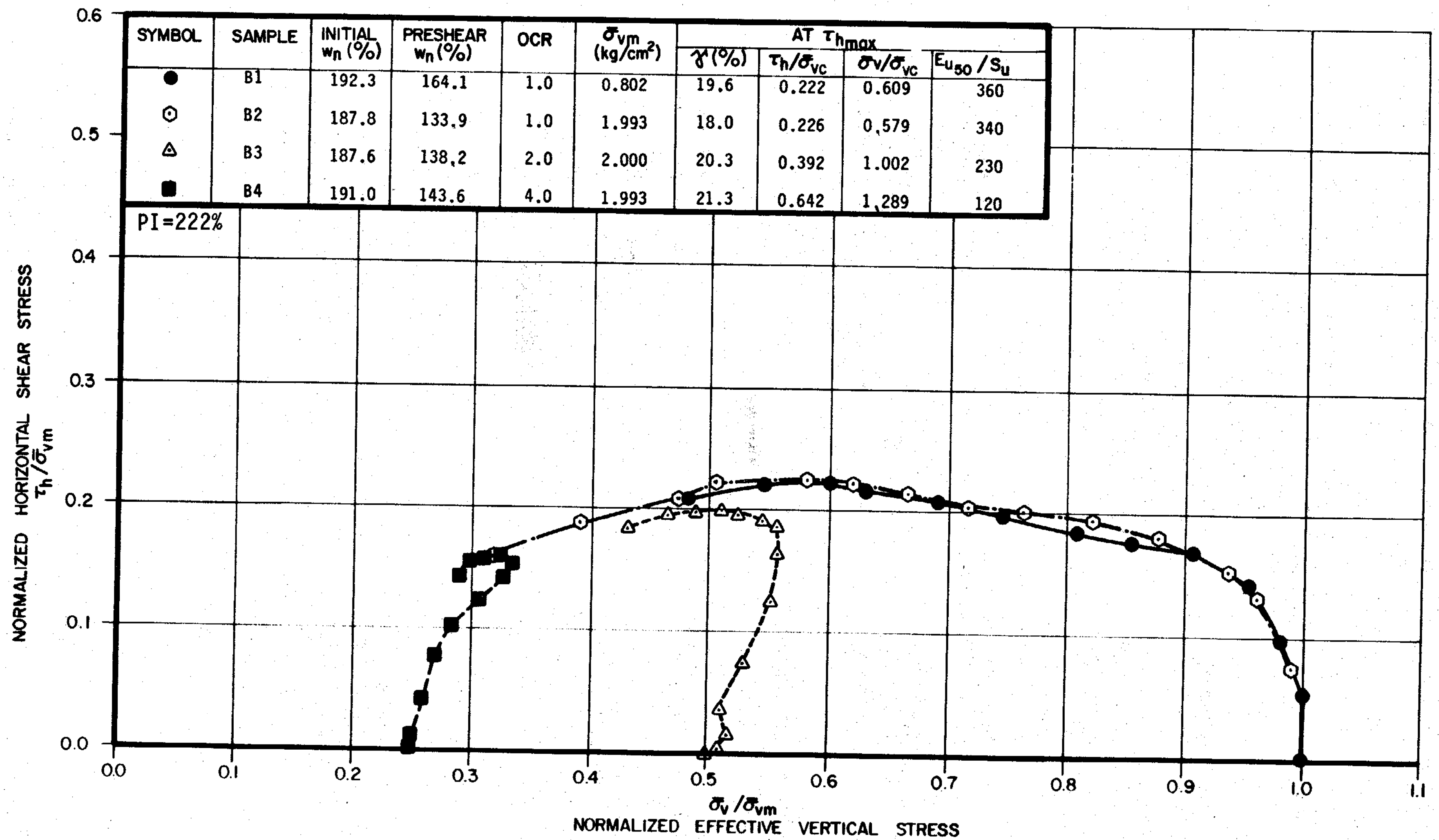

SYMBOL	SAMPLE	INITIAL w_n (%)	PRESHEAR w_n (%)	OCR	$\bar{\sigma}_{vm}$ (kg/cm^2)	AT $\tau_{h\,max}$			
						γ (%)	$\tau_h/\bar{\sigma}_{vc}$	$\bar{\sigma}_v/\bar{\sigma}_{vc}$	E_{u50}/S_u
●	B1	192.3	164.1	1.0	0.802	19.6	0.222	0.609	360
⊙	B2	187.8	133.9	1.0	1.993	18.0	0.226	0.579	340
△	B3	187.6	138.2	2.0	2.000	20.3	0.392	1.002	230
■	B4	191.0	143.6	4.0	1.993	21.3	0.642	1.289	120

NORMALIZED UNDRAINED EFFECTIVE STRESS PATHS FROM CK_oUDSS TESTS ON AGRICO-SADDLE CREEK PHOSPHATIC CLAY

FIGURE 3-2

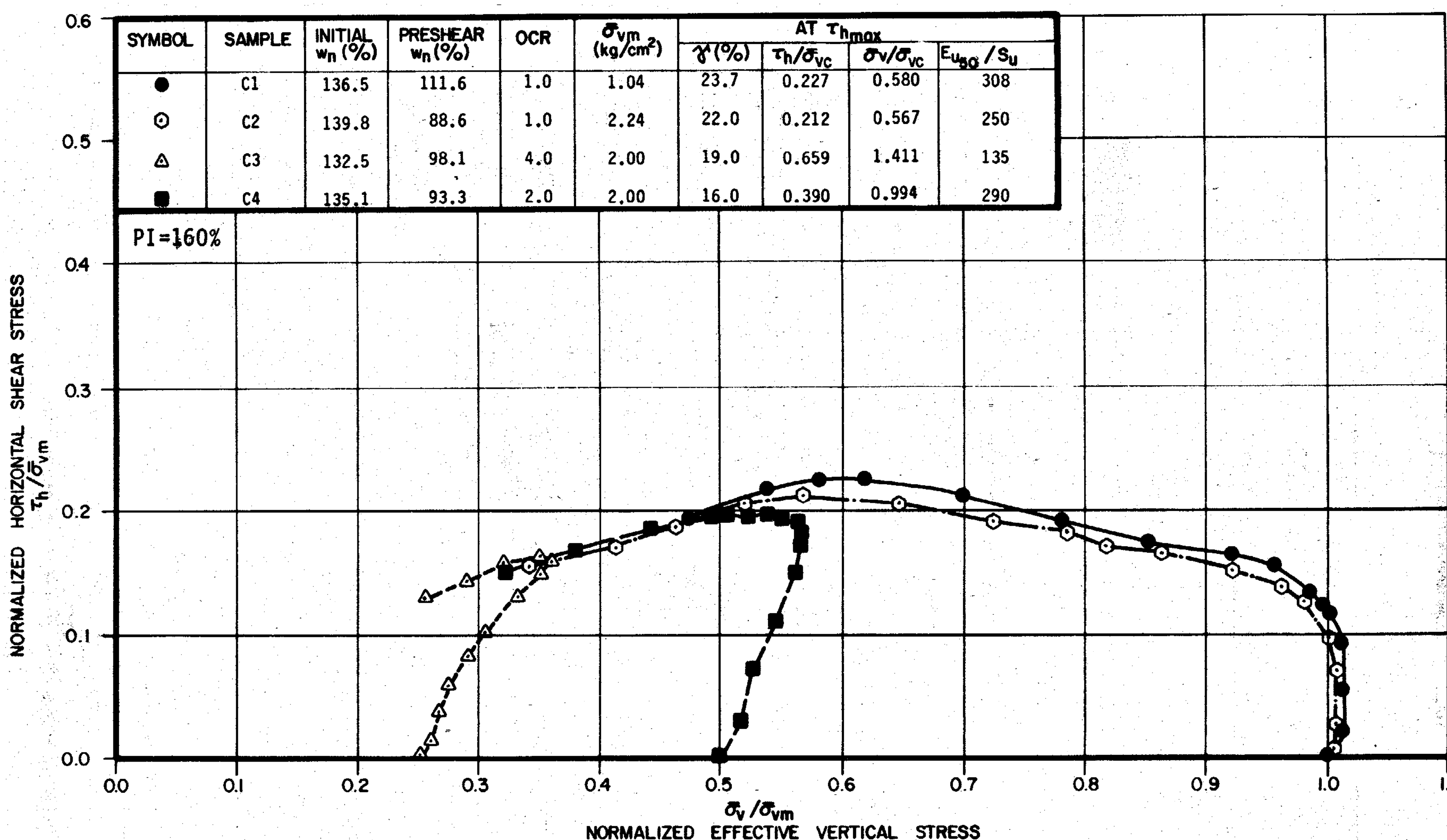

SYMBOL	SAMPLE	INITIAL w_n (%)	PRESHEAR w_n (%)	OCR	$\bar{\sigma}_{vm}$ (kg/cm^2)	AT $\tau_{h max}$ γ (%)	$\tau_h/\bar{\sigma}_{vc}$	$\bar{\sigma}_v/\bar{\sigma}_{vc}$	E_{u50}/S_u
●	C1	136.5	111.6	1.0	1.04	23.7	0.227	0.580	308
⊙	C2	139.8	88.6	1.0	2.24	22.0	0.212	0.567	250
△	C3	132.5	98.1	4.0	2.00	19.0	0.659	1.411	135
■	C4	135.1	93.3	2.0	2.00	16.0	0.390	0.994	290

NORMALIZED UNDRAINED EFFECTIVE STRESS PATHS FROM CK_oUDSS TESTS ON USSAC-ROCKLAND PHOSPHATIC CLAY

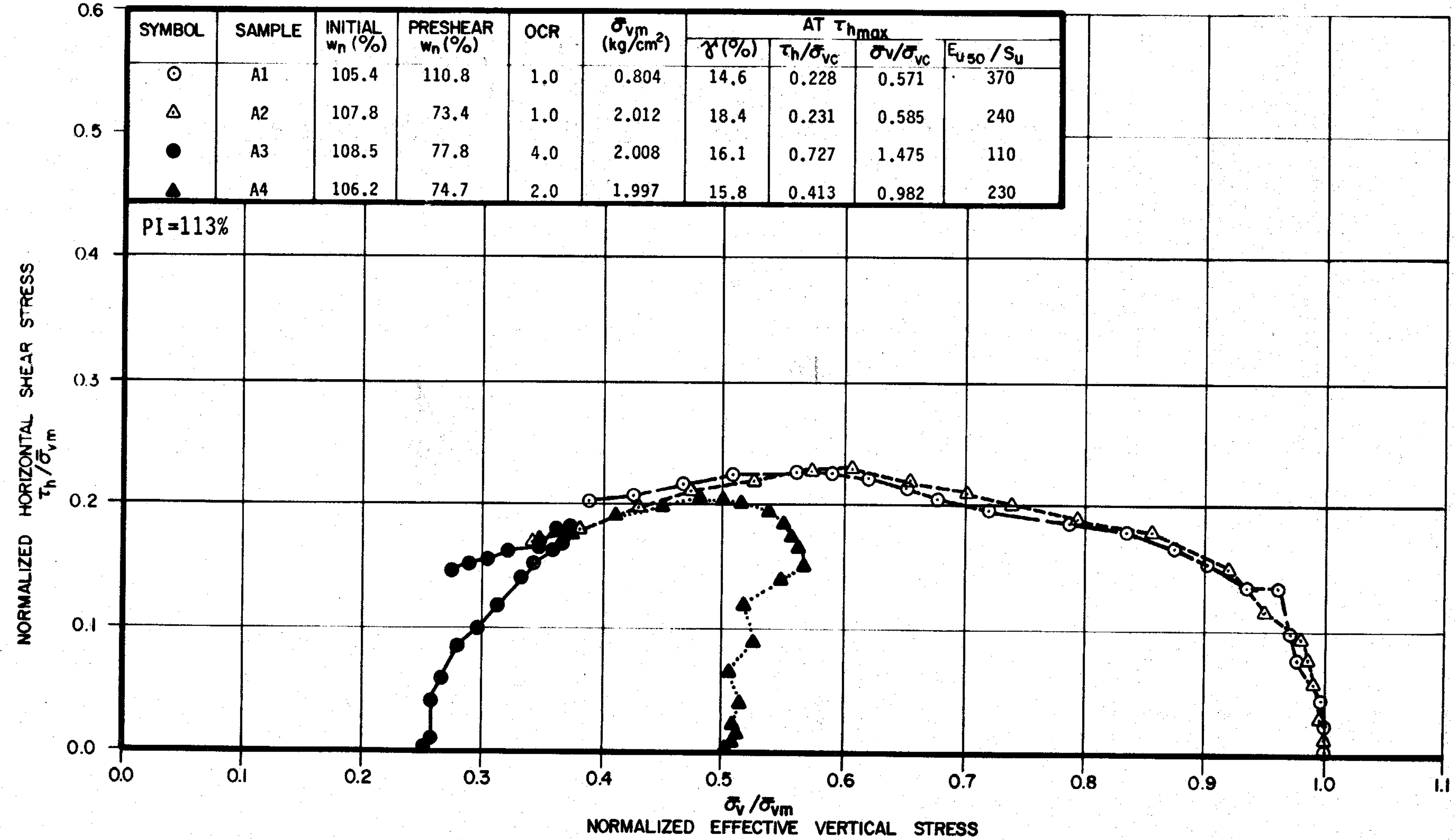

SYMBOL	SAMPLE	INITIAL w_n (%)	PRESHEAR w_n (%)	OCR	$\bar{\sigma}_{vm}$ (kg/cm^2)	AT $\tau_{h max}$ γ (%)	$\tau_h/\bar{\sigma}_{vc}$	$\bar{\sigma}_v/\bar{\sigma}_{vc}$	E_{u50}/S_u
⊙	A1	105.4	110.8	1.0	0.804	14.6	0.228	0.571	370
△	A2	107.8	73.4	1.0	2.012	18.4	0.231	0.585	240
●	A3	108.5	77.8	4.0	2.008	16.1	0.727	1.475	110
▲	A4	106.2	74.7	2.0	1.997	15.8	0.413	0.982	230

FIGURE 3-3

NORMALIZED UNDRAINED EFFECTIVE STRESS PATHS
FROM CK_0UDSS TESTS
ON CF MINING-HARDEE PHOSPHATIC CLAY

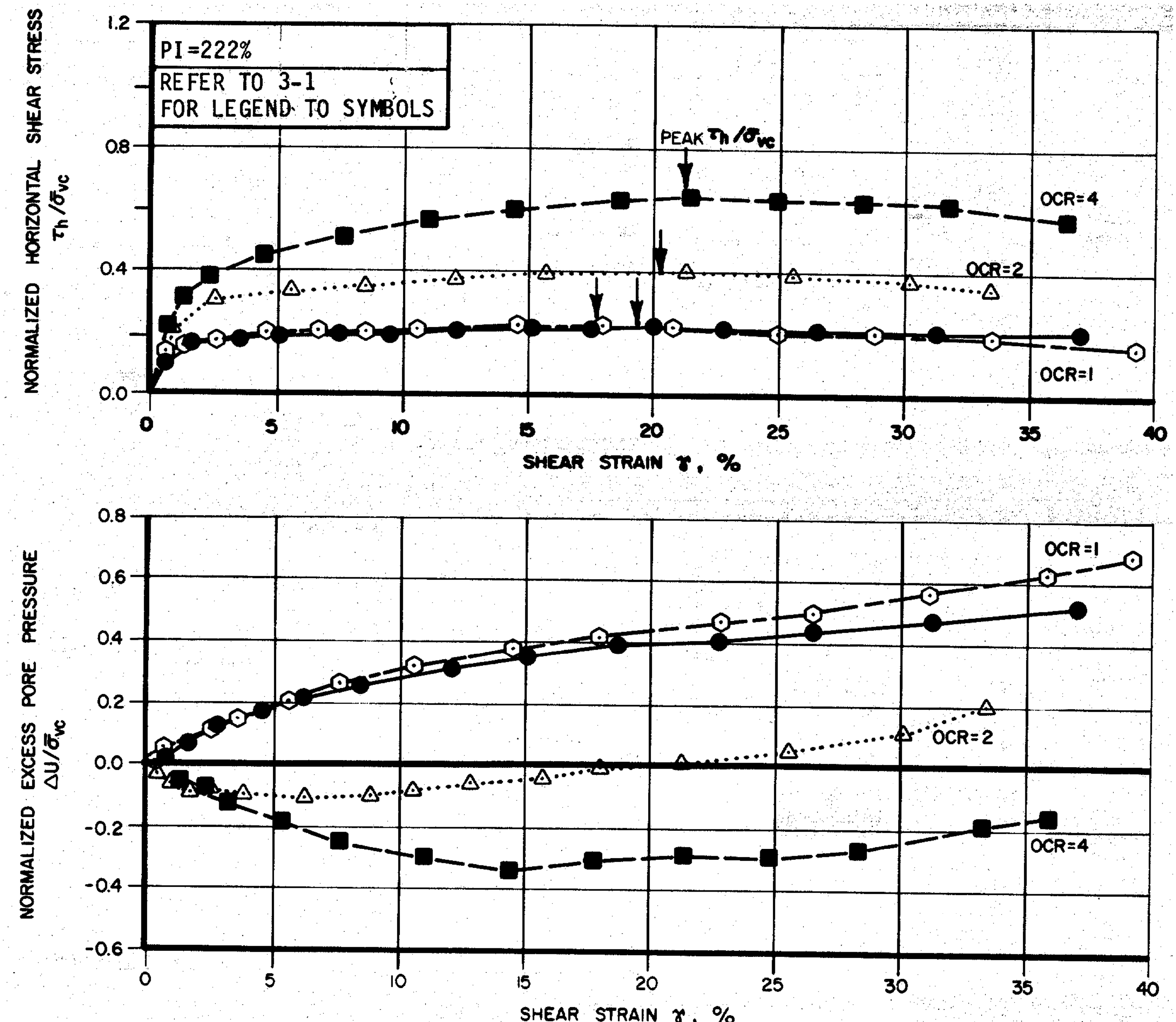

NORMALIZED UNDRAINED STRESS-STRAIN BEHAVIOR FROM CK_0UDSS TESTS ON AGRICO-SADDLE CREEK PHOSPHATIC CLAY

FIGURE 3-4

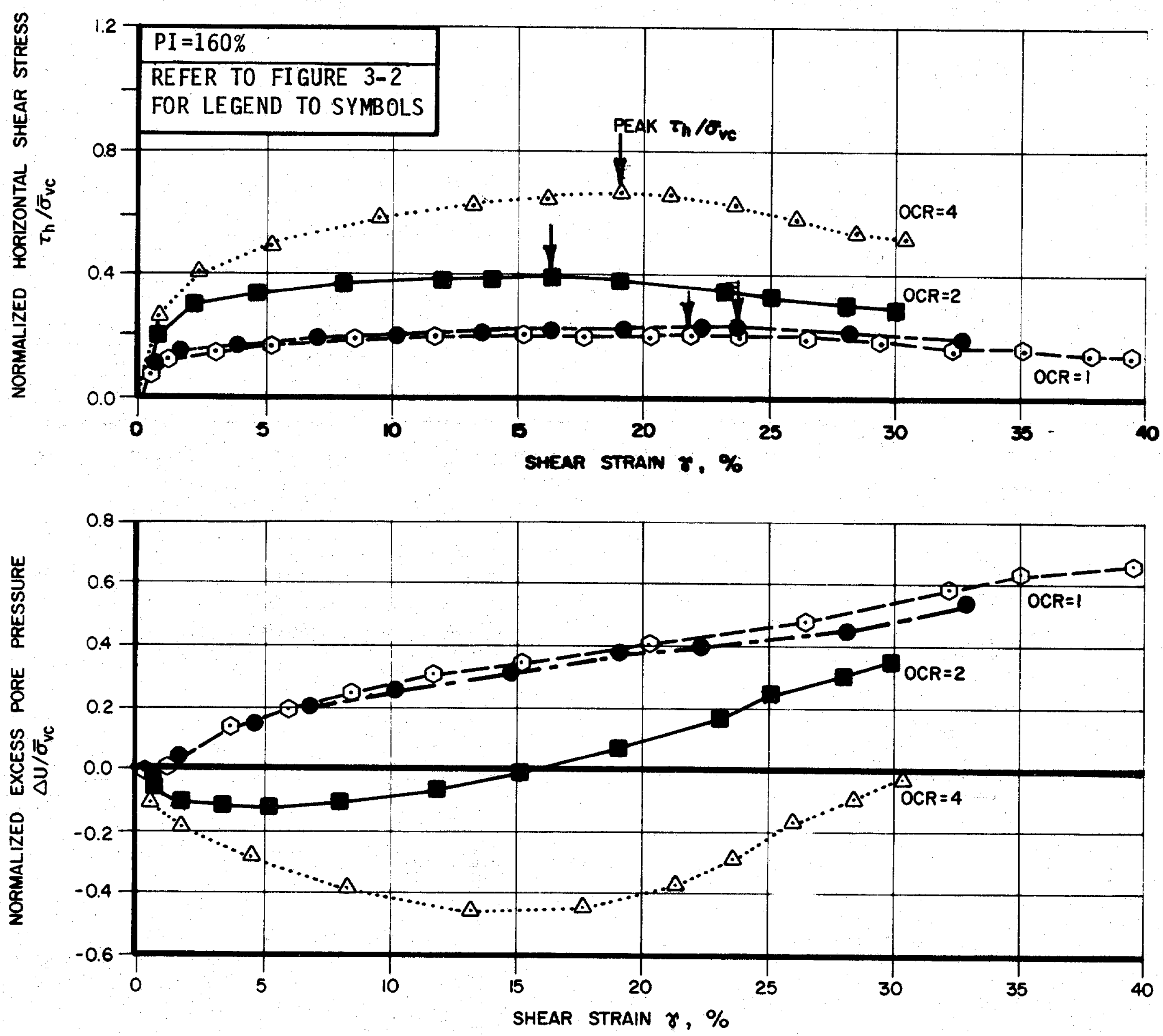

NORMALIZED UNDRAINED STRESS-STRAIN BEHAVIOR FROM CK_oUDSS TESTS ON USSAC-ROCKLAND PHOSPHATIC CLAY

FIGURE 3-5

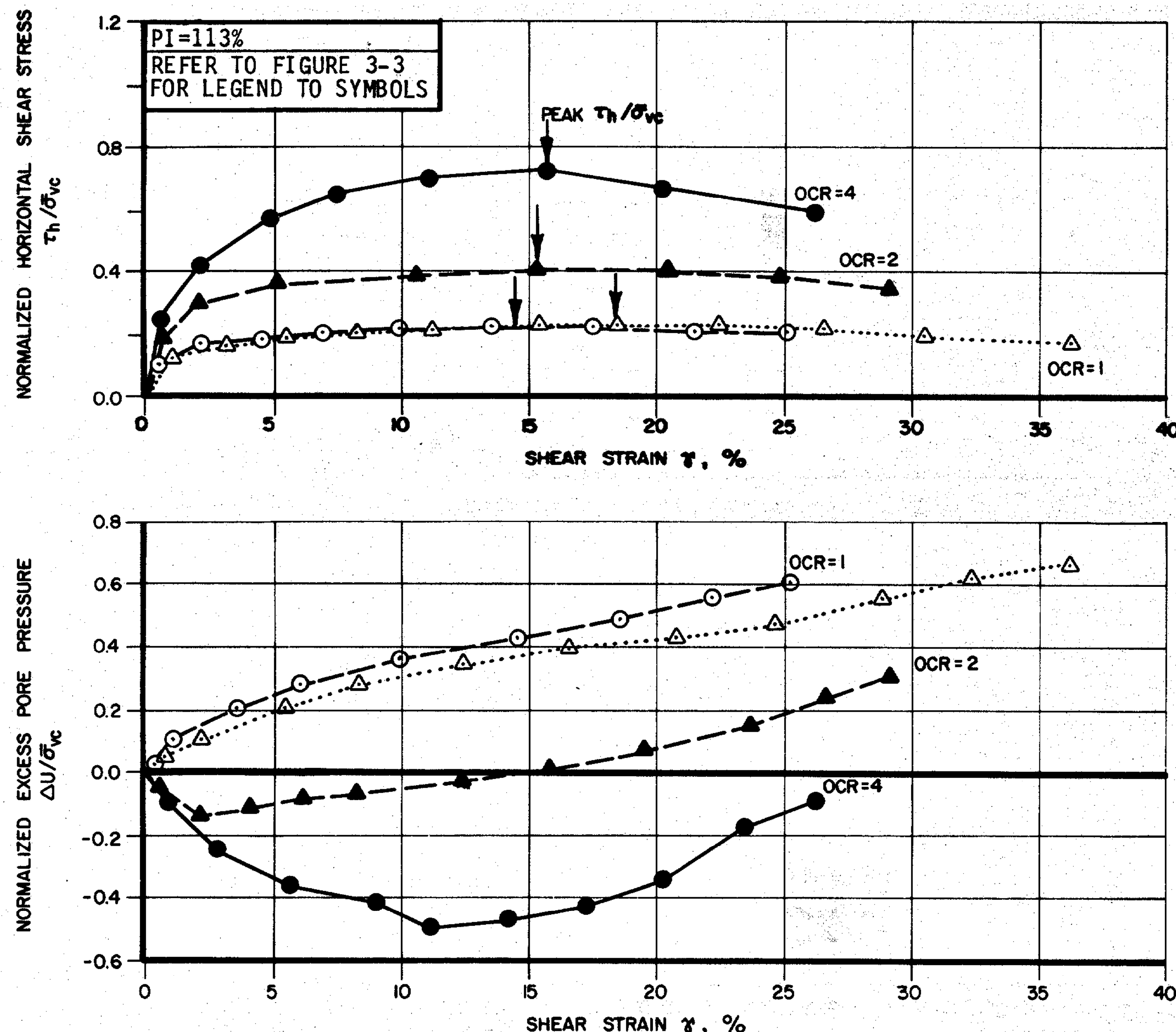

NORMALIZED UNDRAINED STRESS-STRAIN BEHAVIOR FROM CK_0UDSS TESTS ON CF MINING-HARDEE PHOSPHATIC CLAY

FIGURE 3-6

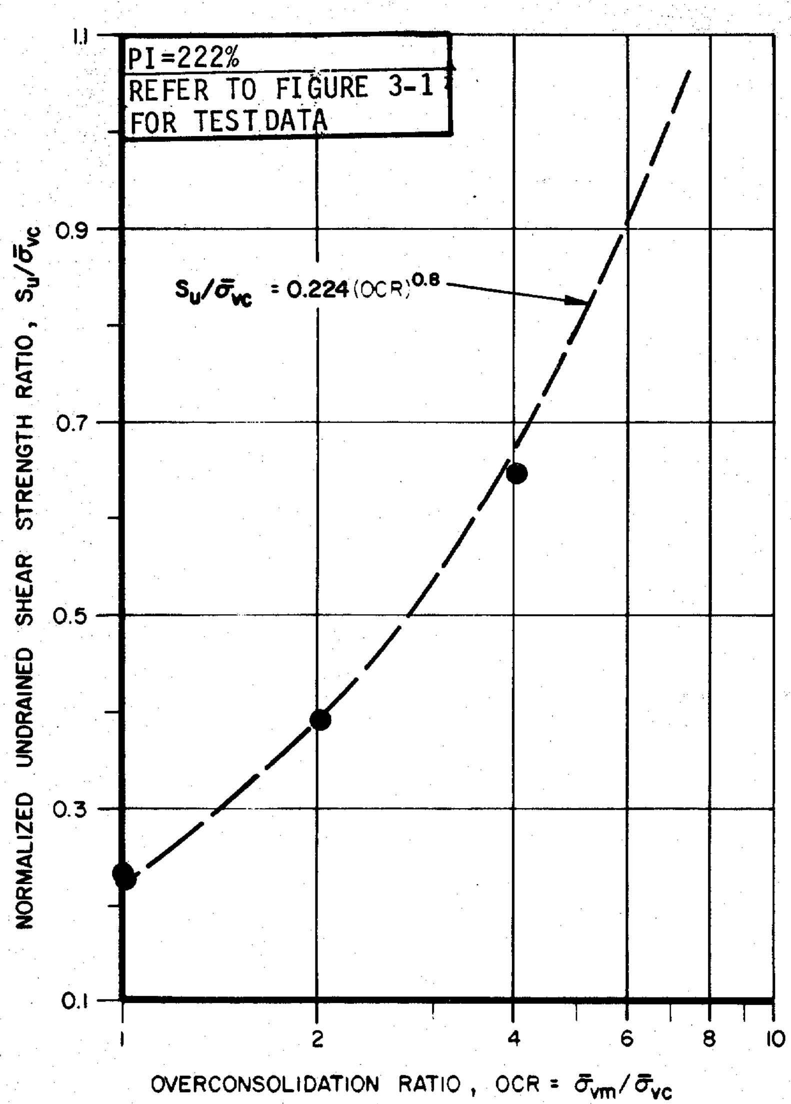

NORMALIZED UNDRAINED SHEAR STRENGTH RATIO VERSUS OVERCONSOLIDATION RATIO FROM CK_0UDSS TESTS ON AGRICO-SADDLE CREEK PHOSPHATIC CLAY

FIGURE 3-7

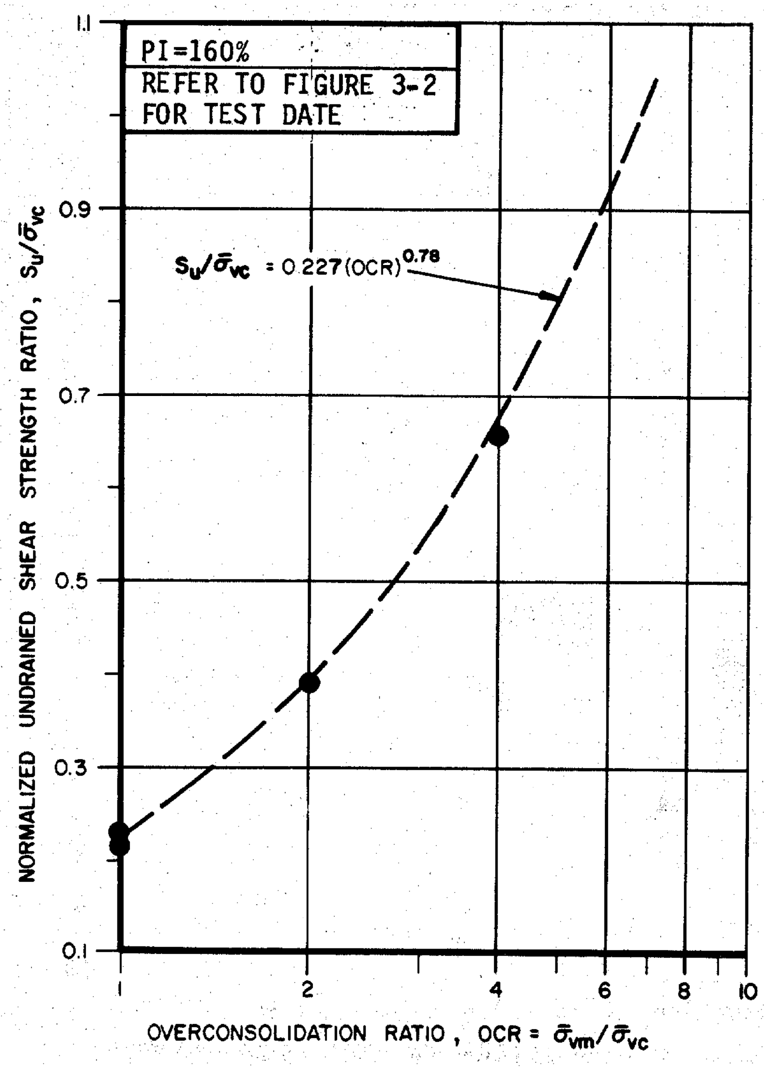

NORMALIZED UNDRAINED SHEAR STRENGTH RATIO VERSUS OVERCONSOLIDATION RATIO FROM CK_0UDSS TESTS ON USSAC-ROCKLAND PHOSPHATIC CLAY

FIGURE 3-8

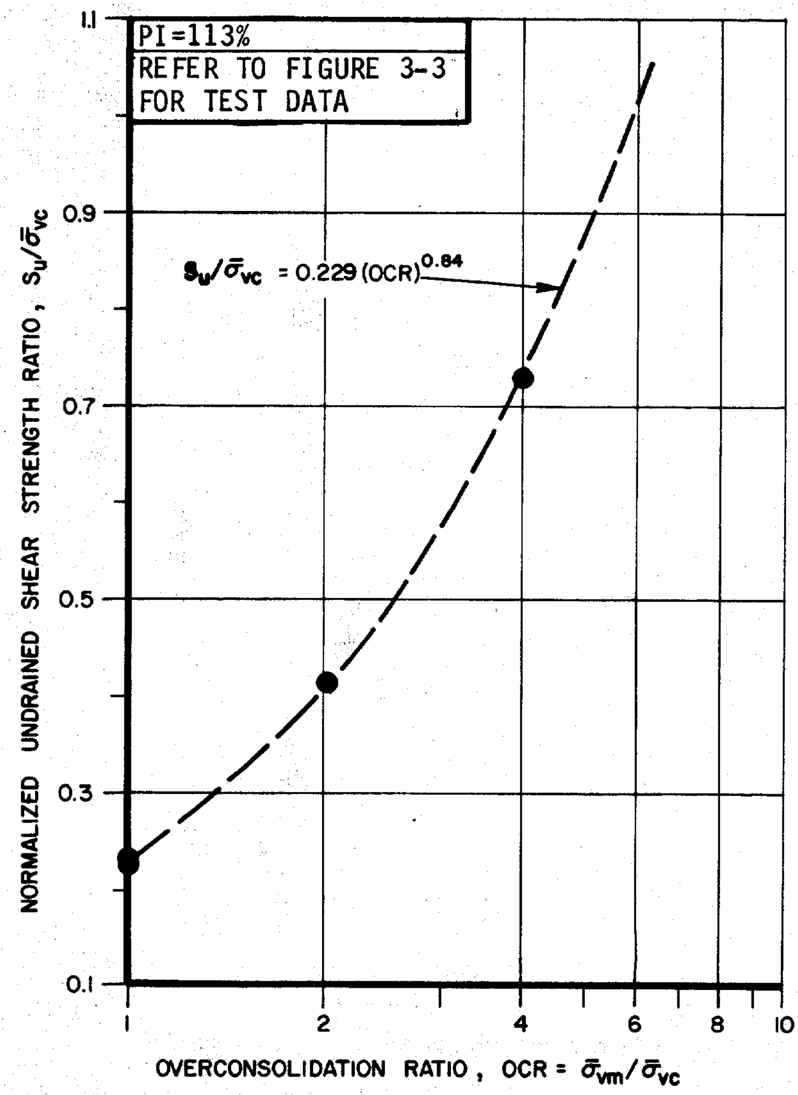

NORMALIZED UNDRAINED SHEAR STRENGTH RATIO VERSUS OVERCONSOLIDATION RATIO FROM CK_0UDSS TESTS ON CF MINING-HARDEE PHOSPHATIC CLAY

FIGURE 3-9

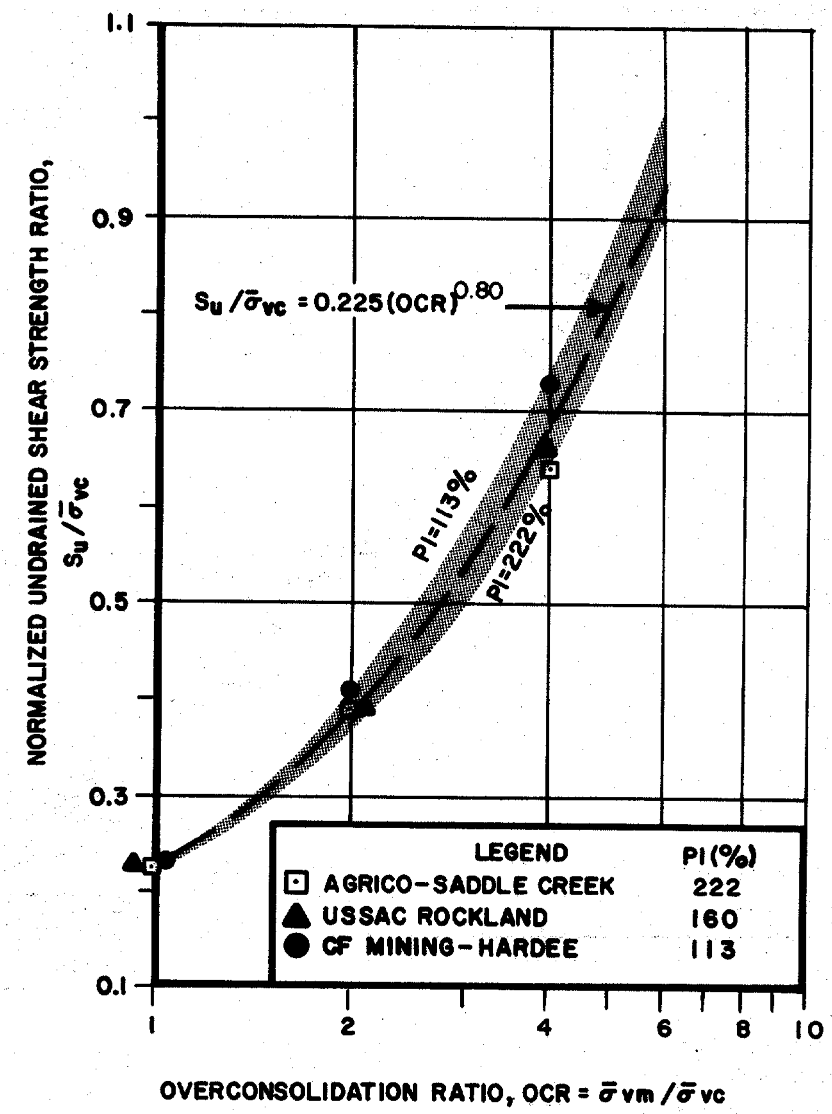

COMPARISON OF NORMALIZED UNDRAINED SHEAR STRENGTH RATIO VERSUS OVERCONSOLIDATION RATIO FROM CK_oUDSS TESTS ON PHOSPHATIC CLAYS

FIGURE 3-10

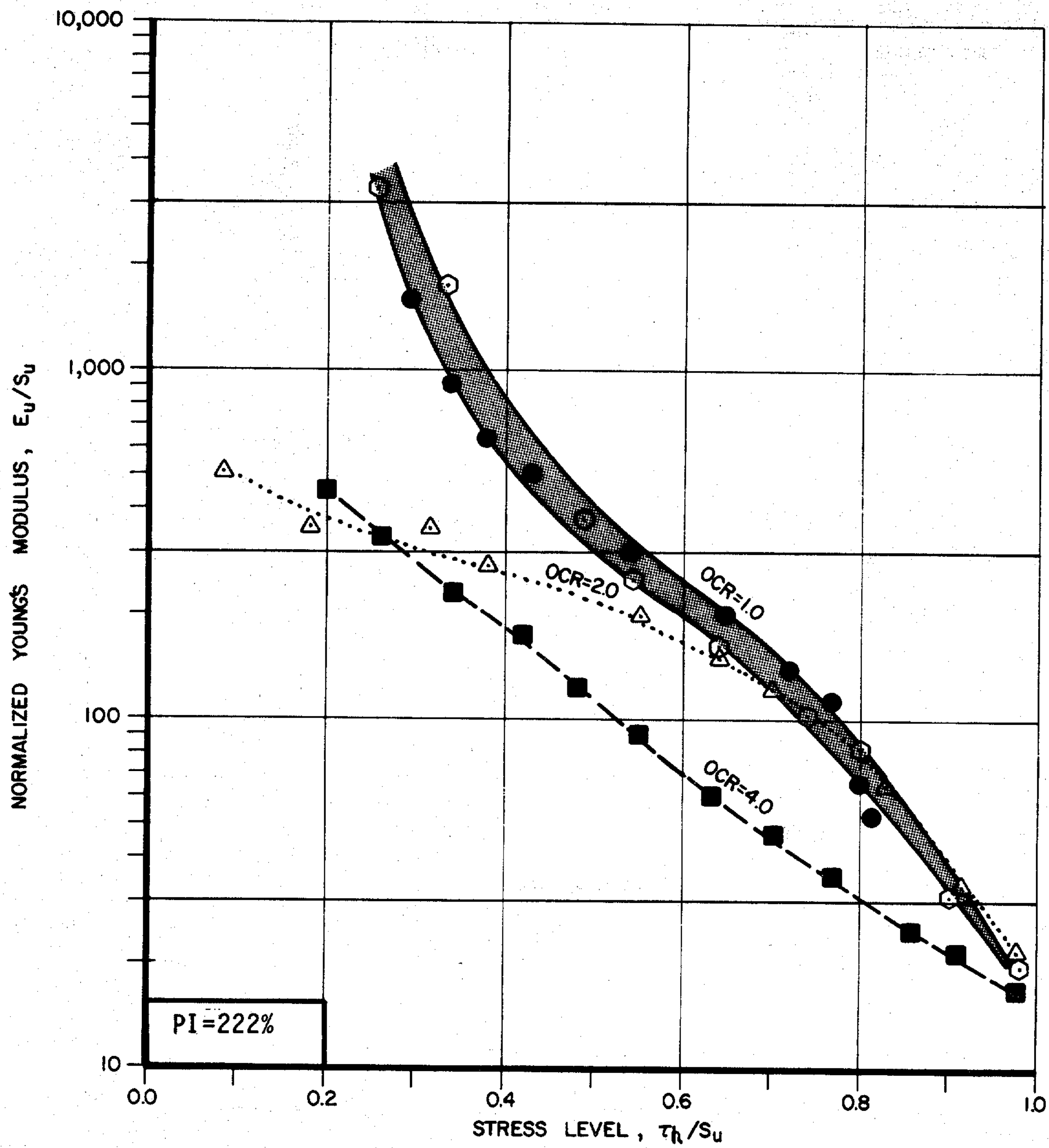

NORMALIZED UNDRAINED YOUNG'S MODULUS VERSUS STRESS LEVEL FROM CK_0UDSS TESTS ON AGRICO-SADDLE CREEK PHOSPHATIC CLAY

FIGURE 3-11

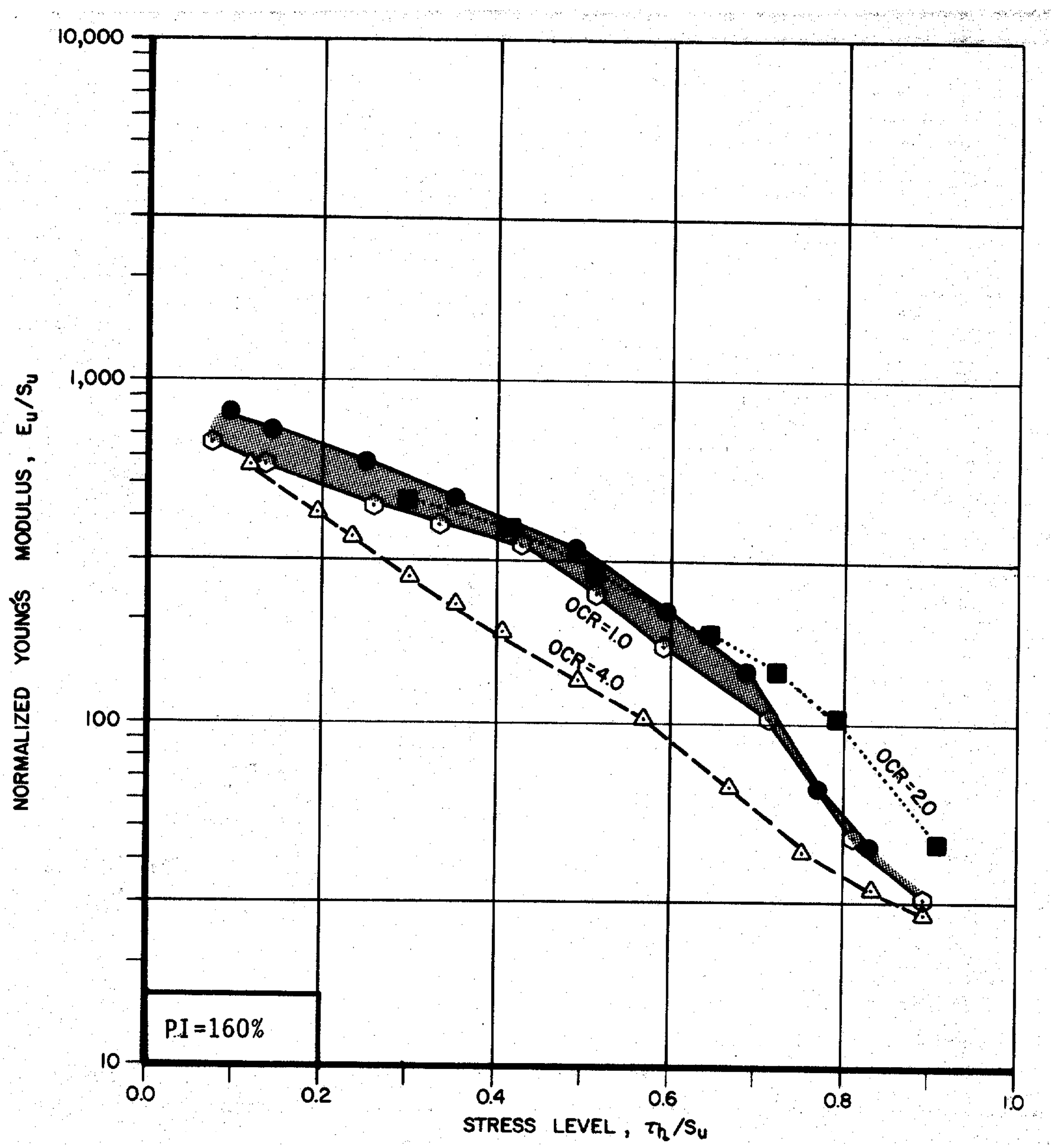

NORMALIZED UNDRAINED YOUNG'S MODULUS VERSUS STRESS LEVEL FROM CK $_0$UDSS TESTS ON USSAC-ROCKLAND PHOSPHATIC CLAY

FIGURE 3-12

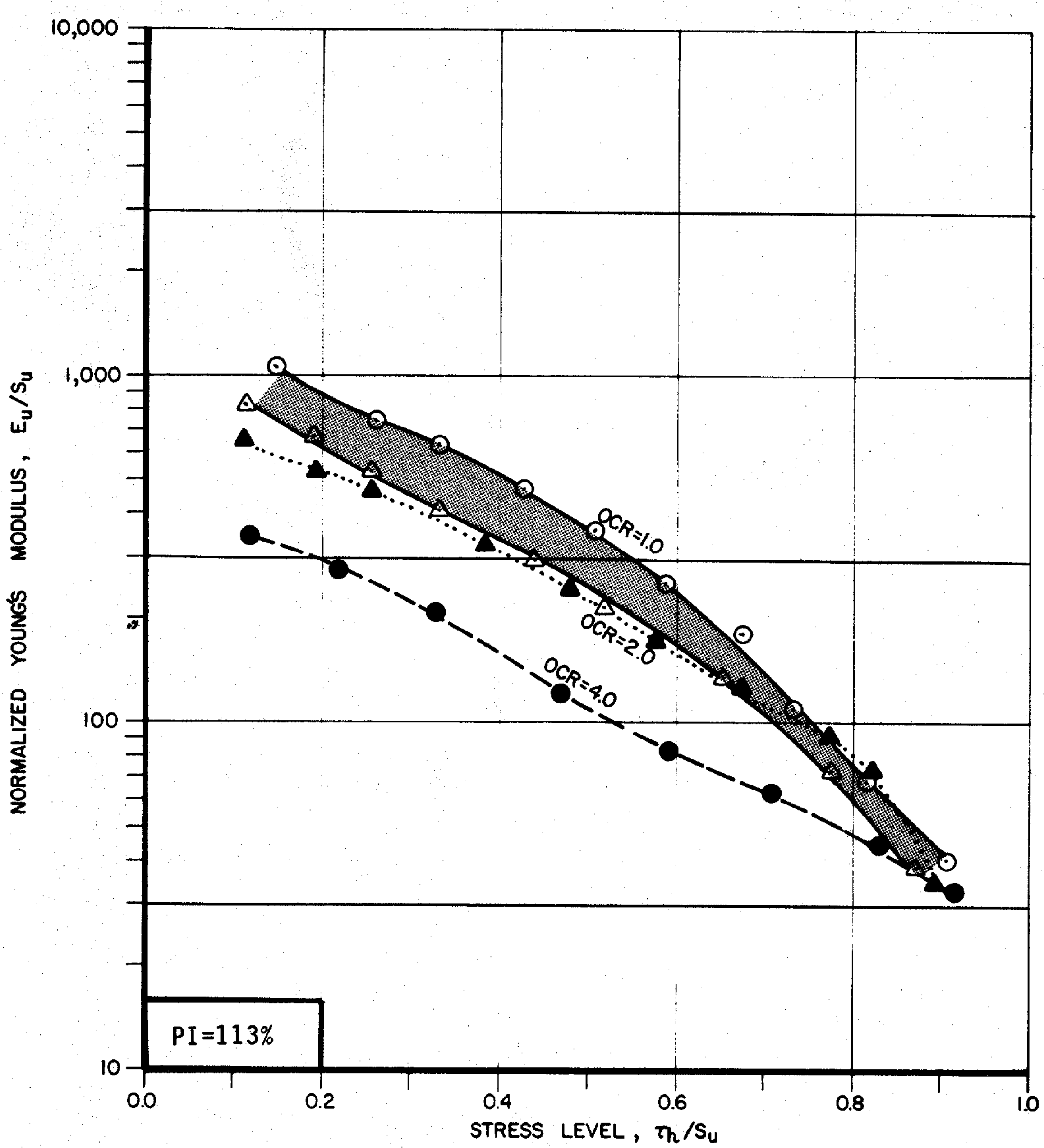

NORMALIZED UNDRAINED YOUNG'S MODULUS VERSUS STRESS LEVEL FROM CK_oUDSS TESTS ON CF MINING-HARDEE PHOSPHATIC CLAY

FIGURE 3-13

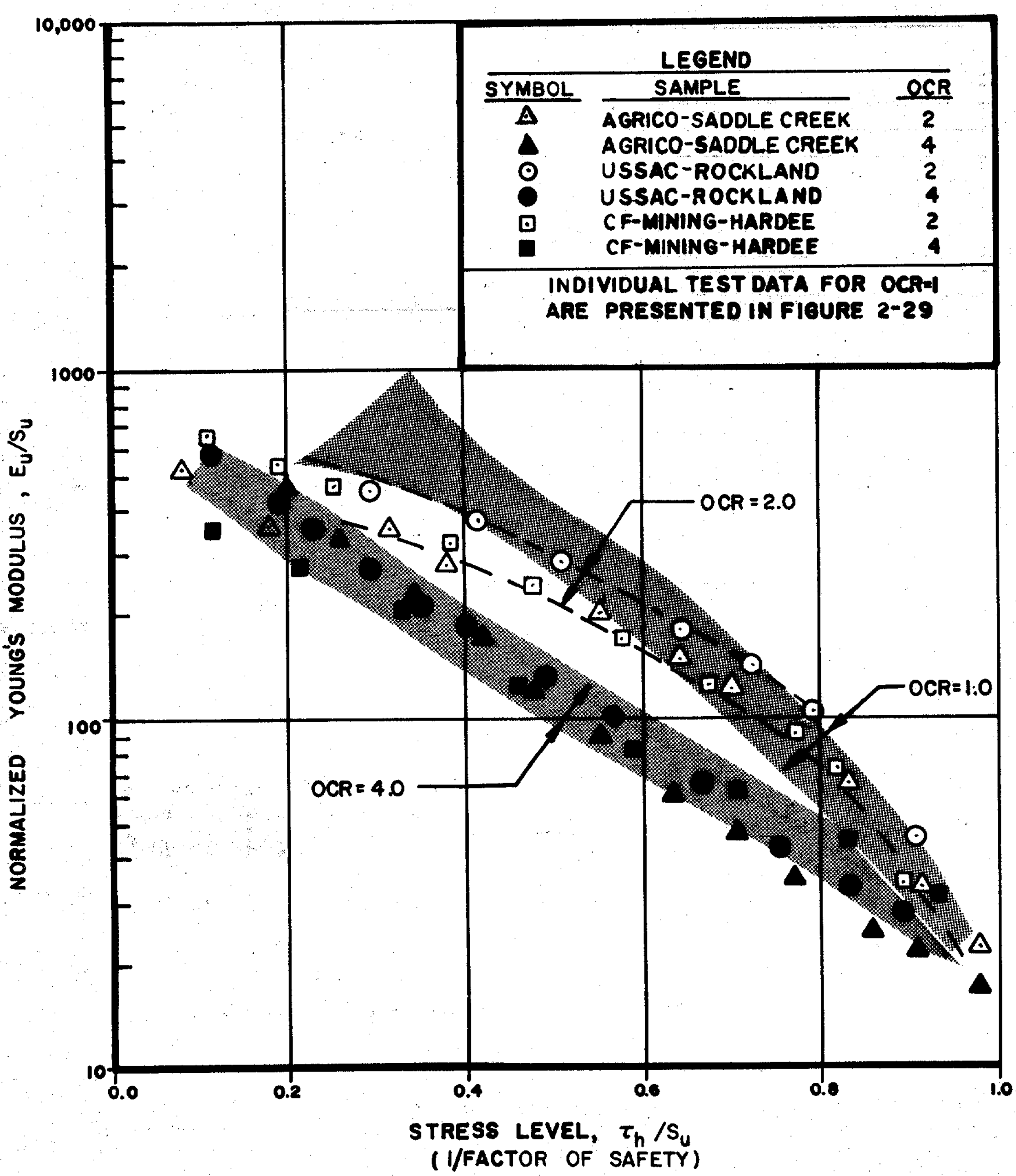

SUMMARY OF NORMALIZED UNDRAINED YOUNG'S MODULUS VERSUS STRESS LEVEL FROM CK$_0$UDSS TESTS ON NORMALLY CONSOLIDATED AND OVERCONSOLIDATED PHOSPHATIC CLAYS

FIGURE 3-14

FIGURE 3-15

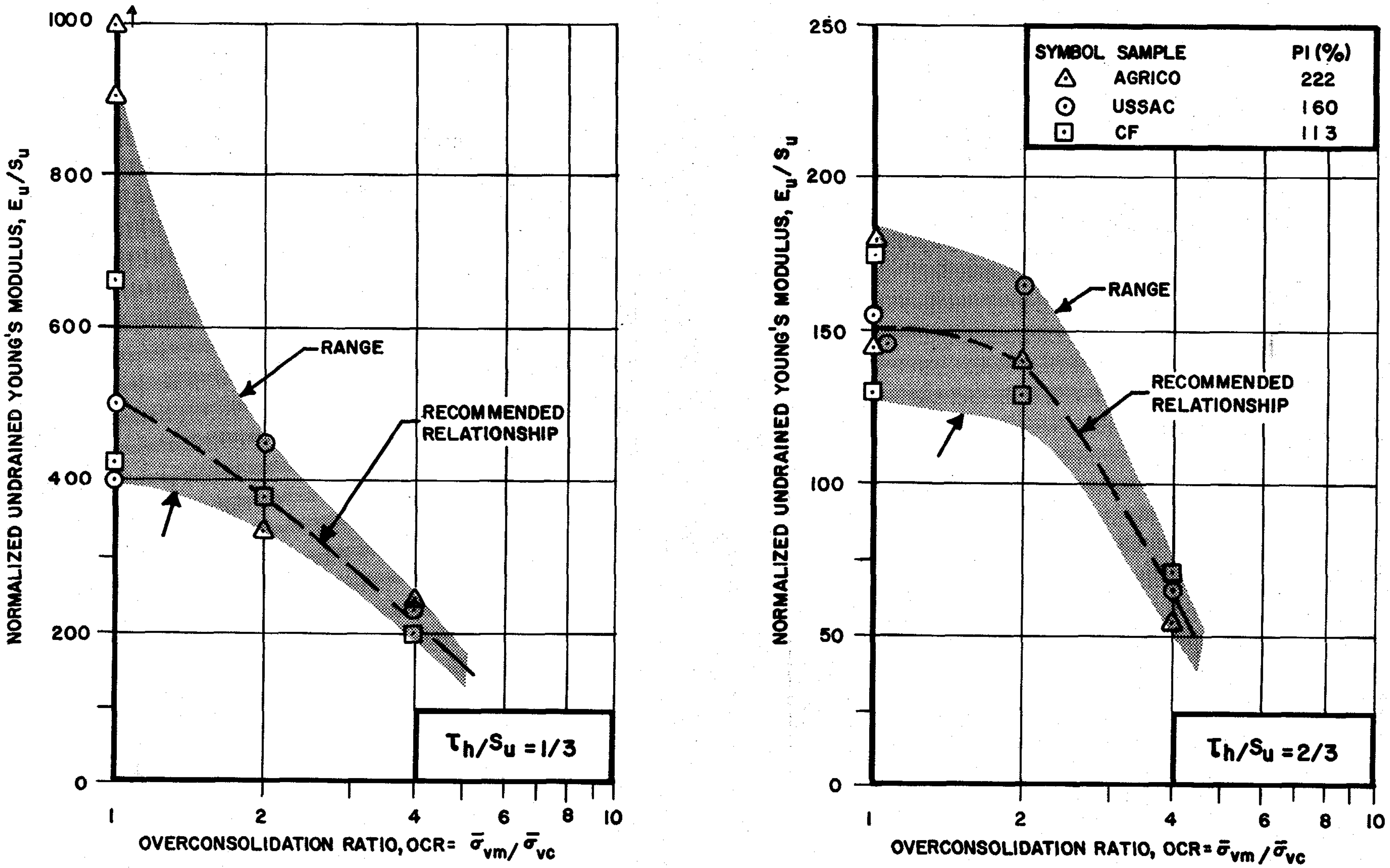

NORMALIZED UNDRAINED YOUNG'S MODULUS VERSUS OVERCONSOLIDATION RATIO FROM CK_oUDSS TESTS ON PHOSPHATIC CLAYS

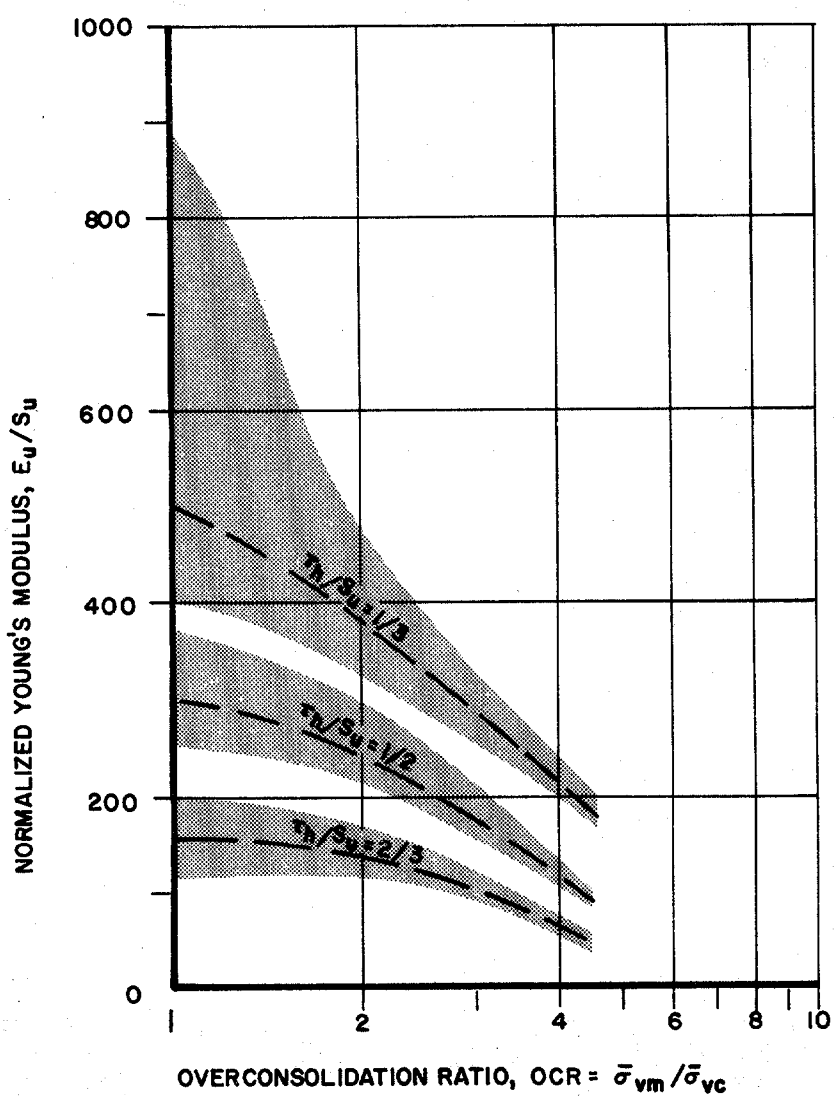

RECOMMENDED STRESS LEVEL DEPENDENT NORMALIZED UNDRAINED YOUNG'S MODULUS VERSUS OVERCONSOLIDATION RATIO FROM CK_0UDSS TESTS ON PHOSPHATIC CLAY

FIGURE 3-16

Section 4

STRESS-STRAIN-STRENGTH PROPERTIES OF SAND-CLAY MIXES

4.1 Test Methods and Test Procedures

Three phosphatic clays representative of the range in plasticity determined on samples obtained from twelve differing mine sites were mixed with tailings sand (at sand-clay ratios, SCR, ranging from 0:1 to 3:1)* to determine the undrained behavior and undrained shear strength of sand-clay mixes. Phosphatic clays selected for this investigation were from the Agrico-Saddle Creek mine (PI = 222%), the USSAC-Rockland mine (PI = 160%), and the CF Mining-Hardee mine (PI = 113%). These three clays are representative of relatively high, average and "low" plasticity phosphatic clays, respectively, and should reflect the effect of sand-clay mix on the range of phosphatic clays likely to occur in Florida. Atterberg limits of the Agrico, USSAC and CF sand-clay mixes were presented in Volume 4 "Consolidation Behavior of Phosphatic Clays" (Section 4.3.2), and are re-tabulated below for comparison:

	Agrico		CF		USSAC	
SCR	PI (%)	LL (%)	PI (%)	LL (%)	PI (%)	LL (%)
0:1	222	268	113	143	160	195
1:1	76	108	50	72	69	93
3:1	27	52	19	37	25	43

As shown, the addition of sand substantially reduces the plasticity of a sand-clay mix.

Sand-clay mix shear strength properties were investigated via $\overline{\text{CIUC}}$ and CK_0UDSS tests performed on normally consolidated samples. Test specimens were prepared as described in Section 2.3.2. They were trimmed from larger block samples pre-consolidated from a slurry to effective vertical consolidation stresses of 0.1 to 0.2 kg/cm^2 for sand-clay mixes, and 0.3 to 0.5 kg/cm^2 for phosphatic clays without sand. All test samples were consolidated prior to shear to effective stresses in excess of those used during sample preparation (i.e., 1.0 kg/cm^2 or more). Hence, all test specimens were normally consolidated prior to shear.

$\overline{\text{CIUC}}$ and CK_0UDSS test data on normally consolidated phosphatic clays (i.e., SCR = 0:1) were presented in Section 2. In addition to tests performed at a sand-clay ratio of 0:1, $\overline{\text{CIUC}}$ and CK_0UDSS tests were performed on each of 3 phosphatic clays at sand-clay ratios of 1:1 and 3:1. A total of 18 $\overline{\text{CIUC}}$ tests and 7 CK_0UDSS

*See Volume 3 "Sedimentation Behavior of Phosphatic Clays" and Volume 4 "Consolidation Behavior of Phosphatic Clays" for sand-clay ratio terminology used in this report and methods used to prepare sand-clay mixes in the laboratory.

tests were performed at sand-clay ratios of 1:1 and 3:1. Test procedures were in accordance with the methodologies outlined in Section 2.2.1 and 2.3.2.

4.2 $\overline{\text{CIUC}}$ Test Results

The undrained stress-strain-strength behavior of phosphatic clays (SCR = 0:1) from $\overline{\text{CIUC}}$ tests was presented for each individual test in Appendix A. The corresponding behavior of sand-clay mixes is included in Appendix B. Pertinent results from $\overline{\text{CIUC}}$ tests are summarized in Tables 4-1, 4-2 and 4-3, for the Agrico-Saddle Creek, USSAC-Rockland and CF Mining-Hardee sand-clay mixes, respectively.

4.2.1 Stress-Strain Behavior

Stress paths and normalized stress-strain behavior of phosphatic clays and sand-clay mixes (up to SCR = 3:1) were not significantly different. However, as illustrated in Figure 4-1, the strain at failure generally decreased* with the addition of sand resulting in a corresponding increase in undrained modulus: at a sand-clay ratio of 0:1, the vertical strain, ε_v, at maximum stress difference averaged about 8%; corresponding strains for a sand-clay ratio of 3:1 equalled 4 to 5%. Strain-softening effects were also slightly more noticeable for the sand-clay mixes.

The pore pressure A-factor at maximum stress difference generally ranged from 1.0 to 1.2 for the three phosphatic clays and averaged about 1.1 at a sand-clay ratio of 0:1. As shown in Figure 4-1, the A-factor at failure was somewhat reduced at a sand-clay ratio of 1:1 with a gross average value of about 1.0. However, with the addition of more sand to sand-clay ratios of 3:1, the A-factor at maximum stress difference experienced a considerable increase with characteristic average values generally ranging from 1.2 to 1.3.

4.2.2 Undrained Shear Strength

The effect of sand-clay ratio on the undrained shear strength, s_u, normalized with respect to the isotropic consolidation stress, $\bar{\sigma}_c$, and the one-dimensional vertical consolidation stress**, $\bar{\sigma}_{vc}$, is illustrated in Figure 4-2. As shown, the normalized undrained shear strength ratio $s_u/\bar{\sigma}_c$ increases moderately with the addition of sand up to a sand-clay ratio of about 1:1. With the continued addition of sand, $s_u/\bar{\sigma}_c$ decreases in magnitude. These changes in $s_u/\bar{\sigma}_c$ with variation in sand-clay ratio reflect primarily the observed change in the A-factor at failure with varying sand-clay ratio (see Section 4.2.1).

As shown in Figure 4-2, trends in $s_u/\bar{\sigma}_{vc}$ with changes in sand-clay ratio are very similar but more subdued than observed for $s_u/\bar{\sigma}_c$. Figure 4-3 illustrates the effect

*except for the Agrico-Saddle Creek sand-clay mix at a sand-clay ratio of 1:1.
**based on the "simple clay principle" and assuming K_o = 0.60 as explained in Section 2.2.4.

of clay plasticity on $s_u/\bar{\sigma}_{vc}$ for various sand-clay ratios. The following normalized undrained shear strength ratios, $s_u/\bar{\sigma}_{vc}$, are believed representative of sand-clay mixes based on $\overline{\text{CIUC}}$ test data:

Phosphatic Clay	PI (%)	SCR =	$s_u/\bar{\sigma}_{vc}$ 0:1	1:1	3:1
Agrico-Saddle Creek	222		0.26	0.30	0.29
USSAC-Rockland	160		0.28	0.29	0.26[5]
CF Mining-Hardee	113		0.29	0.31	0.26
Average			0.28	0.30	0.27

These values are characteristic of the shear strength in compression, $s_u(V)$, when the clay is sheared with the major principal stress in the vertical direction. They are much higher than one would predict when strain compatibility along a failure surface is taken into consideration (see Section 2.4).

4.2.3 Undrained Modulus

The effect of sand-clay ratio on the normalized undrained modulus, E_u/s_u, as a function of stress level is depicted in Figures 4-4, 4-5 and 4-6 for the Agrico-Saddle Creek, USSAC-Rockland and CF Mining-Hardee sand-clay mixes, respectively. As shown, the undrained modulus of the highly plastic Agrico-Saddle Creek clay is not significantly affected by the addition of sand except at high sand-clay ratios and high stress levels (Figure 4-4). On the other hand, the addition of sand substantially increases the undrained modulus of the USSAC-Rockland (Figure 4-5) and CF Mining-Hardee (Figure 4-6) phosphatic clays.

4.2.4 Angle of Internal Friction

The effective angle of internal friction, $\bar{\phi}$, was determined from undrained $\overline{\text{CIUC}}$ tests on sand-clay mixes at maximum obliquity, maximum stress difference, and tangency to the effective stress paths (see Appendices A and B). Figure 4-7 presents average values and ranges in $\bar{\phi}_u$ as a function of sand-clay ratio. As shown, $\bar{\phi}_u$ for all three phosphatic clays increases with increased sand-clay ratio; the increase is most prominent for the highly plastic Agrico-Saddle Creek clay.*

As noted in Section 2.2.6, the angle of internal friction under drained conditions, $\bar{\phi}_d$, is anticipated to be on the order of 25° at a sand-clay ratio of 0:1. Based on data presented in Figure 4-7, $\bar{\phi}_d$ is expected to increase with increased sand-clay ratio: values of $\bar{\phi}_d$ of 27° and 28° are believed applicable at sand-clay ratios of 1:1 and 3:1, respectively.

*The higher $\bar{\phi}$ value at a sand-clay ratio of 3:1 compared to $\bar{\sigma}$ at a sand-clay ratio of 0:1 is primarily responsible for the increase in $s_u/\bar{\sigma}_{vc}$ ratio observed for the Agrico-Saddle Creek clay at a sand-clay ratio of 3:1.

4.3 CK_oUDSS Test Results

Section 2.3.5 presented results of CK_oUDSS tests on phosphatic clays (SCR = 0:1). Normalized effective stress paths at varying sand-clay ratios (SCR = 0:1, 1:1 and 3:1) for the Agrico, USSAC and CF clays are compared in Figures 4-8, 4-9 and 4-10, respectively. The normalized stress-strain behavior is depicted in Figures 4-11, 4-12 and 4-13, respectively.

4.3.1 Stress-Strain Behavior

The normalized CK_oUDSS stress paths in Figures 4-8, 4-9 and 4-10 show a continuous decrease in vertical effective stress during undrained shear. Stress paths at varying sand-clay ratios are not significantly different. However, as illustrated in Figures 4-11 through 4-13, the shear strain at failure decreased substantially with the addition of sand resulting in a corresponding increase in undrained modulus. Moreover, strain softening effects become more prominent with the addition of sand particularly at a sand-clay ratio of 3:1. The reduction in shear strain at failure, γ_f, is clearly illustrated in Figures 4-14, 4-15 and 4-16 for the Agrico, USSAC and CF sand-clay mixes, respectively. The shear strain at failure averaged about 19.4% at a sand-clay ratio of 0:1, and equalled 1.5 to 3.0% at a sand-clay ratio of 3:1, a very marked reduction.

Normalized excess pore pressures, $\Delta u/\bar{\sigma}_{vc}$, generated during undrained shear increased significantly with the addition of sand as shown in Figures 4-11 through 4-13. However, positive excess pore pressures generated at "failure", i.e., at $s_u=(\tau_h)_{max}$ were generally not significantly different at varying sand-clay ratios; a slight reduction in $\Delta u/\bar{\sigma}_{vc}$ at failure is generally noted with increasing sand-clay ratio (i.e., SCR of 3:1 compared to 0:1).

Trends in the normalized undrained shear strength ratio, $s_u(DSS)/\bar{\sigma}_{vc}$, are presented in Figures 4-14, 4-15 and 4-16 for the Agrico, USSAC and CF sand-clay mixes, respectively. As shown, $s_u/\bar{\sigma}_{vc}$ generally increases slightly with the addition of sand up to a sand-clay ratio of about 1:1 (except for the CF Mining-Hardee clay where such an increase was not noted). With the continued addition of sand, $s_u/\bar{\sigma}_{vc}$ decreases in magnitude. These behavioral trends are consistent with those observed in $\overline{\text{CIU}}$C tests (Section 4.2).

4.3.2 Undrained Shear Strength Ratio

The effect of sand-clay ratio on the normalized undrained shear strength, $s_u/\bar{\sigma}_{vc}$, is illustrated in Figure 4-17 which summarizes results from CK_oUDSS tests on sand-clay mixes. A marked similarity in trends is observed for all three phosphatic clays* in spite of significant differences in plasticity. The limited effect of clay plasticity on $s_u/\bar{\sigma}_{vc}$ for various sand-clay ratios is more clearly depicted in Figure 4-18.

*except the CF Mining-Hardee clay at a sand-clay ratio of 1:1.

Based on CK_0UDSS test data, the following normalized undrained shear strength ratios are believed representative of sand-clay mixes:

Phosphatic Clay	PI (%)	SCR =	$s_u/\bar{\sigma}_{vc}$ 0:1	1:1	3:1
Agrico-Saddle Creek	222		0.224	0.236	0.202
USSAC-Rockland	160		0.220	0.235	0.197
CF Mining-Hardee	113		0.229	0.214	0.190
Gross Average			0.225	0.228	0.196

Because the plasticity of the phosphatic clay seems to have only a small effect on the normalized undrained shear strength, gross average $s_u/\bar{\sigma}_{vc}$ values of 0.225, 0.228, 0.214 and 0.196 probably characterize the shear strength of normally consolidated sand-clay mixes at sand-clay ratios of 0:1, 1:1, 2:1 and 3:1, respectively, for a wide range of phosphatic clays.

Figure 4-19 presents the variation in $s_u/\bar{\sigma}_{vc}$ (from both $\overline{CIUC}$ and CK_0UDSS tests) with changes in plasticity index of the sand-clay mix (rather than the plasticity index of the phosphatic clay per se as illustrated previously in Figures 4-3 and 4-18). As shown, trends in $s_u/\bar{\sigma}_{vc}$ versus plasticity index of the mix are generally consistent based on both types of tests. The addition of a "small" quantity of sand to a sand-clay ratio of 1:1 results in a reduced plasticity index* and an increased $s_u/\bar{\sigma}_{vc}$ ratio compared to that of phosphatic clay without sand. With the continued addition of sand to a sand-clay ratio of 3:1, the plasticity index decreases substantially to values characteristic of lean clays (PI = 19 to 27%) rather than high plasticity clays, and $s_u/\bar{\sigma}_{vc}$ also experiences a decrease in magnitude. The ratio $s_u(\overline{CIUC})/s_u(DSS)$ decreases from about 0.8 at a sand-clay ratio of 0:1 to about 0.7 at a sand-clay ratio of 3:1 indicating that the lower plasticity sand-clay mixes are more anisotropic than phosphatic clay without sand.

4.3.3 Undrained Modulus

Variations in the normalized undrained secant Young's modulus, E_u/s_u, with stress level and sand-clay ratio are illustrated in Figures 4-20, 4-21 and 4-22 for the Agrico-Saddle Creek, USSAC-Rockland, and CF Mining-Hardee clays, respectively. In spite of some scatter, the trends observed are similar for all three clays: E_u/s_u increases with increased sand-clay ratio. The increase in undrained modulus at a given stress level with increasing sand-clay ratio is clearly depicted in Figure 4-23.

Figure 4-24 presents an overview of the data from CK_0UDSS tests performed on sand-clay mixes using all three phosphatic clays. As shown, E_u/s_u increases with

*From the plasticity index range 113% to 222% to the PI range of 50% to 76%.

increased sand-clay ratio particularly at sand-clay ratios in excess of 1:1. Figure 4-25 illustrates the degree of scatter in E_u/s_u versus sand-clay ratio at stress levels of 33% and 67%, corresponding to factors of safety of 3 and 1.5. Although E_u/s_u generally increases with reduced clay plasticity particularly at high stress levels, the scatter between tests on a given phosphatic clay (particularly at low stress levels) can be as large as the scatter from one phosphatic clay to the other. Hence, a single stress level dependent relationship between E_u/s_u and sand-clay ratio may be used for all three phosphatic clays with the bands in Figure 4-25 showing potential deviation in E_u/s_u at a given sand-clay ratio.

4.4 **Effect of Sand-Clay Ratio on Undrained Stress-Strain-Strength Behavior**

As detailed in Sections 4.2 and 4.3, the addition of sand to phosphatic clays causes subtle changes to the undrained stress-strain-strength characteristics, namely:

- a reduction in the strain at failure and more prominent strain-softening effects particularly at high sand-clay ratios.
- an increase in positive excess pore pressures generated during undrained shear particularly at high sand-clay ratios at large strains subsequent to failure.
- a slight increase in the normalized undrained shear strength $s_u/\bar{\sigma}_{vc}$ at sand-clay ratios up to 1:1, and a moderate decrease in $s_u/\bar{\sigma}_{vc}$ with the continued addition of sand up to a sand-clay ratio of 3:1.
- an increase in the normalized undrained modulus E_u/s_u.
- a slight to moderate increase in the angle of internal friction, $\bar{\phi}$.

Most of the above trends reflect the change in plasticity of the sand-clay mix and the transition from an extremely plastic clay (SCR = 0:1), to a high plasticity clay (SCR = 1:1), to a much leaner clay (SCR = 3:1). Note that at sand-clay ratios up to 3:1, particle to particle contact between sand grains is not likely, and hence the sand acts as a filler within the clay matrix. The sand grains contribute to rendering the mix somewhat stiffer and less deformable (increased modulus), but may somewhat hamper the preferred structure of clay particles resulting in a slight reduction in the undrained shear strength at a sand-clay ratio of 3:1.

4.5 **Recommended Properties for Use in Design and Predictions**

4.5.1 Undrained Shear Strength Ratio

As demonstrated in Section 2.4, CK_oUDSS tests provide a reasonably reliable estimate for the *in situ* undrained shear strength. A marked similarity in the magnitude and trends of variation in $s_u/\bar{\sigma}_{vc}$ with increasing sand-clay ratio was noted for sand-clay mixes prepared with three phosphatic clays in spite of significant differences in phosphatic clay plasticity. Hence, the following gross average CK_oUDSS normalized undrained shear strength ratios are believed applicable for a wide range of phosphatic clays:

SCR	$s_u/\bar{\sigma}_{vc}$
0:1	0.225
1:1	0.228
2:1	0.214
3:1	0.196

The above values are applicable to normally consolidated sand-clay mixes. (The increase in $s_u/\bar{\sigma}_{vc}$ with overconsolidation ratio can be accounted for as described in Section 3.4).

4.5.2 Undrained Modulus

As detailed in Section 2.3.5, normalized undrained secant modulus data, E_u/s_u, versus stress level from CK_0UDSS tests are recommended for use in predicting undrained deformations. As shown in Figures 4-24 and 4-25, E_u/s_u increases with increased sand-clay ratio. Data presented in these figures may be used to predict undrained deformations of normally consolidated sand-clay mixes.

4.5.3 Effective Stress Failure Envelope

For drained effective stress type stability analyses that may be performed to assess long-term performance of normally consolidated sand-clay mixes, the following sand-clay ratio dependent effective angle of internal friction, $\bar{\phi}_d$, may be used:

SCR	$\bar{\phi}_d$
0:1	25.0°
1:1	27.0°
2:1	27.5°
3:1	28.0°

Section 4.2.4 outlined the basis for these recommended values.

Table 4-1

SUMMARY OF RELEVANT PARAMETERS FROM $\overline{CIU}C$ TEST RESULTS ON AGRICO SADDLE-CREEK SAND-CLAY MIXES

SCR	Test Sample	$s_u/\bar{\sigma}_c$	$s_u/\bar{\sigma}_{vc}$*	At $(\sigma_1-\sigma_3)_{max}$ ϵ(%)	At $(\sigma_1-\sigma_3)_{max}$ A Factor	At $(\sigma_1-\sigma_3)_{max}$ $\bar{\phi}$	At $(\bar{\sigma}_1/\bar{\sigma}_3)_{max}$ $\bar{\phi}$
0:1	S2	0.29	0.28	8.1	1.24	31.1°	32.6°
	S8	0.27	0.25	6.9	1.28	28.2°	29.8°
	S9	0.29	0.25	6.7	1.14	29.5°	31.1°
	Average	0.28	0.26	7.2	1.22	29.6°	31.1°
1:1	S1	0.34	0.31	9.3	1.10	36.6°	38.8°
	S2	0.36	0.30	9.6	0.94	32.7°	33.4°
	Average	0.35	0.30	9.5	1.02	34.6°	36.1°
3:1	S1	0.33	0.30	17.3?	1.27	43.2°	43.2°
	S2	0.29	0.28	4.0	1.22	30.9°	33.6°
	S3	0.34	0.29	5.8	1.10	34.6°	36.4°
	Average	0.32	0.29	4.9	1.20	36.2°	37.7°

*Based on "simple clay principle" and assuming $K_o = 0.60$.

Table 4-2

SUMMARY OF RELEVANT PARAMETERS FROM $\overline{\text{CIUC}}$ TEST RESULTS ON USSAC-ROCKLAND SAND-CLAY MIXES

SCR	Test Sample	$s_u/\bar{\sigma}_c$	$s_u/\bar{\sigma}_{vc}$*	At$(\sigma_1-\sigma_3)_{max}$ ε(%)	At$(\sigma_1-\sigma_3)_{max}$ A Factor	At$(\sigma_1-\sigma_3)_{max}$ $\bar{\phi}$	At$(\bar{\sigma}_1/\bar{\sigma}_3)_{max}$ $\bar{\phi}$
0:1	S1	0.33	0.29^5	8.4	1.05	32.4°	34.8°
	S2	0.34	0.30	11.4	1.05	34.2°	35.6°
	S3	0.27	0.26	7.6	1.13	24.9°	26.3°
	S4	0.28	0.27	8.9	1.23	26.8°	26.8°
	Average	0.30^5	0.28	9.1	1.11	29.6°	30.9°
1:1	S1	0.35	0.30	9.6	1.09	35.5°	36.6°
	S2	0.36	0.29	6.7	0.92	30.6°	31.9°
	S3	0.31	0.27^5	4.0	0.99	25.7°	27.4°
	S4	0.34	0.30	6.3	1.02	30.7°	31.7°
	Average	0.34	0.29	6.7	1.00	30.6°	31.9°
3:1	S2	0.28	0.26^5	4.7	1.37	33.0°	35.0°
	S3	0.30	0.26	3.3	1.17	29.8°	31.9°
	Average	0.29	0.26^5	4.0	1.27	31.4°	33.5°

*Based on "simple clay principle" and assuming K_o = 0.60.

Table 4-3

SUMMARY OF RELEVANT PARAMETERS FROM $\overline{CIU}C$ TEST RESULTS ON CF MINING-HARDEE SAND-CLAY MIXES

SCR	Test Sample	$s_u/\bar{\sigma}_c$	$s_u/\bar{\sigma}_{vc}$*	ε(%)	At$(\sigma_1-\sigma_3)_{max}$ A Factor	At$(\sigma_1-\sigma_3)_{max}$ $\bar{\Phi}$	At$(\bar{\sigma}_1/\bar{\sigma}_3)_{max}$ $\bar{\Phi}$
0:1	S1	0.32	0.27	5.7	1.03	28.6°	29.8°
	S3	0.34	0.30	7.4	0.92	29.3°	29.9°
	S4	0.33	0.30	10.3	1.03	30.2°	31.3°
	Average	0.33	0.29	7.8	0.99	29.4°	30.3°
1:1	S1	0.39	0.32	5.3	0.85	31.5°	33.2°
	S2	0.32$_5$	0.29	7.0	1.09	29.9°	30.4°
	Average	0.35^5	0.31	6.2	0.97	30.7°	31.8°
3:1	S2	0.27	0.26	2.5	1.30	30.2°	34.1°
	S3	0.27	0.24	1.9	1.19	25.6°	28.0°
	S4	0.27	0.27	10.0	1.41	34.5°	34.6°
	Average	0.27	0.26	4.8	1.30	30.1°	32.2°

*Based on "simple clay principle" and assuming K_o = 0.60.

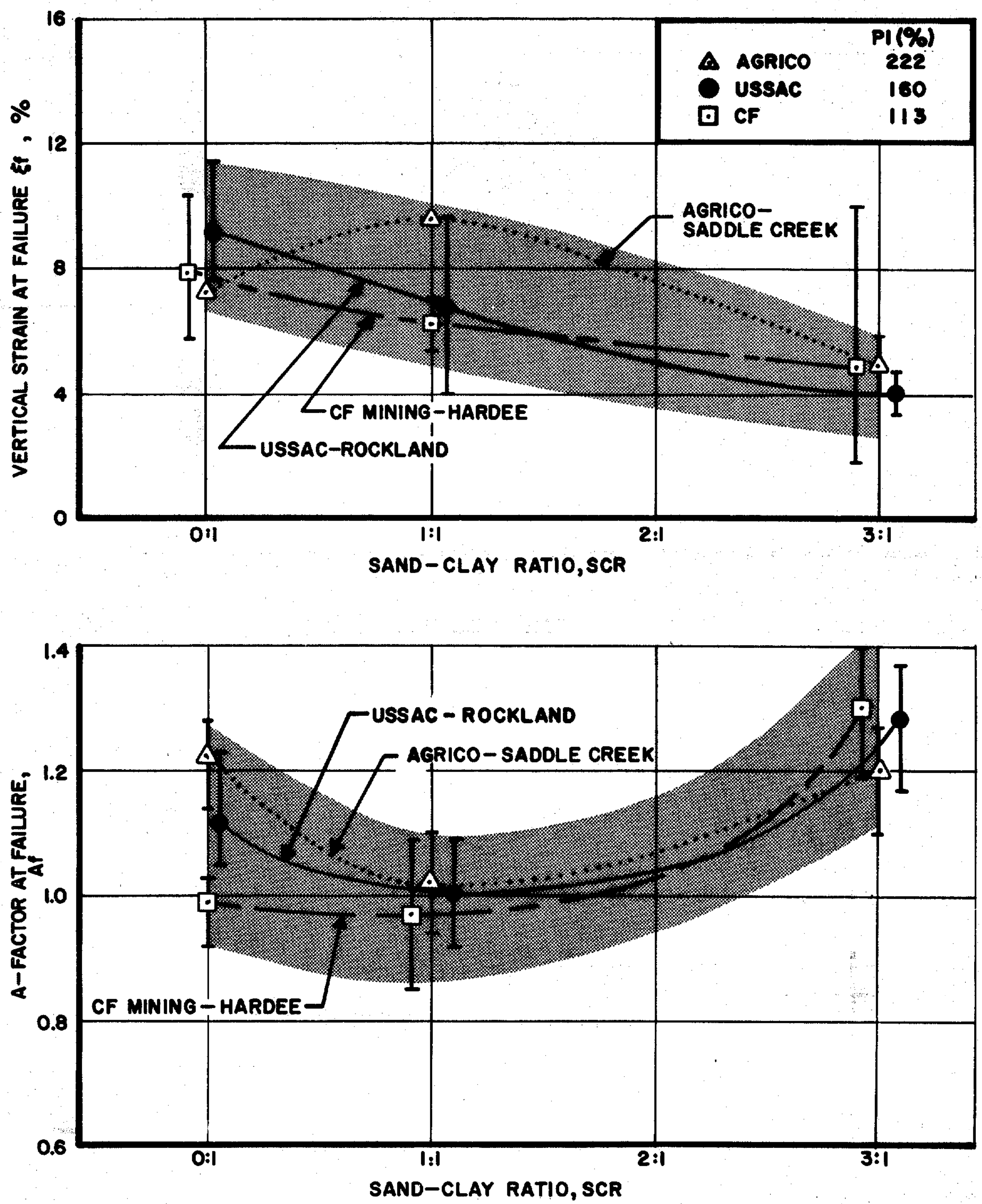

VARIATION OF STRAIN AND A-FACTOR AT FAILURE WITH SAND-CLAY RATIO FROM CIUC TESTS ON SAND-CLAY MIXES

FIGURE 4-1

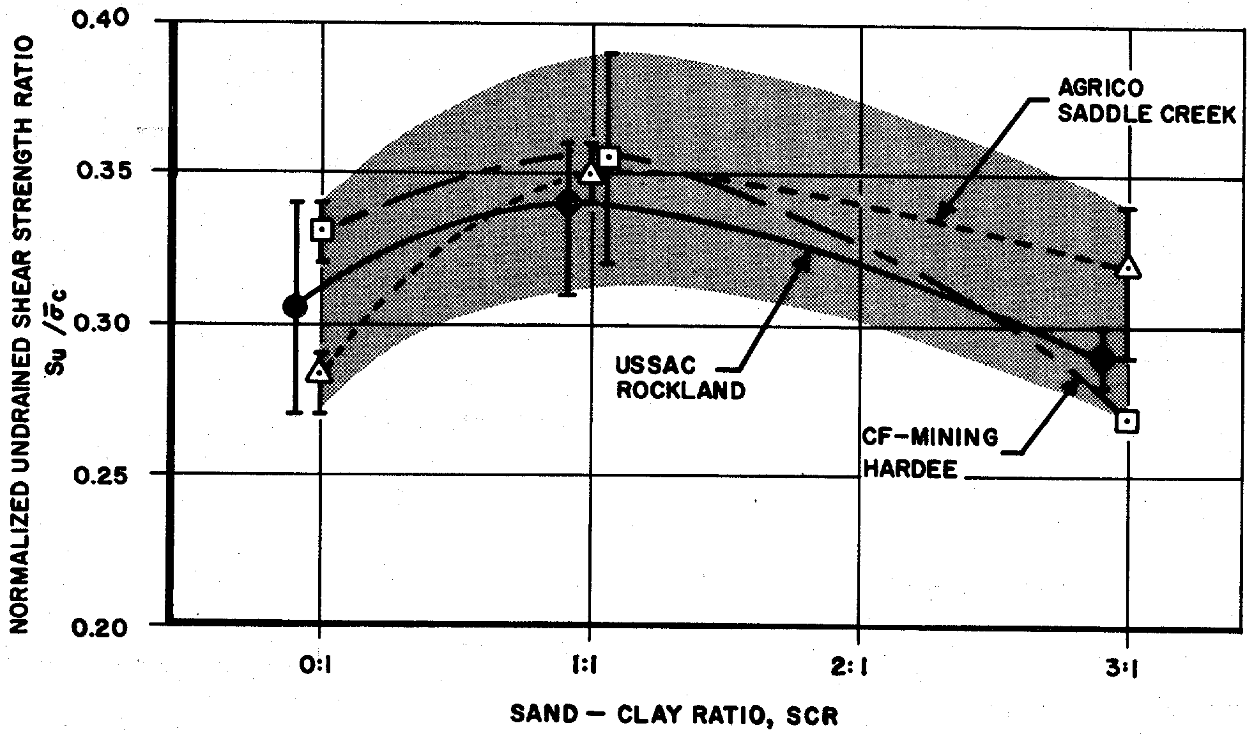

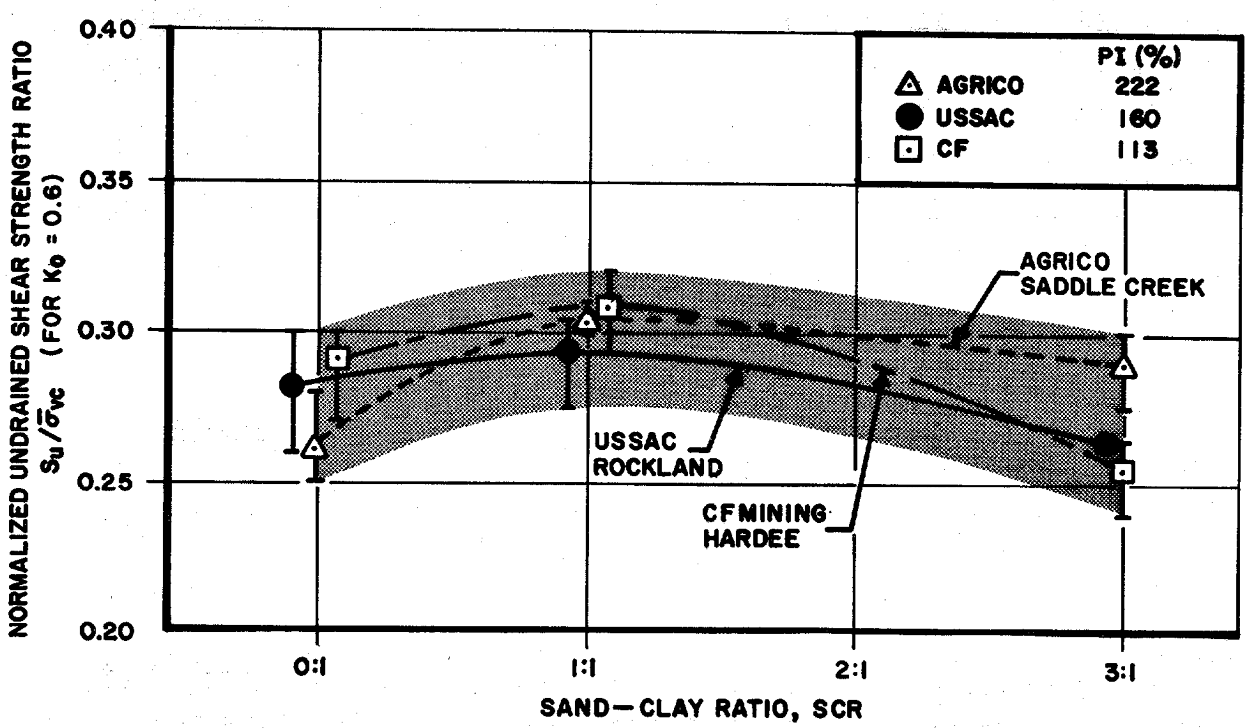

NORMALIZED UNDRAINED SHEAR STRENGTH VERSUS SAND-CLAY RATIO FROM CIUC TESTS ON SAND-CLAY MIXES

FIGURE 4-2

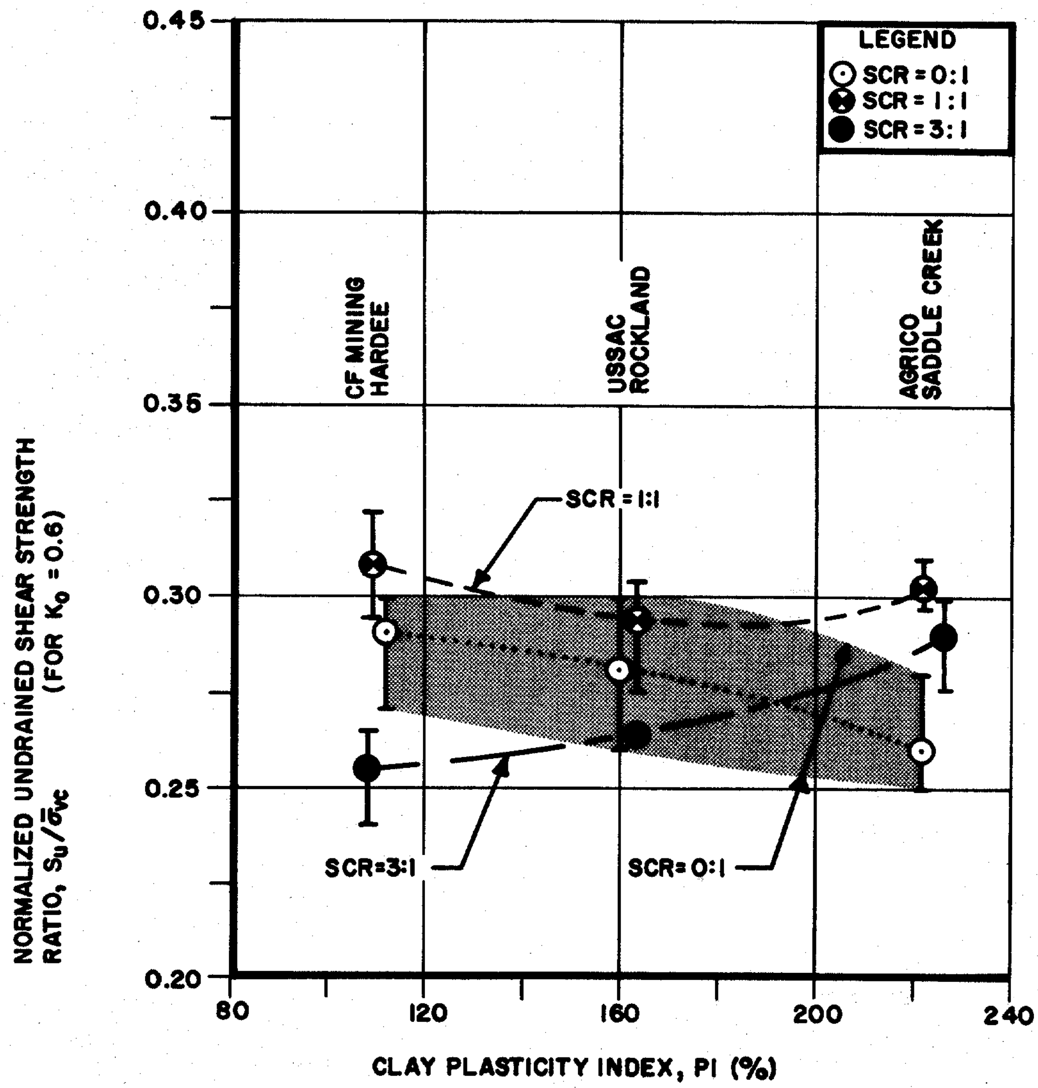

NORMALIZED UNDRAINED SHEAR, STRENGTH RATIO VERSUS PHOSPHATIC CLAY PLASTICITY INDEX FROM CIUC TESTS ON SAND-CLAY MIXES

FIGURE 4-3

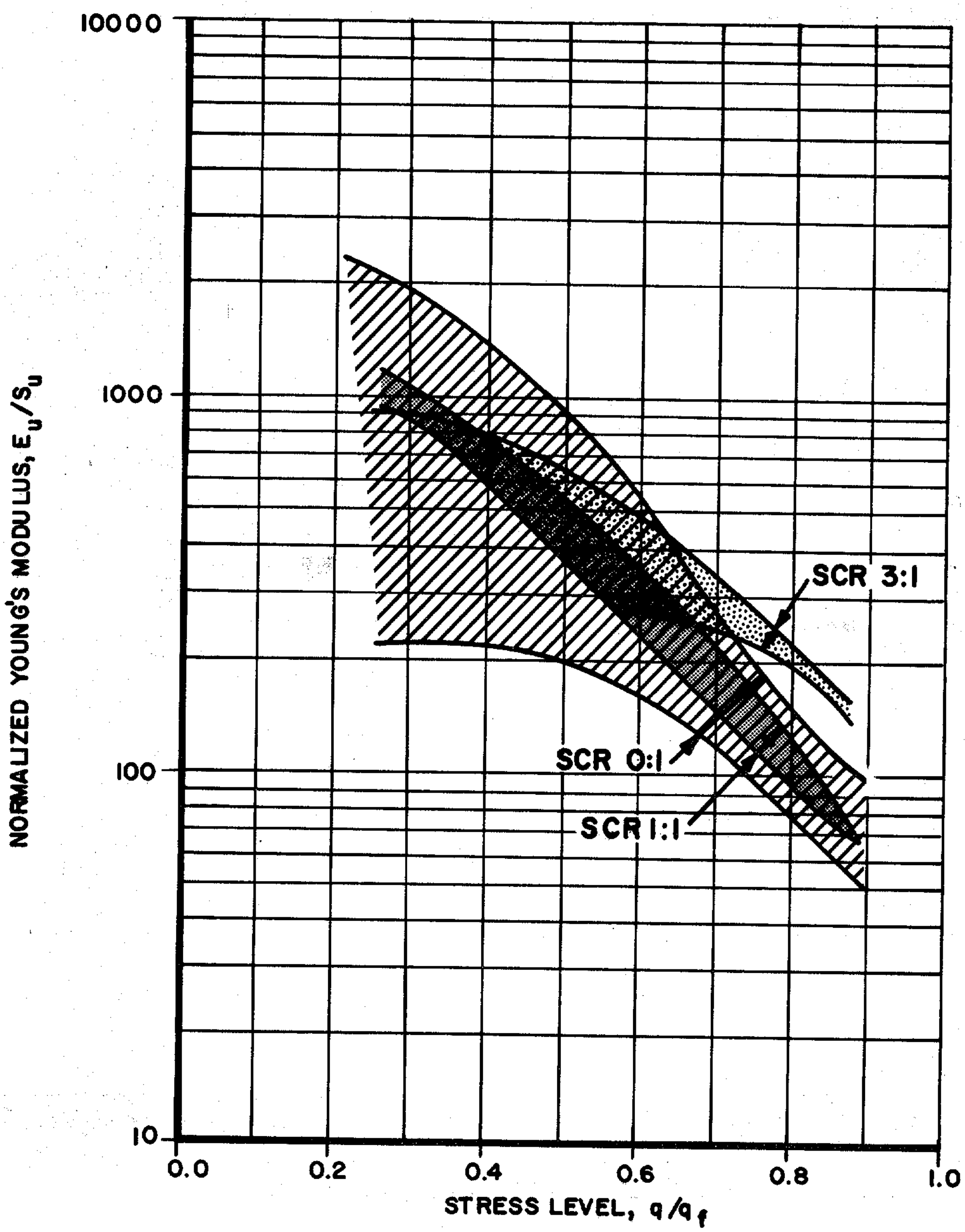

NORMALIZED UNDRAINED YOUNG'S MODULUS VERSUS STRESS LEVEL FROM CIUC TESTS ON AGRICO-SADDLE CREEK SAND-CLAY MIXES

FIGURE 4-4

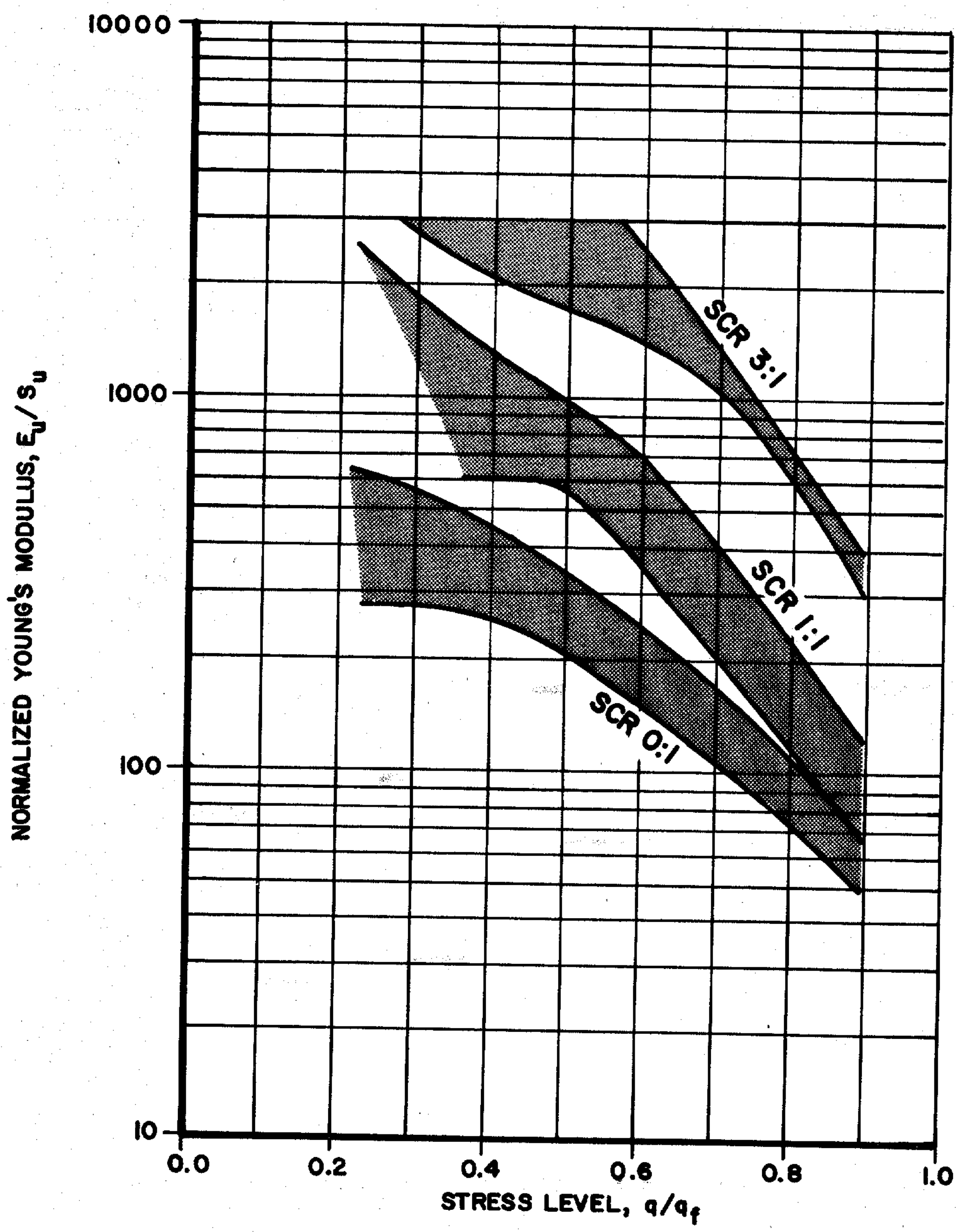

NORMALIZED UNDRAINED YOUNG'S MODULUS VERSUS STRESS LEVEL FROM CIUC TESTS ON USSAC-ROCKLAND SAND-CLAY MIXES

FIGURE 4-5

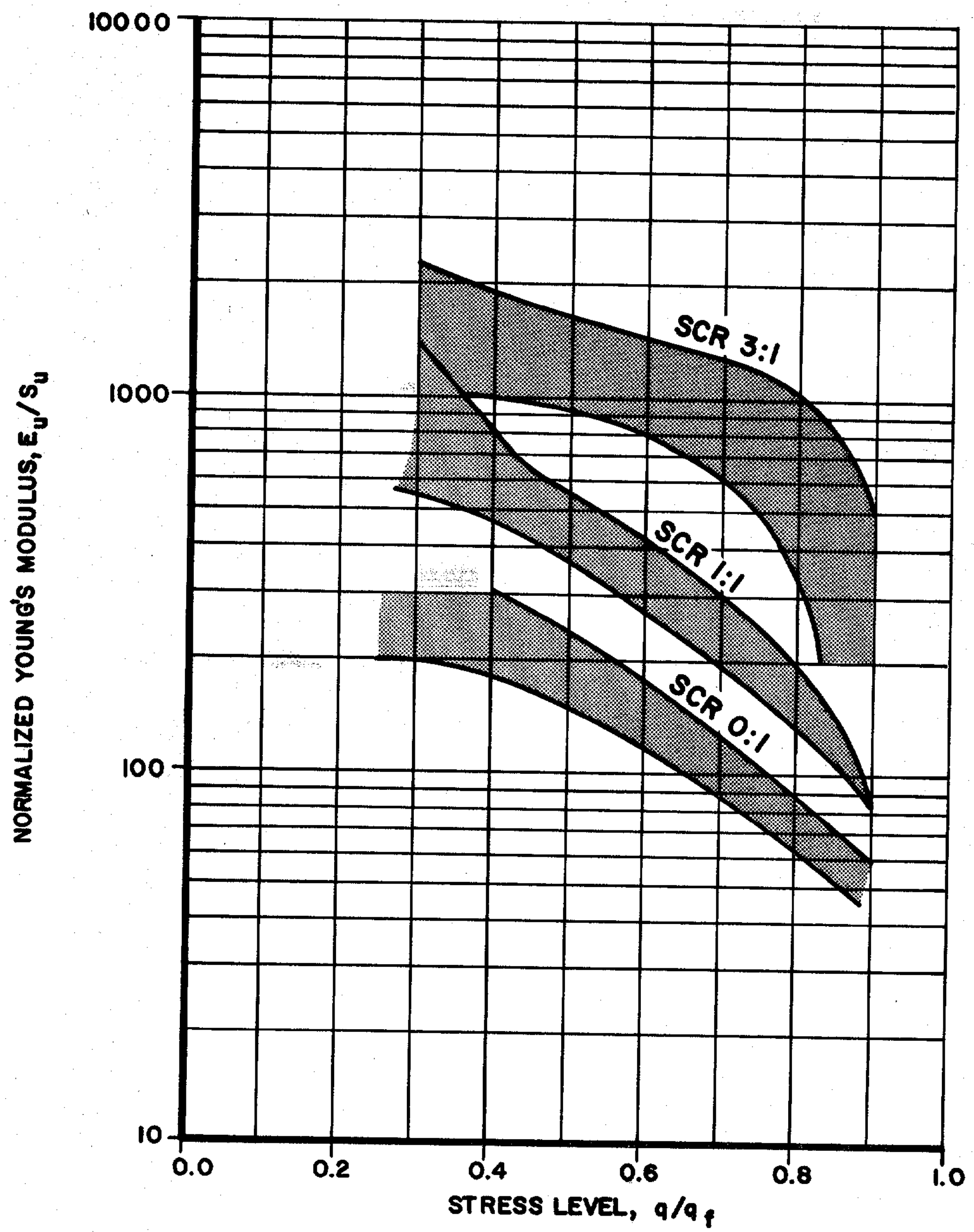

NORMALIZED UNDRAINED YOUNG'S MODULUS VERSUS STRESS LEVEL FROM CIUC TESTS ON CF MINING-HARDEE SAND-CLAY MIXES

FIGURE 4-6

FIGURE 4-7

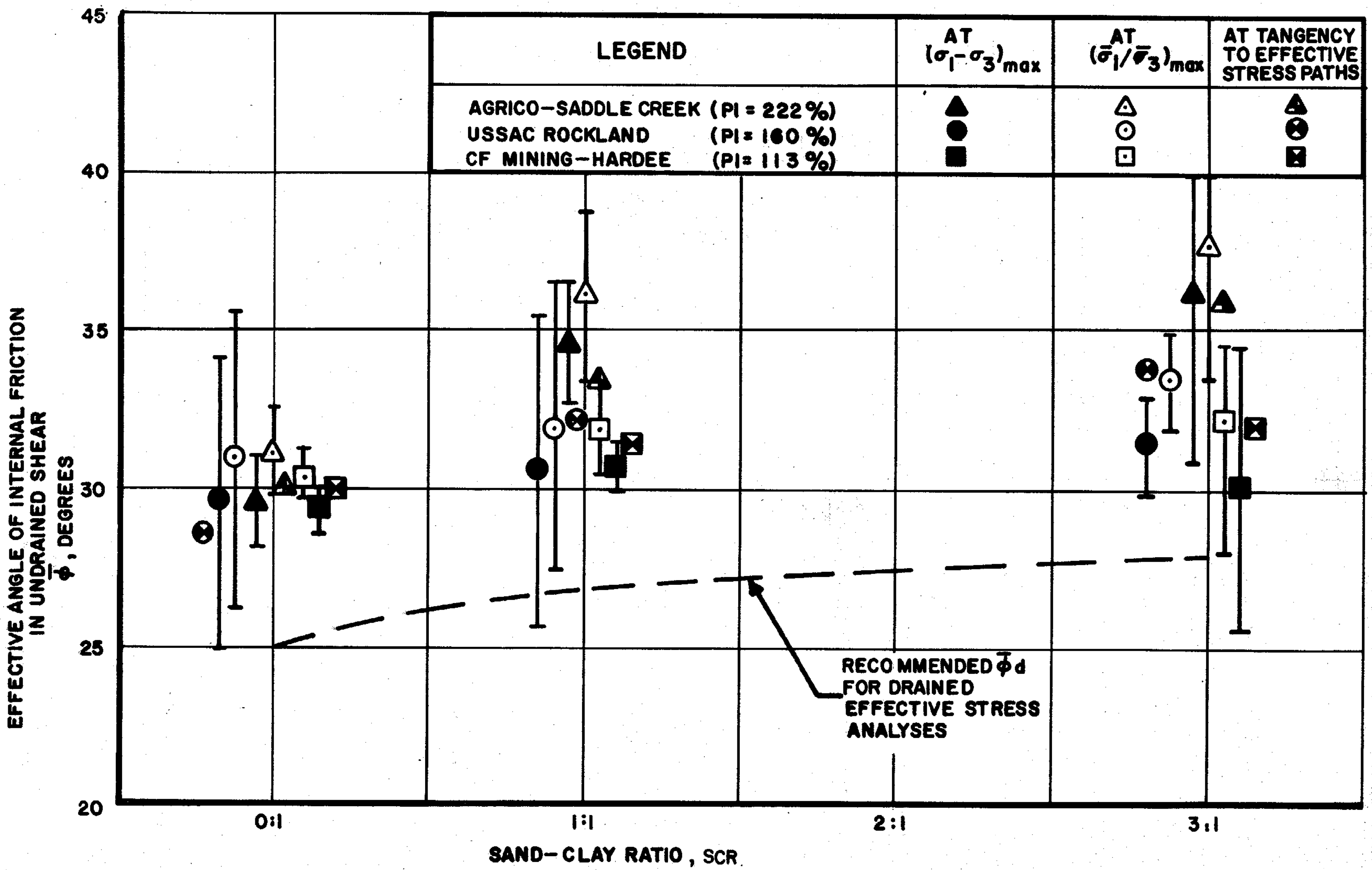

EFFECTIVE ANGLE OF INTERNAL FRICTION VERSUS SAND-CLAY RATIO FROM $\overline{\text{CIUC}}$ TESTS ON SAND-CLAY MIXES

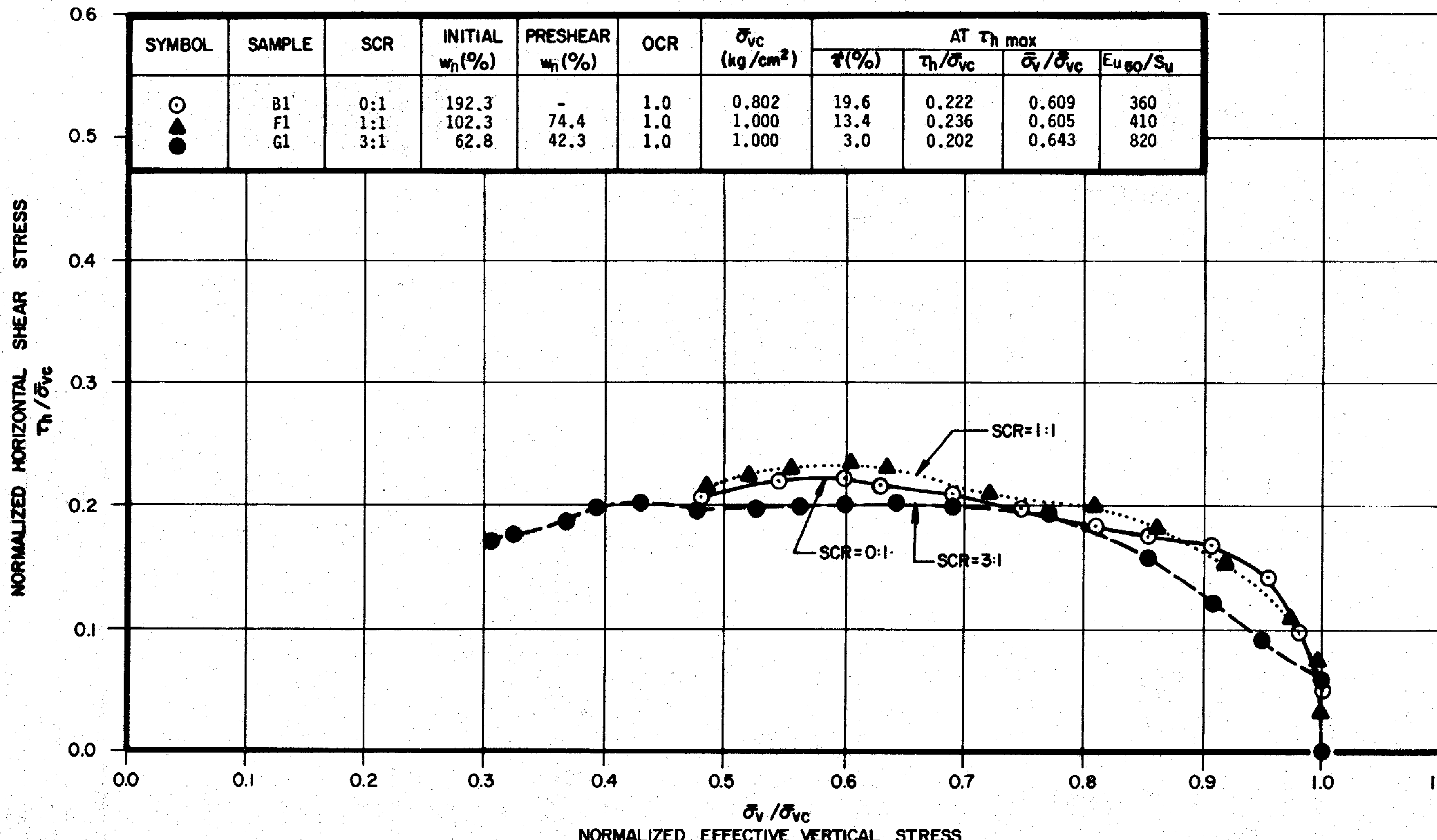

SYMBOL	SAMPLE	SCR	INITIAL w_n(%)	PRESHEAR w_n(%)	OCR	$\bar{\sigma}_{vc}$ (kg/cm²)	AT τ_h max γ(%)	$\tau_h/\bar{\sigma}_{vc}$	$\bar{\sigma}_v/\bar{\sigma}_{vc}$	E_{u50}/S_u
⊙	B1	0:1	192.3	-	1.0	0.802	19.6	0.222	0.609	360
▲	F1	1:1	102.3	74.4	1.0	1.000	13.4	0.236	0.605	410
●	G1	3:1	62.8	42.3	1.0	1.000	3.0	0.202	0.643	820

NORMALIZED UNDRAINED EFFECTIVE STRESS PATHS
FROM CK_0 UDSS TESTS
ON AGRICO-SADDLE CREEK SAND-CLAY MIXES

SYMBOL	SAMPLE	SCR	INITIAL w_n(%)	PRESHEAR w_n(%)	OCR	$\bar{\sigma}_{vc}$ (kg/cm^2)	AT $\tau_{h\,max}$ γ(%)	$\tau_h/\bar{\sigma}_{vc}$	$\bar{\sigma}_v/\bar{\sigma}_{vc}$	$E_{u\,50}/S_u$
⊙	C2	0:1	136.5	111.6	1.0	1.04	22.0	0.212	0.567	308
■	I1	1:1	106.4	61.4	1.0	1.05	12.6	0.235	0.590	415
▲	H1	3:1	47.2	32.9	1.0	1.05	2.0	0.197	0.644	1580

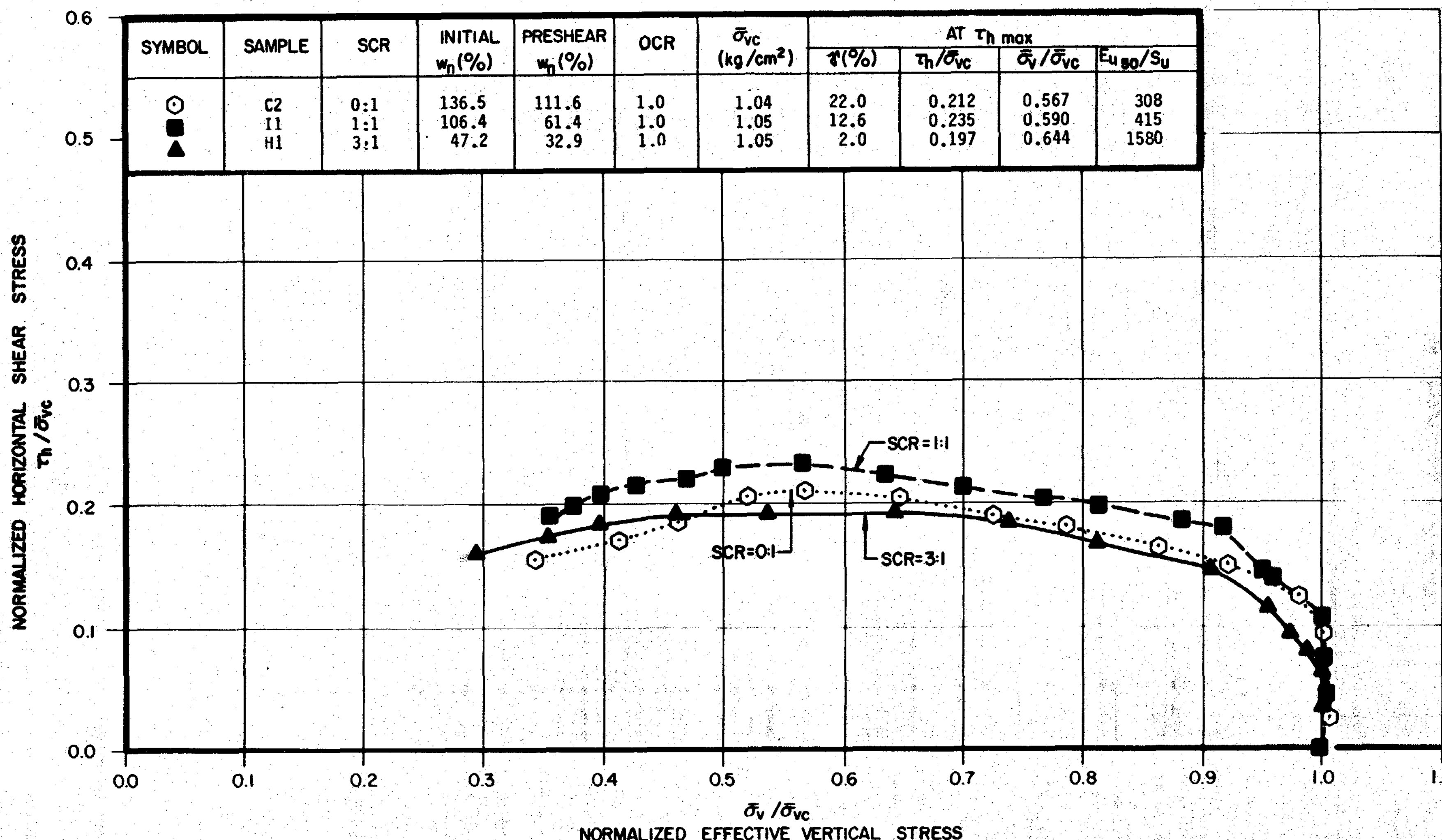

NORMALIZED UNDRAINED EFFECTIVE STRESS PATHS FROM CK$_0$UDSS TESTS ON USSAC-ROCKLAND SAND-CLAY MIXES

FIGURE 4-10

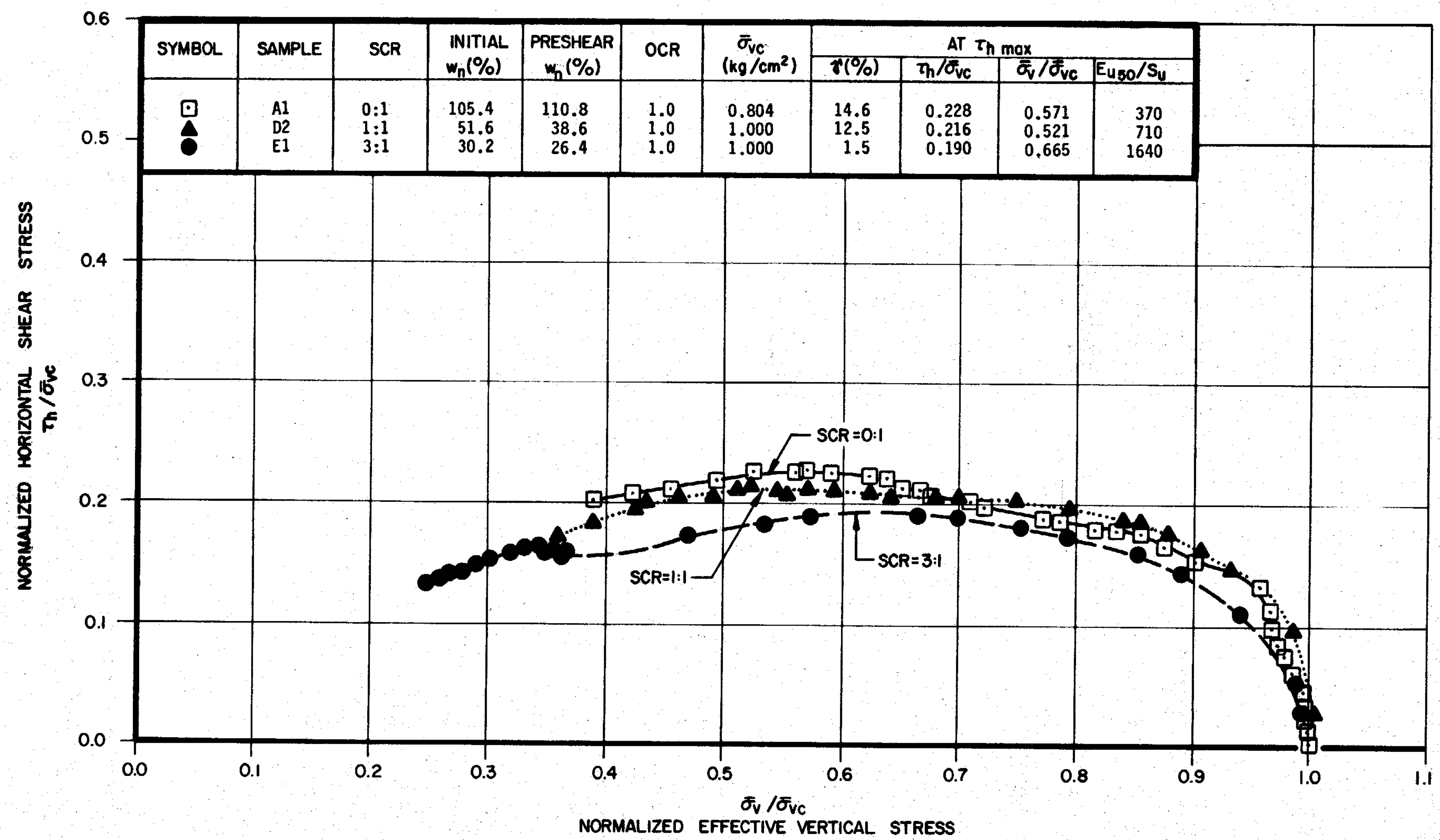

SYMBOL	SAMPLE	SCR	INITIAL w_n(%)	PRESHEAR w_n(%)	OCR	$\bar{\sigma}_{vc}$ (kg/cm^2)	AT τ_h max			
							γ(%)	$\tau_h/\bar{\sigma}_{vc}$	$\bar{\sigma}_v/\bar{\sigma}_{vc}$	E_{u50}/S_u
⊡	A1	0:1	105.4	110.8	1.0	0.804	14.6	0.228	0.571	370
▲	D2	1:1	51.6	38.6	1.0	1.000	12.5	0.216	0.521	710
●	E1	3:1	30.2	26.4	1.0	1.000	1.5	0.190	0.665	1640

NORMALIZED UNDRAINED EFFECTIVE STRESS PATHS FROM CK_oUDSS TESTS ON CF MINING-HARDEE SAND-CLAY MIXES

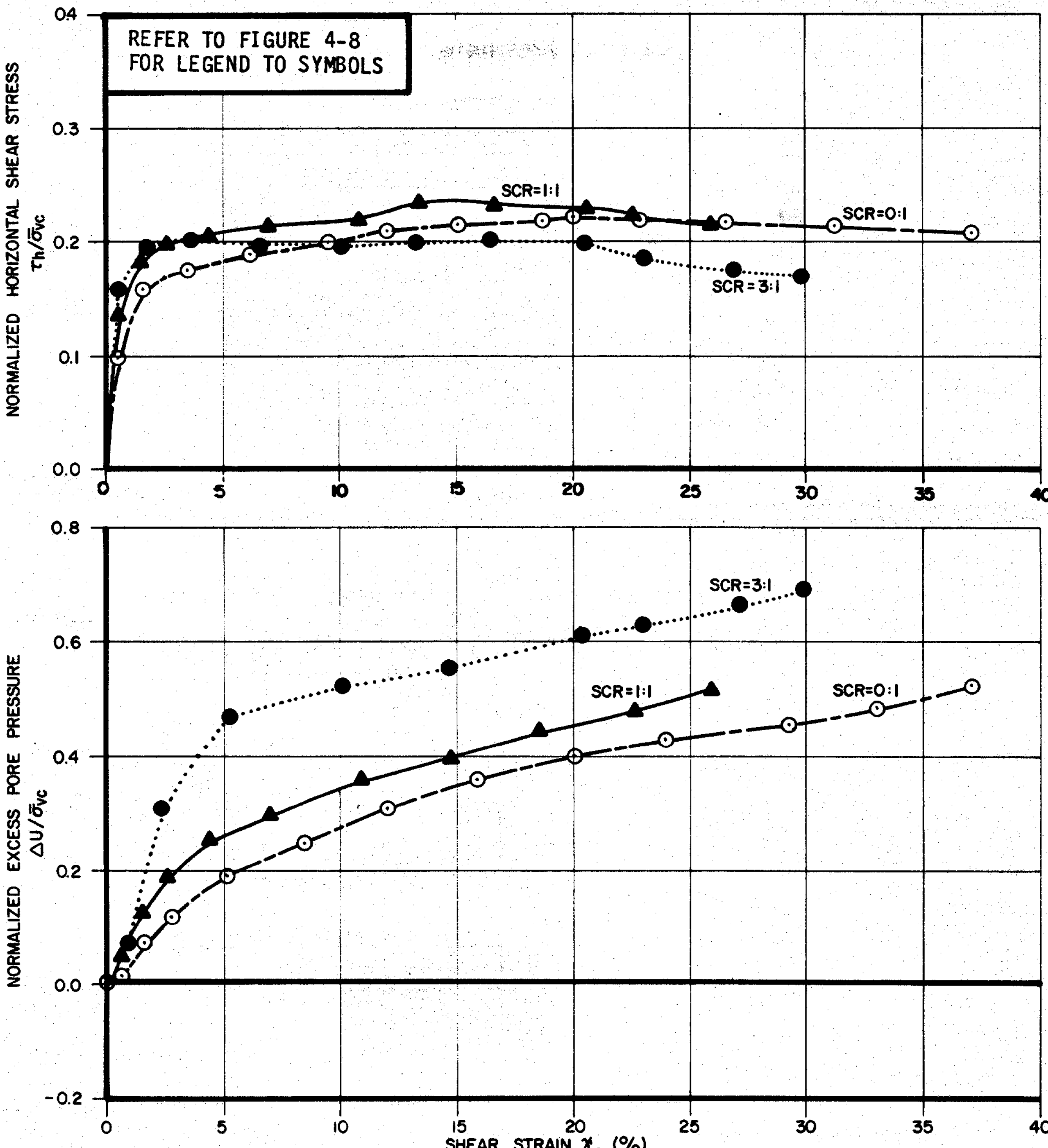

NORMALIZED UNDRAINED STRESS-STRAIN BEHAVIOR FROM CK_0UDSS TESTS ON AGRICO-SADDLE CREEK SAND-CLAY MIXES

FIGURE 4-11

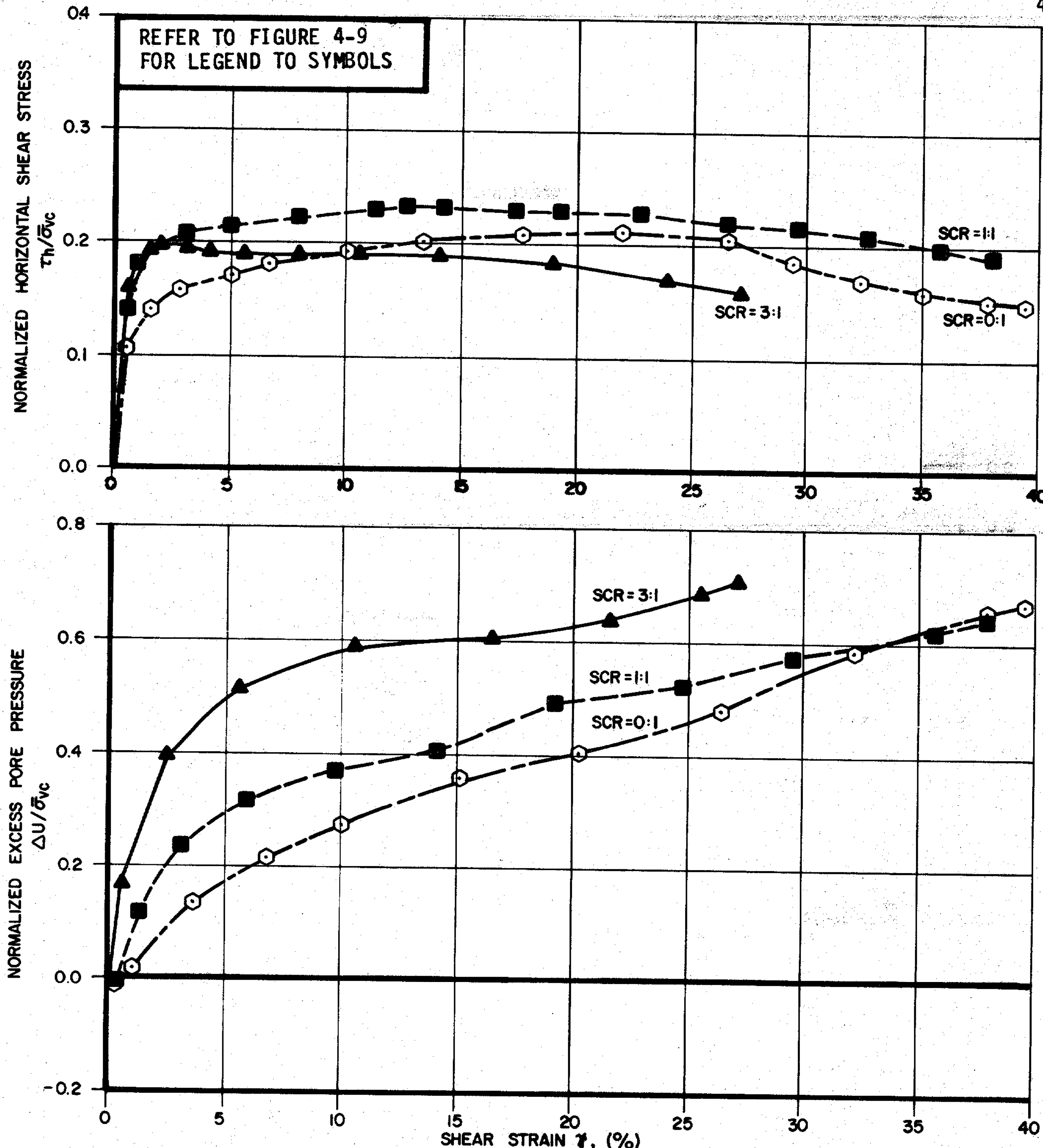

NORMALIZED UNDRAINED STRESS-STRAIN BEHAVIOR FROM CK_0UDSS TESTS ON USSAC-ROCKLAND SAND-CLAY MIXES

FIGURE 4-12

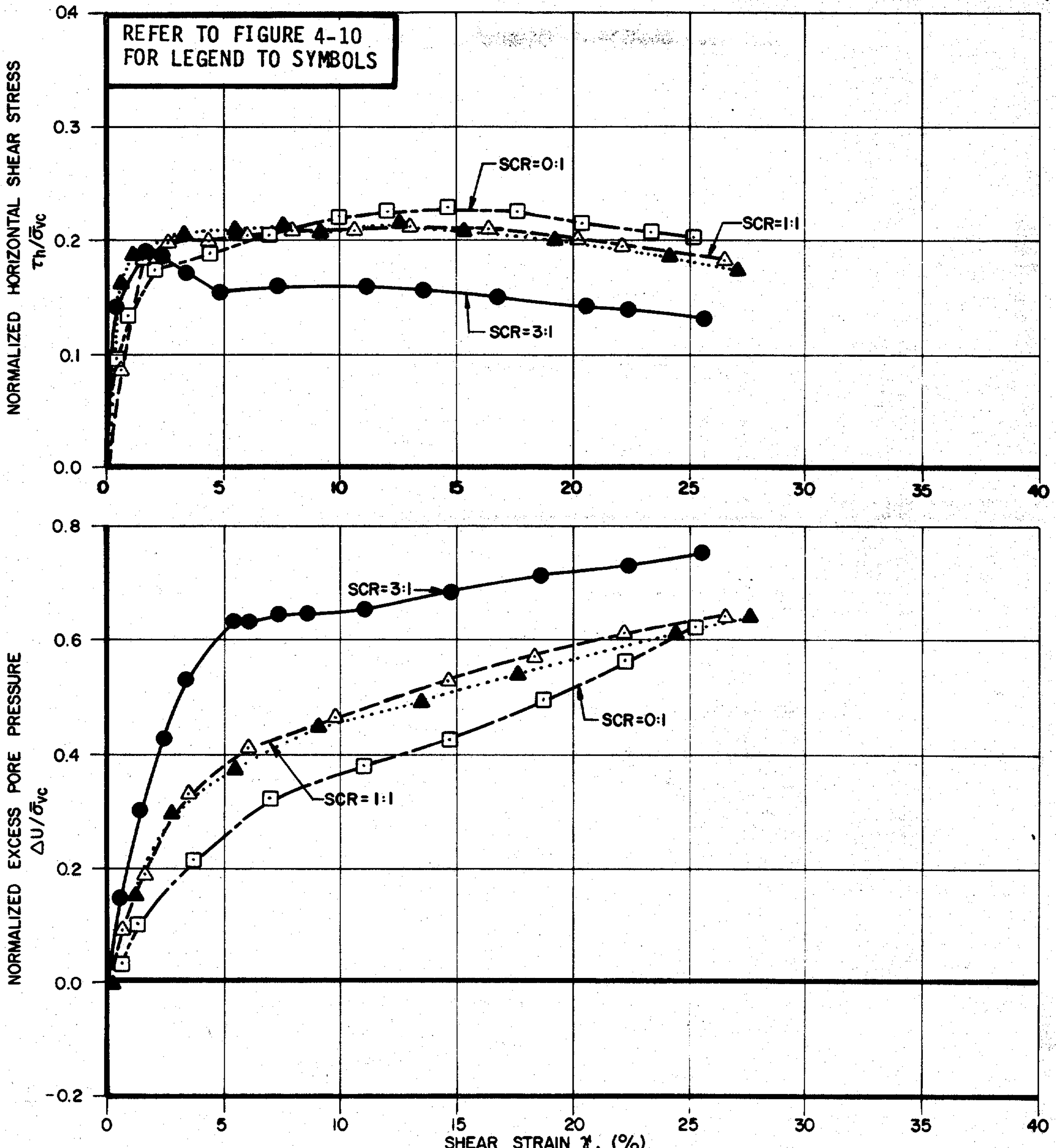

NQRMALIZED UNDRAINED STRESS-STRAIN BEHAVIOR
FROM CK_oUDSS TESTS
ON CF MINING-HARDEE SAND-CLAY MIXES

FIGURE 4-13

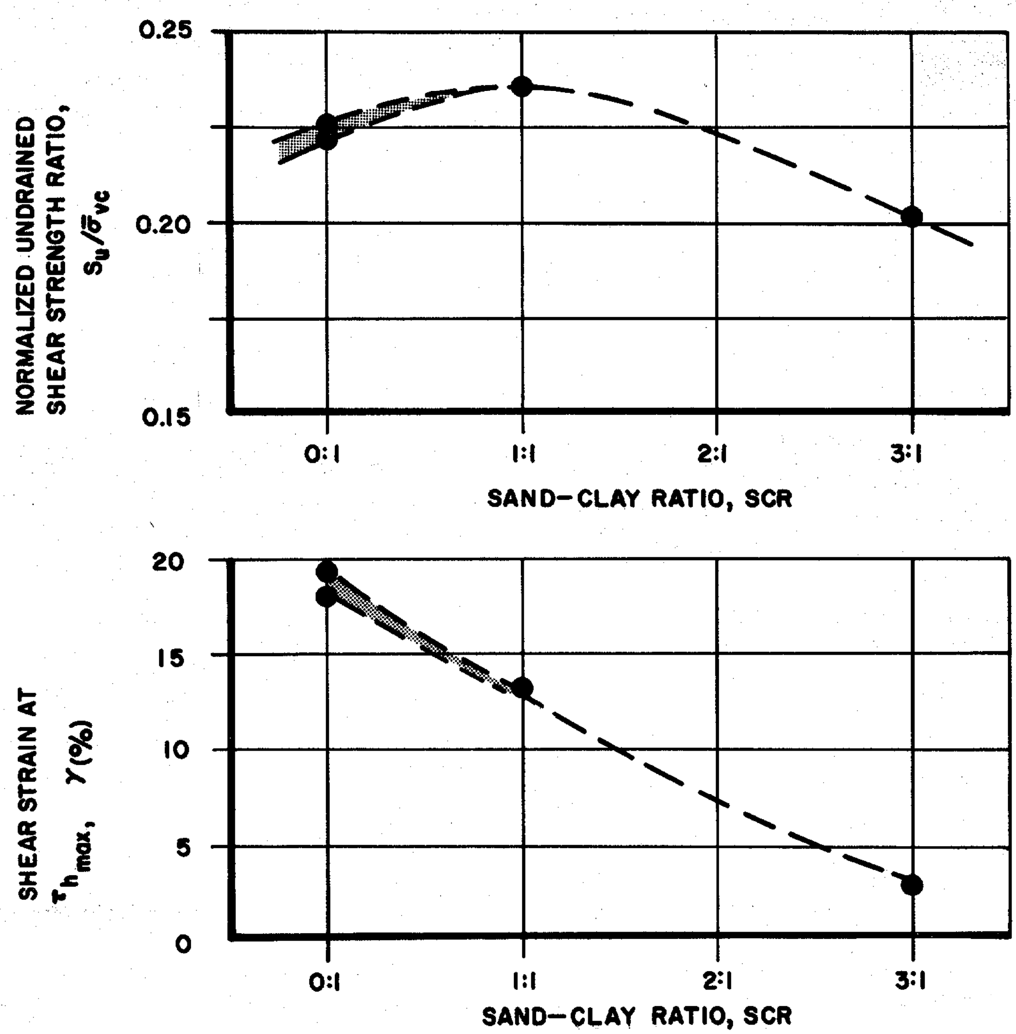

EFFECT OF SAND-CLAY RATIO ON SHEAR STRENGTH AND FAILURE STRAIN OF AGRICO-SADDLE CREEK SAND-CLAY MIXES FROM CK_0UDSS TESTS

FIGURE 4-14

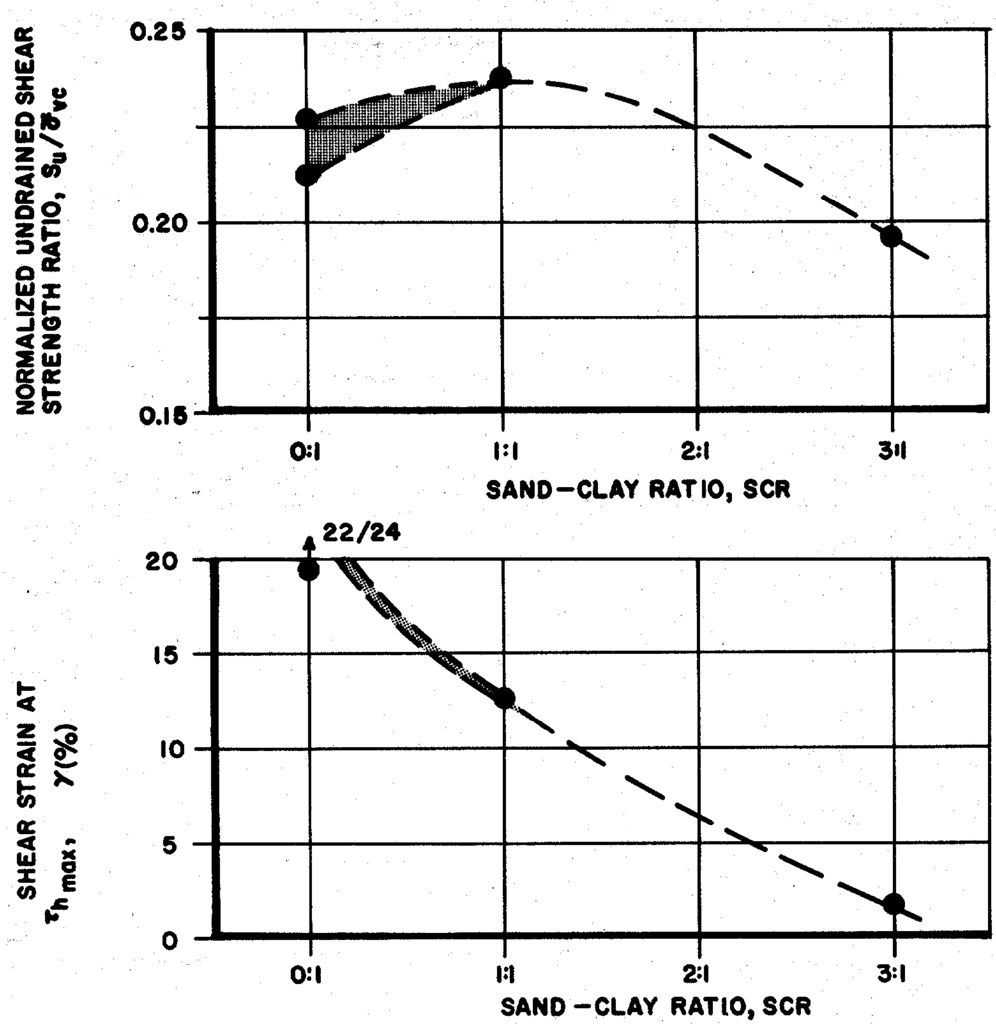

EFFECT OF SAND-CLAY RATIO ON SHEAR STRENGTH AND FAILURE STRAIN OF USSAC-ROCKLAND SAND-CLAY MIXES FROM CK_OUDSS TESTS

FIGURE 4-15

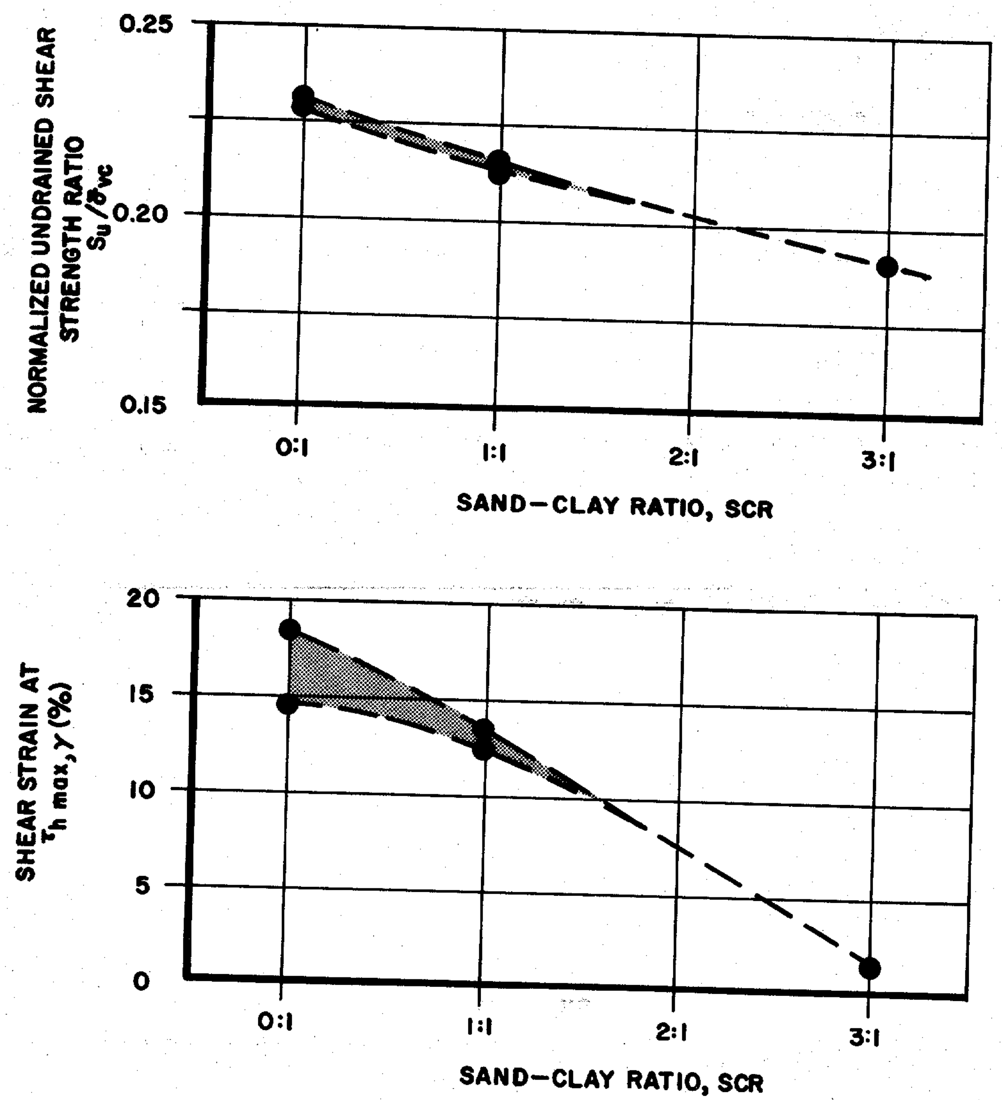

EFFECT OF SAND-CLAY RATIO ON SHEAR STRENGTH AND FAILURE STRAIN OF CF MINING-HARDEE SAND-CLAY MIXES FROM CK_OUDSS TESTS

FIGURE 4-16

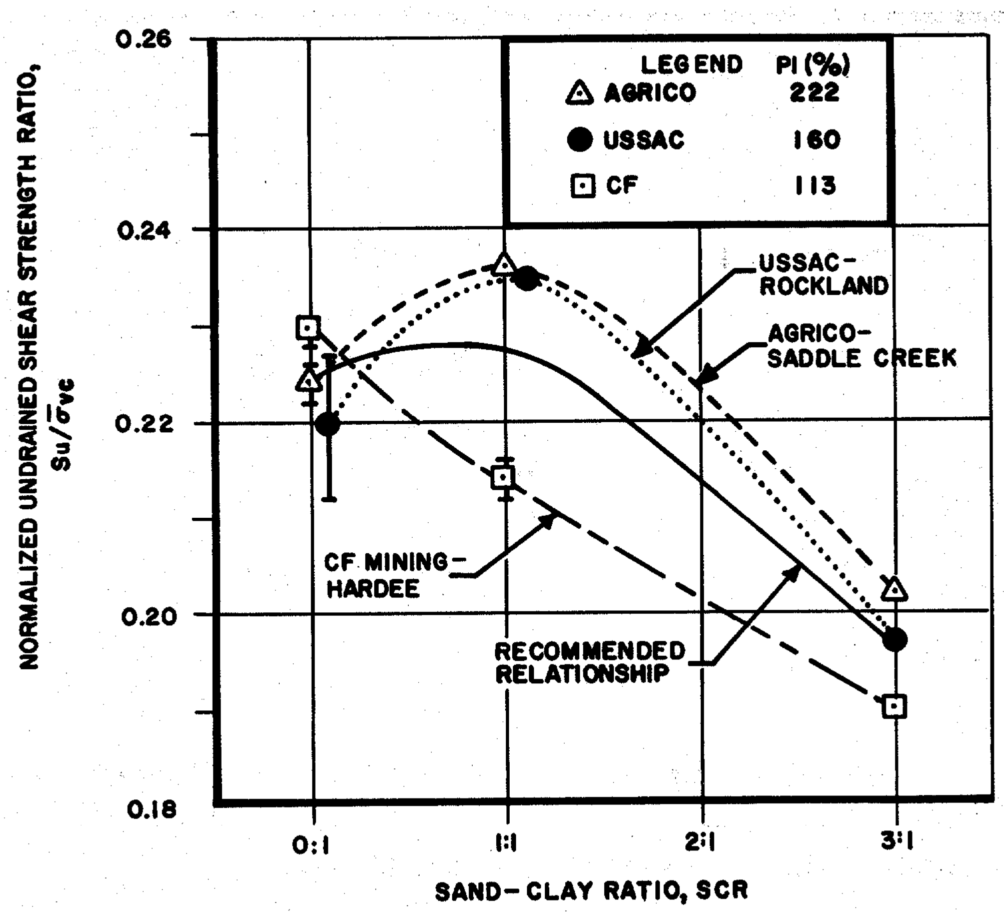

NORMALIZED UNDRAINED SHEAR STRENGTH VERSUS SAND-CLAY RATIO FROM CK_oUDSS TESTS ON SAND-CLAY MIXES

FIGURE 4-17

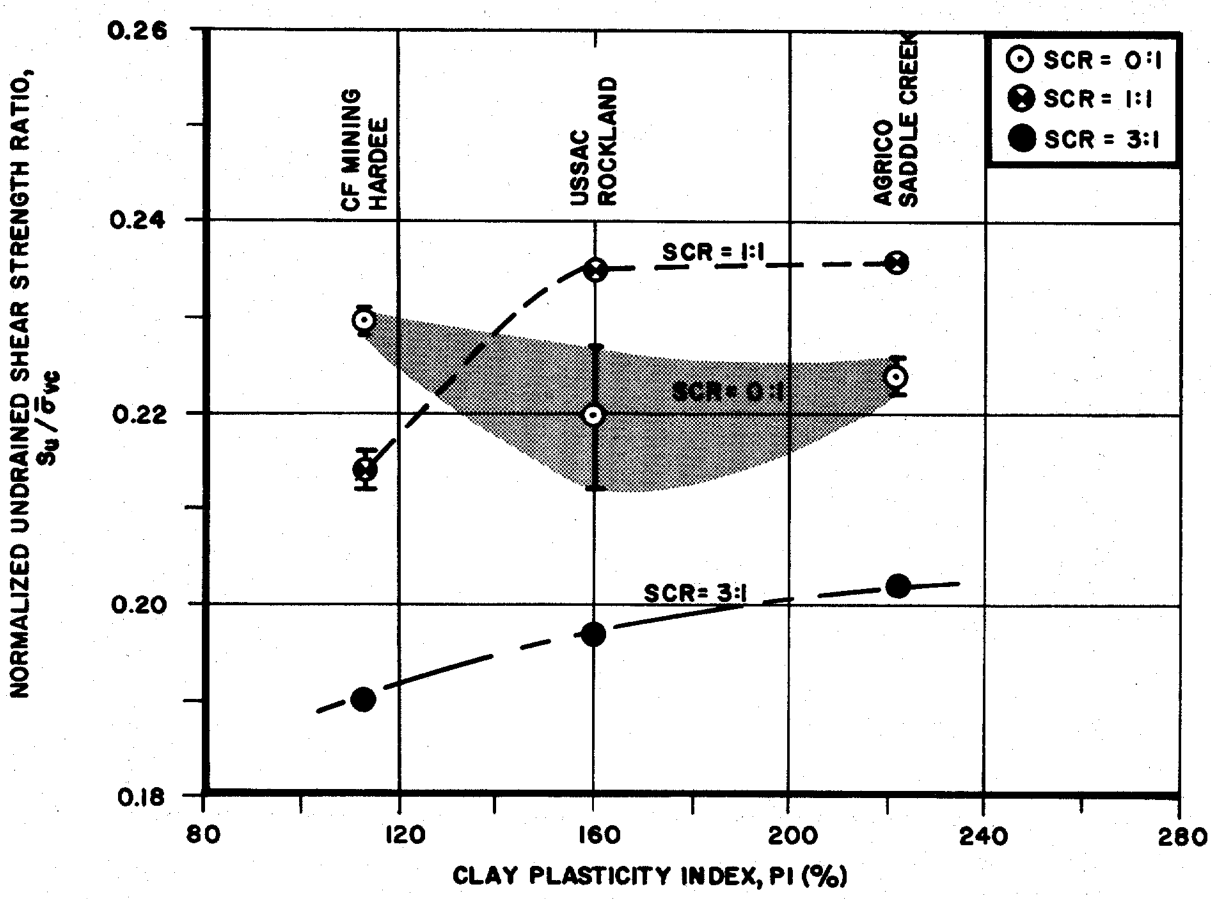

NORMALIZED UNDRAINED SHEAR STRENGTH RATIO VERSUS PHOSPHATIC CLAY PLASTICITY INDEX FROM CK_0UDSS TESTS ON SAND-CLAY MIXES

FIGURE 4-18

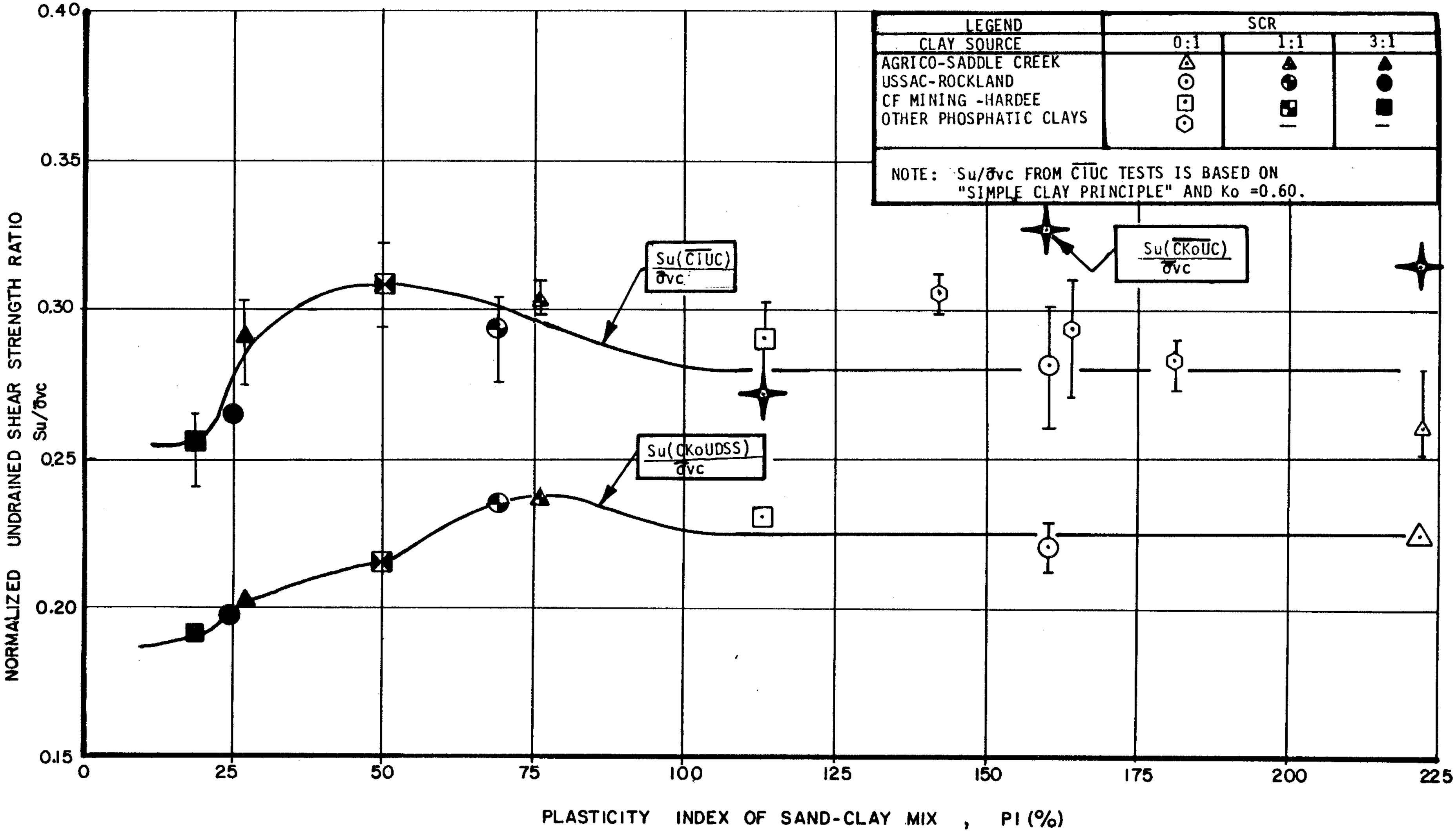

FIGURE 4-19

NORMALIZED UNDRAINED SHEAR STRENGTH VERSUS PLASTICITY INDEX OF SAND-CLAY MIXES FROM $\overline{\text{CIUC}}$ AND CK_oUDSS TESTS

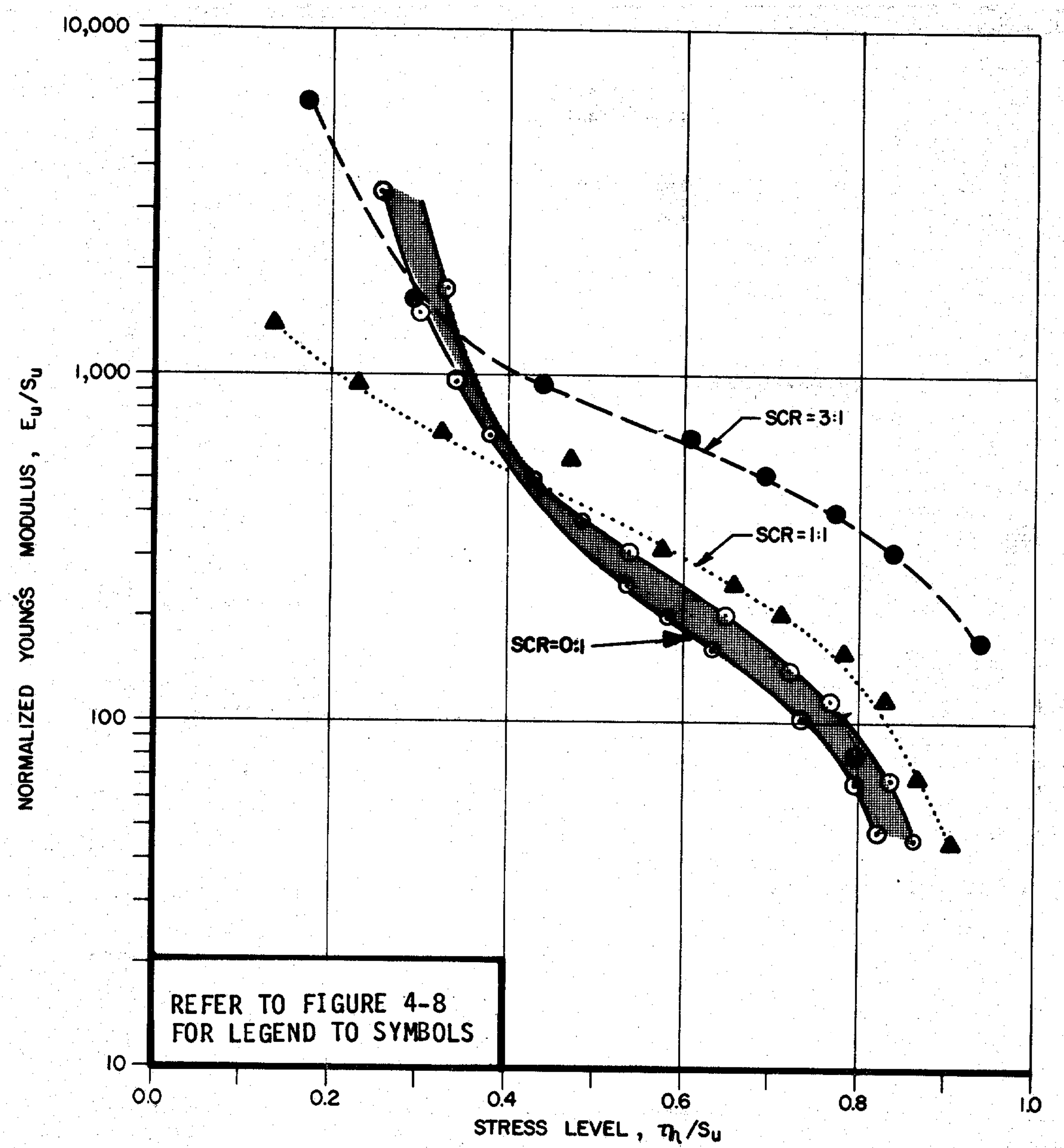

NORMALIZED UNDRAINED YOUNG'S MODULUS VERSUS STRESS LEVEL FROM CK_0UDSS TESTS ON AGRICO-SADDLE CREEK SAND-CLAY MIXES

FIGURE 4-20

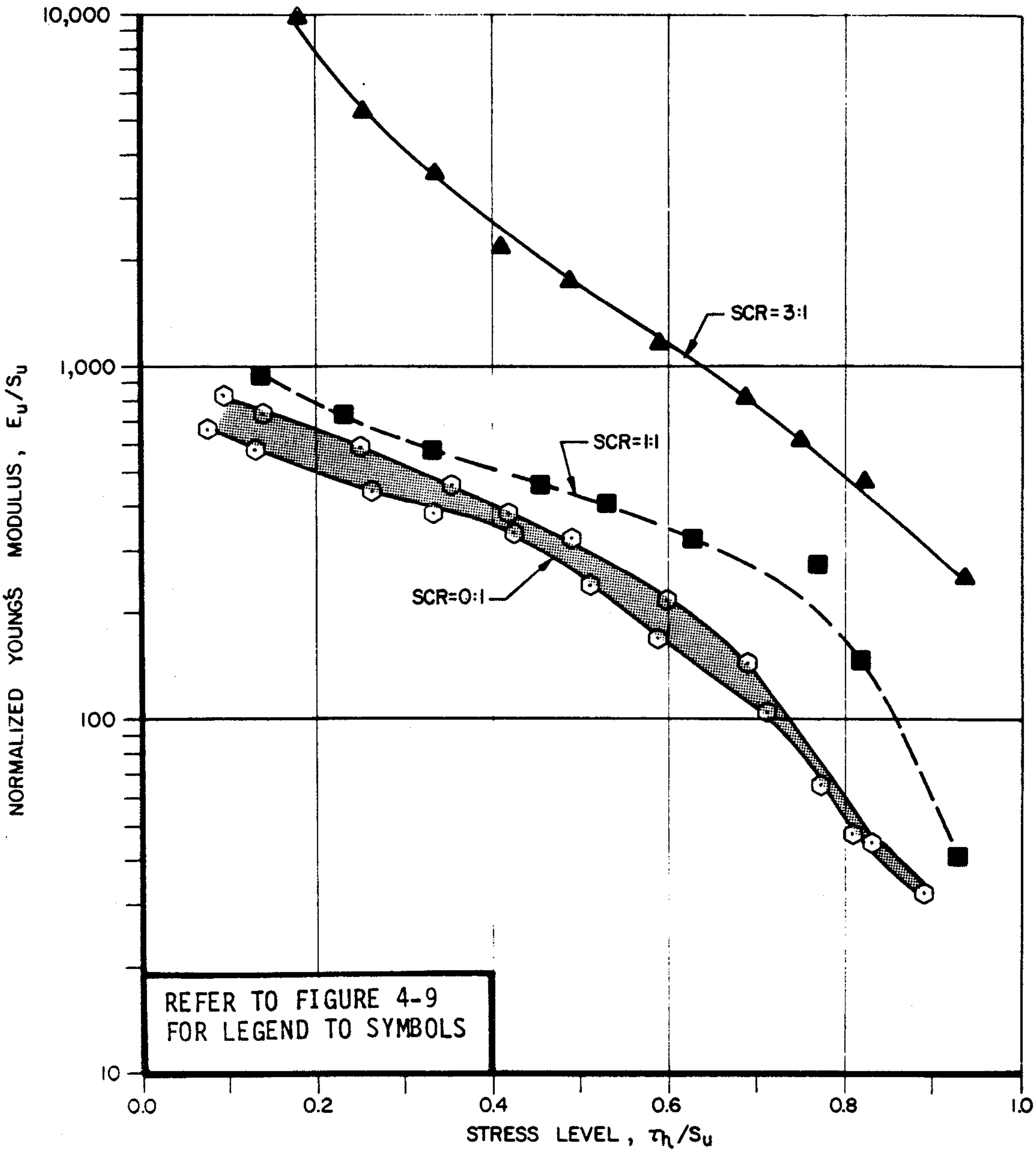

NORMALIZED UNDRAINED YOUNG'S MODULUS VERSUS STRESS LEVEL FROM CK_0UDSS TESTS ON USSAC-ROCKLAND SAND-CLAY MIXES

FIGURE 4-21

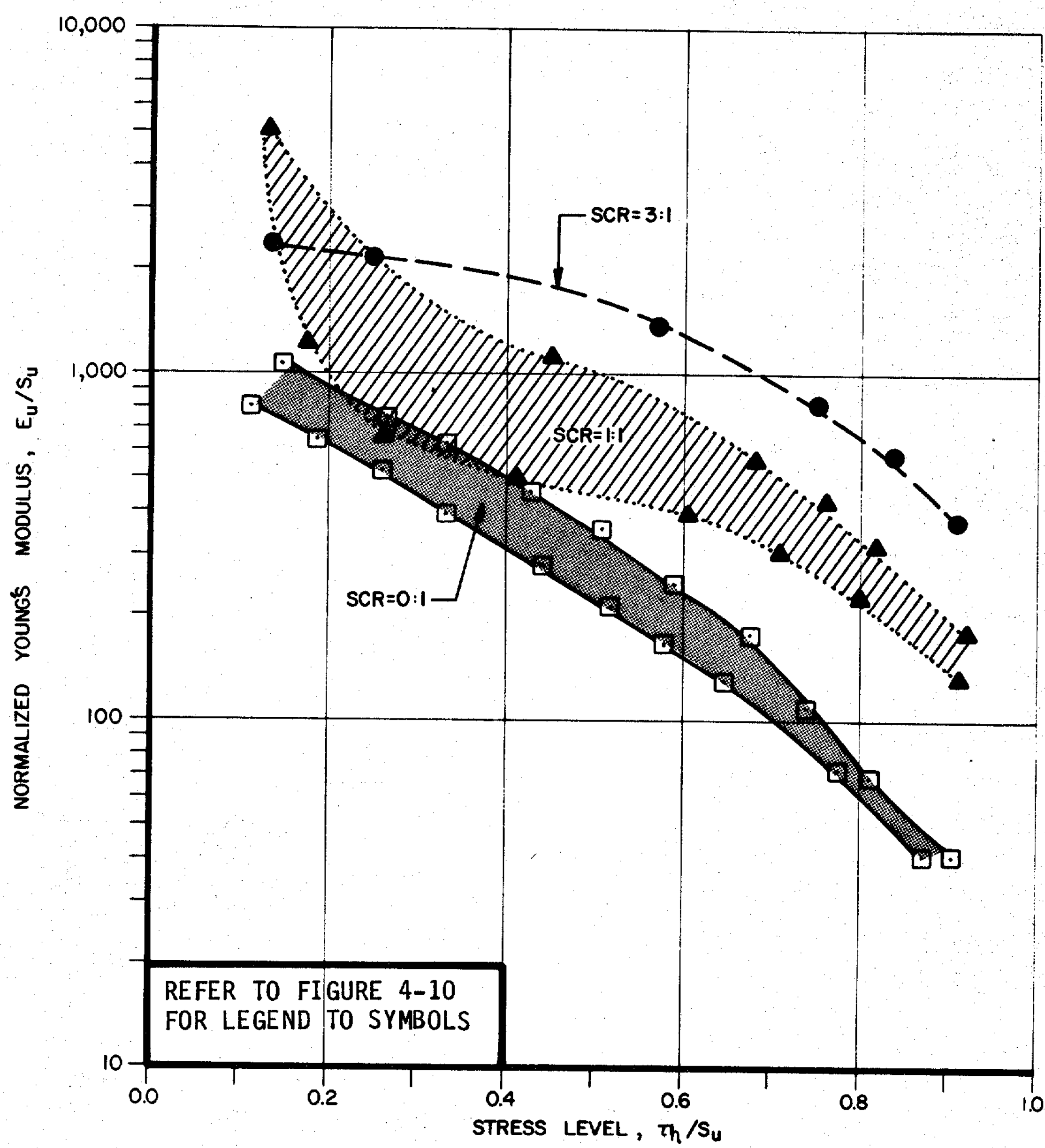

NORMALIZED UNDRAINED YOUNG'S MODULUS VERSUS STRESS LEVEL FROM CK_0UDSS TESTS ON CF MINING-HARDEE SAND-CLAY MIXES

FIGURE 4-22

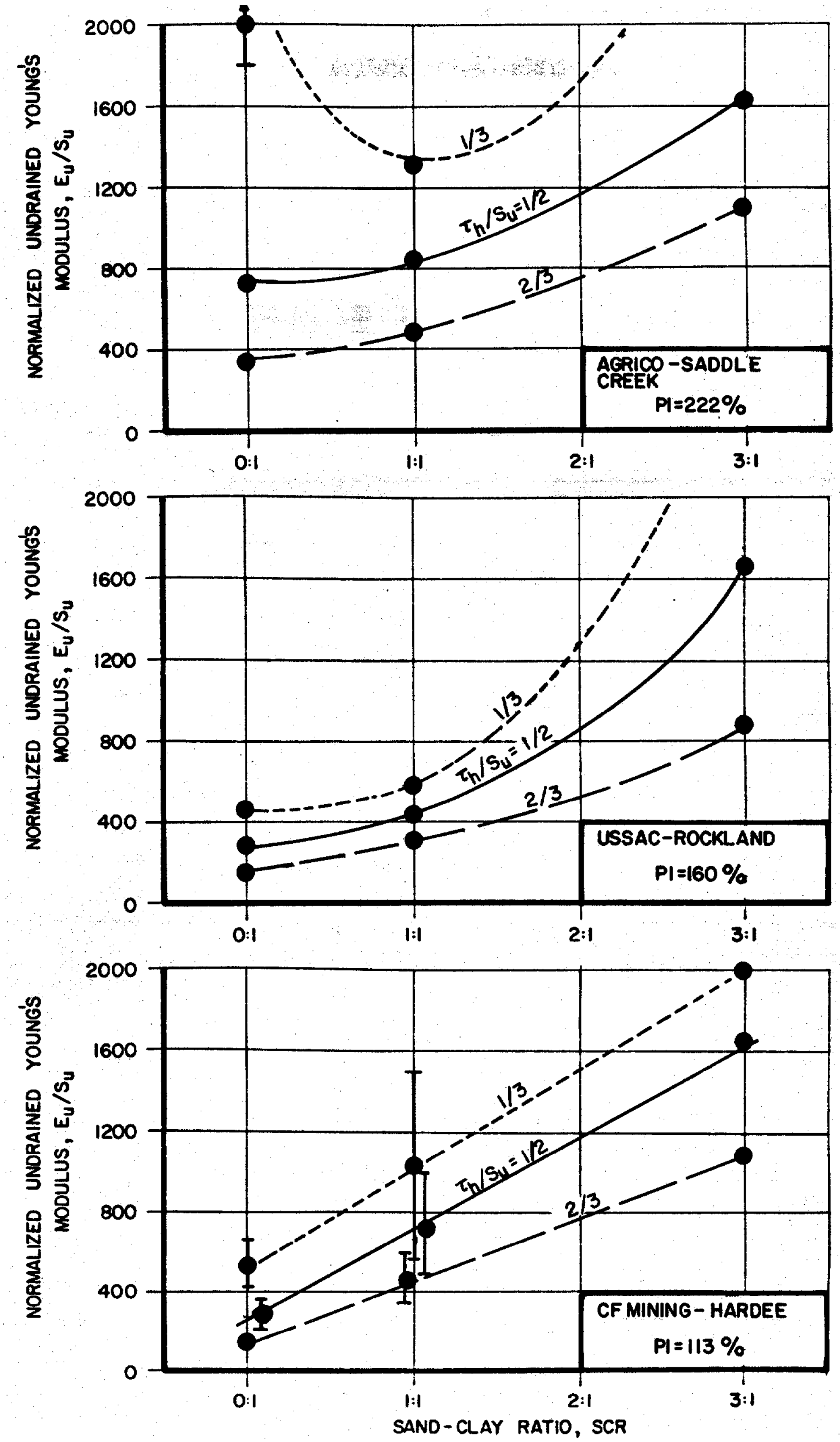

EFFECT OF SAND-CLAY RATIO ON UNDRAINED MODULUS OF SAND-CLAY MIXES FROM CK_OUDSS TESTS

FIGURE 4-23

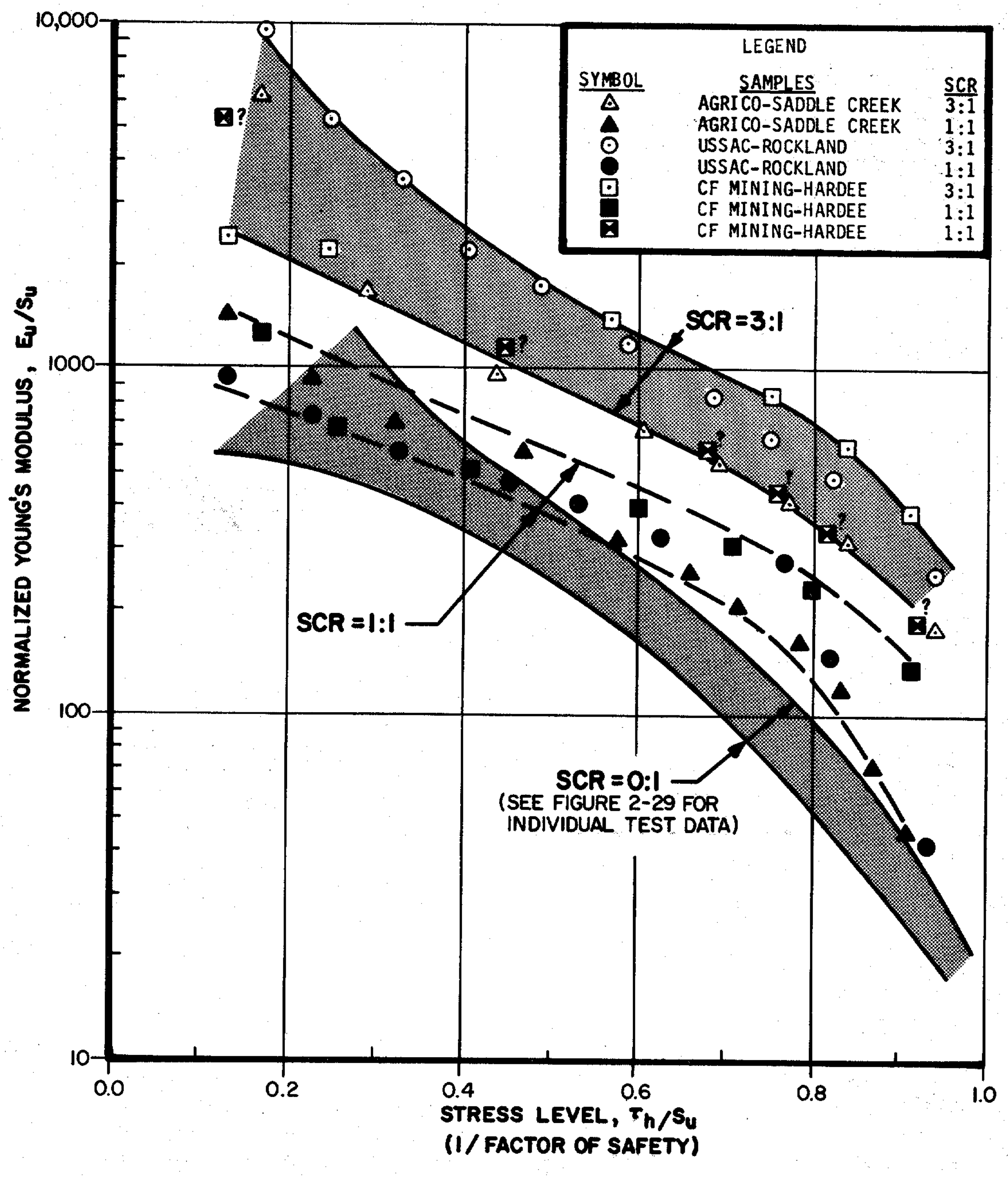

SUMMARY OF NORMALIZED UNDRAINED YOUNG'S MODULUS VERSUS STRESS LEVEL FROM CK_OUDSS TESTS ON SAND-CLAY MIXES

FIGURE 4-24

FIGURE 4-25

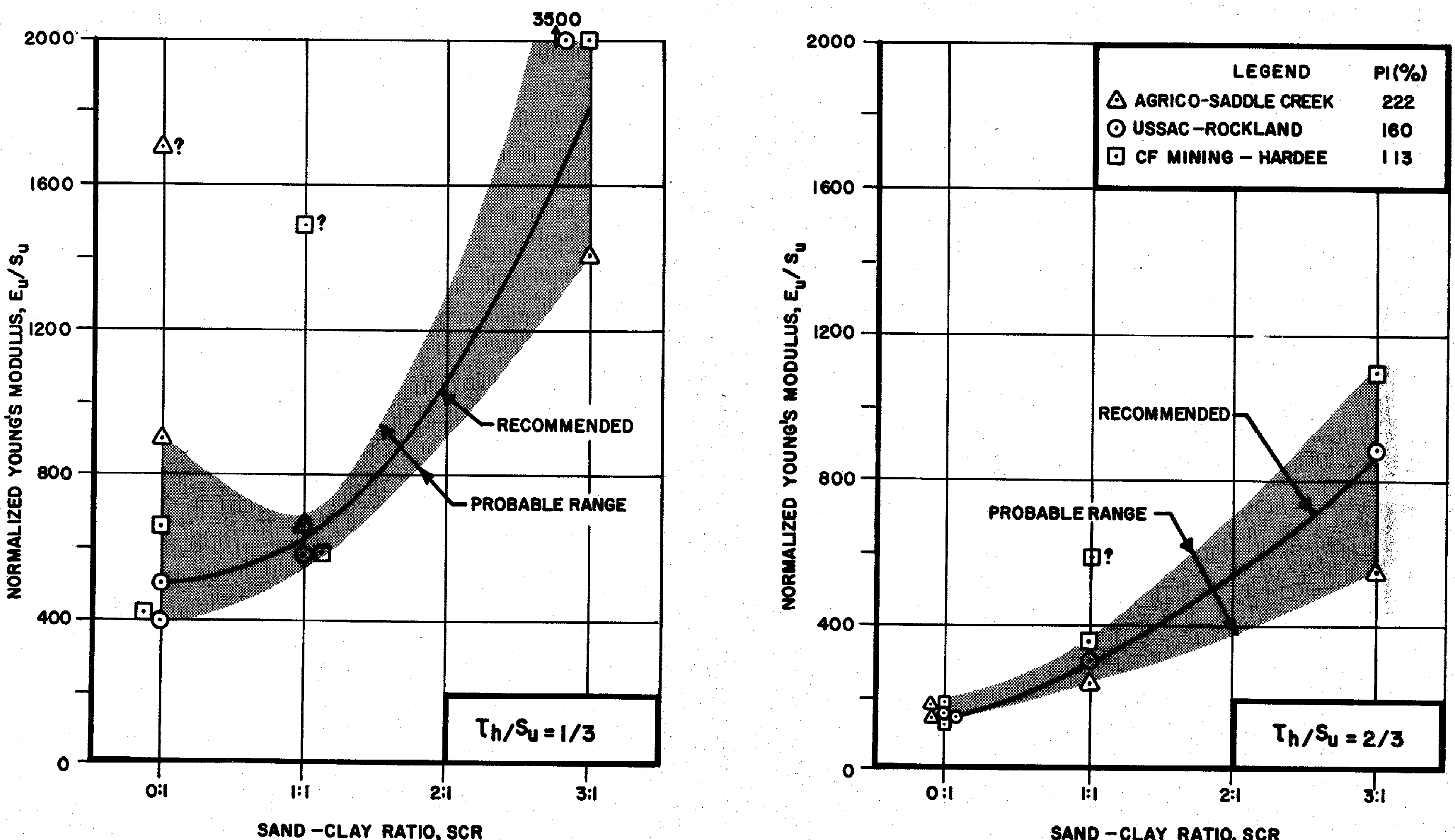

NORMALIZED UNDRAINED YOUNG'S MODULUS VERSUS SAND-CLAY RATIO AT SELECTED STRESS LEVELS FROM CK_oUDSS TESTS ON SAND-CLAY MIXES

Section 5

REFERENCES

Alpan, I. (1967). "The Empirical Evaluation of the Coefficients K_o and K_{oR} Soils and Foundations, Volume 7, No. 1.

Bishop, A.W. and Henkel, D.J. (1962). The Measurement of Soil Properties in the Triaxial Test. Edward Arnold, 2nd Edition, London.

Bjerrum, L. and Landva, A. (1966). "Direct Simple Shear Tests on Norwegian Quick Clays?" Geotechnique, Volume 16, No. 1.

Bromwell, L.G. and Radan, D.J. (1979). "Disposal of Phosphate Mining Wastes." Current Geotechnical Practice in Mine Waste Disposal, American Society of Civil Engineers, New York.

Brooker, E.W. and Ireland, H.O. (1965). "Earth Pressures at Rest Related to Stress History." Canadian Geotechnical Journal, Volume 2, No. 1.

Casagrande, A. (1932). "Research on the Atterberg Limits of Soils." Public Roads, October.

Department of the Navy (1971). Soil Mechanics, Foundations, and Earth Structures. NAVFAC DM-7.

Fuleihan, N.F. and Ladd, C.C. (1976). "Design and Performance of Atchafalaya Flood Control Levees." Research Report R76-24, No. 543, Department of Civil Engineering, Massachusetts Institute of Technology, Cambridge, Massachusetts.

Ladd, C.C., Foott, R., Ishihara, K., Schlosser, F. and Poulos, R.G. (1977). "Stress-Deformation and Strength Characteristics." State-of-the-Art Report, IX International Conference on Soil Mechanics and Foundation Engineering, Tokyo, Japan.

Ladd, C.C. (1975). "Foundation Design of Embankments Constructed on Connecticut Valley Varved Clays." Massachusetts Institute of Technology, Department of Civil Engineering, R75-7, SO 343.

Ladd, C.C. and Foott, R. (1974). "New Design Procedure for Stability of Soft Clays." Journal of the Geotechnical Engineering Division, American Society of Civil Engineers, Volume 100, No. GT-7.

Ladd, C.C., Williams, C.E., Connell, D.H. and Edgers, L. (1972). "Engineering Properties of Soft Foundation Clays at Two South Louisiana Levee Sites." Massachusetts Institute of Technology, Department of Civil Engineering, R72-26, SO 304.

Ladd, C.C. (1971). "Strength Parameters and Stress-Strain Behavior of Saturated Clays." Massachusetts Institute of Technology, Department of Civil Engineering, R71-23, SO 278.

Ladd, C.C. (1964). "Stress-Strain Behavior of Saturated Clay and Basic Strength Principles." Massachusetts Institute of Technology, Department of Civil Engineering, R64-17.

Mesri, G. (1975). Discussion on "New Design Procedure for Stability of Soft Clays." Journal of the Geotechnical Engineering Division, American Society of Civil Engineers, Volume 101, No. GT-4.

Roma, J.R. (1976). "Geotechnical Properties of Phosphate Clays," submitted in partial fulfillment of the requirements of the degree of Master of Science in Civil Engineering, Department of Civil Engineering, Massachusetts Institute of Technology, Cambridge, Massachusetts.

Skempton, A.W. and Northey, R.D. (1952). "The Sensitivity of Clays." Geotechnique, Volume III.

Appendix A

STRESS-STRAIN-STRENGTH BEHAVIOR OF NORMALLY CONSOLIDATED PHOSPHATIC CLAYS FROM $\overline{\text{CIUC}}$ TESTS

Appendix A

LIST OF FIGURES

Note: Stress-strain curves are normalized with respect to the pre-shear isotropic effective consolidation stress, $\bar{\sigma}_c$.

FIGURE A-1

SAMPLE	INITIAL		FINAL		$S_u/\bar{\sigma}_c$	$(\sigma_1-\sigma_3)_{max}$			$(\bar{\sigma}_1/\bar{\sigma}_3)_{max}$		
	w_n (%)	γ_t (pcf)	w_n (%)	γ_t (pcf)		ξ (%)	$\bar{\phi}$	$\bar{A}$ FACTOR	ξ (%)	$\bar{\phi}$	$\bar{A}$ FACTOR
S2	211.5	75.7	213.3	78.6	0.29	8.1	31.1°	1.24	11.1	32.6°	1.35
S6	198.5	80.9	122.3	87.8	0.37	8.3	35.1°	0.97	10.5	36.1°	1.00
S8	190.1	77.7	109.4	90.0	0.27	6.9	28.2°	1.28	10.9	29.8°	1.42
S9	205.1	76.9	130.6	86.5	0.29	6.7	29.5°	1.14	10.6	31.1°	1.26

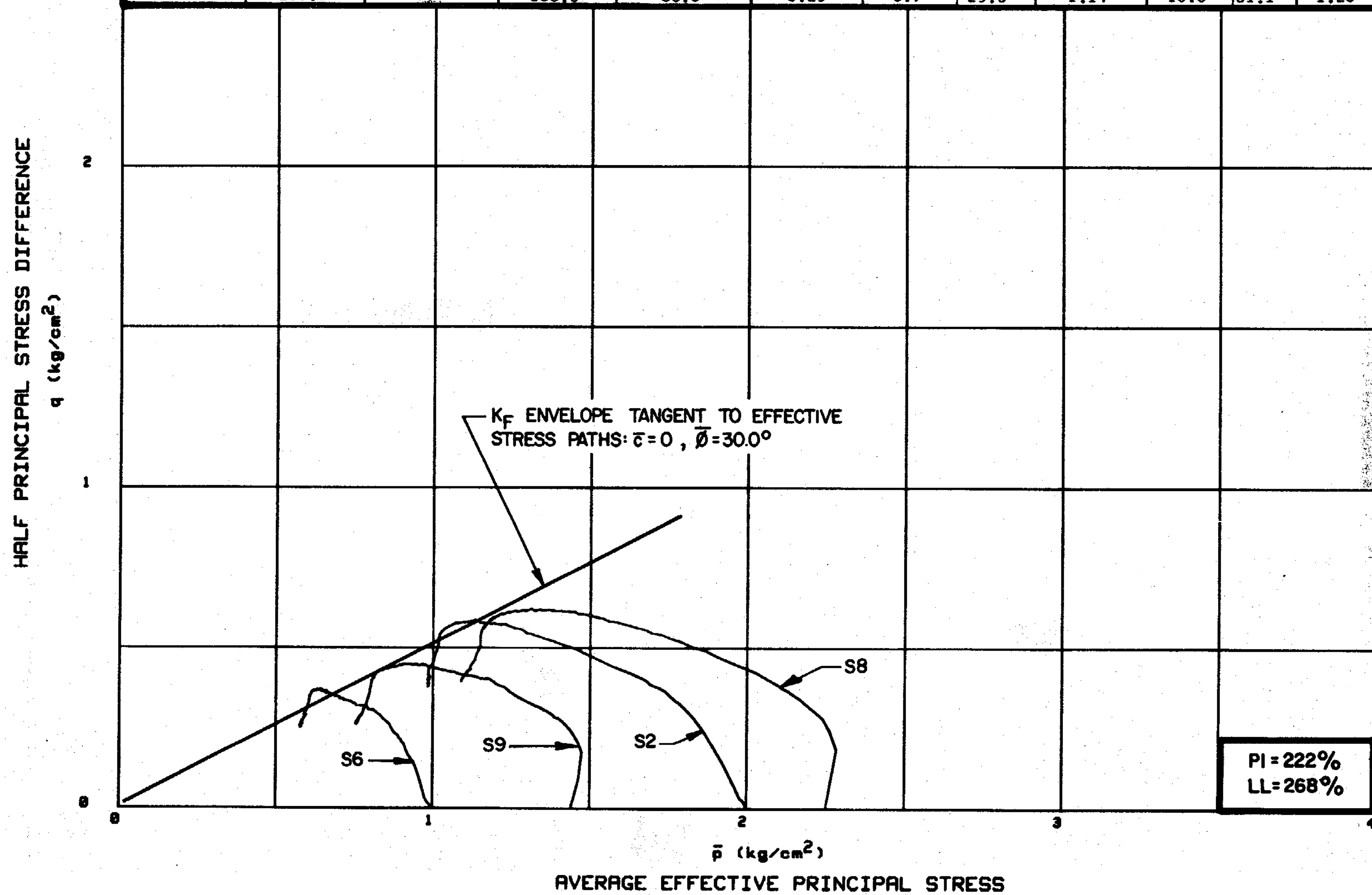

UNDRAINED EFFECTIVE STRESS PATHS FROM $\overline{\text{CIUC}}$ TESTS ON AGRICO-SADDLE CREEK PHOSPHATIC CLAY

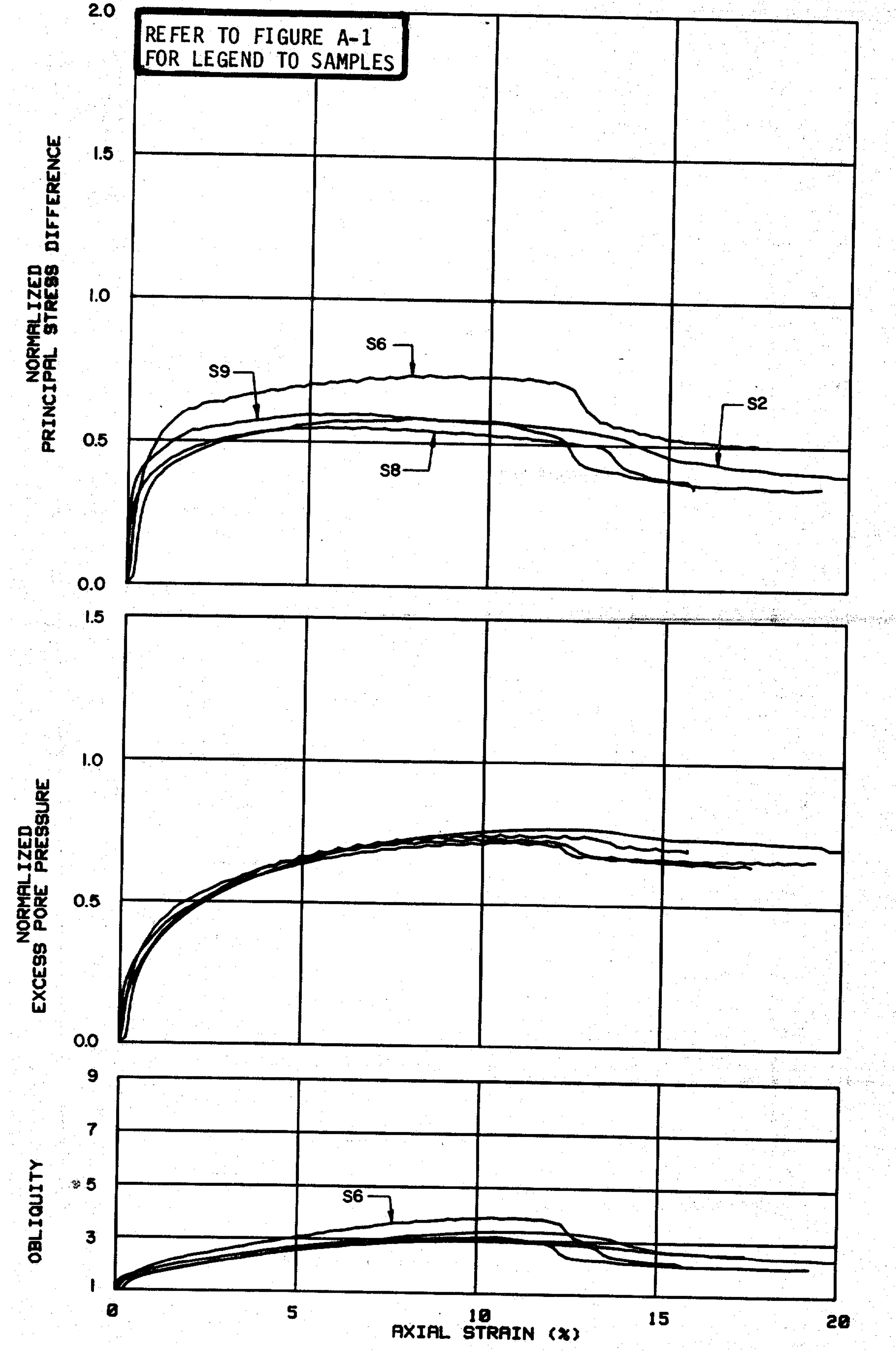

UNDRAINED STRESS-STRAIN BEHAVIOR FROM $\overline{\text{CIU}}$C TESTS ON AGRICO-SADDLE CREEK PHOSPHATIC CLAY

FIGURE A-2

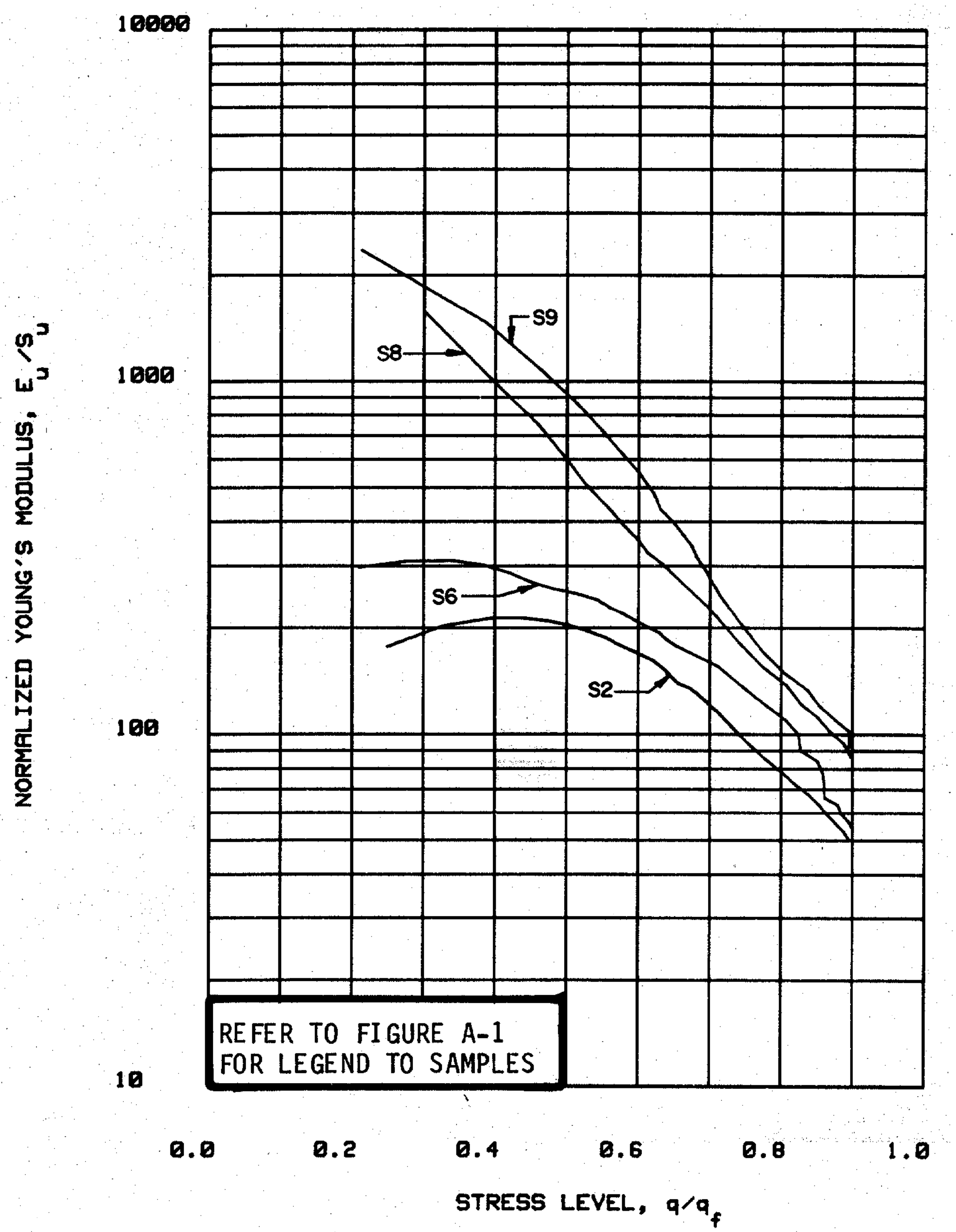

NORMALIZED UNDRAINED YOUNG'S MODULUS VERSUS STRESS LEVEL FROM $\overline{CIU}$C TESTS ON AGRICO-SADDLE CREEK PHOSPHATIC CLAY

FIGURE A-3

SAMPLE	INITIAL		FINAL		$Su/\bar{\sigma}_c$	$(\sigma_1 - \sigma_3)$ max			$(\bar{\sigma}_1 / \bar{\sigma}_3)$max		
	w_n (%)	γ_t (pcf)	w_n (%)	γ_t (pcf)		ξ (%)	$\bar{\phi}$	A FACTOR	ξ (%)	$\bar{\phi}$	A FACTOR
S1	111.5	90.1	86.6	95.4	0.32	5.7	28.6°	1.03	9.6	29.8°	1.17
S3	113.4	91.3	116.4	88.9	0.34	7.4	29.3°	0.92	9.5	29.9°	0.97
S4	112.2	86.8	112.0	89.7	0.33	10.3	30.2°	1.03	14.7	31.3°	1.09
S	116.3	87.2	86.2	95.3	0.37	10.3	33.2°	0.88	15.2	34.0°	0.94
F	115.3	85.3	84.0	96.0	0.31	5.6	26.7°	1.01	10.3	28.9°	1.16

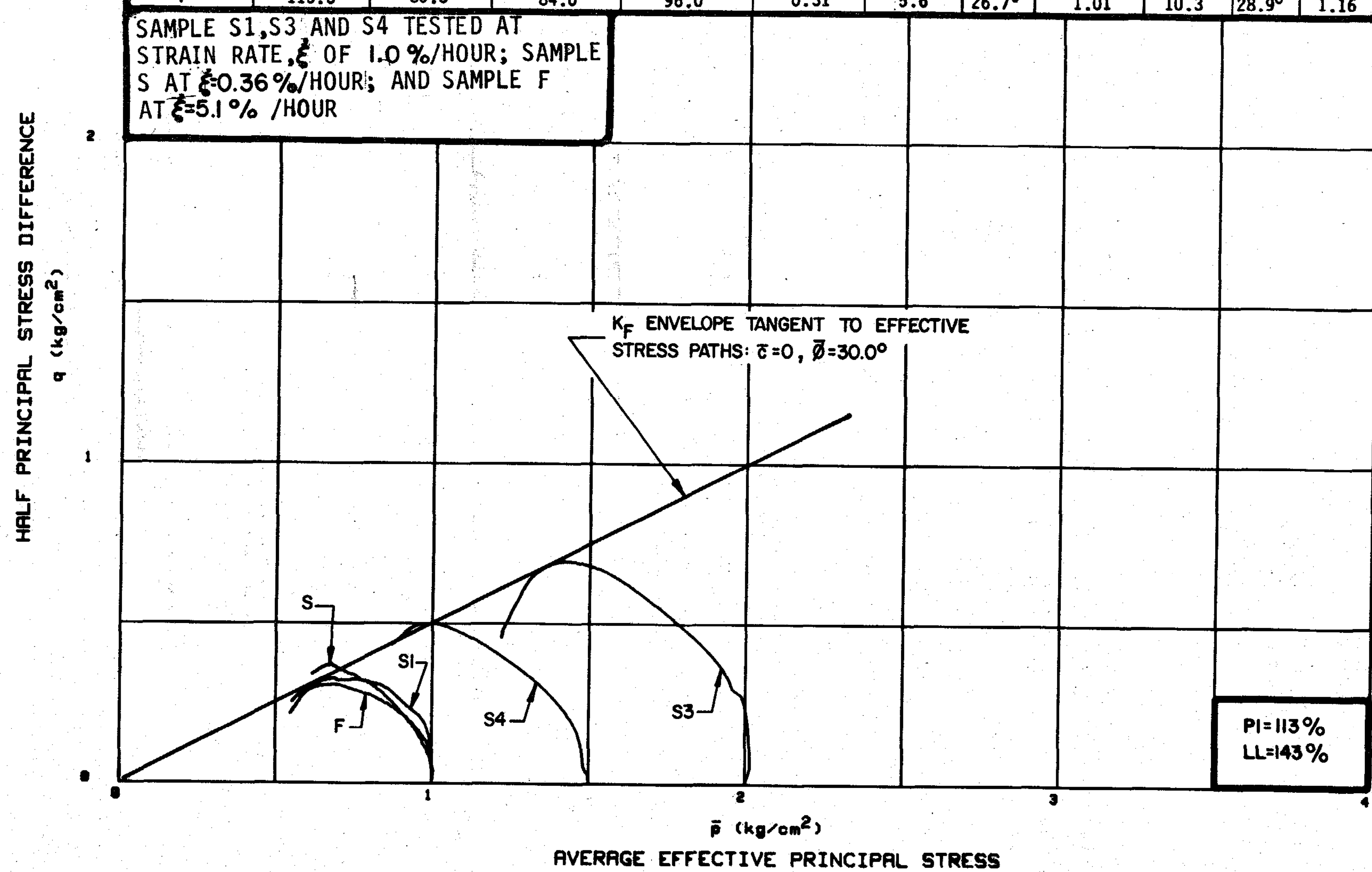

FIGURE A-4

UNDRAINED EFFECTIVE STRESS PATHS FROM $\overline{CIU}C$ TESTS ON CF MINING-HARDEE PHOSPHATIC CLAY

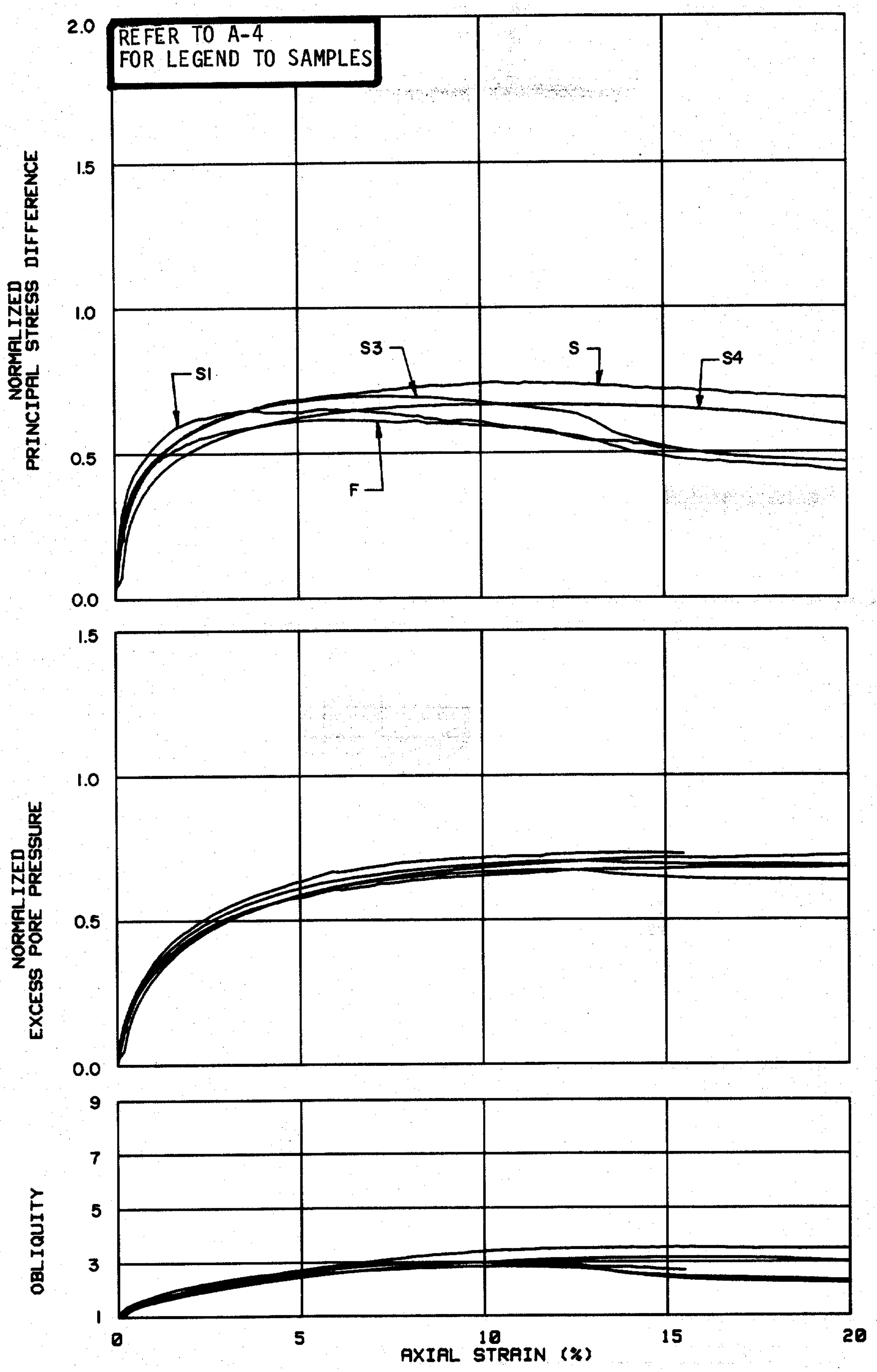

UNDRAINED STRESS-STRAIN BEHAVIOR FROM $\overline{\text{CIU}}$C TESTS ON CF MINING-HARDEE PHOSPHATIC CLAY

FIGURE A-5

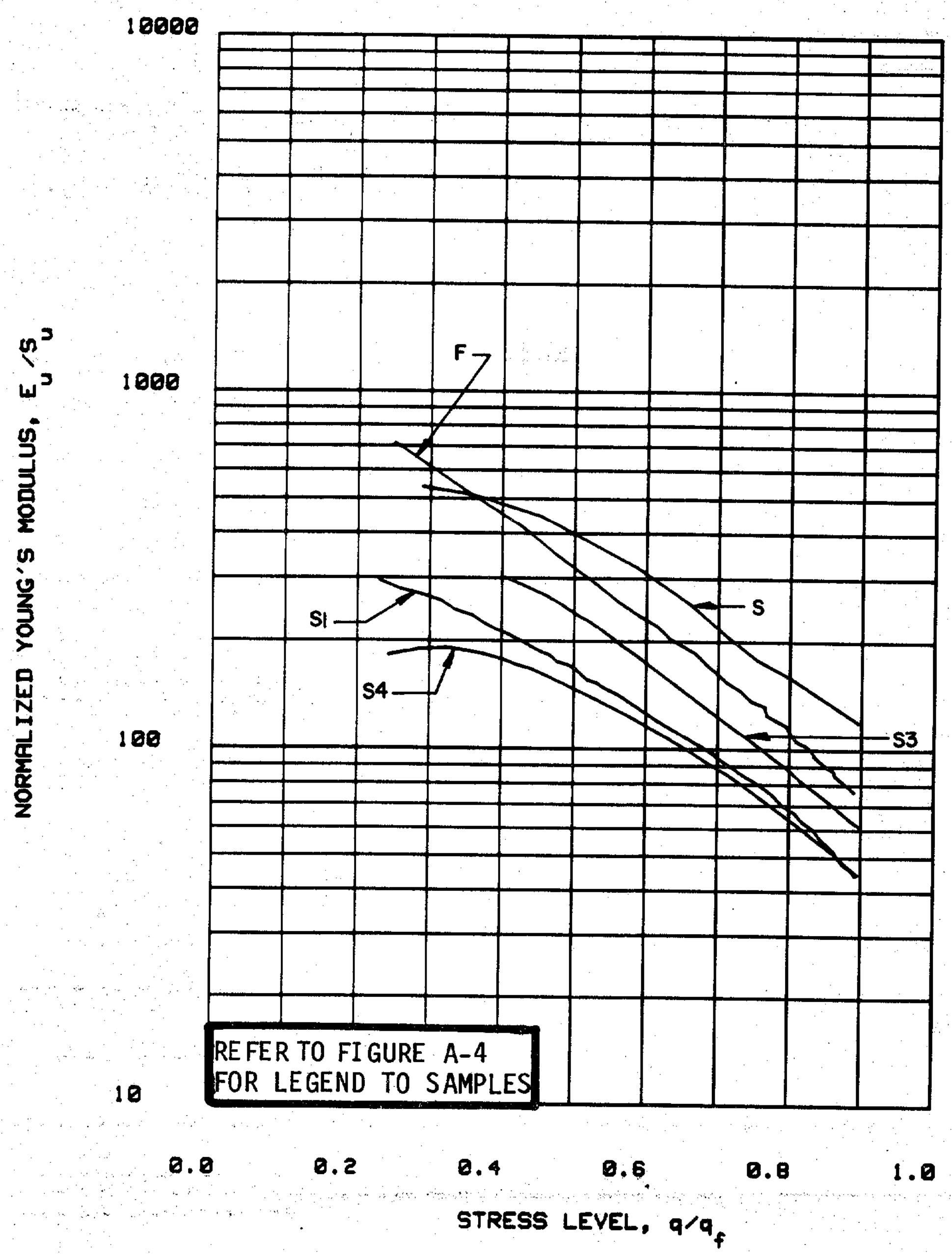

NORMALIZED UNDRAINED YOUNG'S MODULUS VERSUS STRESS LEVEL FROM $\overline{\text{CIU}}$C TESTS ON CF MINING-HARDEE PHOSPHATIC CLAY

FIGURE A-6

FIGURE A-7

SAMPLE	INITIAL		FINAL		$S_u/\bar{\sigma}_c$	$(\sigma_1 - \sigma_3)$ max			$(\bar{\sigma}_1 / \bar{\sigma}_3)$ max		
	w_n (%)	γ_t (pcf)	w_n (%)	γ_t (pcf)		ξ (%)	$\bar{\phi}$	A FACTOR	ξ (%)	$\bar{\phi}$	A FACTOR
S2	168.8	81.2	104.0	91.4	0.35	12.4	30.8°	0.96	14.3	31.4°	0.98
S3	140.1	84.7	92.5	93.9	0.31	12.0	29.8°	1.09	13.9	30.3°	1.11
S4	140.3	84.3	114.3	89.4	0.32	7.5	29.5°	1.05	11.3	31.1°	1.17

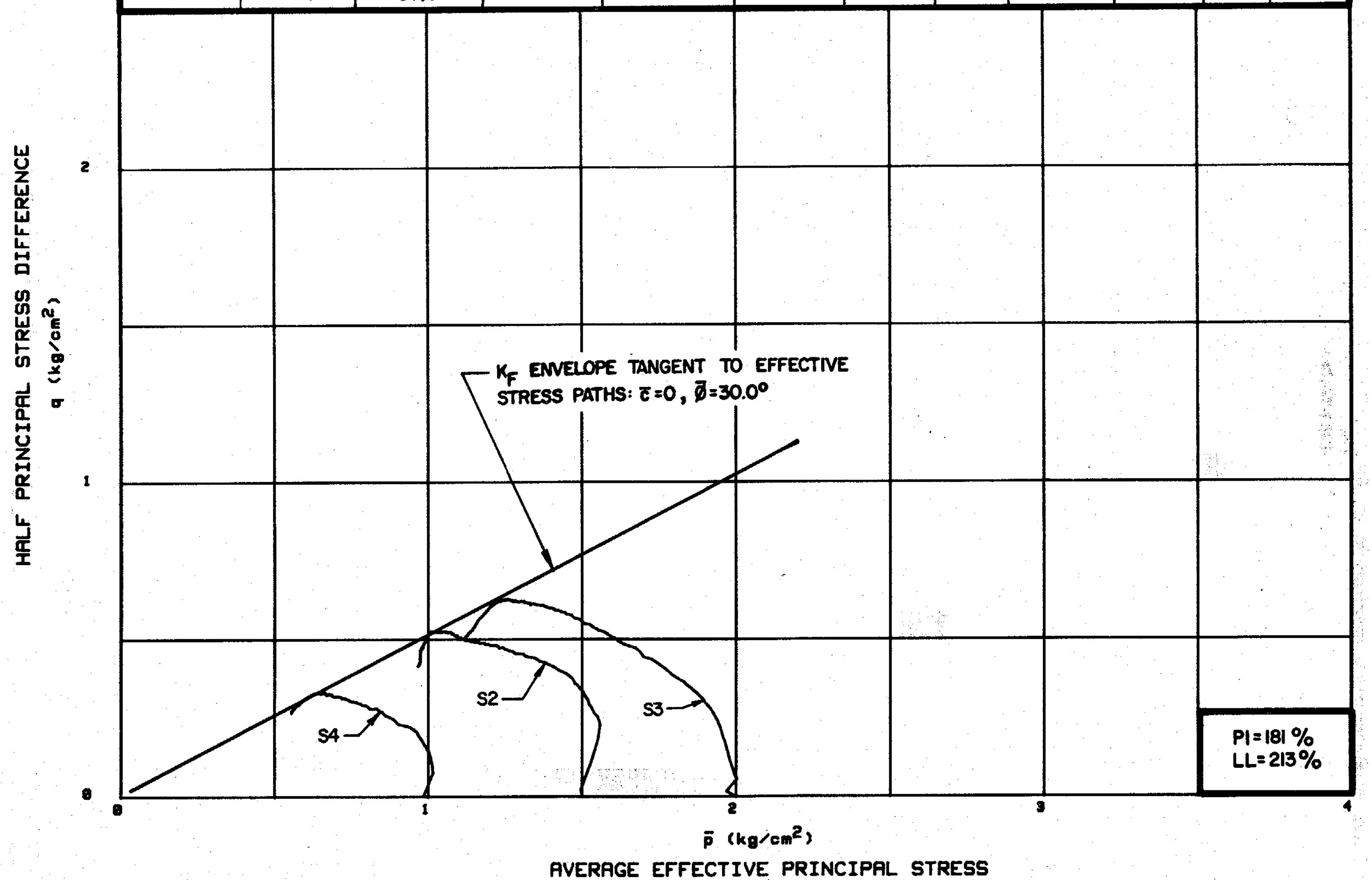

UNDRAINED EFFECTIVE STRESS PATHS FROM $\overline{\text{CIU}}$C TESTS ON IMC-NORALYN PHOSPHATIC CLAY

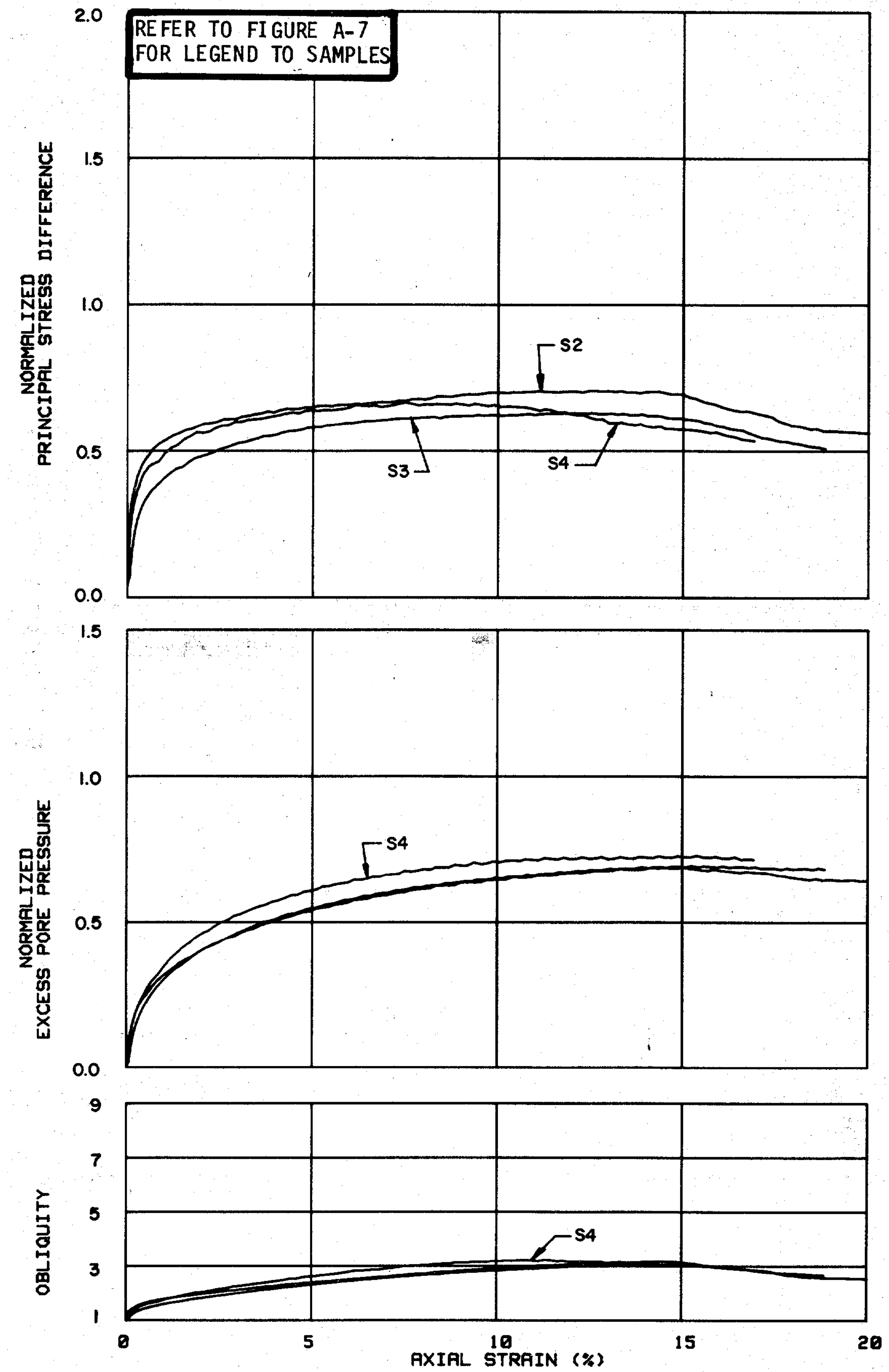

UNDRAINED STRESS-STRAIN BEHAVIOR FROM $\overline{CIU}C$ TESTS ON IMC-NORALYN PHOSPHATIC CLAY

FIGURE A-8

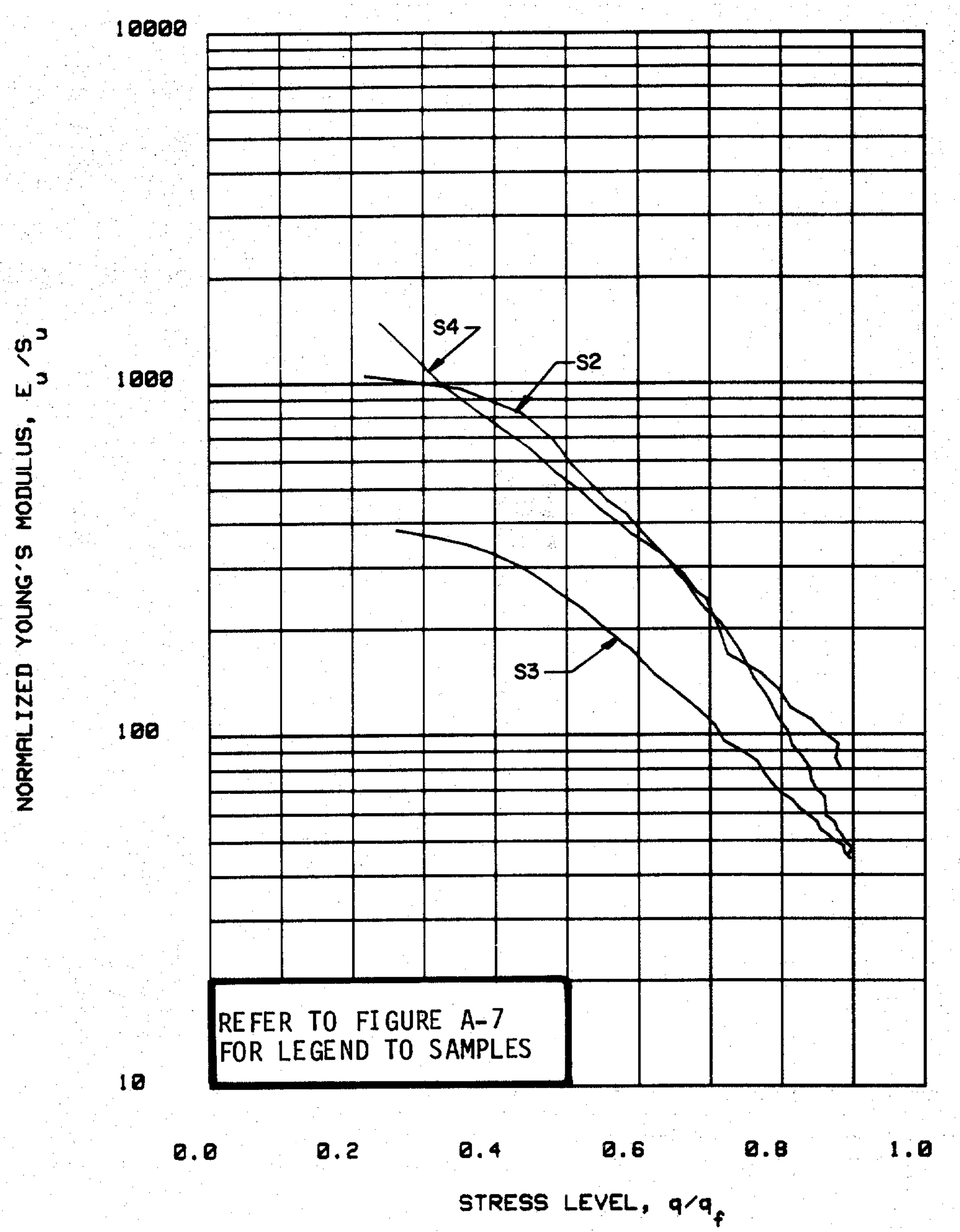

NORMALIZED UNDRAINED YOUNG'S MODULUS VERSUS STRESS LEVEL FROM $\overline{CIU}C$ TESTS ON IMC-NORALYN PHOSPHATIC CLAY

FIGURE A-9

SAMPLE	INITIAL		FINAL		$S_u/\bar{\sigma}_c$	$(\bar{\sigma}_1 - \bar{\sigma}_3)$ max			$(\bar{\sigma}_1 / \bar{\sigma}_3)$ max		
	w_n (%)	γ_t (pcf)	w_n (%)	γ_t (pcf)		ξ (%)	$\bar{\phi}$	A FACTOR	ξ (%)	$\bar{\phi}$	A FACTOR
S1	166.4	83.6	108.2	90.9	0.36	11.9	30.7°	0.89	14.3	31.2°	0.93
S2	156.3	84.1	95.2	93.9	0.31	8.6	26.7°	1.02	11.1	27.4°	1.08
S3	122.5	86.8	89.2	95.4	0.34	12.0	32.4°	1.02	14.4	33.2°	1.05

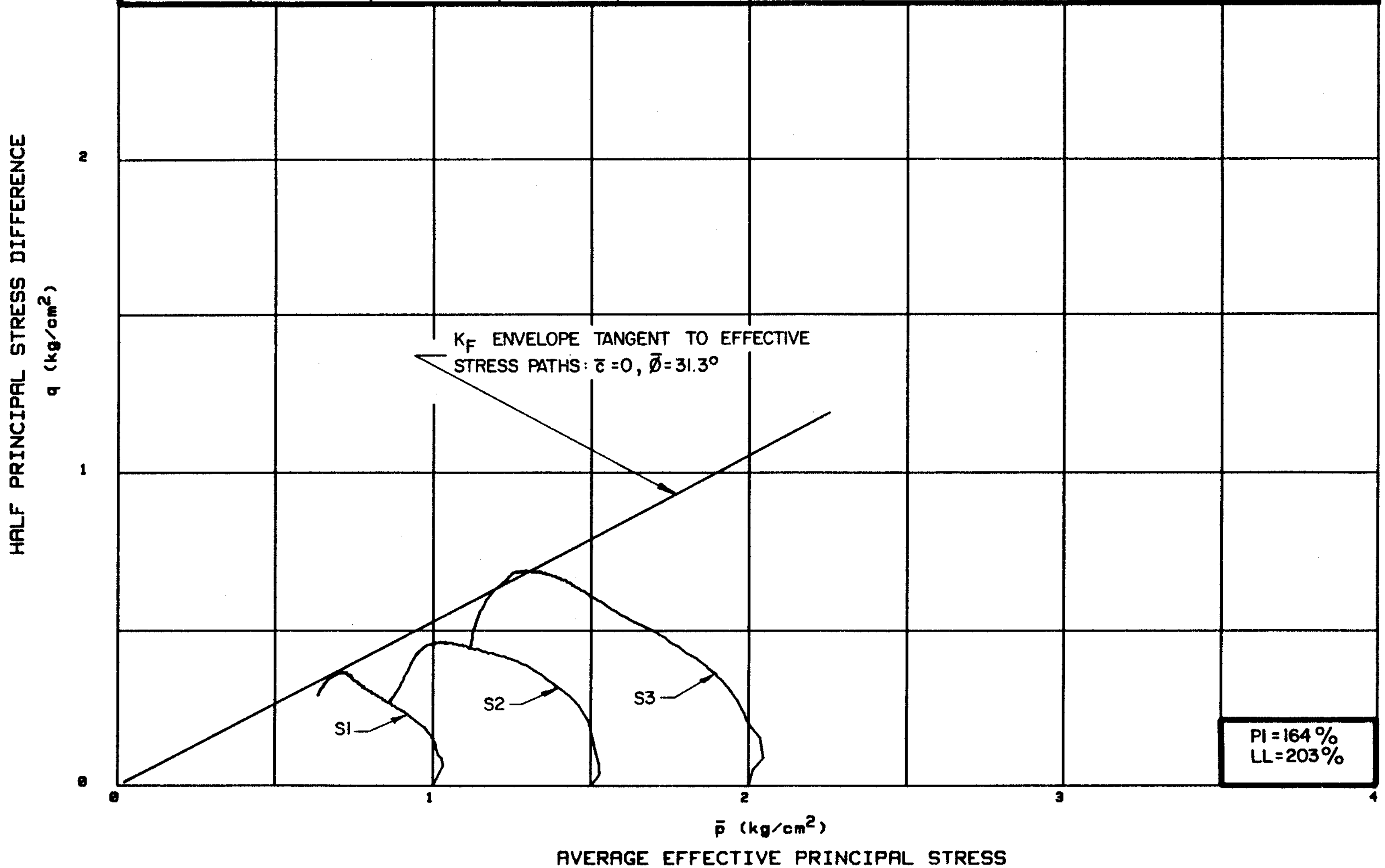

UNDRAINED EFFECTIVE STRESS PATHS FROM $\overline{CIU}$C TESTS ON MOBIL-NICHOLS PHOSPHATIC CLAY

FIGURE A-10

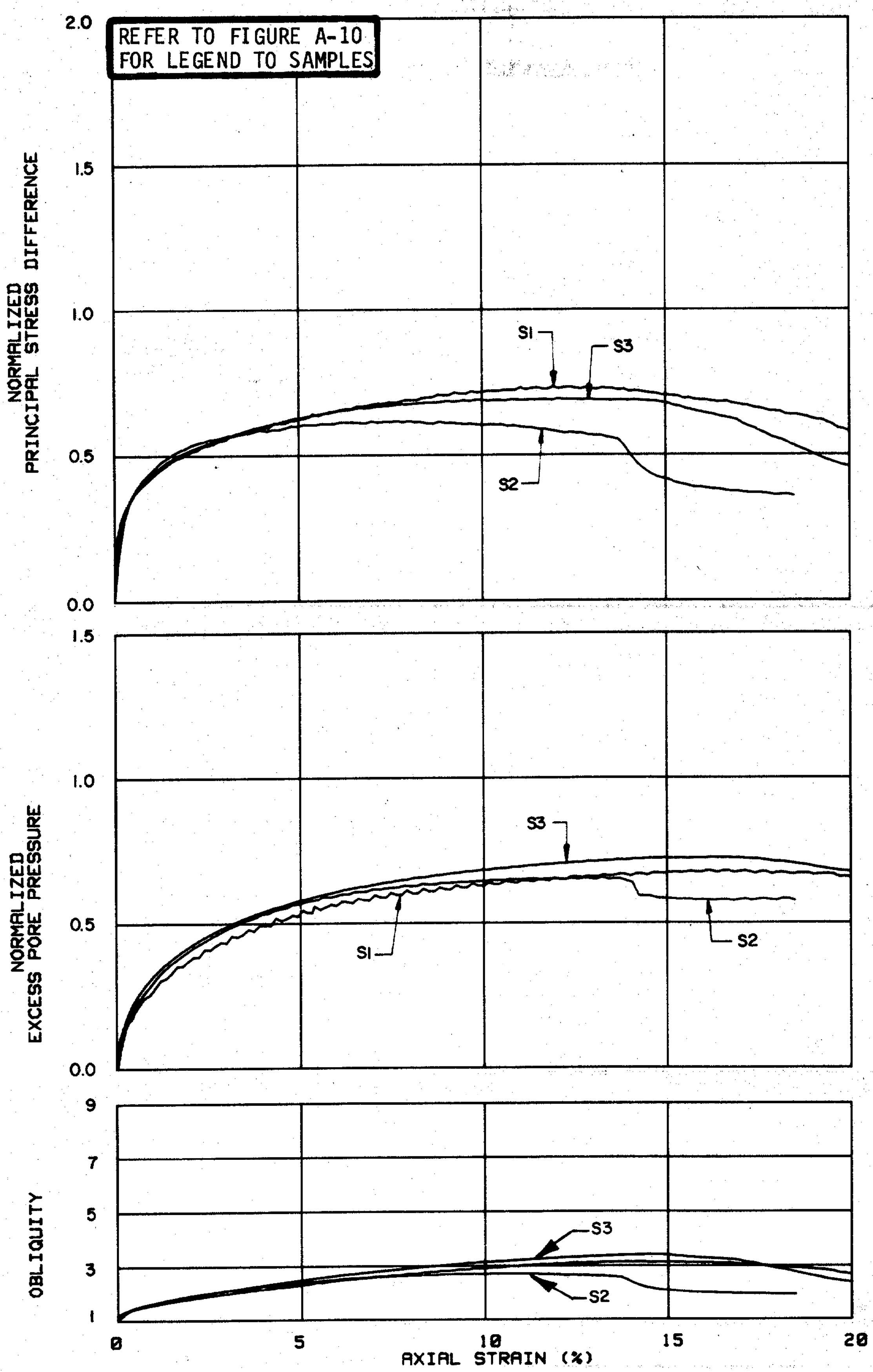

UNDRAINED STRESS-STRAIN BEHAVIOR FROM CIUC TESTS ON MOBIL-NICHOLS PHOSPHATIC CLAY

FIGURE A-11

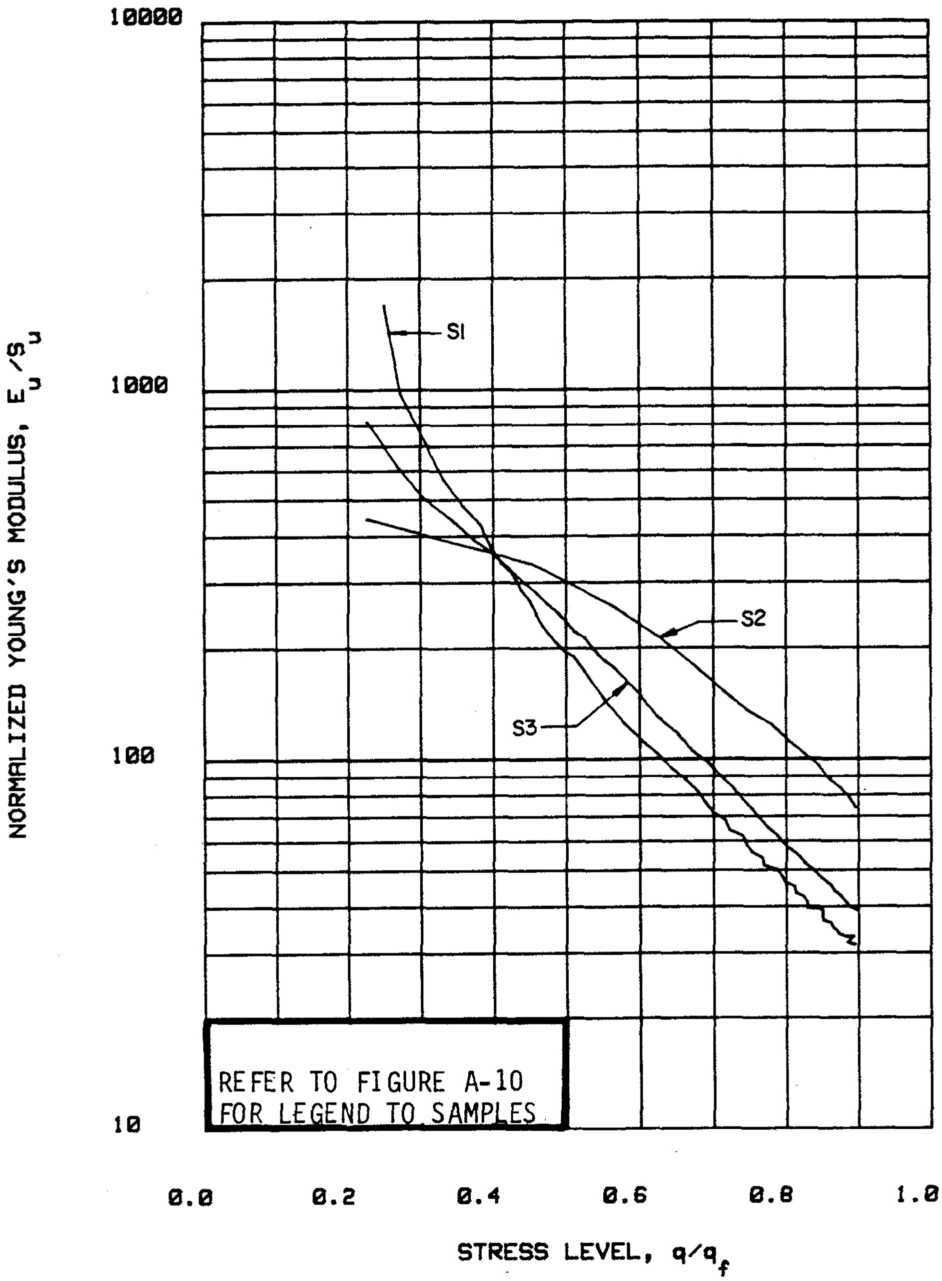

NORMALIZED UNDRAINED YOUNG'S MODULUS VERSUS STRESS LEVEL FROM $\overline{\text{CIU}}$C TESTS ON MOBIL-NICHOLS PHOSPHATIC CLAY

FIGURE A-12

SAMPLE	INITIAL w_n (%)	INITIAL γ_t (pcf)	FINAL w_n (%)	FINAL γ_t (pcf)	$Su/\bar{\sigma}_c$	$(\sigma_1-\sigma_3)$ max ξ (%)	$(\sigma_1-\sigma_3)$ max $\bar{\phi}$	$(\sigma_1-\sigma_3)$ max A FACTOR	$(\bar{\sigma}_1/\bar{\sigma}_3)$max ξ (%)	$(\bar{\sigma}_1/\bar{\sigma}_3)$max $\bar{\phi}$	$(\bar{\sigma}_1/\bar{\sigma}_3)$max A FACTOR
S1	150.8	78.8	106.7	90.5	0.39	-	-	-	-	-	-
S2	154.7	79.5	105.7	90.7	0.35	12.1	43.2°	1.19	17.0	45.8°	1.33
S4	146.4	76.1	91.7	93.7	0.32	8.7	33.0°	1.14	13.0	35.6°	1.25
S6	153.8	81.2	89.4	94.5	0.31	12.6	35.1°	1.24	17.2	36.4°	1.33
S8	151.9	77.8	106.9	90.4	0.33	12.7	39.5°	1.26	16.0	41.1°	1.33

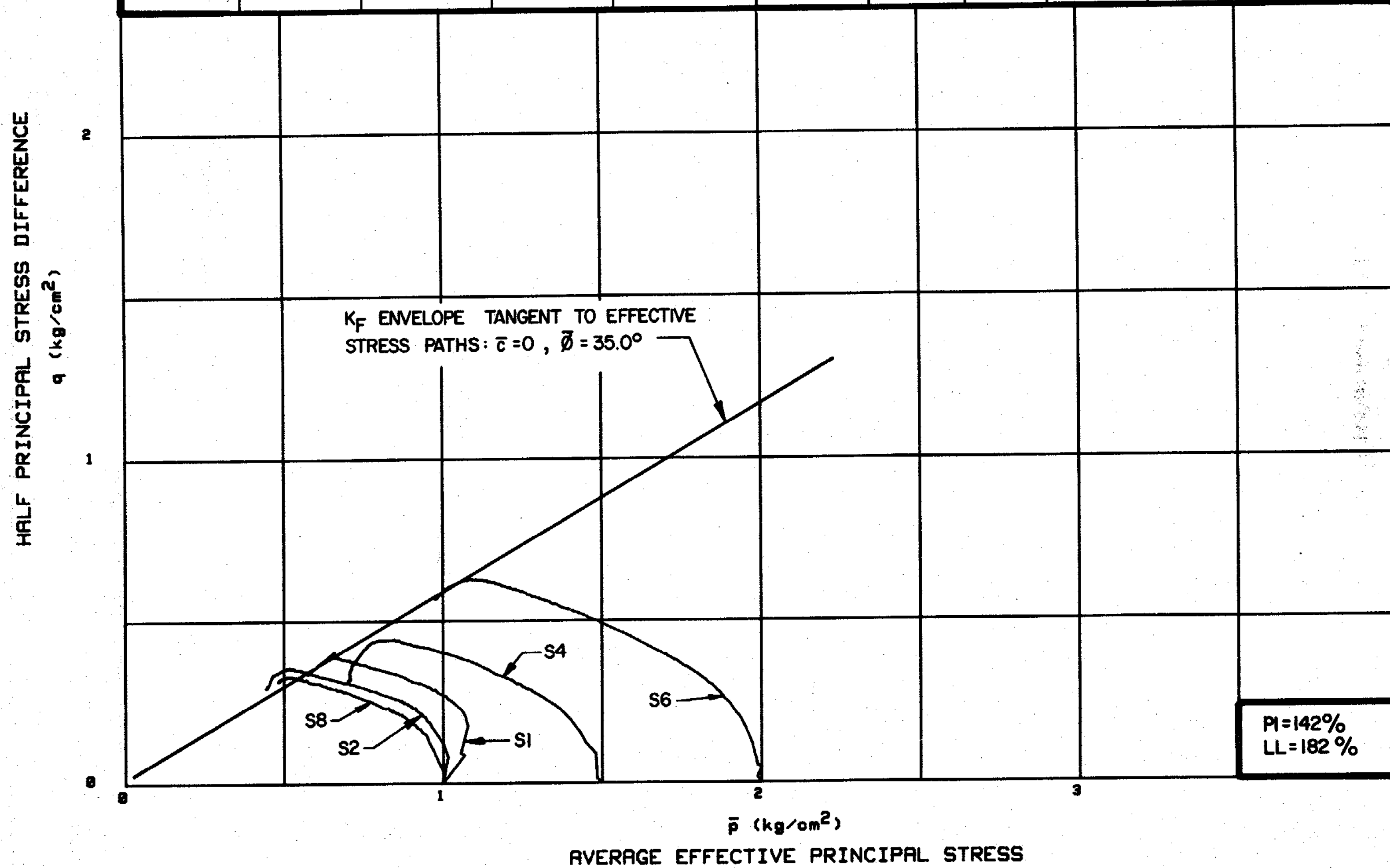

FIGURE A-13

UNDRAINED EFFECTIVE STRESS PATHS FROM $\overline{\text{CIU}}$C TESTS ON OCCIDENTAL-SUWANNEE RIVER PHOSPHATIC CLAY

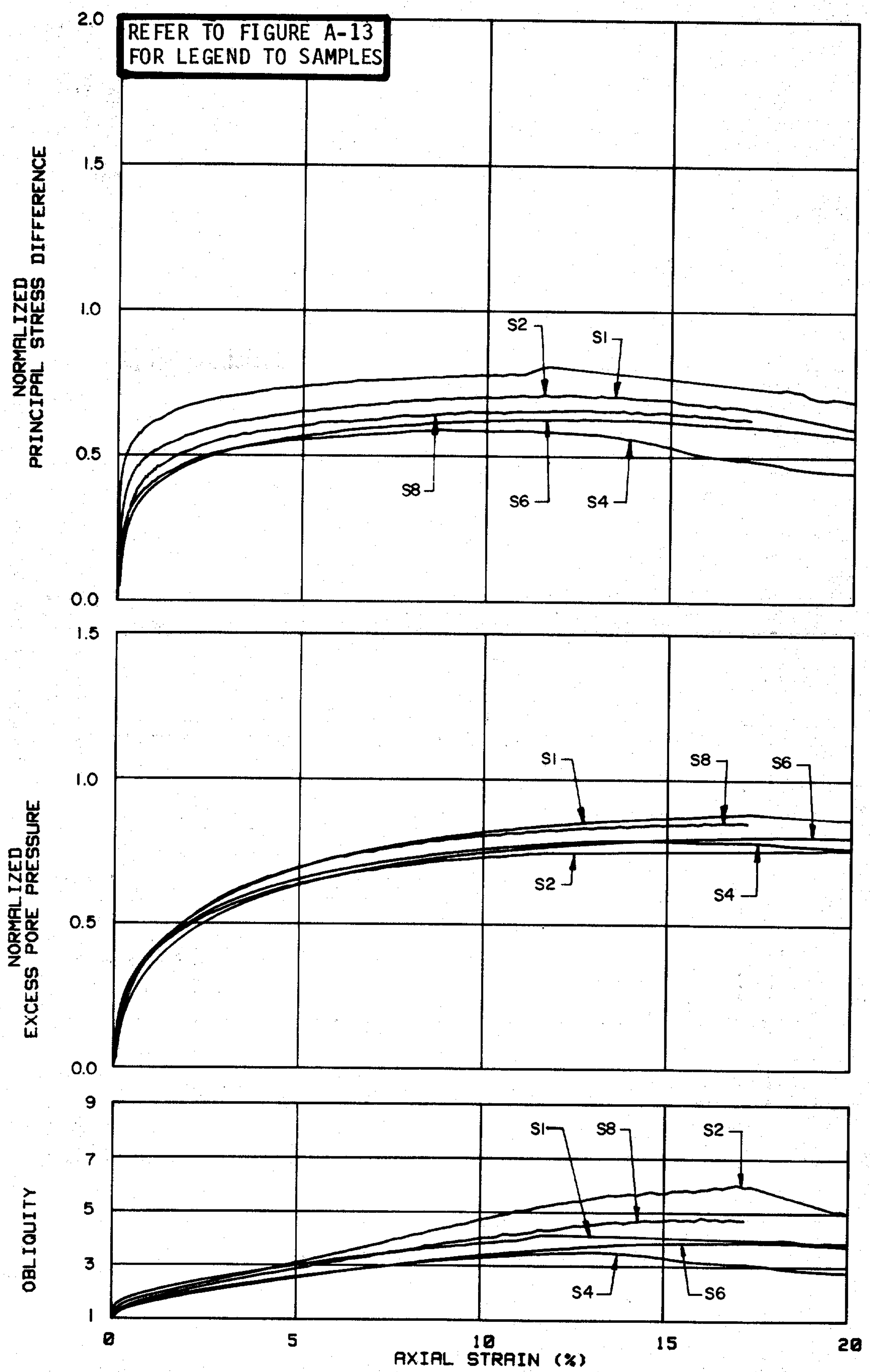

UNDRAINED STRESS-STRAIN BEHAVIOR FROM $\overline{\text{CIU}}$C TESTS
ON OCCIDENTAL-SUWANNEE RIVER PHOSPHATIC CLAY

FIGURE A-14

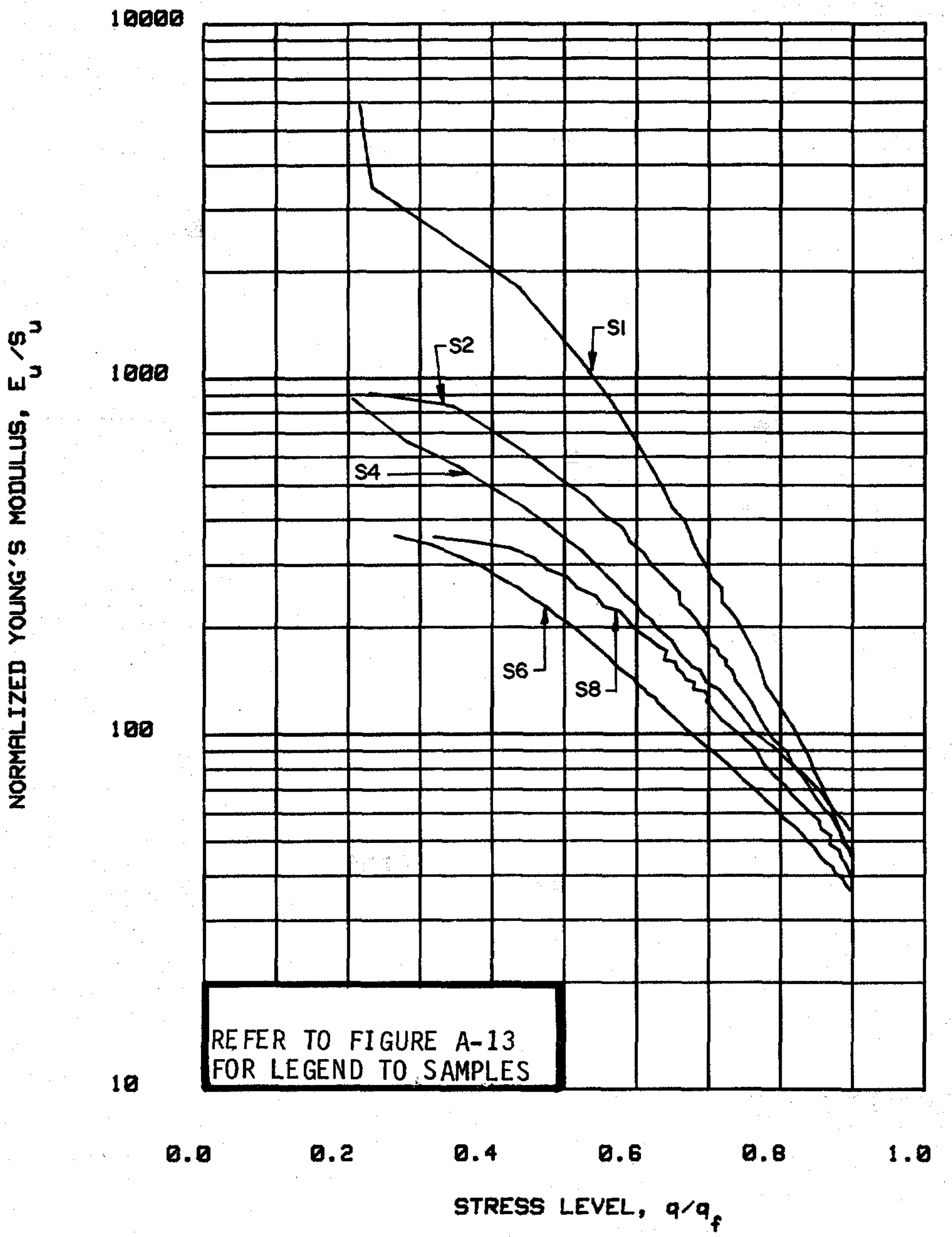

NORMALIZED YOUNG'S MODULUS VERSUS STRESS LEVEL FROM CIUC TESTS ON OCCIDENTAL-SUWANNEE RIVER PHOSPHATIC CLAY

FIGURE A-15

FIGURE A-16

SAMPLE	INITIAL		FINAL		$S_u/\bar{\sigma}_c$	$(\bar{\sigma}_1 - \bar{\sigma}_3)_{max}$			$(\bar{\sigma}_1 / \bar{\sigma}_3)_{max}$		
	w_n (%)	γ_t (pcf)	w_n (%)	γ_t (pcf)		ξ (%)	$\bar{\phi}$	A FACTOR	ξ (%)	$\bar{\phi}$	A FACTOR
S1	143.4	85.2	110.0	90.1	0.33	8.4	32.4°	1.05	12.8	34.8°	1.16
S2	143.2	90.9	99.1	92.4	0.34	11.4	34.2°	1.05	14.7	35.6°	1.12
S3	139.8	83.9	90.7	94.4	0.27	7.6	24.9°	1.13	10.3	26.3°	1.22
S4	139.6	85.5	91.3	94.1	0.28	8.9	26.8°	1.23	9.4	26.8°	1.26
S	139.4	85.7	111.8	89.8	0.38	5.0	33.9°	0.86	9.5	39.0°	1.02
F	141.1	86.6	110.1	90.1	0.36	4.9	26.4°	0.79	9.4	28.5°	0.91

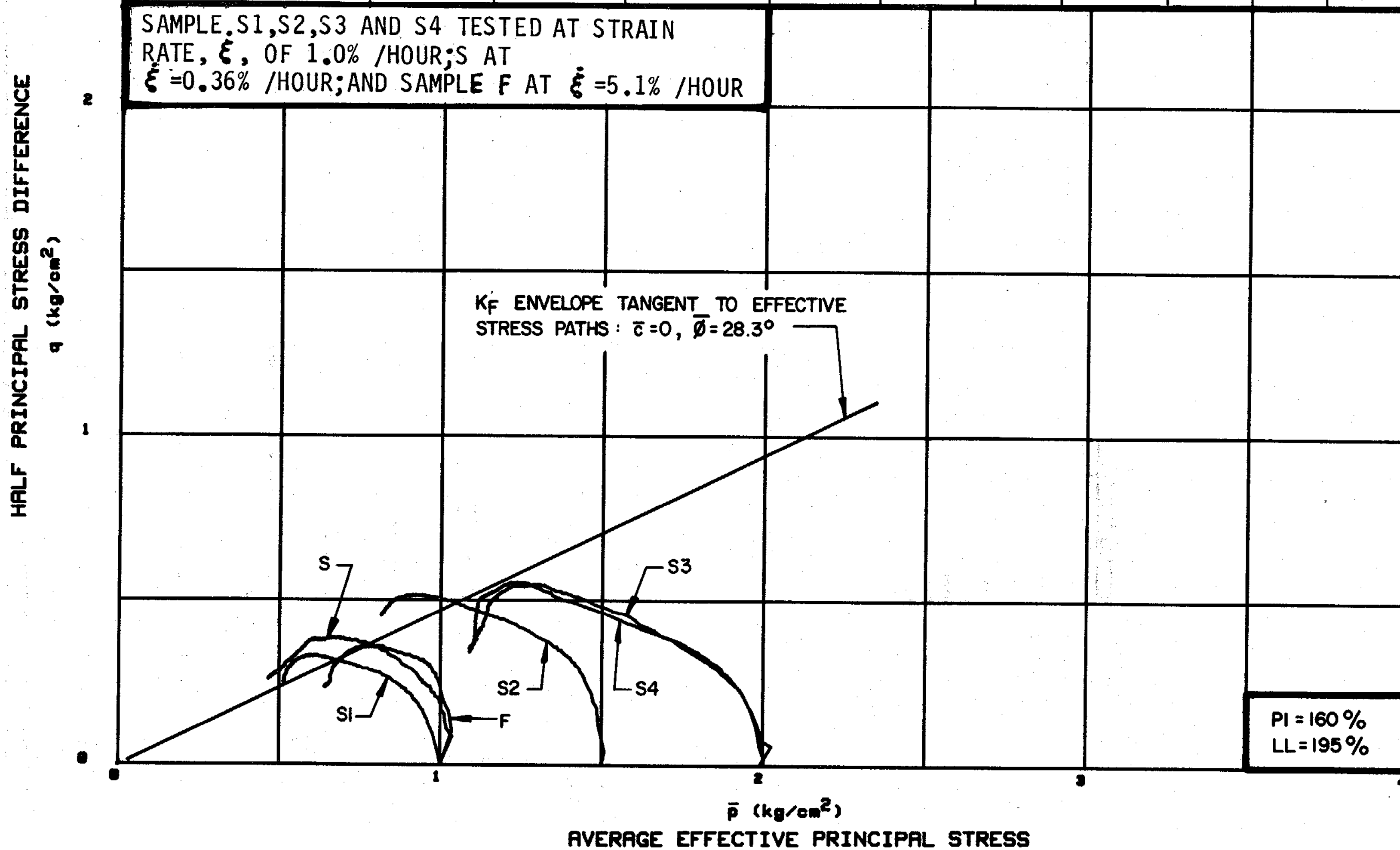

UNDRAINED EFFECTIVE STRESS PATHS FROM CIUC TESTS ON USSAC-ROCKLAND PHOSPHATIC CLAY

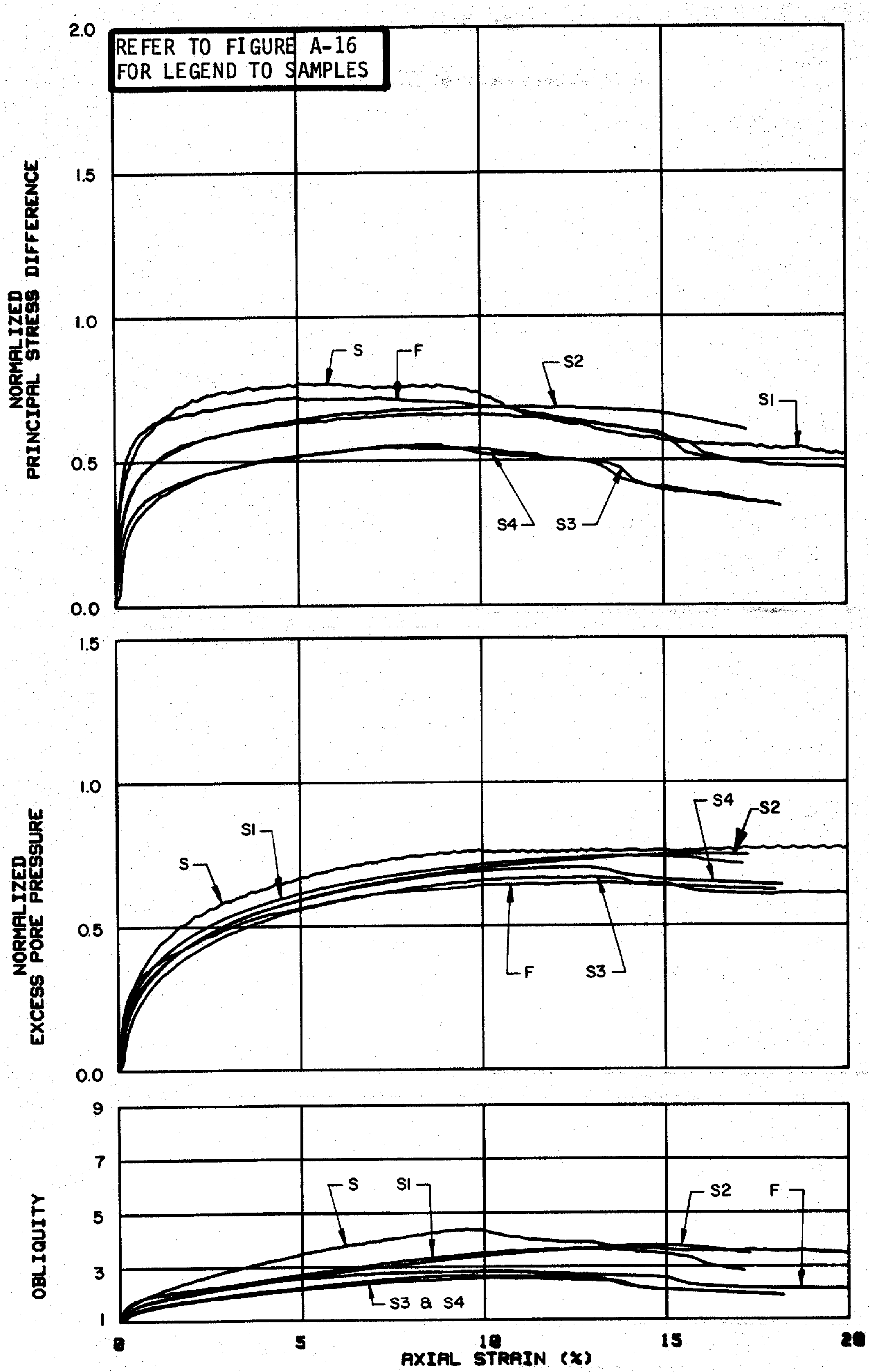

UNDRAINED STRESS-STRAIN BEHAVIOR FROM $\overline{\text{CIUC}}$ TESTS ON USSAC-ROCKLAND PHOSPHATIC CLAY

FIGURE A-17

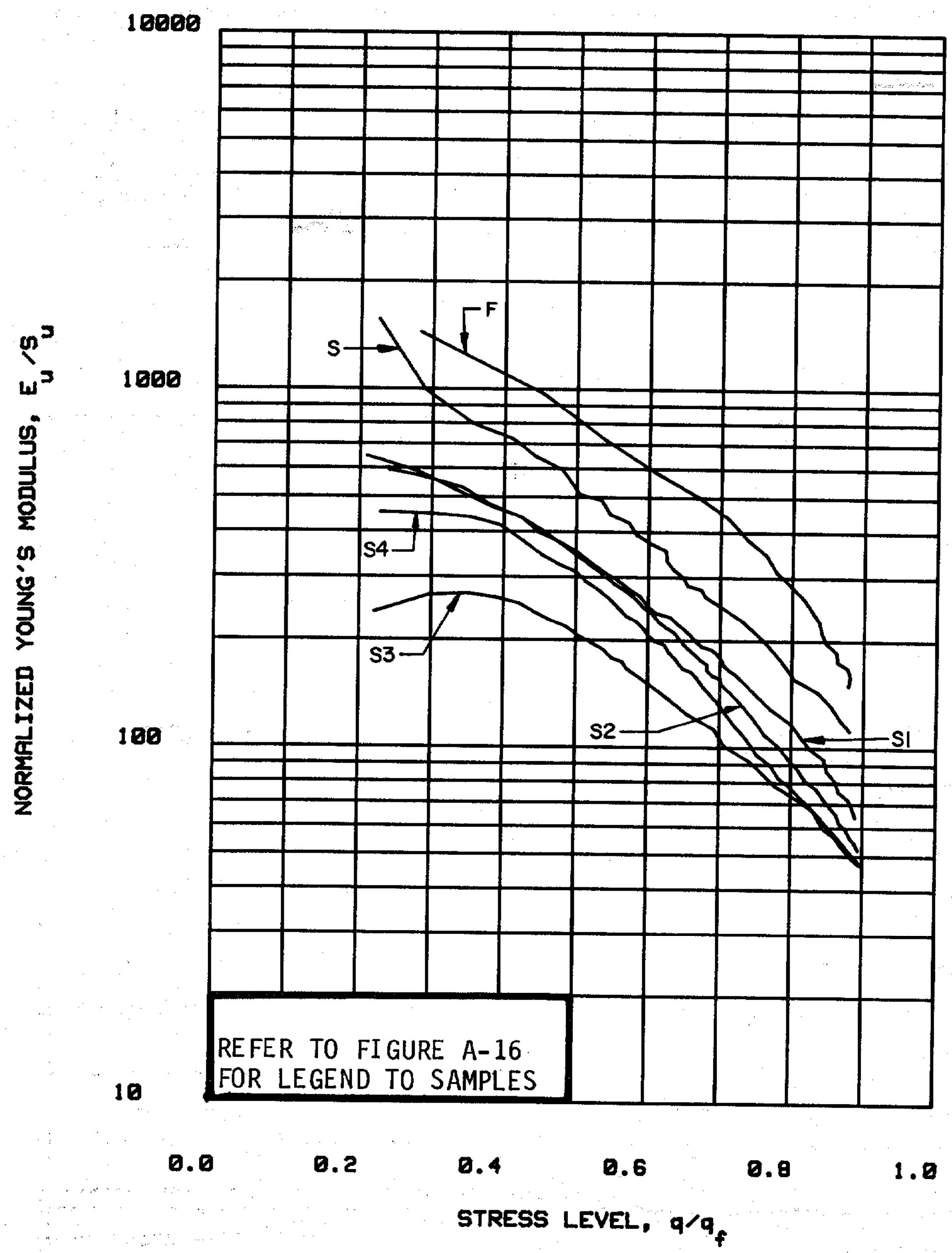

NORMALIZED UNDRAINED YOUNG'S MODULUS VERSUS STRESS LEVEL FROM CIUC TESTS ON USSAC-ROCKLAND PHOSPHATIC CLAY

FIGURE A-18

Appendix B

STRESS-STRAIN-STRENGTH BEHAVIOR OF NORMALLY CONSOLIDATED SAND-CLAY MIXES FROM $\overline{\text{CIUC}}$ TESTS

Appendix B

LIST OF FIGURES

<u>Note:</u> Stress-strain curves are normalized with respect to the pre-shear isotropic effective consolidation stress, $\bar{\sigma}_c$.

SAMPLE	INITIAL		FINAL		$S_u/\bar{\sigma}_c$	$(\sigma_1 - \sigma_3)$ max			$(\bar{\sigma}_1 / \bar{\sigma}_3)$ max		
	w_n (%)	γ_t (pcf)	w_n (%)	γ_t (pcf)		ξ (%)	$\bar{\phi}$	A FACTOR	ξ (%)	$\bar{\phi}$	A FACTOR
S1	118.6	87.2	72.4	98.3	0.34	9.3	36.6°	1.10	14.4	38.8°	1.16
S2	119.5	87.1	61.3	102.4	0.36	9.6	32.7°	0.94	13.2	33.4°	0.99

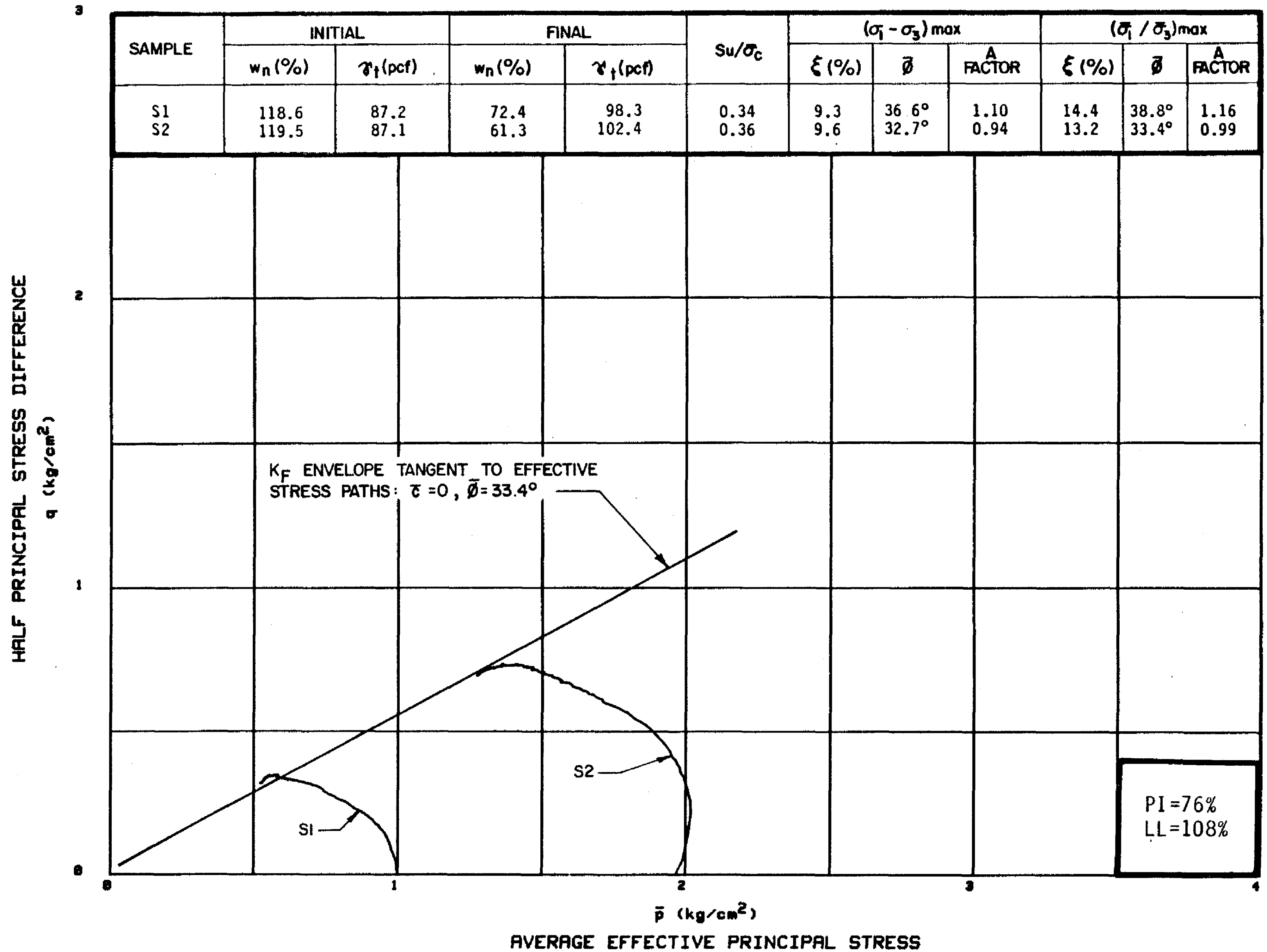

FIGURE B-1

UNDRAINED EFFECTIVE STRESS PATHS FROM $\overline{CIU}$C TESTS ON AGRICO-SADDLE CREEK SAND-CLAY MIX WITH SCR = 1:1

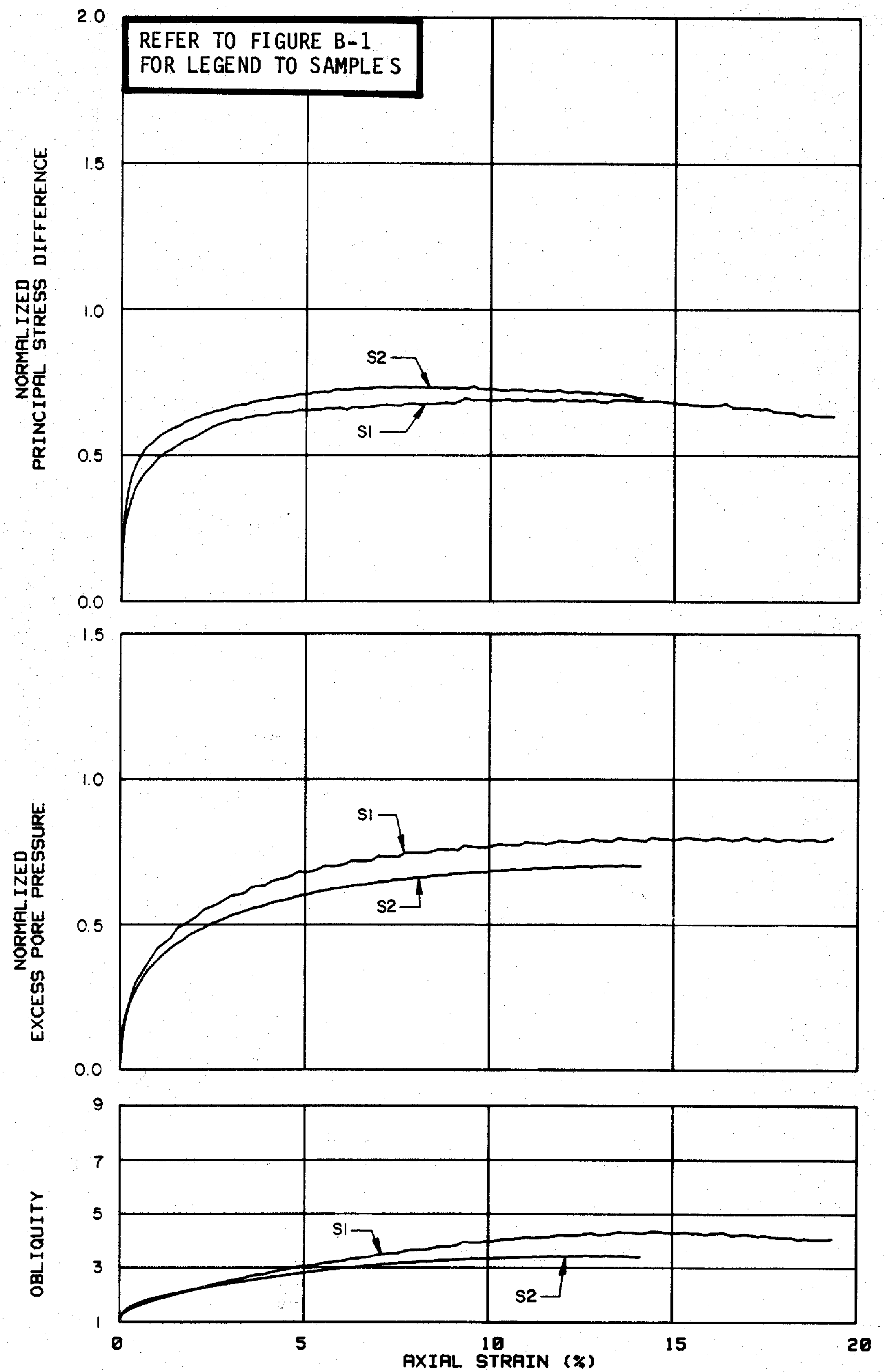

UNDRAINED STRESS-STRAIN BEHAVIOR FROM $\overline{\text{CIUC}}$ TESTS ON AGRICO-SADDLE CREEK SAND-CLAY MIX WITH SCR = 1:1

FIGURE B-2

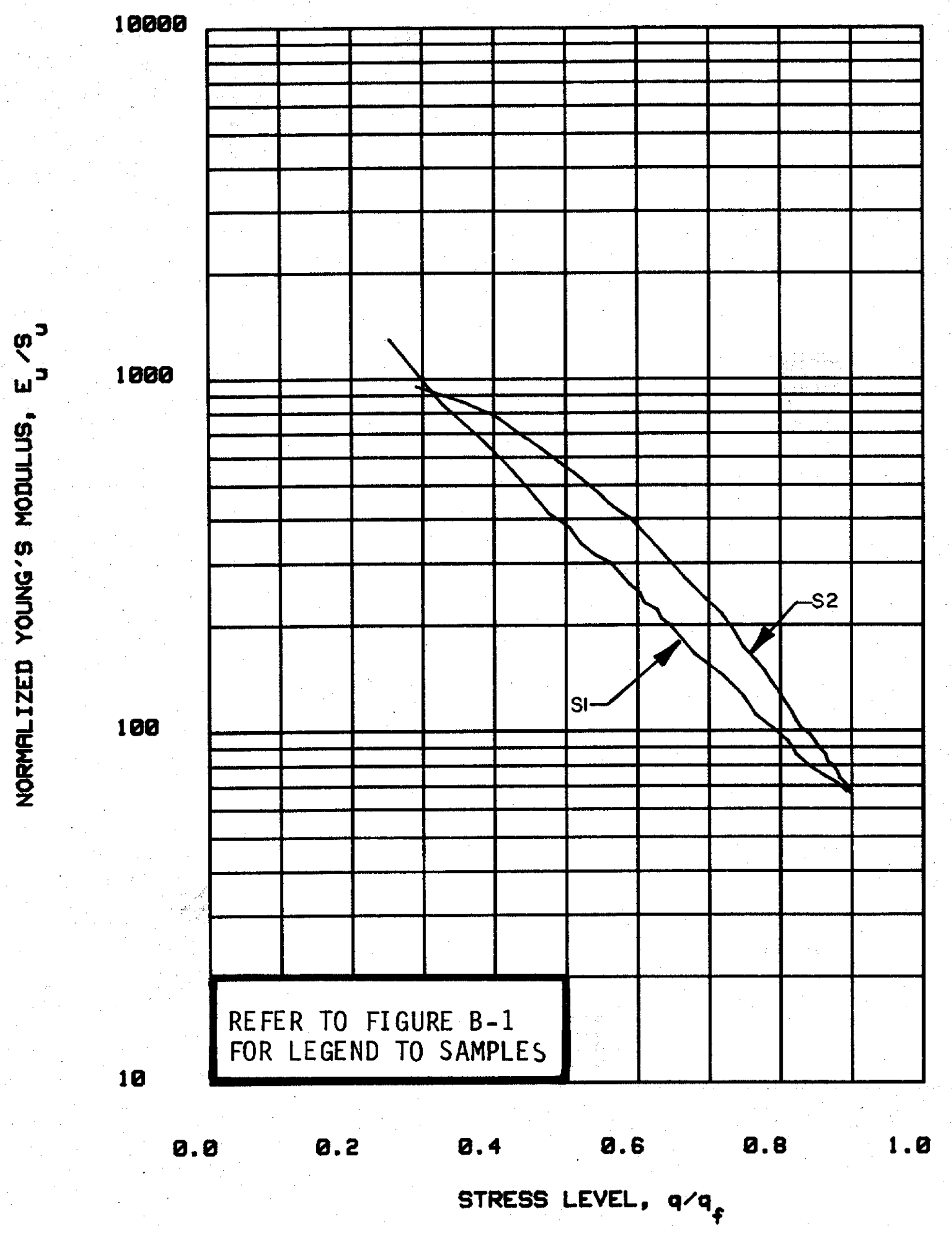

NORMALIZED UNDRAINED YOUNG'S MODULUS VERSUS STRESS LEVEL FROM CIUC TESTS ON AGRICO-SADDLE CREEK SAND-CLAY MIX SCR = 1:1

FIGURE B-3

SAMPLE	INITIAL w_n (%)	INITIAL γ_t (pcf)	FINAL w_n (%)	FINAL γ_t (pcf)	$S_u/\bar{\sigma}_c$	$(\sigma_1 - \sigma_3)_{max}$ ξ (%)	$(\sigma_1 - \sigma_3)_{max}$ $\bar{\phi}$	$(\sigma_1 - \sigma_3)_{max}$ A FACTOR	$(\bar{\sigma}_1/\bar{\sigma}_3)_{max}$ ξ (%)	$(\bar{\sigma}_1/\bar{\sigma}_3)_{max}$ $\bar{\phi}$	$(\bar{\sigma}_1/\bar{\sigma}_3)_{max}$ A FACTOR
S1	72.3	101.5	42.9	111.4	0.33	17.3	43.2°	1.27	17.3	43.2°	1.27
S2	58.0	102.7	40.2	113.0	0.29	4.0	30.9°	1.22	7.4	33.6°	1.34
S3	70.8	101.6	35.8	115.7	0.34	5.8	34.6°	1.10	11.2	36.4°	1.15

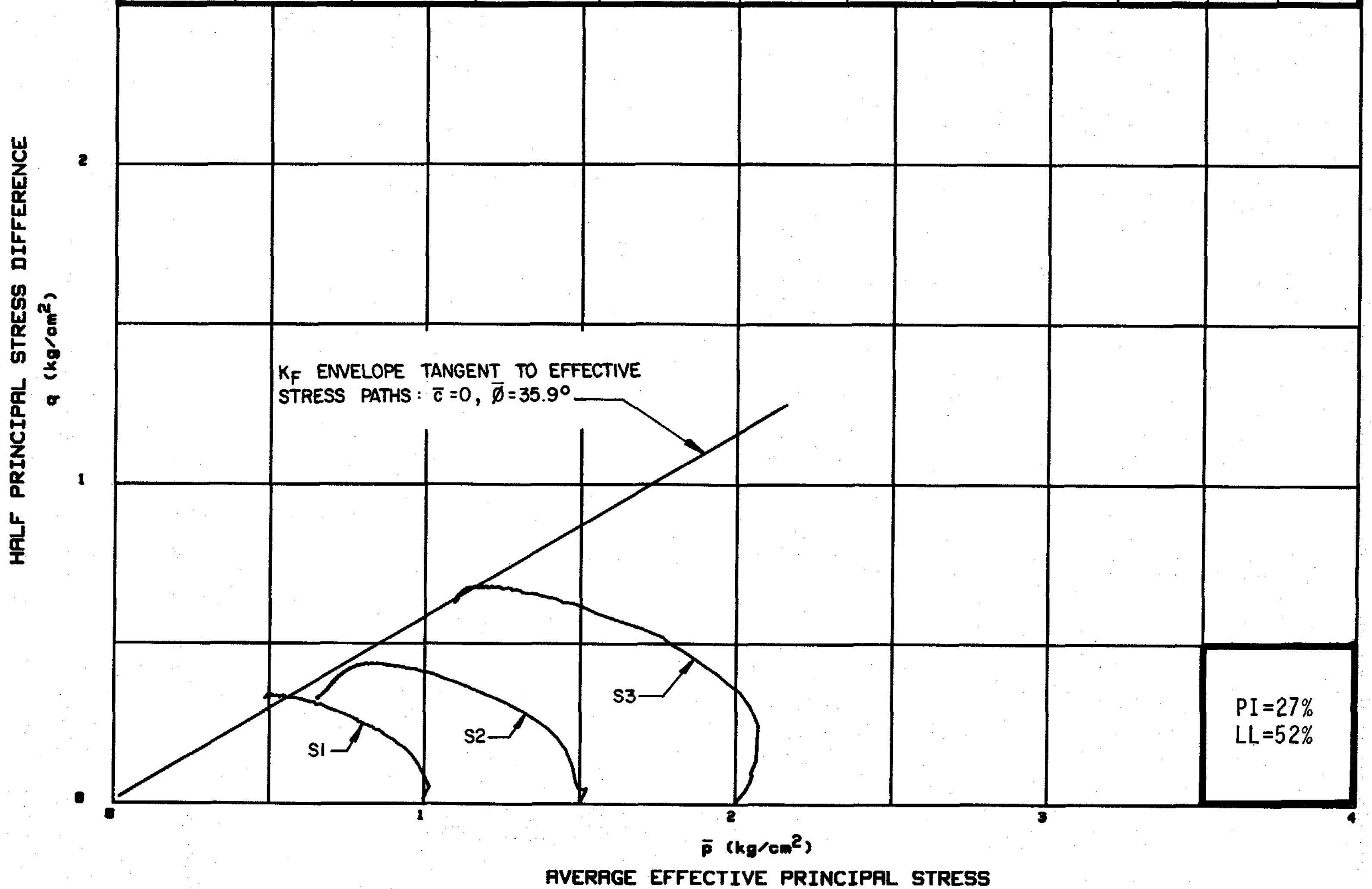

FIGURE B-4

UNDRAINED EFFECTIVE STRESS PATHS FROM $\overline{\text{CIUC}}$ TESTS ON AGRICO-SADDLE CREEK SAND-CLAY MIX WITH SCR: 3:1

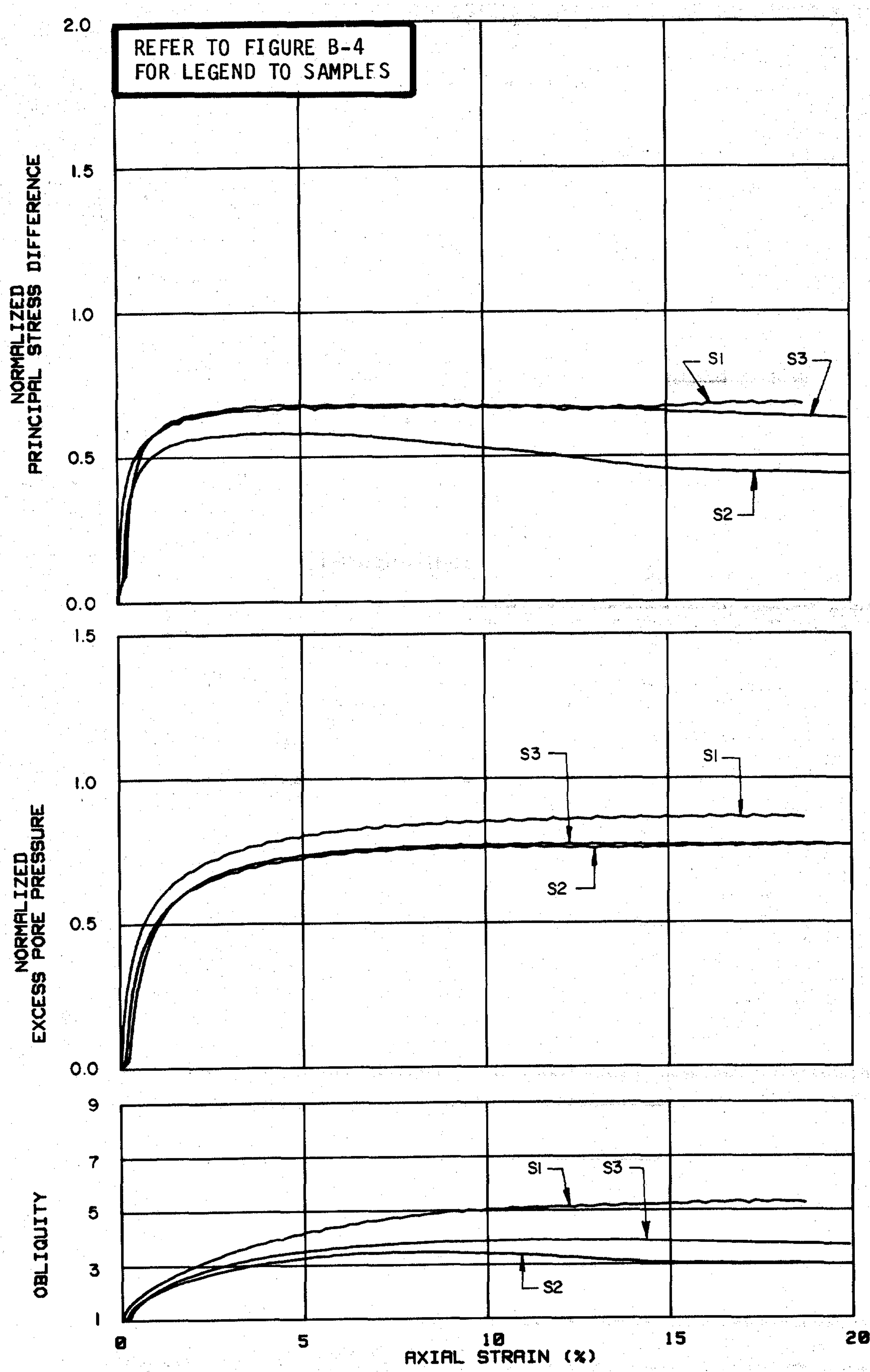

UNDRAINED STRESS-STRAIN BEHAVIOR FROM $\overline{\text{CIU}}$C TESTS ON AGRICO-SADDLE CREEK SAND-CLAY MIX WITH SCR = 3:1

FIGURE B-5

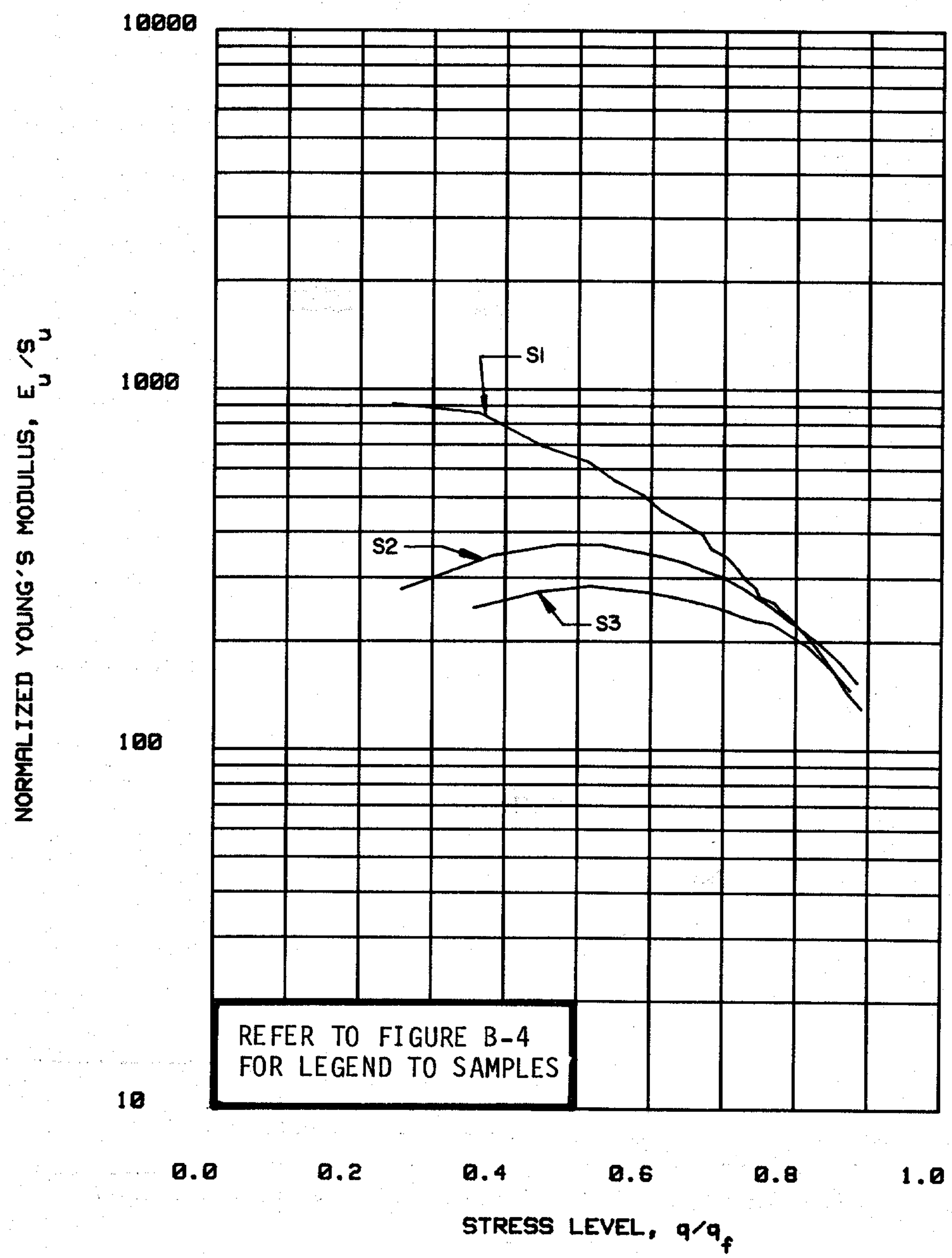

NORMALIZED UNDRAINED YOUNG'S MODULUS VERSUS STRESS LEVEL FROM CIUC TESTS ON AGRICO-SADDLE CREEK SAND-CLAY MIX WITH SCR : 3:1

FIGURE B-6

FIGURE B-7

SAMPLE	INITIAL		FINAL		$Su/\bar{\sigma}_c$	$(\sigma_1 - \sigma_3)$ max			$(\bar{\sigma}_1 / \bar{\sigma}_3)$max		
	w_n (%)	γ_t (pcf)	w_n (%)	γ_t (pcf)		ξ (%)	$\bar{\phi}$	A FACTOR	ξ (%)	$\bar{\phi}$	A FACTOR
S1	61.1	108.8	40.1	113.3	0.39	5.3	31.5°	0.85	8.8	33.2°	0.93
S2	60.7	102.5	35.1	116.9	0.32	7.0	29.9°	1.09	9.7	30.4°	1.17

PI AND LL VALUES ARE ESTIMATED BASED ON LINEAR REGRESSION BETWEEN PI AND LL FOR VALUES AT SCR= 0:1, 2:1 and 3:1

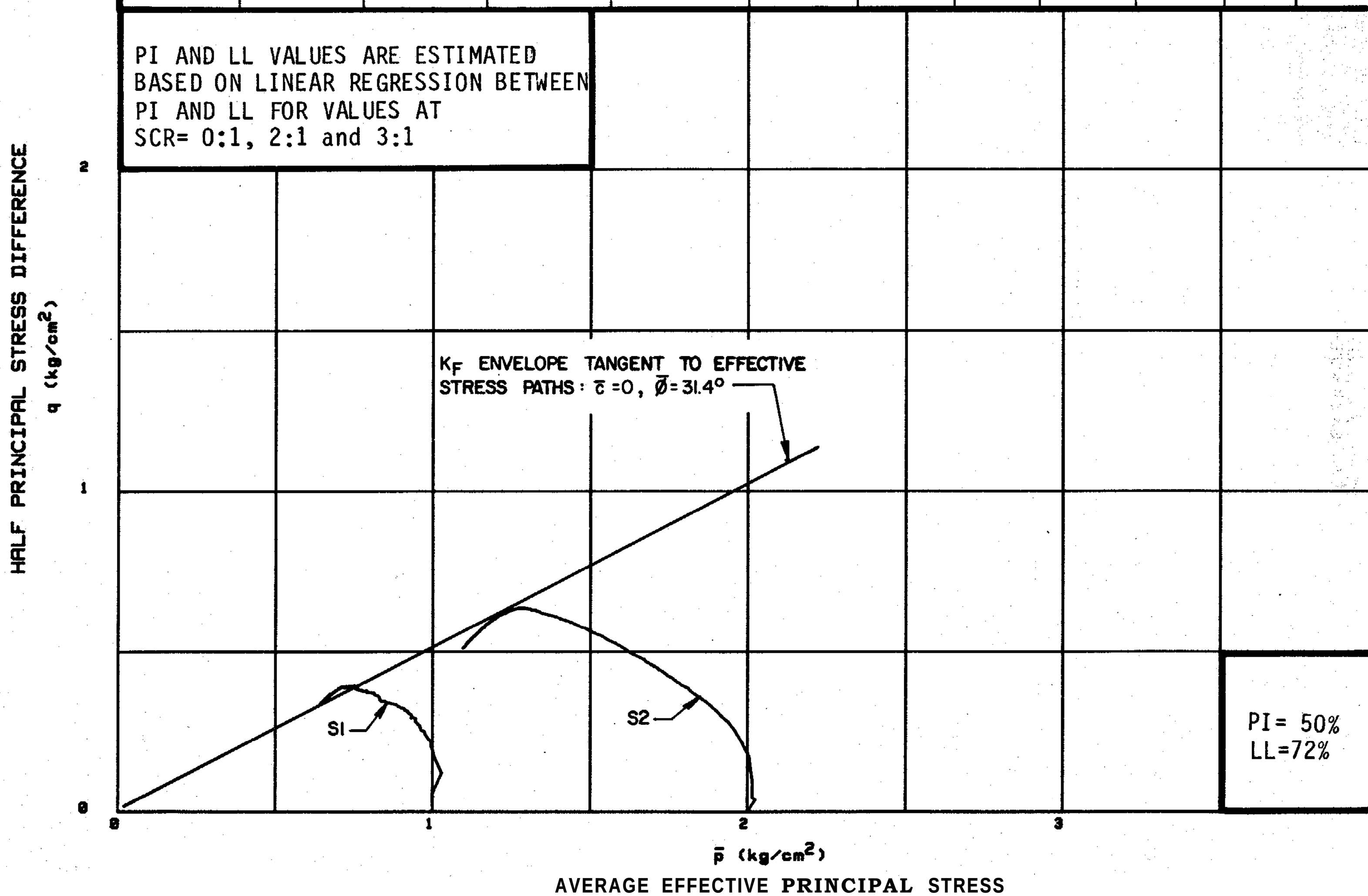

PI= 50%
LL=72%

UNDRAINED EFFECTIVE STRESS PATHS FROM $\overline{\text{CIUC}}$ TESTS ON CF MINING-HARDEE SAND-CLAY MIX WITH SCR : 1:1

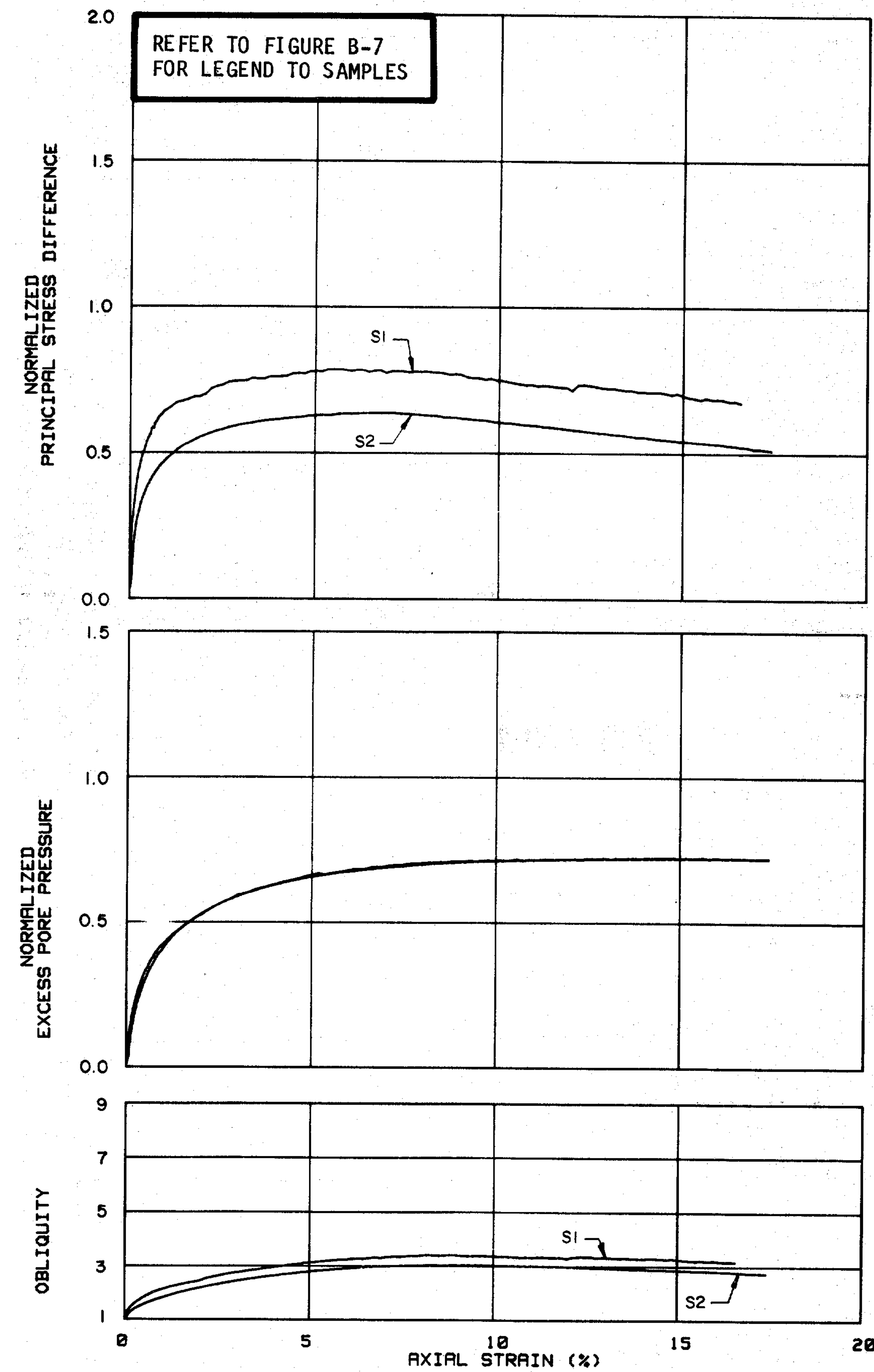

UNDRAINED STRESS-STRAIN BEHAVIOR FROM $\overline{\text{CIUC}}$ TESTS ON CF MINING-HARDEE SAND-CLAY MIX WITH SCR : 1:1

FIGURE B-8

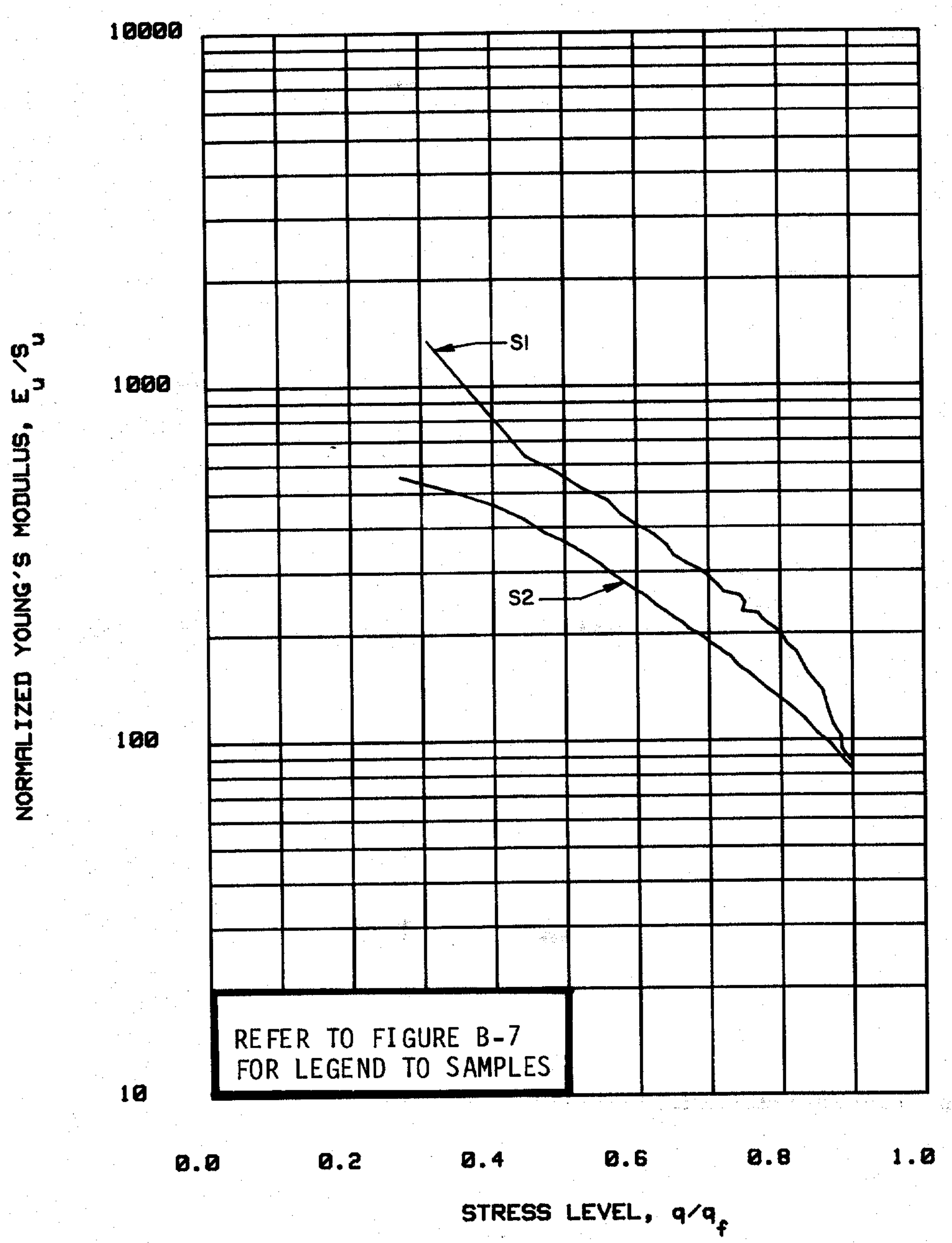

NORMALIZED UNDRAINED YOUNG'S MODULUS VERSUS STRESS LEVEL FROM $\overline{\text{CIU}}$C TESTS ON CF MINING-HARDEE SAND-CLAY MIX WITH SCR : 1:1

FIGURE B-9

SAMPLE	INITIAL		FINAL		$S_u/\bar{\sigma}_c$	$(\sigma_1 - \sigma_3)_{max}$			$(\bar{\sigma}_1 / \bar{\sigma}_3)_{max}$		
	w_n (%)	γ_t (pcf)	w_n (%)	γ_t (pcf)		ξ (%)	$\bar{\phi}$	A FACTOR	ξ (%)	$\bar{\phi}$	A FACTOR
S1	31.6	111.1	25.7	124.9	0.17	10.8	31.4°	2.30	10.8	34.4°	2.30
S2	37.3	109.2	30.3	120.4	0.27	2.5	30.2°	1.30	11.8	34.1°	1.49
S3	37.6	107.6	28.5	121.9	0.27	1.9	25.6°	1.19	4.2	28.0°	1.33
S4	31.3	112.0	23.1	127.9	0.27	10.0	34.5°	1.41	9.9	34.6°	1.41

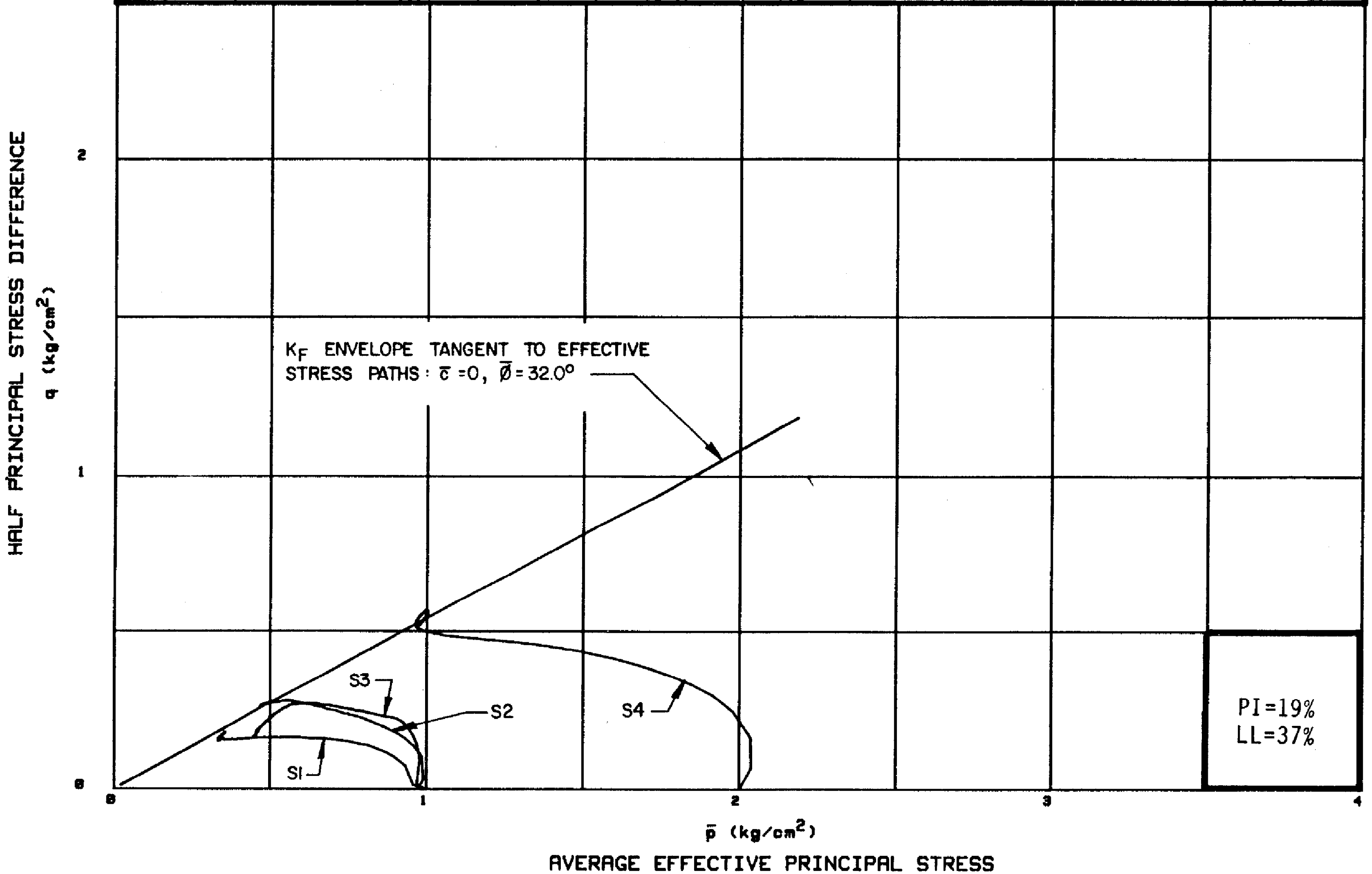

FIGURE B-10

UNDRAINED EFFECTIVE STRESS PATHS FROM $\overline{\text{CIU}}$C TESTS ON CF MINING-HARDEE SAND-CLAY MIX WITH SCR = 3:1

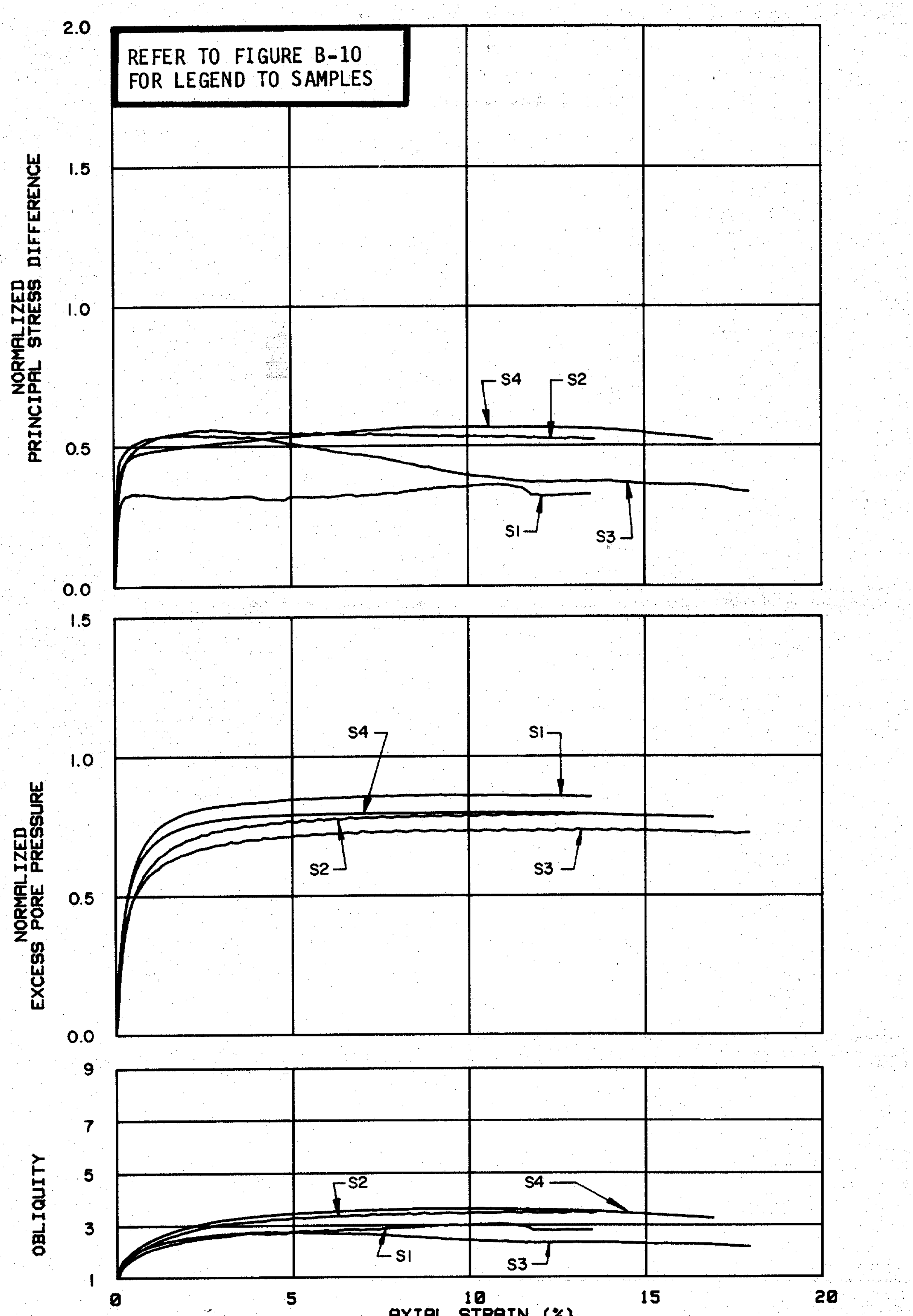

UNDRAINED STRESS-STRAIN BEHAVIOR FROM $\overline{\text{CIU}}$C TESTS ON CF MINING-HARDEE SAND-CLAY MIX WITH SCR : 3:1

FIGURE B-11

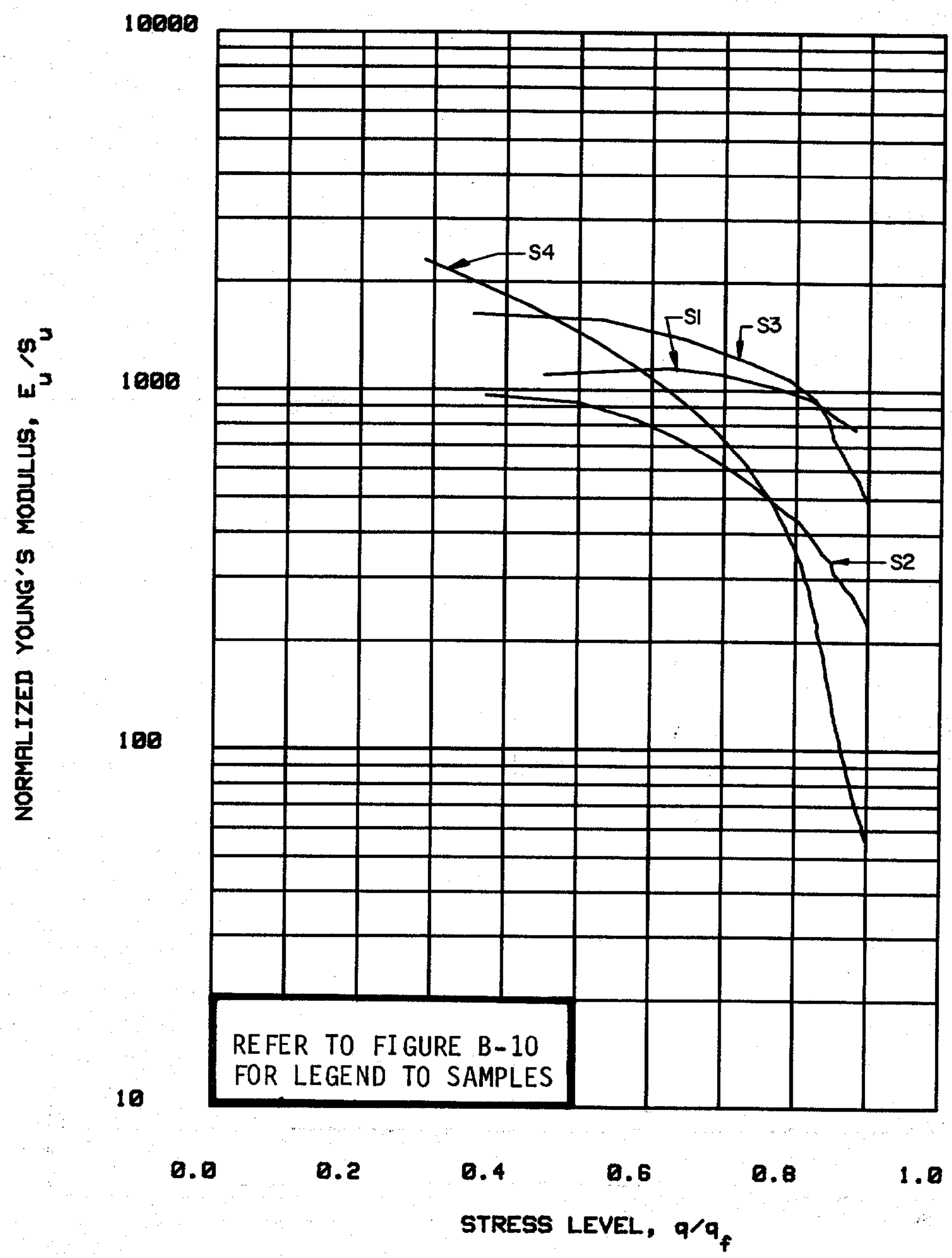

NORMALIZED UNDRAINED YOUNG'S MODULUS VERSUS STRESS LEVEL FROM $\overline{\text{CIU}}$C TESTS ON CF MINING-HARDEE SAND-CLAY MIX WITH SCR : 3 :1

FIGURE B-12

FIGURE B-13

SAMPLE	INITIAL		FINAL		$Su/\bar{\sigma}_c$	$(\sigma_1 - \sigma_3)$ max			$(\bar{\sigma}_1 / \bar{\sigma}_3)$ max		
	w_n (%)	γ_t (pcf)	w_n (%)	γ_t (pcf)		ξ (%)	$\bar{\phi}$	A FACTOR	ξ (%)	$\bar{\phi}$	A FACTOR
S1	111.7	85.3	58.8	104.0	0.35	9.6	35.5°	1.09	14.1	36.6°	1.15
S2	72.4	96.0	49.2	108.3	0.36	6.7	30.6°	0.92	10.0	31.9°	1.00
S3	71.9	96.4	49.7	108.1	0.31	4.0	25.7°	0.99	7.2	27.4°	1.14
S4	111.4	89.6	49.4	108.3	0.34	6.3	30.7°	1.02	8.5	31.7°	1.08

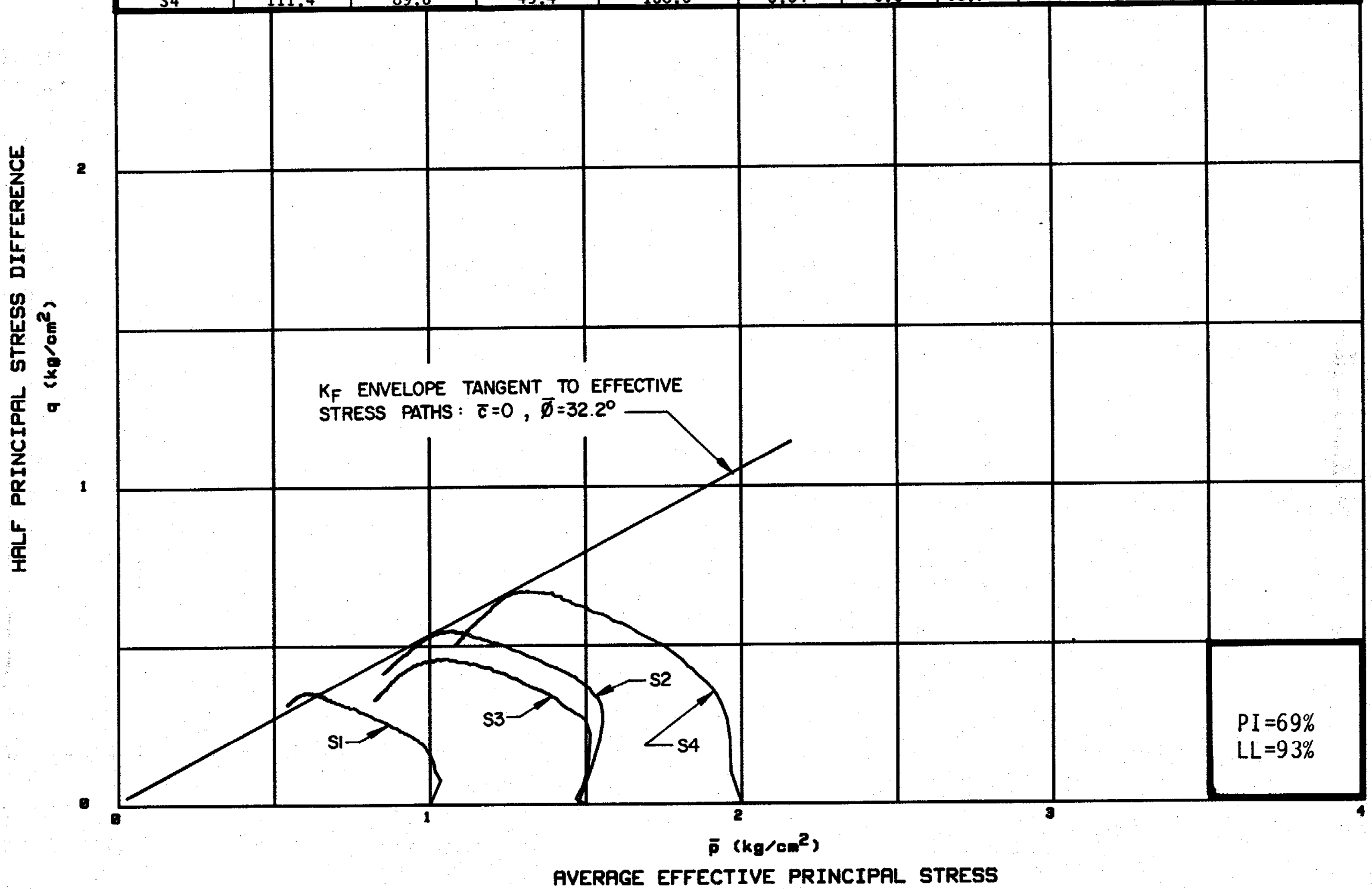

UNDRAINED EFFECTIVE STRESS PATHS FROM $\overline{CIU}$C TESTS ON USSAC-ROCKLAND SAND-CLAY MIX WITH SCR = 1:1

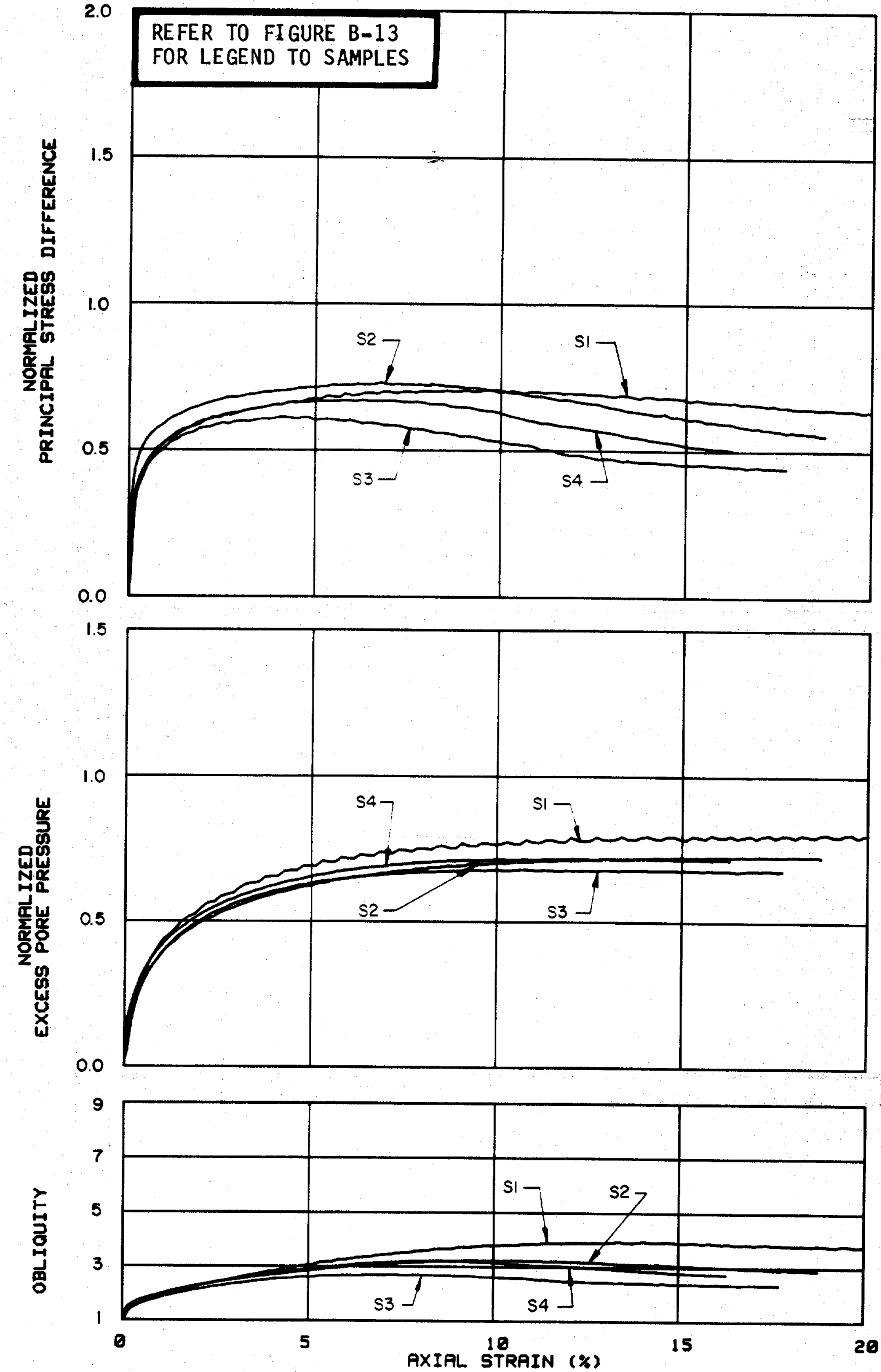

UNDRAINED STRESS-STRAIN BEHAVIOR FROM $\overline{\text{CIU}}$C TESTS ON USSAC-ROCKLAND SAND-CLAY MIX WITH SCR : 1:1

FIGURE B-14

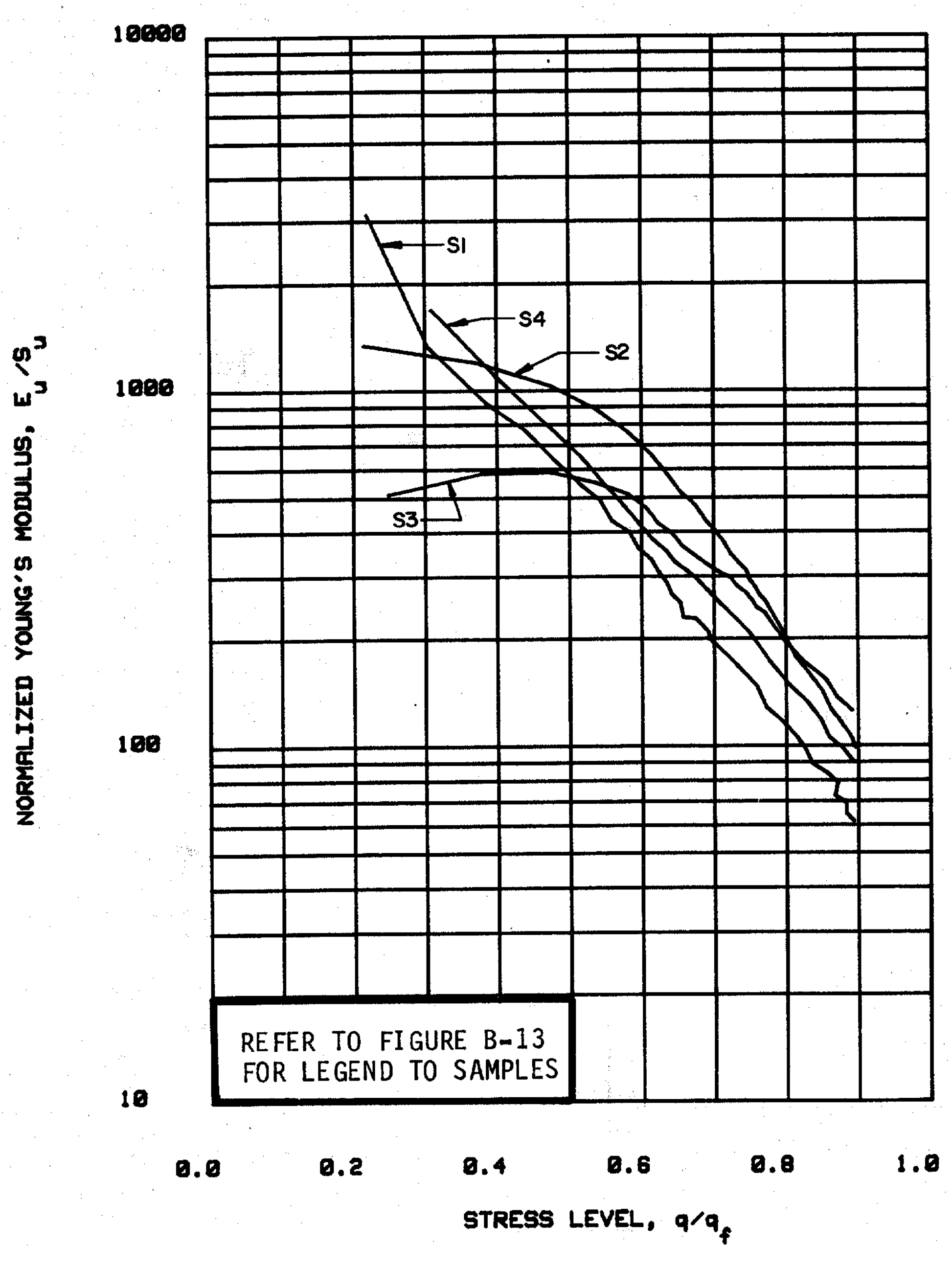

NORMALIZED UNDRAINED YOUNG'S MODULUS VERSUS STRESS LEVEL FROM CIUC TESTS ON USSAC-ROCKLAND SAND-CLAY MIX WITH SCR = 1:1

FIGURE B-15

SAMPLE	INITIAL		FINAL		$Su/\bar{\sigma}_c$	$(\sigma_1 - \sigma_3)$ max			$(\bar{\sigma}_1 / \bar{\sigma}_3)$max		
	w_n (%)	γ_t (pcf)	w_n (%)	γ_t (pcf)		ξ (%)	$\bar{\phi}$	A FACTOR	ξ (%)	$\bar{\phi}$	A FACTOR
S1	43.0	108.0	33.3	118.0	0.38	7.1	38.6°	1.00	11.4	39.1°	1.05
S2	53.6	102.0	27.7	122.5	0.28	4.7	33.0°	1.37	10.3	35.0°	1.41
S3	42.6	108.8	29.2	121.2	0.30	3.3	29.8°	1.17	12.4	31.9°	1.33

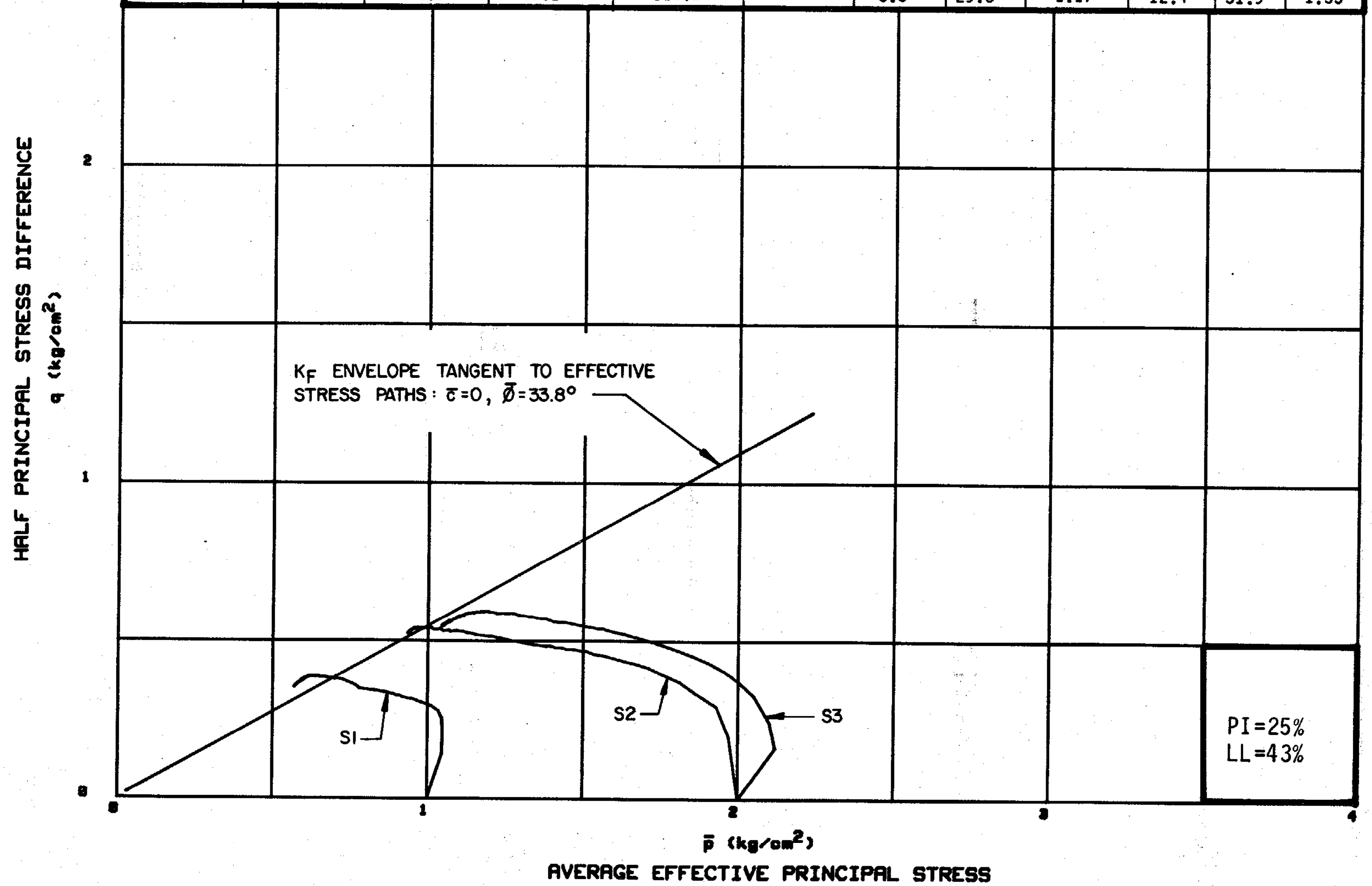

FIGURE B-16

UNDRAINED EFFECTIVE STRESS PATHS FROM $\overline{\text{CIUC}}$ TESTS
ON USSAC-ROCKLAND SAND-CLAY MIX WITH SCR: 3:1

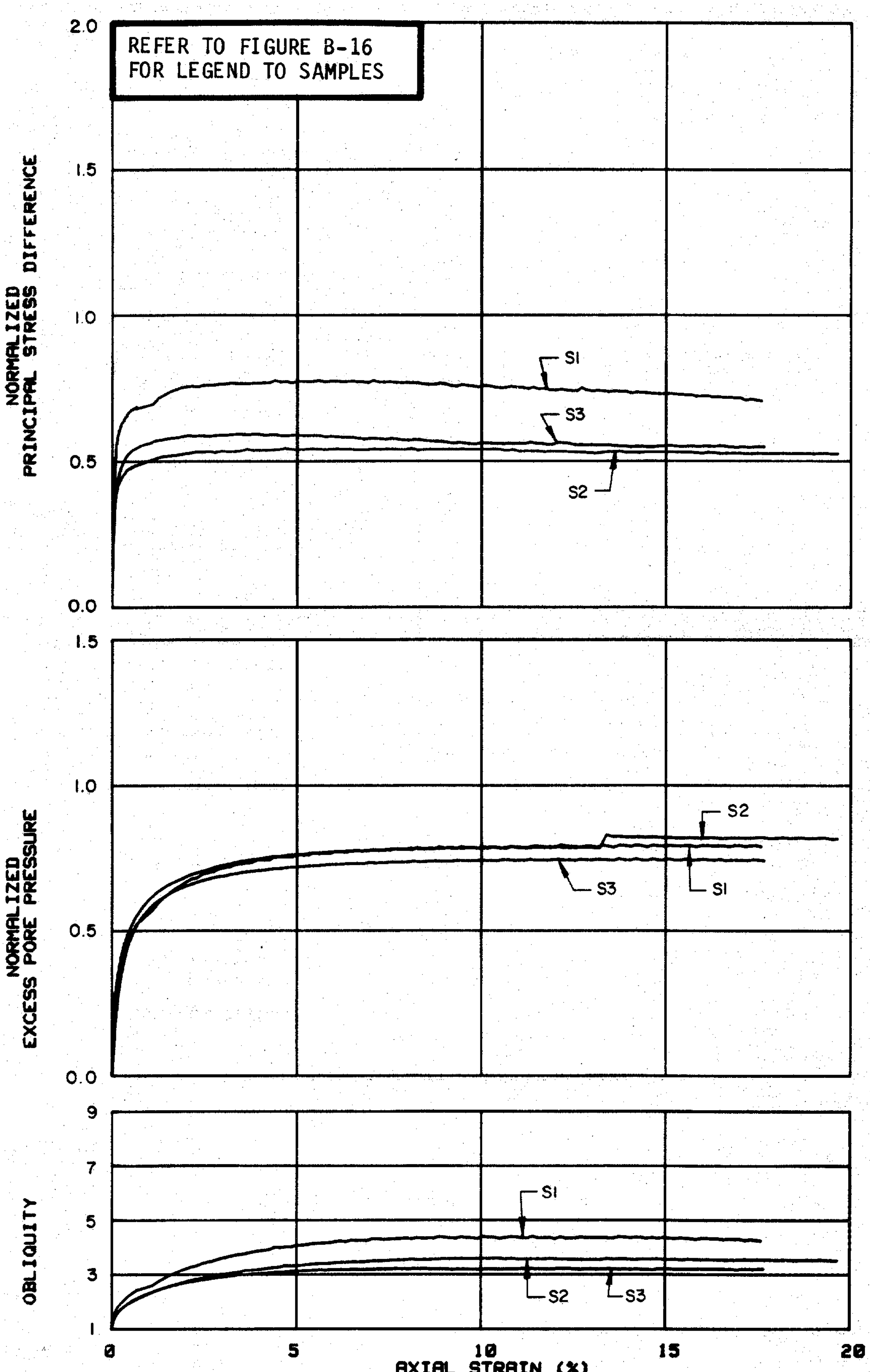

UNDRAINED STRESS-STRAIN BEHAVIOR FROM $\overline{\text{CIUC}}$ TESTS
ON USSAC-ROCKLAND SAND-CLAY MIX WITH SCR = 3:1

FIGURE B-17

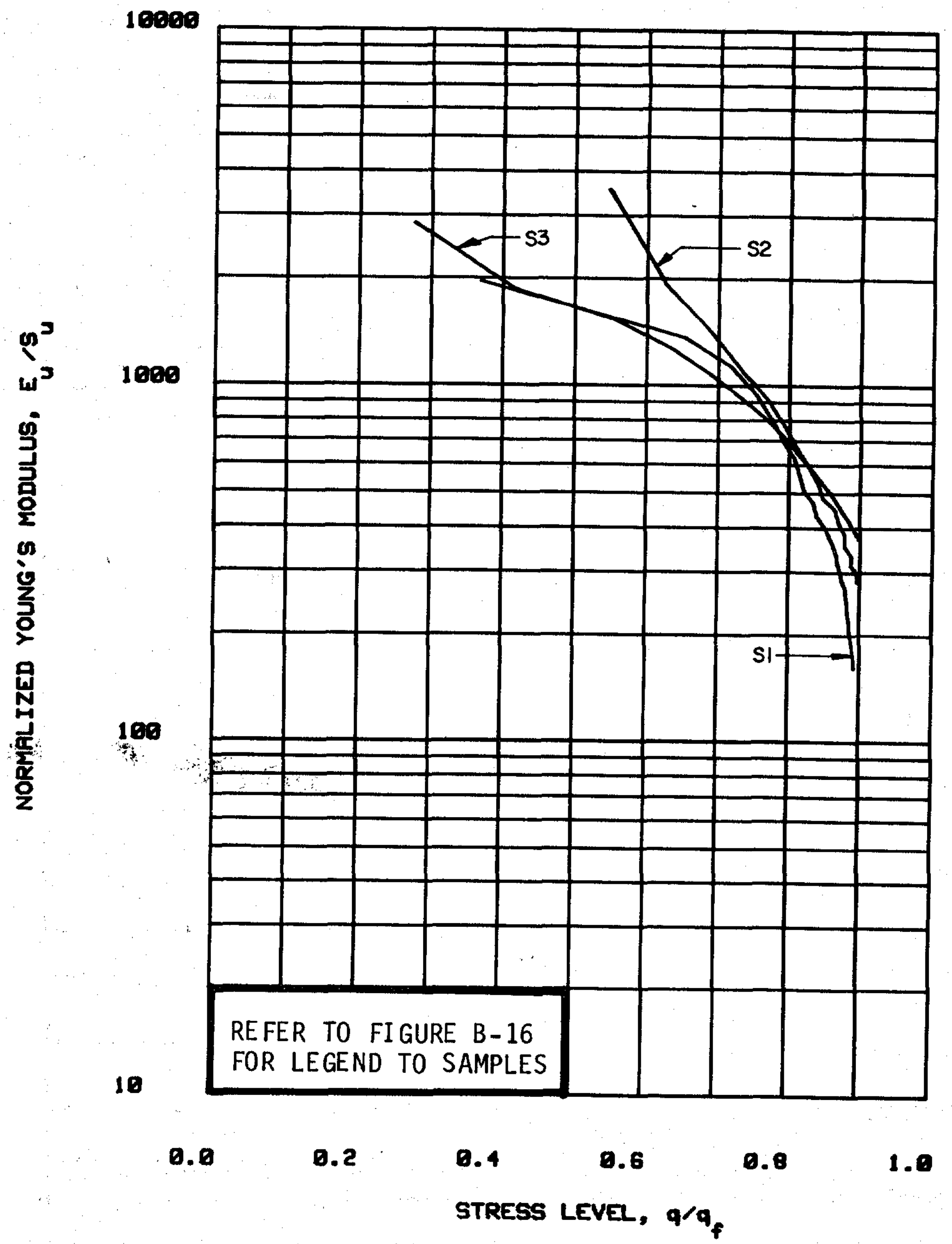

NORMALIZED UNDRAINED YOUNG'S MODULUS VERSUS STRESS LEVEL FROM $\overline{\text{CIU}}$C TESTS ON USSAC-ROCKLAND SAND-CLAY MIX WITH SCR = 3:1

FIGURE B-18